UNIVERSIDADE DE LISBOA

FACULDADE DE CIÊNCIAS

Ciências
ULisboa

Unraveling the metabolome of grapevine
through FT-ICR-MS: from nutritional value to pathogen resistance

"Documento Definitivo"

Doutoramento em Bioquímica

Especialidade em Regulação Bioquímica

Marisa Raquel Gomes Maia

Tese orientada por:

Doutora Marta Sousa Silva

Professora Doutora Andreia Figueiredo

Documento especialmente elaborado para a obtenção do grau de doutor

2021

UNIVERSIDADE DE LISBOA

FACULDADE DE CIÊNCIAS

Unraveling the metabolome of grapevine

through FT-ICR-MS: from nutritional value to pathogen resistance

Doutoramento em Bioquímica

Especialidade em Regulação Bioquímica

Marisa Raquel Gomes Maia

Tese orientada por:

Doutora Marta Sousa Silva

Professora Doutora Andreia Figueiredo

Júri:
Presidente:
● Doutor Manuel Eduardo Ribeiro Minas da Piedade, Professor Catedrático e Presidente do Departamento de Química e Bioquímica da Faculdade de Ciências da Universidade de Lisboa
Vogais:
● Doutor Philippe Schmitt-Kopplin, Professor, Research Unit Analytical BioGeoChemistry (BGC) do Helmholtz Zentrum München (Alemanha)
● Doutora Maria do Rosário Fernandes Félix, Professora Auxiliar, Escola de Ciências e Tecnologia da Universidade de Évora
● Doutor Francisco Manuel Lemos Amado, Professor Associado com Agregação, Departamento de Química da Universidade de Aveiro
● Doutor Manuel Pedro Salema Fevereiro, Professor Auxiliar com Agregação, Instituto de Tecnologia Química e Biológica António Xavier da Universidade Nova de Lisboa
● Doutora Marta Filomena de Sousa Silva Ferreira, Equiparada a Investigadora Principal, Faculdade de Ciências da Universidade de Lisboa (orientadora)

2021

"The goal is not to be better than the other man, but your previous self."

The 14th Dalai Lama (Tenzin Gyatso)

The Nobel Peace Prize 1989

"Self-respect without the respect of others is like a jewel which will not stand the daylight."

Alfred Nobel - The founder of the Nobel Prize

(1833-1896)

"Perhaps it is good to have a beautiful mind, but an even greater gift is to discover a beautiful heart."

Russell Crowe as John Nash

(In a Beautiful Mind movie)

ACKNOWLEDGMENTS

I know this is not very usual, but first of all I would like to thank Marisa Maia for deciding 4 years ago, after an incredible journey of a master thesis, to accept the challenge of doing a PhD in metabolomics applied to plant science. Looking back to the beginning of this journey, 4 years later I am writing this acknowledgement. Everyone said "You can do it!", but there were times I did not believe in it. I kept on insisting and insisting and never gave up, and look at me now: "I DID IT!". I knew you got it in you girl!

This journey presents many landmarks, being the first my supervisors. My particular gratitude goes to Professor Doctor Andreia Figueiredo, for her guidance, support, patience and knowledge transmitted. I am forever grateful for your dedication to make sure that I had the most solid PhD thesis and papers published, learned the most of this PhD and continuously pushing me to think about everything in my results. All of those things to make me not only a better scientist but also started to build my path into a more independent and critical minded scientist. I would also like to acknowledge my supervisor Doctor Marta Sousa e Silva. I want to thank you both for all the support and opportunities to work abroad, to attend international conferences and training schools around the world.

I acknowledge also Professor Doctor Carlos Cordeiro, my PhD advisor, and Professor Doctor António Ferreira, from the *Laboratório de FTICR e Espectrometria de Massa Estrutural*, of *Faculdade de Ciências* of University of Lisbon in Portugal, for all the scientific constructive discussions and support.

I am immensely grateful to all my colleagues at Grapevine Pathogen Systems Lab (GPS_Lab) from Biosystems and Integrative Sciences Institute (BioISI). I cannot turn into words what you mean to me. I am so happy to be part of something that was created by pure hard working and lovely people that always have each other's backs. GPS_Lab is all of us. It started as an idea and look at us now. We built this together, we continued to grow not only as a group but personally, as friends as a unison. I enjoyed every day working with all of you. Thank you for always supporting me and putting up with a lot of my ****. I know I can be a bit ("BIT") annoying sometimes. But I know you love me, even if it's just a bit. Everything is possible when you have the right people walking beside you, and at GPS_Lab everything is possible. When I say everything, I really mean it. You can be doing qPCR in the morning and at 5 pm you can be enjoying a glass of wine and cheese in the office. It's a mystery every day. People say that there are different types of home, and GPS_Lab is definitely a HOME to me.

reminding me that it's the small things that matter in life. I also want it to be written that I am sorry for not always having the time to be with you. You kept saying "You are always working!". I know we cannot recover the lost time, but I will make sure for now on, things will change.

I also want to thank Alexandre Cardoso (my Tupperware Boss [I wrote the word]) for its motivation speeches through the years. I want to thank especially this one: "Congratulations Marisa for your incredible work. You achieved all your goals. You will be an amazing scientist". I want to thank him all the adventures and the support during these 4 years.

I want to thank all my friends (the list is long) for their friendship and always saying "If there is someone who can do it, it's you!". I want to also thank my friends (you know who you are) that kept asking me during these 4 years: "Why are you doing a PhD?"; "When do you finish to get a real job?"; "Are you still studying?"; "You should leave science, there are great opportunities out there for you!". Because I am very stubborn and persistent, and without them I would not have in the back of my mind the strength to prove them wrong about science.

To Ioana and Cláudia from Departamento de Química e Bioquímica (DQB) secretary, for all the support and kindness. To the Biochemistry PhD coordinator Professor Doctor Carlos Farinha, for all the advices.

RESUMO (PORTUGUESE ABSTRACT)

O metaboloma de um organismo engloba todas as pequenas moléculas químicas resultantes do metabolismo, denominadas de metabolitos. A metabolómica é um ramo das abordagens "Ómicas" que envolve a identificação e quantificação dos metabolitos e/ou variações destes em processos celulares, células individuais ou tecidos, bem como a compreensão destes nos diferentes sistemas biológicos. Apesar destes termos apenas terem surgido há aproximadamente 20 anos atrás, as abordagens de metabolómica têm sido cada vez mais utilizadas para estudar e compreender melhor, não só os diferentes Reinos existentes na Natureza, como também para explorar as interações entre regulação genética e o meio ambiente, mutações, mudanças de fenótipos, identificação de biomarcadores, avaliação da qualidade de produtos bem como a descoberta de novos medicamentos, entre outros.

O reino vegetal contém uma grande diversidade de metabolitos (aproximadamente 200000). A grande maioria destes metabolitos ainda é desconhecida e até agora os identificados são estruturalmente diferentes e as suas propriedades e funções biológicas são consideradas muito importantes em biologia vegetal. Sendo assim, uma abordagem não dirigida de metabolómica de plantas, tem como alvo um elevado número de metabolitos, em que grande parte tem estrutura desconhecida. Considera-se então um desafio para qualquer técnica analítica, quando um número tão elevado de compostos naturais desconhecidos com propriedades tão diferentes, necessitam de ser analisados simultaneamente.

Existem várias técnicas disponíveis que permitem fazer estudos de metabolómica como a Ressonância Magnética Nuclear (*Nuclear Magnetic Resonance*, NMR) e Espectrometria de Massa (*Mass spectrometry*, MS) ou a combinação destas técnicas com processos de separação cromatográficos como a cromatografia gasosa (*gas chromatography*, GC) ou líquida (*liquid chromatography*, LC). Contudo, há que ter em conta que é necessária uma técnica analítica que permita a análise de amostras extremamente complexas e a identificação/deteção de dezenas de milhares de compostos individuais. Os limites de deteção por NMR são baixos e apesar da combinação destas técnicas com GC e LC possibilitarem a deteção de um elevado número de compostos, os processos cromatográficos demoram muito tempo e normalmente necessitam de vários passos de limpeza do equipamento. Normalmente a técnica escolhida para estudos de metabolómica de plantas é MS. Dentro dos equipamentos atuais, a espectrometria de massa de ressonância ciclotrónica de ião com transformada de Fourier (*Fourier Transform Ion Cyclotron Resonance Mass Spectrometry*, FT-ICR-MS) é uma das tecnologias com maior potencial na análise metabolómica global de plantas (**CAPÍTULO I**). Esta técnica combina não só a elevada resolução com a elevada exatidão de massa, permitindo a identificação na ordem das centenas de milhares de compostos, como também permite uma rápida e fácil aquisição de resultados a partir da injeção direta da amostra.

A videira (*Vitis vinifera* L.) é atualmente uma das plantas de fruto mais cultivadas em todo o mundo devido à sua importância económica na indústria vitivinícola. Em 2020, a área mundial coberta por vinhas para produção de uvas, passas de uva, vinho e outros produtos foi de 7.3 milhões de hectares. Com um mercado global de 29.6 biliões de euros, esta planta desempenha um papel fundamental na economia de muitos países. A União Europeia é líder mundial na produção de vinho, tendo quase metade da área vitivinícola. Devido ao seu fácil cultivo e inúmeras aplicações, Portugal tem 194 kha de superfície de vinha, sendo o 5 º país da Europa com maior área coberta por vinhas. Como resultado, em 2020, Portugal produziu 6,4 milhões de hectolitros de vinho, dos quais 3,1 foram exportados, tornando o país no 11 º produtor mundial de vinho e o 5 º na Europa. A receita total desta indústria foi de 846 milhões de euros para Portugal.

De todos os produtos vitícolas, e apesar das uvas e do vinho serem maioritariamente os mais comercializados, alguns países como a Turquia, Arábia Saudita, Grécia, Bulgária, Roménia e Vietname cultivam algumas espécies de videira especificamente para a produção de folhas para consumo na alimentação. Em Portugal, as folhas de algumas cultivares de videira começaram já a ser analisadas para a inclusão na dieta, devido ao seu conteúdo antioxidante e compostos fenólicos. Os seus benefícios para a saúde têm sido cada vez mais estudados, tendo-se demonstrado que este produto pode ser utilizado, por exemplo, para o tratamento de dores crónicas, processos inflamatórios e pressão arterial elevada. Estas propriedades, o valor nutricional, o sabor e a qualidade são devidos a uma grande diversidade de compostos secundários que as folhas de videira possuem.

Esta dissertação teve como foco principal a utilização de FT-ICR-MS para a caracterização do metaboloma total de folhas de diferentes espécies de videira. Foram efetuadas diferentes análises de modo a detetar metabolitos com possível interesse nutricional, outros associados à defesa intrínseca da planta e quais os metabolitos ativados após infeção com um patógeno.

De modo a valorizar este produto secundário das vinhas, o valor nutricional de folhas de videira foi avaliado a partir de uma análise do metaboloma de folhas de videira de *V. vinifera* cv. Pinot noir por FT-ICR-MS (**CAPÍTULO II**). Foram identificados diferentes compostos que possuem diferentes propriedades nutricionais e farmacológicas, particularmente compostos fenólicos. A classe metabólica mais representada em folhas de videira foi a classe dos lípidos, em que os ácidos gordos representam quase 50% do total de lípidos detetados. A atividade antioxidante de folhas de videira foi também avaliada. Os resultados obtidos demonstram que as folhas de videira têm uma elevada atividade antioxidante semelhante aos frutos vermelhos, reconhecidos no mercado por serem alimentos de referência desta propriedade.

A grande maioria das cultivares de *V. vinifera* utilizadas na produção de vinho são suscetíveis a variadas doenças das quais podemos destacar o míldio, o oídio e a podridão cinzenta. Estas doenças são causadas, respetivamente, pelo oomicete *Plasmopara viticola* (Berk. et Curt.) Berl. et de Toni e pelos fungos *Erysiphe necator* (Schweinf.) Burrill e *Botrytis cinerea* (Pers.).

P. viticola e *E. necator* são patógenos biotróficos obrigatórios, retiram nutrientes dos tecidos vivos da planta e desenvolvem estruturas para invadir as células da planta e obter produtos do seu metabolismo sem matar a planta. Este ciclo de vida contrasta com o de patógenos necrotróficos, *B. cinerea*, que matam os tecidos da planta à medida que se propaga, alimentando-se de células mortas. O modo de infeção destes patógenos também é diferente. O *P. viticola* invade a planta pelos estomas e o *E. necator* promove feridas no tecido da planta, pela secreção de enzimas líticas, por onde entra. *B. cinerea* entra no hospedeiro através de uma infeção local através de feridas. Em condições climáticas adequadas, estas doenças reduzem drasticamente o fitness da planta e a qualidade da uva, com perdas significativas, chegando a atingir 75% da vinha, levando consequentemente a uma diminuição na produção de vinho e à sua comercialização.

A aplicação preventiva de produtos químicos é a abordagem mais usada pelos viticultores para controlar esses patógenos. Esta abordagem não é a mais eficaz, nem compatível com um desenvolvimento sustentável, nem segura para a saúde pública. Para além disto, as alterações climáticas têm afetado bastante a viticultura levando cada vez mais ao aparecimento de vários surtos mais agressivos de doenças. Na última década, surgiram exigências crescentes de práticas agrícolas mais sustentáveis. As diretrizes da União Europeia exigem a redução e o uso sustentável de produtos químicos (Diretiva 2009/128 / CE e Metas da Agenda 2030 para o Desenvolvimento Sustentável), de modo a aumentar a segurança para o consumidor e paralelamente reduzir os custos de produção. Para fazer frente a estas exigências, os produtores reforçam a necessidade de criação de novas variedades por meio de programas de melhoramento. Este processo envolve o cruzamento natural de plantas com características desejadas. Apesar das diferentes cultivares de videira serem extremamente suscetíveis a estes patógenos, existe um grau de diferenciação entre estas, desde as altamente suscetíveis até às mais tolerantes. Algumas espécies Americanas e Asiáticas de *Vitis* são tolerantes ao *P. viticola*, *E. necator* e *B. cinerea*, pelo que, uma possível alternativa na prevenção da infeção por estes patógenos é a criação de híbridos a partir da combinação de videiras com tolerâncias eficazes, e duráveis aos patógenos, com cultivares de *V. vinifera* com boa qualidade de uva para a produção de vinho. No entanto, um programa bem-sucedido de reprodução de plantas melhoradas com características de tolerância requer, não só uma compreensão dos mecanismos de tolerância inata de cultivares contra os fungos/oomicetes, mas também a identificação de biomarcadores de tolerância. De entre estes, os biomarcadores metabólicos

podem revelar-se particularmente úteis. Uma análise metabólica da videira é de elevada importância visto que as plantas contêm um metaboloma único que varia com as condições ambientais, o desenvolvimento da planta e infeções patogénicas. Para além disto, estes biomarcadores serão importantes em programas de melhoramentos para uma rápida seleção de cultivares com características de interesse. Em relação às folhas de videira, visto que é o primeiro órgão que estes patógenos infetam, estas podem possuir na sua composição biomarcadores de tolerância ou suscetibilidade contra estas doenças.

Nos **CAPÍTULOS III**, **IV** e **V**, o metaboloma de vários genótipos de *Vitis*, com diferentes graus de tolerância a fungos/oomicetes, foi comparado de modo a compreender melhor os mecanismos de defesa intrínsecos da videira, associados a estas doenças, de modo a permitir uma fácil e rápida caracterização das videiras.

A partir da comparação do metaboloma de duas *V. vinifera* (*V. vinifera* cv. Trincadeira e *V. vinifera* cv. Regent, suscetível e tolerante a patógenos, respetivamente) foi possível a discriminação destas cultivares e a identificação de compostos discriminativos (**CAPÍTULO III**). Uma comparação semelhante foi analisada entre uma *Vitis vinifera* (*V. vinifera* cv. Cabernet Sauvignon, suscetível) e uma espécie de *Vitis* (*Vitis rotundifolia*, tolerante) (**CAPÍTULO IV**). Os resultados obtidos permitiram uma discriminação entre estes genótipos a partir do metaboloma e perceber que o metaboloma da *Vitis rotundifola* apresenta uma maior complexidade de fórmulas químicas. A partir destes resultados foi possível perceber que apesar do metaboloma da videira ser bastante complexo, permite discriminar não só entre espécies como também variedades dentro da mesma espécie.

Sendo assim, foi efetuado um estudo com um maior número de variedades de videira, com diferentes graus de tolerância a patógenos, para perceber as características intrínsecas de defesa das videiras (**CAPÍTULO V**). No total foram destacados sete compostos com um padrão de acumulação maior em apenas videiras suscetíveis. As vias metabólicas destes compostos foram analisadas e a expressão de genes, que codificam para enzimas de síntese ou degradação para estes compostos, foi quantificada por reação de polimerase de cadeia em tempo real. Como a expressão de genes de interesse tem de ser normalizada com genes de referência, a estabilidade de dez genes foi avaliada e foram estabelecidos genes de referência para este tipo de dados. Os três genes mais estáveis (*ubiquitin-conjugating enzyme* – UBQ; *SAND family protein* - SAND e e*longation factor 1-alpha* - EF1α) foram considerados para normalizar os dados. Os resultados obtidos demonstram um aumento significativo de catequina e derivados nas cultivares suscetíveis a patógenos. Estes resultados estão de acordo com os dados de expressão do gene envolvido na biossíntese da catequina e derivados [*leucoanthocyanidin reductase 2* gene (*LAR2*)], mais expresso em videiras suscetíveis. Estes dados apontam para um possível biomarcador associado à suscetibilidade.

Foi também avaliado os diferentes compostos envolvidos na interação e defesa da videira a um dos patógenos, *P. viticola*. Os resultados obtidos encontram-se representados nos **CAPÍTULOS VI** e **VII**.

De modo a utilizar diretamente os dados obtidos do equipamento de MS (dados *raw*) para distinguir rapidamente o metaboloma de videira após infeção com um patógeno (sem a sua identificação prévia dos compostos), foi efetuada uma análise do metaboloma de videira de *V. vinifera* cv. Trincadeira 24 horas após infeção com *P. viticola*. Os dados obtidos permitiram uma rápida e de fácil visualização separação do metaboloma de videira infetado e do não infetado (**CAPÍTULOS VI**).

Por último, e como o *P. viticola* infecta a planta a partir da entrada na cavidade estomática, uma análise preliminar não direcionada do metaboloma de *V. vinifera* cv. Trincadeira foi efetuada com recurso a imagens por espectrometria de massa de ionização/dessorção a laser assistida por matriz de ressonância ciclotrónica de ião com transformada de Fourier (*Matrix-Assisted Laser Desorption/Ionization Mass Spectrometry Imaging* - MALDI-FT-ICR-MSI), de modo a identificar os metabolitos responsáveis pela interação videira-*P. viticola* (**CAPÍTULOS VII**). A sacarose foi putativamente identificada, estando mais acumulada na superfície das folhas de videira infetadas com *P. viticola*. Para além disso, a distribuição da sacarose na folha verifica-se maioritariamente nos veios da folha. Estes resultados estão de acordo com o modo de infeção do patógeno, levando à hipótese do *P. viticola* extrair a sacarose da videira para se reproduzir.

Cada capítulo desta tese foi escrito como um artigo científico e cada um possui o seu próprio resumo, introdução, materiais e métodos, resultados e discussão, conclusão, agradecimentos e referências bibliográficas.

Os resultados obtidos nesta tese de doutoramento, irão ser uma mais valia para elucidar quais as bases moleculares inerentes à tolerância/suscetibilidade das videiras bem como perceber melhor os mecanismos de defesa da videira perante doenças. Permitirão também construir ferramentas de análise, para a identificação dos diferentes graus de tolerância/suscetibilidade a patógenos, em programas de melhoramento e análise de linhagens.

Palavras-chave: FT-ICR-MS; Metabolómica; *Vitis vinifera*; *Plasmopara viticola*

x

ABSTRACT

Grapevine (*Vitis vinifera* L.) is one of most important fruit crops in the world due to its numerous food products, namely fresh and dried table grapes, wine and intermediate products, with a high economic importance worldwide.

Concerning nutritional value, grapes are highly studied and a great diversity of secondary bioactive metabolites has already been identified. However, an important grapevine by-product, also containing a high nutritional value, but sometimes disregarded is grapevine leaves. They are an abundant source of compounds with interest in human health and are already included in human diet in several countries. The study of the nutritional values of this by-product is essential towards the improvement of food systems. Hence, in this PhD dissertation an untargeted metabolomic profiling of the leaves of *Vitis vinifera* cultivar 'Pinot noir' was performed by Fourier-transform ion cyclotron-resonance mass spectrometry (FT-ICR-MS), (**CHAPTER II**). Numerous compounds with diverse nutritional and pharmacological properties, particularly polyphenols and phenolic compounds, several phytosterols and fatty acids (the most represented lipids' secondary class), were identified. Grapevine leaves were also evaluated for their antioxidant capacity. It was found that leaves present a high antioxidant capacity, similar to berries, putting grapevine leaves at the top of the list of foods with the highest antioxidant activity.

Traditional premium cultivars of wine and table grapes are highly susceptible to various diseases. Grapevine downy mildew, powdery mildew and gray mold are caused, respectively, by the biotrophic oomycete *Plasmopara viticola* (Berk. & Curt.) Berl. & de Toni) Beri, et de Toni], by the biotrophic fungus *Erysiphe necator* (Schweinf.) Burrill) and by the necrotrophic fungus *Botrytis cinerea* Pers.).

In Europe, disease management became one of the main tasks for viticulture, being the current strategy, for disease control, the massive use of fungicides and pesticides in each growing season. This practice has several associated problems, from the environmental impact to the economical level, and even in human health.

The alternative approach to the application of pesticides is breeding for resistance, clearly the most effective and sustainable approach, particularly if coupled to the selection of desirable traits from local grapevine cultivars. However, a successful breeding program of grape plants with increased resistance traits against pathogens requires not only an understanding of the innate resistance mechanisms of cultivars against fungi/oomycetes, but also the identification of biomarkers of tolerance or susceptibility. Among these, metabolic biomarkers may prove particularly useful, not only because they can be determined in a high

throughput way but, above all, because metabolites provide an accurate image of the metabolic state of the plant. To better understand the metabolic differences associated with intrinsic defence mechanisms of grapevine to pathogens, the metabolome of several genotypes with different tolerance degrees to fungal/oomycete pathogens was compared through an untargeted metabolomics approach by FT-ICR-MS (**CHAPTERS III, IV and V**).

First, a comparison of two *Vitis vinifera* (*V. vinifera* cv. Trincadeira e *V. vinifera* cv. Regent, susceptible and tolerant, respectively, to pathogens) was performed and discriminatory compounds between these two cultivars, were identified (**CHAPTER III**). Also, through the comparison of the metabolome of one *Vitis vinifera* (*V. vinifera* cv. Cabernet Sauvignon, susceptible to pathogens) and one *Vitis* species (*Vitis* rotundifolia, tolerant), was possible to distinguish both genotypes and determine that *Vitis rotundifolia* metabolome appeared to be more complex according to the chemical formulas analysed (**CHAPTER IV**). Albeit grapevine metabolome is complex, it is possible to distinguish *Vitis* species and different genotypes within the same species.

Ultimately, to identify compounds that contribute to the segregation between susceptible and tolerant grapevines, eleven *Vitis* genotypes, were compared at the metabolite level (**CHAPTER V**). From all the metabolites identified, seven compounds with a higher accumulation on susceptible genotypes were selected. Their metabolic pathways were analysed and the expression profile of biosynthesis and/or degradation enzymes coding genes was evaluated by Real-time Polymerase Chain Reaction (qPCR). qPCR studies require as internal controls one or more reference genes. Hence, in this study, ten possible reference genes were tested and the three most stable reference genes (*ubiquitin-conjugating enzyme* – UBQ, *SAND family protein* - SAND and *elongation factor 1-alpha* - EF1α) were established for our analysis and selected for qPCR data normalization. Our data revealed that the *leucoanthocyanidin reductase 2* gene (*LAR2*) presented a significant increase of expression in susceptible genotypes, in accordance with catechin accumulation in this analysis group, being a possible metabolic constitutive biomarker, associated to susceptibility.

The interaction of grapevine-*P.viticola* was also analysed by FT-ICR-MS (**CHAPTERS VI and VII**). The metabolome of *Vitis vinifera* cv. Trincadeira after 24 hours post-infection (hpi) was analysed and, based only on the chemical profile and representation plots, the discrimination between infected and non-infected grapevine leaves was possible (**CHAPTER VI**). A further analysis of *Vitis vinifera* cv. Trincadeira infected with *P. viticola* was performed through Matrix-assisted laser desorption/ionization (MALDI) FT-ICR-MS imaging, to identify leaf surface compounds related to the grapevine-pathogen interaction (**CHAPTER VII**). Putatively identified sucrose ions were more abundant on *P. viticola* infected leaves when compared to control ones. Also, sucrose was mainly located around the veins, which is

an indicator of the correlation of putatively identified sucrose at *P. viticola* infection sites, leading to the hypothesis that the pathogen is extracting sucrose from grapevine to reproduce.

Each chapter was written as a scientific article and has its own abstract, introduction, materials and methods, results and discussion, conclusion, acknowledgments and references.

The results obtained in this PhD thesis are a starting point on the elucidation of the molecular mechanisms related to the intrinsic tolerance/susceptibility to different pathogens. Also, these results can be used for the development of new approaches and help to improve breeding and introgression line programs.

Keywords: FT-ICR-MS; Metabolomics; *Vitis vinifera*; *Plasmopara viticola*

DECLARAÇÃO

De acordo com o disposto no artigo n.º 32 do Regulamento de Estudos de Pós – Graduação da Universidade de Lisboa, Despacho n.º 8631/2020, publicado no Diário da República, 2.ª série — N.º 175 — 8 de setembro de 2020 – Pág. 236, e após aprovação pelo Gabinete de Estudos Pós-graduados da Faculdade de Ciências da Universidade de Lisboa, esta dissertação de Doutoramento foi escrita em capítulos, enquadrados por uma introdução e conclusão gerais, representando cada capítulo um trabalho de investigação da autoria da aluna Marisa Raquel Gomes Maia, correspondendo a tarefas/objetivos propostos no plano de doutoramento.

Os trabalhos apresentados foram aceites e publicados em revistas indexadas, com e sem fator de impacto, e com comités de seleção de reconhecido mérito internacional. Trabalhos submetidos para revisão e em preparação para submissão também estão representados nesta dissertação:

- **Maia, M.**, McCann, A., Malherbe, C., Far, J., Cunha, J., Eiras-Dias, J., Cordeiro, C., Eppe, G., De Pauw, E., Figueiredo, A., Sousa Silva, M., 2021. Grapevine leaf MALDI-FT-ICR-MS imaging reveals sucrose localisation patterns associated to *P. viticola* development. Metabolites (***Submitted***)
- **Maia, M.**, Figueiredo, A., Cordeiro, C., Sousa Silva, M., 2021. FT-ICR-MS-Based metabolomics: a deep dive into plant metabolism. Mass Spectrom. Rev. 1–22. https://doi.org/10.1002/mas.21731
- **Maia, M.**, Ferreira, A.E.N., Cunha, J., Eiras-Dias, J., Cordeiro, C., Figueiredo, A., Sousa Silva, M., 2021. Comparison of the chemical diversity of *Vitis rotundifolia* and *Vitis vinifera* cv. 'Cabernet Sauvignon.' Ciência Téc. Vitiv. 36, 1–8. https://doi.org/10.1051/ctv/20213601001
- **Maia, M.**, Ferreira, A.E.N., Nascimento, R., Monteiro, F., Traquete, F., Marques, A.P., Cunha, J., Eiras-Dias, J.E., Cordeiro, C., Figueiredo, A., Sousa Silva, M., 2020. Integrating metabolomics and targeted gene expression to uncover potential biomarkers of fungal/oomycetes-associated disease susceptibility in grapevine. Sci. Rep. 10, 15688. https://doi.org/10.1038/s41598-020-72781-2
- **Maia, M.**, Ferreira, A.E.N., Laureano, G., Marques, A.P., Torres, V.M., Silva, A.B., Matos, A.R., Cordeiro, C., Figueiredo, A., Sousa Silva, M., 2019a. *Vitis vinifera* "Pinot noir" leaves as a source of bioactive nutraceutical compounds. Food Funct 10, 3822–3827. https://doi.org/10.1039/c8fo02328j
- **Maia, M.**, Ferreira, A.E.N., Marques, A.P., Figueiredo, J., Freire, A.P., Cordeiro, C., Figueiredo, A., Sousa Silva, M.S., 2019b. Uncovering markers for downy mildew

resistance in grapevine through mass spectrometry-based metabolomics. Rev. Ciênc. Agr. 41, 48–53. https://doi.org/10.19084/RCA.17066

- **Maia, M.**, Maccelli, A., Nascimento, R., Ferreira, A.E.N., Crestoni, M.E., Cordeiro, C., Figueiredo, A., Sousa Silva, M., 2019. Early detection of *Plasmopara viticola*-infected leaves through FT-ICR-MS metabolic profiling. Acta Hortic. 575–580. https://doi.org/10.17660/ActaHortic.2019.1248.77

Em cumprimento com o disposto no referido despacho e com o gabinete de estudos pós-graduados da Faculdade de Ciências da Universidade de Lisboa, esclarece-se ser da minha responsabilidade a execução das experiências que estiverem na base dos resultados apresentados (exceto quando referido em contrário), assim como a interpretação e discussão dos mesmos.

Lisboa, 21 de setembro de 2021

Marisa Raquel Gomes Maia

INDEX

INDEX OF FIGURES

XXIV

INDEX OF TABLES

INDEX OF SUPPLEMENTARY FIGURES

INDEX OF SUPPLEMENTARY TABLES

xxx

ABBREVIATIONS, SYMBOLS AND UNITS

Abbreviations

60S	*60S ribosomal protein L18*
ACT	*Actin*
ANR	*Anthocyanidin reductase*
AP2M	*Arabidopsis adaptor protein-2 MU-adaptin*
BC	Before Christ
BKI	BestKeeper Index
BLAST	Basic Local Alignment Search Tool
BP	Base pairs
C16:0	Hexadecanoic acid
C16:1	Palmitoleic acid
C16:1t	Trans-Hexadecanoic acid
C17:0	Heptadecanoic acid
C18:0	Octadecanoic acid / stearic acid
C18:1	Oleic acid
C18:2	Linoleic acid / Omega-6
C18:3	alpha-Linolenic acid / Omega-3
CAN	Portuguese Ampelographic Grapevine Collection (*Coleção Ampelográfica Nacional*)
cDNA	Complementary DNA
COMT	Caffeic acid O-methyltransferase
Cq	Quantification cycle
Ct	Threshold cycle
DBE	Double-bond equivalents
DNA	Deoxyribonucleic acid
EF1α	*Elongation factor 1-alpha*
ESI	Electrospray Ionization
F3'5'H	*Flavonoid 3',5'-hydroxylase*
FAME	Fatty Acids' Methyl Esters
FAO	Food and Agriculture Organization of the United Nations
FAs	Fatty acids
FatB	*Fatty acyl-ACP thioesterase B*
FC	Fold-change
FDR	False Discovery Rate
FT-ICR-MS	Fourier Transform Ion Cyclotron Resonance Mass Spectrometry

Fw	Fresh Weight
GAPDH	*Glyceraldehyde-3-phosphate dehydrogenase*
gDNA	genomic deoxyribonucleic acid
HMDB	Human Metabolome Data Base
hpi	Hours post infection
IA	Index of Atherogenicity
IMPL1	*Myo-inositol monophosphatase*
IT	Index of Thrombogenicity
JA	Jasmonic acid
KEGG	Kyoto Encyclopedia of Genes and Genomes
LAR2	*Leucoanthocyanidin reductase 2 gene*
MDA	Malonaldehyde
mQTL	Metabolic Quantitative Trait Loci
MS	Mass spectrometry
MUFAs	Monounsaturated Fatty Acids
NMR	Nuclear Magnetic Resonance
O/C	Oxygen/Carbon
OIV	International Organisation of Vine and Wine (*Organisation Internationale de la vigne et du vin*)
OPLS-DA	Orthogonal Partial Least Squares Discriminant Analysis
PCA	Principal Component Analysis
PLS-DA	Partial Least Squares - Discriminant Analysis
PUFA-n3	Polyunsaturated Fatty Acids-n3
PUFA-n6	Polyunsaturated Fatty Acids-n6
PUFAs	Polyunsaturated Fatty Acids
qPCR	quantitative Polymerase Chain Reaction
QTLs	Quantitative Trait Loci
REN	Resistance to *Erysiphe necator*
RGs	Reference Genes
RNA	Ribonucleic acid
ROS	Reactive Oxygen Species
RPV	Resistance to *Plasmopara viticola*
SA	Salicylic acid
SAND	*SAND family protein*
SD	Standard deviation
SO4	Selection Oppenheim 4
SV	Stability value
TE	Trolox Equivalent

TEAC	Trolox Equivalent Antioxidant Capacity
TPR7B	*Tetratricopeptide repeat protein 7B*
UBQ	*Ubiquitin-conjugating enzyme*
UFGT	*UDP-glucose:flavonoid 3-O-glucosyltransferase*
VIP	Variable Importance in Projection
VIVC	*Vitis* International Variety Catalogue
VK	van Krevelen
α-TUB	*alpha-Tubulin 3-chain*
β-TUB	*beta-Tubulin 1-chain*

Symbols and Units

T	Tesla
cm	Centimetres
Da	Dalton
eg	For example - abbreviation of the Latin expression *exempli gratia*
et al.	And others - abbreviation for the Latin expression *et alia*
g	Centrifugal Force
g	Grams
h	Hours
kha	Thousands of hectares
Km	Kilometres
m	Meters
m/z	Mass-to-charge ratio
mg	Milligrams
mha	Millions of hectares
min	Minutes
mL	Millilitres
mm	Millimetres
mM	Millimolar
mt	Millions of quintals
nm	Nanometres
ppm	Parts per million
r	Pearson correlation coefficient
T	Temperature (°C)
Ta	Annealing temperature
Tm	Melting temperature

µg	Microgram
µL	Microliter

CHAPTER I

Introduction

The sections in this chapter are organized differently from the paper.

1 INTRODUCTION

1.1 MAJOR REMARKS IN MASS SPECTROMETRY HISTORY

Mass spectrometry (MS) is a major analytical tool in chemistry, biochemistry, pharmacy, medicine and many related fields of science (Gross, 2017; Hiraoka, 2013). Its basic principle relies on the detection, identification and quantification of molecules based on their mass-to-charge (m/z) ratio, providing both molecular weight and structural information (Gross, 2017; Hiraoka, 2013). A mass spectrometer generates multiple ions from the sample under investigation; it then separates them according to their specific m/z, and then records the relative abundance of each ion (Gross, 2017; Hiraoka, 2013). The information delivered by mass alone can be sufficient for the identification of elements and the determination of the molecular formula of an analyte. The relative abundance of isotopes helps to decide which elements contribute to such formula and to estimate the number of atoms of a contributing element. Under the conditions of certain mass spectrometric experiments, fragmentation of ions can deliver information on ionic structure. Thus, MS may elucidate the connectivity of atoms within smaller molecules, identify functional groups, determine the (average) number and eventually the sequence of constituents of macromolecules, and in some cases even yields their three-dimensional structure (Gross, 2017; Hiraoka, 2013).

The field of applications of mass spectrometry are countless ranging from elemental and isotopic analysis, organic and bio-organic analysis, structure elucidation and characterization of ionic species and chemical reactions to coupling to separation techniques, mass spectral imaging and miniaturization. Due to its multiple-applications, MS is now applied in various fields such as biological, non-biological and environmental research; forensic analysis; quality control of drugs, foods and polymers; industry; environmental; military and space exploration (Vestal, 2011).

In order to understand how the field of MS has evolved to the present-day, it is helpful to look back and examine the major advances in the field. The history of Mass Spectrometry, remote to the beginning of the 20th century when Sir Joseph John Thomson developed MS (Thomson, 1897). Sir Thomson was working on another area of research at the time: cathode rays; and prevailed not only to understand what were the nature of cathode rays but also to measure the mass of the unknown particles involved on them. Sir Thomson first used his apparatus to measure electron/mass (early physicists typically reported a charge-to-mass ratio, e/m, rather than the present MS standard of m/z) of these fundamental particles/electrons in 1897 (Thomson, 1910, 1907, 1897). He received the Nobel Prize in Physics in 1906 (Nobel Prize, 1906). His early work led to the discovery of atoms and isotopes and was the foundation of the MS field (Thomson, 1912, 1910, 1908).

On the following years, Francis William Aston's built the first mass spectrometer, to provided means for the atomic characterization of numerous elements (Aston, 1920a, 1920b, 1919). His work was also awarded with the Nobel Prize in chemistry in 1922 (Nobel Prize, 1922). In 1929, Ernest O. Lawrence (Nobel Prize, 1939) invented the cyclotron: a device for accelerating nuclear particles to very high velocities without the use of high voltages (Lawrence et al., 1939), this principle lead to the creation of the first ion cyclotron resonance (ICR) mass spectrometers years later.

Until 1940s, MS was used to measure masses of atoms and to demonstrate the existence of isotopes. Then, mass spectrometers started to become commercially available and MS was firmly established as a useful technique among physicists and industrial chemists. However, at the time, the major application of this technique was for the petroleum industry to control production processes and to measure the abundances of small hydrocarbons in process streams (Westinghouse Electric International Company, 1943).

Besides the slow beginning and small interest in the MS technique, remarkable progresses have been made in the last eighty years. In 1946, William Stephens presents the concept of Time-of-Flight (TOF) mass spectrometry (Stephens, 1946; Wolff and Stephens, 1953), and since then, TOF mass analysers have grown, especially in the biological applications of mass spectrometry. Few years later, in 1949, the beginning of ultra-high resolution mass spectrometry started with the work of John A. Hipple, which developed the ICR mass spectrometer (Hipple et al., 1949).

In the 1950s, Hans Dehmelt (Nobel Prize, 1989), developed a method for using magnetic fields to capture charged particles in a trap: the Penning trap (Dehmelt, 1952, 1951a, 1951b, 1950; Dehmelt and Krüger, 1951a, 1951b, 1950). At the same time, Wolfgang Paul (Nobel Prize, 1989) developed a method to trap charged particles based on electrical currents and electromagnetic fields: quadrupole and quadrupole ion trap (Paul and Steinwedel, 1953). Both these works earn them the Nobel Prize in Physics in 1989. The ion trap technique is the most widely used today and is still being improved for an even wider range of applications.

It was not until the late 1950s and 1960s that scientists really began to understand the complexity of molecules, the fragmentation mechanisms of different classes of organic compounds and determine the structures of unknown molecules by MS (Beynon, 1956; Gohlke, 1959; Ryhage et al., 1965). Also, the urge to discover more and more led to the combination of other techniques with MS: gas chromatography (GC-MS), liquid chromatography (LC-MS) and mass spectrometry imaging (MSI), (Beynon, 1956; Gohlke, 1959; Ryhage et al., 1965). In 1968, Malcolm Dole developed the electrospray ionization (ESI) (Dole et al., 1968). Despite the mass spectrometers available at the time could not detect singly

4

charged ions with masses larger than a few thousand Daltons, below the mass range of macromolecules of biological interest, his experiments opened new insights for MS applications and are the groundwork for modern biological MS research.

A major breakthrough happened in 1974 to John A. Hipple work, when Alan Marshall and Melvin Comisarow realized that Fourier Tranform, a mathematical transformation, could be applied to ICR. The advance was truly revolutionary (Comisarow and Marshall, 1974a). By the 1980s, small organic molecules were routinely being analysed by MS (Fenn et al., 1989; Karas et al., 1985; Lee et al., 1989; Tanaka et al., 1988; Yoshida et al., 1988). Albeit incredible progress, proteins and other macromolecules still could not be detected to address this problem, Franz Hillenkamp, Michael Karas and co-workers were investigating different techniques and developed the Matrix-Assisted Laser Desorption Ionization (MALDI), (Karas et al., 1985; Karas and Hillenkamp, 1988). Also, almost at the same time, John B. Fenn (Nobel Prize, 2002) showed that when a sample (small molecules and macromolecules) is sprayed with an electrical field, small charged drops are formed, and when the water evaporates, ions in gaseous form remain. John Fenn improved the Electrospray (ESI) technique to analyse biological molecules (Fenn et al., 1989). These ionization techniques, MALDI and ESI, triggered the explosive development of mass spectrometry and revolutionized biological MS. Moreover, they are still the dominant forms of macromolecule ionization to this day, especially to ionize proteins and peptides. Also, in that decade, Koichiro Tanaka (Nobel Prize, 2002) showed that laser pulses could blast apart protein molecules so that ions in gaseous form (Tanaka et al., 1988; Yoshida et al., 1988). The 2002 Nobel Prize in Chemistry, was awarded with one half jointly to John B. Fenn and Koichi Tanaka "*for their development of soft desorption ionisation methods for mass spectrometric analyses of biological macromolecules*".

In 2000, Alexander Makarov developed a new type of mass analyser which employs trapping in an electrostatic field: the orbitrap (Makarov, 2000).

Although, all of these mass spectrometers are different and allow the analysis of all types of samples in a different way, the general layout of the equipment's itself is common; they all consist of an ion source, a mass analyser and a detector which are operated under high vacuum conditions.

Due to the advance in MS equipment's and as the applications of MS rapidly expand, incredible progresses have been made in science, particularly during the past decade. There is no single "golden rule" in approaching the wide field of mass spectrometry. Mass spectrometry is an integrated science itself; it is based on physics, quantum mechanics, thermodynamics, physical chemistry, photochemistry, electromagnetism, instrumentation,

and so on. In other words, mass spectrometry is multi-facet rather than to be viewed from a single perspective. It is nowadays an indispensable analytical method in modern science and technology and albeit all the marvellous improvements, it is still a technology in progress.
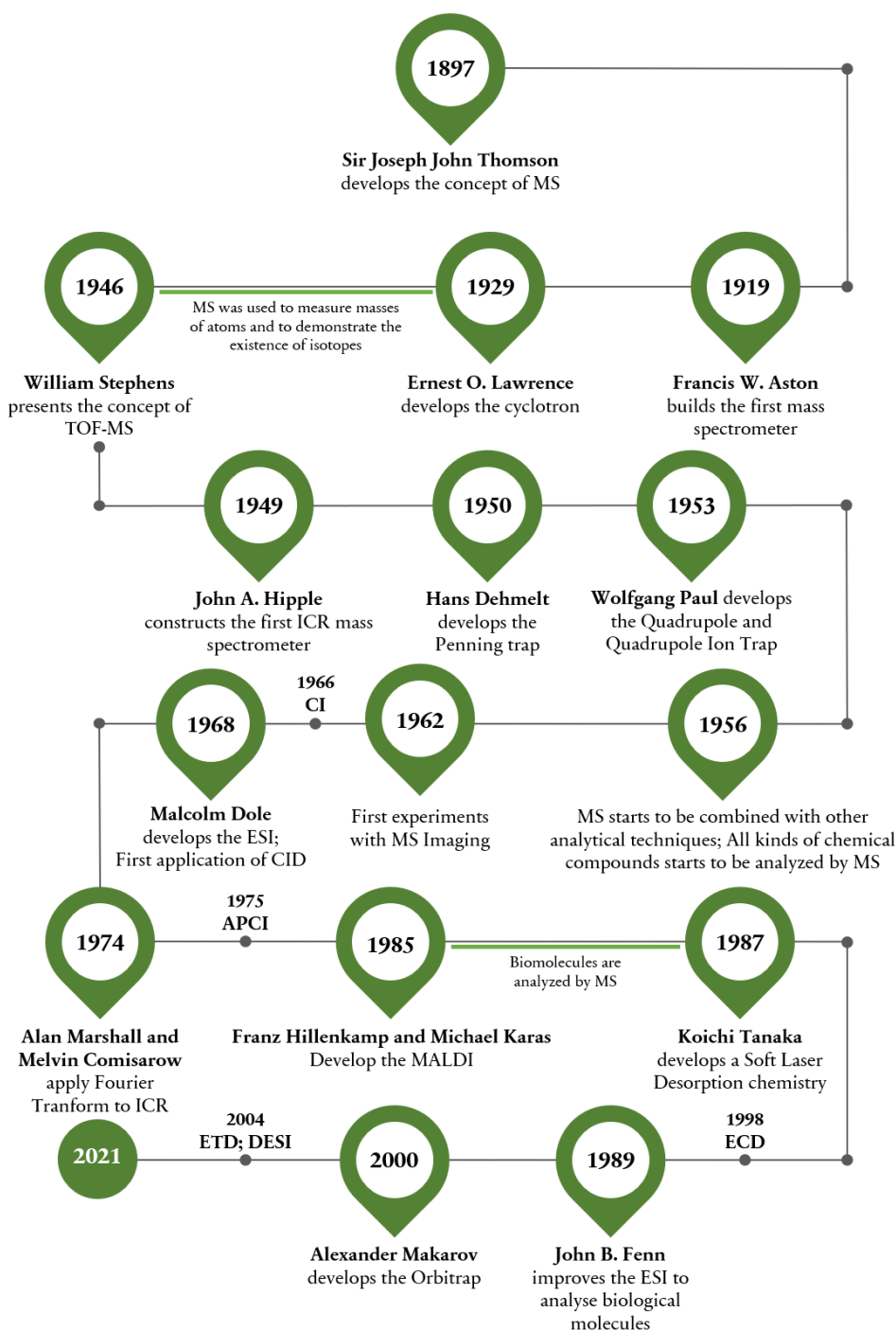
Figure 1.1 - Major milestones in mass spectrometry history. MS – Mass Spectrometry; TOF - Time-of-Flight; ICR - ion cyclotron resonance; CI – Chemical Ionization; ESI - electrospray ionization; CID – Collision Induced Dissociation; APCI - Atmospheric Pressure Chemical Ionization; MALDI - Matrix-Assisted Laser Desorption Ionization; ECD - Electron Capture Dissociation; ETD - Electron Transfer Dissociation; DESI - Desorption Electrospray Ionization.

1.2 PLANT METABOLOMICS

Metabolomics targets an enormous number of compounds of unknown structure (Fiehn, 2002; Sumner et al., 2003; Schauer & Fernie, 2006). This is an extreme challenge in analytical chemistry when a high number of unknown natural compounds with different properties need to be addressed simultaneously (Ohta et al., 2007).

But what is in fact "metabolomics" and the "metabolome"? The term "metabolomics" originates from metabolic profiling, a definition that dates from the early 1970s by researchers at the Baylor College of Pharmacy (Devaux et al., 1971; Horning & Horning, 1971). Years later, in 1998, Oliver and co-workers proposed the concept of "metabolome" (Oliver et al., 1998). Thereafter, many plant chemists conducted research in this area. In 1999, another concept was proposed by Nicholson and co-workers: "metabonomics", defined as "the quantitative measurement of the dynamic multiparametric metabolic response of living systems to pathophysiological stimuli or genetic modification" (Nicholson et al., 1999). Next, in 2001, "metabolomics" concept arose defining the "comprehensive and quantitative analysis of all metabolites in a biological system" (Fiehn, 2001). In short, in a biological sample, the metabolome comprises the total metabolite pool of an organism, a tissue and a cell, at a given moment, which can be unrevealed to characterize genetic background and responses to environmental challenges. Within "OMICs" research areas, metabolomics includes the identification and quantification of small molecule compounds, as well as the understanding of the chemical patterns involved in the regulation of the cellular processes in different biological species (Razzaq et al., 2019). Studies in metabolomics are crucial to explore environment–to-gene interactions, phenotyping, biomarkers identification and drug detection (Razzaq et al., 2019).

Within the different biological systems, plants are the group that contains the highest diversity of metabolites with thousands of compounds already identified and many still unknown (Wang et al., 2019). Hence, it is not only important to develop and improve new analytical techniques and protocols, but also to exploit already existing metabolomic platforms to discover more of the unknown plant metabolome, to explain complex biological pathways and to explore hidden regulatory networks controlling plant growth and development (Foito & Stewart, 2018; Chen et al., 2019; Razzaq et al., 2019; Wang et al., 2019; Castro-Moretti et al., 2020).

In plant metabolomics, several techniques have been applied so far, from nuclear magnetic resonance (NMR) (Aranìbar et al., 2001; Choi et al., 2004; Crockford et al., 2006; Viant et al., 2003) to mass spectrometry (MS) (Gowda and Djukovic, 2014). Although NMR is extremely reproducible and allows absolute quantification of detected signals, it lacks sensitivity as only a limited number of compounds are identified in complex mixtures and

the resolution are not comparable to MS techniques. The choice of mass spectrometry for metabolomics studies has innumerous advantages, namely a higher coverage through the use of separation steps, such as liquid (LC) or gas chromatography (GC) and capillary electrophoresis, which provide robust platforms for metabolomic studies (Tomita & Nishioka, 2005). Regarding ionization methods in MS, the preferred ionization chemistry tends to be electrospray ionization (ESI) and/or matrix-assisted laser desorption/ionization (MALDI). Both ESI and MALDI are soft ionization methods, which means individual naturally occurring metabolites can be ionized with great sensitivity without fragmentation of the molecules (Hiraoka, 2013; Gross, 2017). Furthermore, these methods enable very sensitive measurements allowing the detection of small levels of biological metabolites (in the pico- or femtomolar concentrations), (Tomita & Nishioka, 2005).

1.3   HIGH RESOLUTION PLANT METABOLOMICS: THE CASE OF FT-ICR-MS

For metabolomics analysis, mass spectrometers with high mass resolution, ability to achieve measurements with ppm errors, and ability to differentiate metabolites at the ppb to ppm level, is a prerequisite. These characteristics can only be achieved by using high resolution mass spectrometers, such as time-of-flight (TOF) and Fourier transform (FT) mass spectrometers, including FT ion cyclotron resonance (FT-ICR) and Orbitrap. These mass spectrometers have proven to be the most valuable for analyzing complex mixtures, not only for their mass accuracy and resolution but also due to the fact that direct infusion of the samples without chromatographic separation or derivatization reactions may be achieved (Allwood et al., 2011; Barrow et al., 2005; Haijes et al., 2019).

The majority of the plant-based metabolomics published studies so far use the Orbitrap or TOF equipment (around 700 studies published since 2011 – Pubmed, August 11th, 2021). The main reason is that most recent TOF equipment's can achieve mass resolution values of 30,000–40,000 (Andrews et al., 2011; Pelander et al., 2011) and the resolution power is not affected by chromatography acquisitions rates (Ghaste et al., 2016; Glauser et al., 2013; Hopfgartner, 2011; Park et al., 2021).

On the other hand, FT-ICR and Orbitrap outperform any other commonly used mass spectrometer in terms of absolute resolving power. Orbitrap mass spectrometers are especially useful in shotgun metabolomics as they allow rapid tandem MS spectra acquisition, high mass resolution (up to 240,000) and optional MS^n fragmentation (Ghaste et al., 2016; Herzog et al., 2011; Schuhmann et al., 2012, 2011). Also, these mass spectrometers are capable of rapid polarity switching with high mass accuracy, which simplifies and accelerates the analysis and

improves the metabolome coverage (Ghaste et al., 2016; Glauser et al., 2013; Park et al., 2021; Schuhmann et al., 2012).

Compared to TOF and Orbitrap, FT-ICR-MS had a slower start in metabolomics. Fourier transform ion cyclotron resonance mass spectrometer is an equipment with one of the highest resolution power and sensitivity. Its technical development began in the late 1920s, when Ernest O. Lawrence invented the cyclotron, which uses electrical and magnetic fields to accelerate protons to high velocities in a spiral-shaped path before they collide with their target (Lawrence & Livingston, 1932; Comisarow & Marshall, 1996). A few years later, it was also demonstrated that in ion cyclotron resonance (ICR), the angular frequency of the circular motion of ions species is independent of the radius they are traveling on (Gross, 2017). This principle was used by John A. Hipple to construct the first ICR mass spectrometer (Smith, 1951; Sommer et al., 1951). However, the major breakthrough in this technique happened in 1974 when Fourier transformation was applied to ICR by Alan Marshall and Melvin Comisarow (Comisarow & Marshall, 1974a; 1974b).

Since then, the performance of FT-ICR-MS instruments has steadily improved to reach unprecedented levels of resolving power and mass accuracy (van Agthoven et al., 2011; Hendrickson et al., 2015; Smith et al., 2018; Kanawati & Schmitt-Kopplin, 2019).

In most mass spectrometers, the sample is introduced in the equipment as a solid, liquid or gas, depending on the type of ion source used. Then, the ion species of the sample enter the mass analyzer, are detected and a mass-to-charge ratio (*m/z*) for each ion specie is obtained. In the case of FT-ICR-MS analyzers, ion species are usually generated externally in a separate ion source and then injected into a container known as the "ICR cell" (Kanawati & Schmitt-Kopplin, 2019). This cell is a Penning ion trap in which ion species are confined by a strong magnetic field, typically generated using a superconducting magnet, and possess not only excitation but also detection plates (Junot et al., 2010; Hiraoka, 2013).

In the cell, the ion species must have a coherent ion motion (Junot et al., 2010). To achieve that, the ion cloud present in the cell is excited, though the excitation plates. Due to the magnetic field, the ion species are forced on circular orbits by action of the Lorentz force. Once excited, the ions coherently circulate inside the ICR cell, perpendicular to the magnetic field, with an orbital frequency (cyclotron frequency) depending on their respective *m/z* ratios: ion species of equal *m/z* coherently circulate inside the ICR cell. The trajectories of the ion species induce an image current in the detection plates of the cell, which is amplified and stored as a time domain signal, and is composed of a set of frequencies corresponding to the motion of each ion species of a given *m/z* ratio. These currents are then transformed into frequency domain using a Fourier transform, from which the corresponding *m/z* values are calculated and mass spectra are reconstituted (Barrow et al., 2005; Junot et al., 2010; Hiraoka

2013; Gross, 2017). The Fourier transform is a mathematical operation that transforms one complex-valued function of a real variable into another. In the ICR, the domain of the ions original function is time and after Fourier transformation is the frequency domain (Gross, 2017). Also, to allow a higher resolving power for small molecules a particular ion trap with dynamic harmonization was developed for FT-ICR mass spectrometers (Kostyukevich et al., 2012).

Nowadays, FT-ICR-MS has become one of the best-performing mass analyzers in terms of resolving power (10^5 to $>10^6$), mass accuracy (typically 0.1–2 ppm) and sensitivity (Barrow et al., 2005; Hiraoka, 2013; Gross, 2017). The resolving power and sensitivity of FT-ICR-MS is such that it is possible to detect the naturally abundant elemental isotopes (e.g., ^{13}C, ^{41}K, ^{15}N, ^{18}O, ^{34}S, and ^{37}Cl) and have the isotopic distribution for certain signals. This allows the calculation of highly accurate elemental compositions for the unknown signals, facilitating the selection of potential metabolite candidates prior to their confirmation by comparisons to analytical standards (Allwood et al., 2011). Such characteristics allow unequivocal mass assignment and the resolution of ion species which currently are not distinguishable with other types of mass spectrometers. As an example, this analytical technique has been used for the study of complex organic matter samples, such as crude oils, and is capable of evaluating around 50,000 molecular formulas in each analysis (Folli et al., 2020; Hughey et al., 2002; Smith et al., 2018). Another advantage is the wide range of ionization source types that can be applied to FT-ICR-MS: electrospray ionization (ESI); atmospheric pressure chemical ionization (APCI); atmospheric pressure photoionization (APPI); matrix assisted laser desorption ionization (MALDI); electron impact and chemical ionization (EI and CI respectively), allowing a broader application to different kinds of samples (Allwood et al., 2011). Furthermore, it is possible to select the mode of introducing the sample in the FT-ICR-MS.

Although, most of the FT-ICR-MS based untargeted metabolomics studies use the direct infusion of the sample extracts, FT-ICR-MS has the capability to be coupled to several chromatographic techniques for compound identification and quantification (Schrader & Klein, 2004; Barrow et al., 2005).

Direct infusion mass spectrometry (DIMS) is an attractive approach with several advantages. Data acquisition only takes a few minutes with high throughput experiments and data processing is simpler than LC or GC-MS based approaches (Junot et al., 2014). Still, this imposes several disadvantages as well. Some studies reported that DIMS based approaches are prone to severe matrix effects and the biological material concentration that is introduced into the MS, needs to be optimized, to have high sensitivity and a correct metabolite detection (Madalinski et al., 2008). If not, tandem MS experiments may be affected due to incorrect selection of the precursor ions. Also, using this approach, ion species of biological relevance

could be masked by isomers or isobaric compounds, outlining another drawback (Junot et al., 2014). In addition, one should not disregard the space constraints of the ions directly infused in the FT-ICR cell. This space is limited and therefore the capacity for ion trapping is also limited. As a consequence, the direct infusion of complex samples in FT-ICR, such as plant extracts, may generate ion suppression, lower mass accuracy and decrease in measured frequencies of the trapped ions (Leach et al. 2012; Hohenester et al. 2020).

Some authors suggest that DIMS could be used as a first screening filter used prior to chromatographic and spectral methods (Beckmann et al., 2008). In the case of chromatographic separation, it is important to have in mind that the achievable mass resolving power with FT-ICR-MS is proportional to ICR signal transient length (Park et al., 2021). In other words, longer transient lengths can yield higher resolving power. This becomes a limitation of FT-ICR-MS coupled to chromatographic separation techniques (Park et al., 2021). Nevertheless, this limitation is being addressed by increasing the strength of the magnetic field (Blair et al., 2017; He et al., 2019; Smith et al., 2018; Walker et al., 2017), using multiple parallel mass analyzers (Park et al., 2016; S.-G. Park et al., 2017) and/or several frequency detectors (Cho et al., 2017; Nagornov et al., 2014; Park et al., 2020; Shaw et al., 2018). For instance, FT-ICR-MS coupled with Ultra Performance Liquid Chromatography (UPLC) was used together with stable isotope (^{13}C) allowing background contamination removal with a true positive identification of compounds with biological origin; also it empowered structural isomers discrimination (Giavalisco et al., 2009). The choice between DIMS or LC-MS should take in consideration the high throughput capability and the optimal metabolome coverage.

The application of FT-ICR-MS to plant metabolomics started around the early 2000's and roughly 90 studies have been published until now, the majority being published in the last 10 years. To uncover new metabolites and metabolic pathways, FT-ICR-MS plant metabolomics studies have been focused mainly on untargeted metabolomics approaches (**Table 1.1**). A crude plant extract is analyzed and through the different signal patterns of metabolites it is possible to correlate this information with metabolic pathways and other OMICs approaches, allowing for better understanding of plant regulatory systems. Targeted approaches have also been used in plant metabolomics studies using FT-ICR-MS (**Table 1.2**) allowing the detection of metabolites belonging to a specific class, metabolic pathway or already known compounds, ranging from medicinal to agrochemicals, increasing plants market value and industrial uses. The application of FT-ICR-MS to plant metabolism goes beyond full plant extracts, and some studies have been published on the investigation of intact plant cells and cell compartments (**Table 1.3** and **Table 1.4**). Different plant samples' extraction protocols compatible with FT-ICR-MS have been developed and guidelines for FT-

ICR-MS application in plant science have been published (Allwood et al., 2011; Barrow et al., 2005; Junot et al., 2010), (**Figure 1.2**).
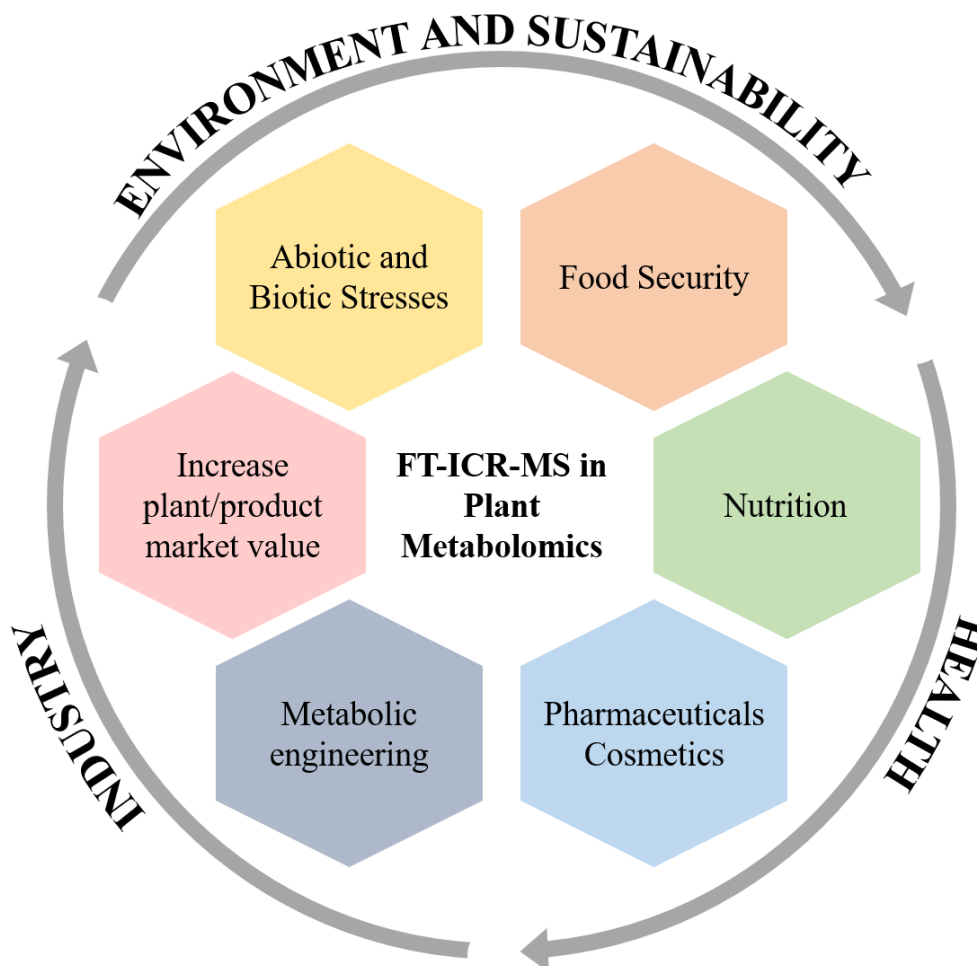
Figure 1.2 - The role of FT-ICR-MS applied to plant metabolomics in different fields.

1.4 UNCOVERING THE PLANT METABOLOME THROUGH UNTARGETED FT-ICR-MS

Untargeted metabolomics approaches aim for comprehensive analysis of all the measurable analytes in a sample, being the biological significance of each metabolite determined during data analysis and metabolite identification (Roberts et al., 2012). Therefore, the chemical identity of each metabolite in the study is not known a priori. The main aim is to maximize the number of metabolites detected and therefore provide the opportunity to observe unexpected changes. The selection of the right powerful analytical technique, capable of detecting and discriminate hundreds to thousands of metabolites in a

complex sample, such as FT-ICR-MS is a step in the right direction to increasing the metabolome coverage (**Table 1.1**).

Table 1.1 - Untargeted FT-ICR-MS plant metabolomics studies (alphabetical order by plant species name). Tesla (T); Direct-infusion mass spectrometry (DIMS); Electrospray ionization (ESI); Atmospheric pressure chemical ionization (APCI); Linear Trap Quadrupole (LTQ); Ultra Performance Liquid Chromatography (UPLC); High-performance liquid chromatography (HPLC); liquid chromatography (LC); Collision-induced dissociation (CID).

Plant (species)		Experimental conditions	Reference
Allium sativum (Garlic) species	DIMS	4.7 T FT-ICR-MS (ESI source; CID)	(Maccelli et al., 2020a)
Ananas comosus var. *comosus* (Pineapple)	DIMS	9.4 T FT-ICR-MS (ESI source; CID)	(Ogawa et al., 2018)
Arabidopsis thaliana	DIMS	7 T FT-ICR-MS (ESI and APCI sources)	(Hirai et al., 2004)
	DIMS	FT-ICR-MS (ESI and APCI sources)	(Tohge et al., 2005a)
	DIMS	7 T FT-ICR-MS (ESI source; SORI-CID)	(Oikawa et al., 2006)
	DIMS	7 T FT-ICR-MS (ESI source; SORI-CID)	(Ohta et al., 2007)
	DIMS	LTQ-FT-ICR-MS	(Giavalisco et al., 2008)
	UPLC	LTQ-FT-ICR-MS	(Giavalisco et al., 2009)
	DIMS	7 T FT-ICR-MS (ESI source)	(Satou et al., 2014)
	DIMS	7 T FT-ICR-MS (ESI source)	(Hansen et al., 2019)
Bellis perennis	UPLC	LTQ-FT-ICR-MS	(Scherling et al., 2010)
Celtis iguanaea	DIMS	9.4 T FT-ICR-MS (ESI source)	(Martins et al., 2014)
Chrysanthellum americanum	DIMS	12 T FT-ICR-MS (ESI source)	(Cao-Ngoc et al., 2020)
Crataegus (Hawthorn)	DIMS	12 T FT-ICR-MS (ESI source)	(Cao-Ngoc et al., 2020)
Dimocarpus longan (Longan)	DIMS	9.4 T FT-ICR-MS (ESI source)	(Chen et al., 2014)
Eugenia calycina (Red pitanga)	DIMS	9.4 T FT-ICR-MS (ESI source)	(Ferreira et al., 2014)
Fragaria x *ananassa*, cv. *Elsanta* (Strawberry fruit)	DIMS	7 T FT-ICR-MS (ESI and APCI sources)	(Aharoni et al., 2002)
Knautia arvensis	UPLC	LTQ-FT-ICR-MS	(Scherling et al., 2010)
Leontodon autumnalis	UPLC	LTQ-FT-ICR-MS	(Scherling et al., 2010)
Lotus corniculatus	UPLC	LTQ-FT-ICR-MS	(Scherling et al., 2010)
Mangifera indica (Mango)	DIMS	9.4 T FT-ICR-MS (ESI source; CID)	(Oliveira et al., 2016)
Medicago truncatula	LC	FT-ICR MS (ESI source)	(Pollier et al., 2013)
Medicago x *varia*	UPLC	LTQ-FT-ICR-MS	(Scherling et al., 2010)
Nicotiana tabacum (Tobacco)	DIMS	7 T FT-ICR-MS (ESI and APCI sources)	(Aharoni et al., 2002)

	DIMS	7 T FT-ICR-MS (ESI and APCI sources)	(Mungur et al., 2005)
Ophiorrhiza pumila (Rubiaceae species)	DIMS	FT-ICR-MS (ESI and APCI sources)	(Yamazaki et al., 2013)
Panax ginseng (Korean ginseng)	DIMS	15 T FT-ICR-MS (ESI source);	(Park et al., 2013)
	HPLC	15 T FT-ICR-MS (ESI source; CID)	
Populus x *canescens* (Poplar)	DIMS	12 T FT-ICR-MS (ESI source)	(Behnke et al., 2010)
		12 T FT-ICR-MS (ESI source)	(Way et al., 2013)
	DIMS	12 T FT-ICR-MS (ESI source)	(Janz et al., 2010)
Populus euphratica (Poplar species)	DIMS	12 T FT-ICR-MS (ESI source)	(Janz et al., 2010)
Populus × canescens syn. *P. alba × P. tremula* (Poplar species)	DIMS	12 T FT-ICR-MS (ESI source)	(Kaling et al., 2015)
Ribes nigrum (blackcurrant)	DIMS	12 T FT-ICR-MS (ESI source)	(Cao-Ngoc et al., 2020)
Solanum lycopersicum cultivars (Tomato)	DIMS	4.7 T FT-ICR-MS (ESI source; CID); 7 T FT-ICR-MS (ESI source)	(Ingallina et al., 2020)
Solanum tuberosum, var. Kennebek (Potato)	DIMS	7 T FT-ICR-MS (ESI source)	(Aliferis and Jabaji, 2012)
Thymus vulgaris (Thyme)	DIMS	7 T FT-ICR-MS (ESI source)	(Shahbazy et al., 2020)
Vitis vinifera (Grapevine)	DIMS	9.4 T FT-ICR-MS (ESI source; SORI-CID)	(Becker et al., 2013)
	DIMS	7 T FT-ICR-MS (ESI source)	(Maia et al., 2016)
	DIMS	12 T FT-ICR-MS (ESI source)	(Adrian et al., 2017)
	DIMS	7 T FT-ICR-MS (ESI source)	(Maia et al., 2018)
	DIMS	7 T FT-ICR-MS (ESI source)	(Marisa Maia et al., 2019a)
	DIMS	7 T FT-ICR-MS (ESI source)	(Marisa Maia et al., 2019b)
	DIMS	7 T FT-ICR-MS (ESI source)	(Nascimento et al., 2019)
Vitis vinifera (Grapevine) and *Vitis* species	DIMS	7 T FT-ICR-MS (ESI source)	(Maia et al., 2020)
	DIMS	7 T FT-ICR-MS (ESI source)	(Maia et al., 2021a)
Zea mays (Maize varieties: Aristis, Tietar and PR33P66)	DIMS	12 T FT-ICR-MS (ESI source)	(Leon et al., 2009)

The beginning of untargeted plant metabolomics studies by FT-ICR-MS dates back to 2002 with Aharoni and co-workers applying a high-throughput FT-ICR-MS-based method to detect metabolic modulation in strawberry fruit development and tobacco flowers overexpressing a strawberry MYB transcription factor (Aharoni et al., 2002). Methanol and acetonitrile extracts were used and over 1000 *m/z* values were detected in those extracts, using a direct infusion of the sample in the FT-ICR-MS. Results have shown not only changes in the levels of a large range of *m/z* values corresponding to known fruit metabolites, but also revealed novel information on the metabolic transition from immature to ripe fruit. Also,

specific *m/z* values discriminated between transgenic and control plants, among which the cyanidin-3-rhamnoglucoside seemed to have a particular role (Aharoni et al., 2002).

Aharoni and co-workers' pioneer work demonstrated the feasibility and utility of FT-ICR-MS approaches for an untargeted and rapid metabolic plant "fingerprinting", starting a new era for plant metabolomics.

Since then, several FT-ICR-MS based plant studies have emerged in which different plants, plant tissues and plant cell compartments were analyzed, metabolite extractions were optimized, and even FT-ICR-MS metabolomics were combined with other OMICs approaches to better reveal gene-to-metabolite networks (**Table 1.1**).

One of the main plants analyzed using FT-ICR-MS, with an untargeted approach, has been *Arabidopsis thaliana* (Giavalisco et al., 2009, 2008; Hansen et al., 2019; Hirai et al., 2004; Ohta et al., 2007; Oikawa et al., 2006; Tohge et al., 2005). This model plant organism was one of the first to have its genome sequenced (Arabidopsis Genome Initiative, 2000) and is now one of the best model plants to study gene-to-metabolite correlation through the integrated analysis of gene expression (transcriptomics) and metabolite accumulation (metabolomics), (Fiehn, 2002; Sumner et al., 2003; Bino et al., 2004; Kopka et al., 2004; Scherling et al., 2010).

Hirai and co-workers were the first to study the *Arabidopsis thaliana* metabolome using FT-ICR-MS (Hirai et al., 2004). In their work, transcriptomics was combined with FT-ICR-MS metabolomics to investigate the gene-to-metabolite networks controlling nitrogen and sulfur, and secondary metabolism. They explored the plant whole-cellular processes under sulfur and nitrogen deficiency and understood that plants adapted to nutrient deficiency had a steady-state transcriptome and metabolome. The study opened new insights for a more precise investigation of gene-to-metabolite networks, aiming for functional genomics and better biotechnological application (Hirai et al., 2004). FT-ICR-MS was also applied to study *A. thaliana* metabolites and metabolic pathways after exposure to different concentrations of glyphosate (Ohta et al., 2007) and herbicidal chemical classes (Oikawa et al., 2006), as well as to study the light/dark regulation (Nakamura et al., 2007) and clarify the cytochrome P450 functions (Kai et al., 2009) in cell cultures.

Also, metabolomics studies in transgenic *A. thaliana* plants over-expressing or with loss of function of genes, helped to elucidate and correlate the impact of select genes with the overall metabolism. The combination of FT-ICR-MS metabolomics analysis with other OMICs was also used in *Arabidopsis thaliana* mutants, to identify key metabolites involved in signaling pathways and to understand their biological roles (Hansen et al., 2019; Tohge et al., 2005). A recent study in *A. thaliana* wild-type and loss-of-function mutant of FER (*feronia*) identified a total of 68 and 52 compounds in positive and negative mode, respectively, with

significant differences between wild-type and mutant plants. Arabidopsides (oxylipins) were found to be significantly enriched in the mutant (Hansen et al., 2019).

FT-ICR-MS has also been applied to study the metabolism of other model plants, such as *Nicotiana tabacum* and *Medicago truncatula*, and of different economically important crops and fruits, to gain deeper insights into the physiological responses of plant species (**Table 1.1**).

The biological activity of plant metabolic extracts towards several bacterial and fungal strains, their antioxidant effects and use in the treatment of specific medical conditions was also evaluated by FT-ICR-MS (Chen et al., 2014; Ferreira et al., 2014; Martins et al., 2014). FT-ICR-MS metabolomics studies were also applied to valorize several plants as a source of health and nutritional bioactive components (Maccelli et al., 2020; Marisa Maia et al., 2019a). As an example, the chemical diversity of eight different hydroalcoholic extracts of white and red crop *A. sativum* and wild *Allium triquetrum*, *A. roseum*, and *A. ampeloprasum*, all originating from the Mediterranean Basin, were evaluated by FT-ICR-MS and 850 and 450 *m/z* values were detected, respectively, by ESI$^+$ and ESI$^-$. The annotation of all these *m/z* values covered all of the main classes of primary and secondary metabolites, including amino acids, alkaloids, organic and fatty acids, nucleotides, vitamins, organosulfur compounds, and flavonoids (Maccelli et al., 2020). In grapevine, FT-ICR-MS allowed the characterization of the leaves of *Vitis vinifera* cv. Pinot noir and their valorization as a source of diverse biologically active phytochemical compounds (Marisa Maia et al., 2019a)

One of the major applications of metabolomics studies is the study of plant metabolite responses to different stimuli *in vitro* that mimics the overall stresses that plants are exposed to every day in the field. Exposure to these environmental stresses reduces and limits the productivity of any plant. Abiotic constraints include radiation, salinity, flood, drought, extremes in temperature, heavy metals, among others. Biotic stressors account for attacks by various pathogens such as fungi, bacteria, oomycetes, nematodes and herbivores. Plants have developed various mechanisms to overcome these stresses. Signaling metabolic pathways play an important role and act as a connecting link between sensing the stress and generating an appropriate biochemical and physiological response (Gull et al., 2019). Several reviews have been published regarding plant metabolism in response to biotic and abiotic stresses (Arbona and Gómez-Cadenas, 2016; Genga et al., 2011; Jorge et al., 2015; Piasecka et al., 2019) and considering the application of FT-ICR-MS, several works have also been published (Adrian et al., 2017; Kaling et al., 2015; Maia et al., 2020; Nascimento et al., 2019; Shahbazy et al., 2020), (**Table 1.1**).

Shahbazya and co-workers studied the distinctive metabolites and metabolic pathways of thyme (*Thymus vulgaris*) plants, responding to drought stress, and highlighted a

possible correlation for the accumulation of carbohydrates and amino acids with osmotic protection as an adaptive stress response mechanism. In this work, it was demonstrated that galactose metabolism is the most significant in thyme (Shahbazy et al., 2020). Janz and co-workers studied the metabolomics changes of two poplar species [*Populus euphratica* (tolerant) and *Populus × canescens* (sensitive)] in response to salinity stress (Janz et al., 2010) and, in the same plant, Kaling and co-workers elucidated the influence of UV-B radiation on overall metabolite patterns in transgenic poplar plants (Kaling et al., 2015). In both studies, hundreds of *m/z* values were found to be discriminant and revealed an up or down-regulation of various metabolic pathways, depending on the experimental conditions, such as, flavonoids, anthocyanins, osmotic adjustment, reactive oxygen species and others.

The study of the effects of *Rhizoctonia solani*, the causal agent of Rhizoctonia disease, was studied by FT-ICR-MS on the global metabolic network of potato sprouts (*Solanum tuberosum*, var. Kennebek) by Aliferis and Jabaji (Aliferis and Jabaji, 2012). An up-regulation of mevalonic acid and deoxy-xylulose pathways leading to the biosynthesis of sesquiterpene alkaloids was reported. Fluctuations on the content of amino, carboxylic and fatty acids in infected potato sprouts were also detected (Aliferis and Jabaji, 2012).

Grapevine metabolomics has also been widely explored by FT-ICR-MS. The first study was performed on a grapevine population, obtained by different crosses, to investigate the metabolism of infected and non-infected leaves with *Plasmopara viticola*, the causal agent of downy mildew disease (Becker et al., 2013). The comparison of MS profiles obtained from control and infected leaves of different levels of resistant grapevines highlighted several classes of metabolites involved in the discrimination between infected and non-infected leaves. Moreover, the high mass accuracy provided by FT-ICR-MS, allowed a precise analysis and critical discrimination between all signals which led to the identification of 19 possible markers between inoculated and healthy samples. Several studies have followed, the chemical diversity of different *Vitis* species, including grapevine (*Vitis vinifera*) was explored, and the metabolites present in grapevine with and without pathogen interaction were identified (Adrian et al., 2017; Maia et al., 2021, 2020; Marisa Maia et al., 2019b; M. Maia et al., 2019; Nascimento et al., 2019).

Plant development associated metabolism is another focus of untargeted FT-ICR-MS studies (Aharoni et al., 2002; Ogawa et al., 2018; Oliveira et al., 2016). Pineapple (*Ananas comosus* var. *comosus*) and mango (*Mangifera indica*) are some of the most cultivated plants in tropical areas and highly exported to other countries. The maturation of these fruits indicates the best stage for harvesting and determines the correct time for fruit consumption. In both works, the metabolism of different maturation stages of these plants was studied, and the results pointed to primary (mainly sugars) and secondary (mainly phenolic compounds) metabolites as the most abundant in the third stage of maturation (Ogawa et al., 2018;

Oliveira et al., 2016). More recently, Ingallina and co-workers thoroughly analyzed and compared the metabolic profile of two tomato cultivars (Torpedino di Fondi and San Marzano) in different ripening stages by FT-ICR-MS untargeted analysis combined with NMR spectroscopy (Ingallina et al., 2020). The different tomato extracts were analyzed in both positive and negative ionization modes, detecting up to 1646 different molecular formulas in only one extract. Some metabolites were shared by all extracts and others were found to possibly be considered marker compounds, being detected only in one extract (Ingallina et al., 2020). In grapevine leaves direct infusion FT-ICR metabolomics was done with the focus to improve metabolome coverage, through the use of different solvents in sequential elutions from the solid phase extraction, allowed the extraction of polar and non-polar compounds, covering all major metabolic classes in plants (Maia et al., 2016).

To cope with the increase in metabolomics biological studies, there is an ever-growing need for faster and more comprehensive analysis methods. As metabolites vary widely in both concentration and chemical behavior, there is still no single analytical procedure allowing the unbiased and comprehensive structural elucidation and determination of all metabolites present in a given biological system (Kueger et al., 2012). But the ever-increasing resolving power and the improved mass accuracy by commercially available FT-ICR-MS, significantly boosts untargeted metabolomics studies. Moreover, the capability of having a higher metabolome coverage, using direct infusion, metabolites are analyzed in a high-throughput way, providing a rapid analysis of complex metabolite samples, eliminating the time-consuming separation approaches.

1.5   TARGETING METABOLIC PLANT COMPOUNDS BY FT-ICR-MS

Targeted metabolomics can be described as the measurement of defined groups of chemically characterized and biochemically annotated metabolites with established biological importance at the start of the study before data acquisition is performed. Targeted methods have a greater selectivity and sensitivity than untargeted methods, but targeted studies can only be performed if an authentic chemical standard of the metabolite is available or if the fragmentation pattern of the compound is known (Roberts et al., 2012).

Most FT-ICR-MS-targeted-based plant metabolomics studies are related to the detection of plant compounds or classes with nutritional, medicinal or pharmaceutical value, identification and characterization of plant compounds already known to have interesting health properties and for cultivation improvement and marketing (**Table 1.2**).

Table 1.2 - Targeted FT-ICR-MS plant metabolomics studies (alphabetical order by plant species name). Tesla (T); Direct-infusion mass spectrometry (DIMS); Electrospray ionization (ESI); Sustained off-resonance irradiation (SORI); Collision-induced dissociation (CID); Infrared multiple photon dissociation (IRMPD); Ultra Performance Liquid Chromatography (UPLC); High-performance liquid chromatography (HPLC); liquid chromatography (LC); Linear Trap Quadrupole (LTQ); ultraviolet detection (UV); matrix-assisted laser desorption/ionization (MALDI).

Plant (species)	Experimental conditions		Reference
Acanthopanax senticosus Harms	DIMS	7T FT-ICR-MS (ESI source; SORI-CID)	(Zhou et al., 2012)
Allium cepa (Onion)	LC	7 T FT-ICR-MS (ESI source)	(Nakabayashi et al., 2013)
	LC	7 T FT-ICR-MS (ESI source)	(Nakabayashi et al., 2016)
Allium fistulosum (Green onion)	LC	7 T FT-ICR-MS (ESI source)	(Nakabayashi et al., 2016)
Allium sativum (Garlic)	LC	7 T FT-ICR-MS (ESI source)	(Nakabayashi et al., 2016)
Arabidopsis thaliana plants	DIMS	9.4 T FT-ICR-MS (ESI source)	(Qin et al., 2011)
Artocarpus altilis		FT-ICR-MS (ESI source)	(Huong et al., 2012)
Asparagus officinalis cv. Purple Passion	DIMS	9.4 T FT-ICR-MS (ESI source)	(Sakaguchi et al., 2008)
Camellia sinensis (Black tea)	DIMS	9.4 T FT-ICR-MS (ESI source)	(Kuhnert et al., 2010)
Cerbera manghas	DIMS	FT-ICR-MS (ESI source)	(Zhang et al., 2010)
Fallopia convolvulus	DIMS	FT-ICR-MS (ESI source)	(Brennan et al., 2013)
Ginkgo biloba	DIMS	HPLC-LTQ-FT-ICR-MS (ESI source; CID)	(Beck and Stengel, 2016)
Ibervillea sonorae	DIMS	FT-ICR-MS	(Vidal-Gutiérrez et al., 2021)
Medicago truncatula	UPLC	FT-ICR-MS (ESI source; CID)	(Pollier et al., 2011)
Morus alba (Mulberries)	DIMS	15 T FT-ICR-MS (ESI source)	(Park et al., 2017)
	DIMS	7T FT-ICR-MS (ESI source; CID)	(Xiao et al., 2017)
Panax ginseng (Red ginseng)	DIMS	7T FT-ICR-MS (ESI source; CID)	(Du et al., 2012)
Piper methysticum (Kava)	DIMS	4.7 T FT-ICR-MS (ESI source; SORI-CID; IRMPD)	(Warburton and Bristow, 2006)
Polygonum multiflorum	HPLC	LTQ-(7 T)-FT-ICR-MS (ESI source; CID)	(Yang et al., 2019)
Salvia miltiorrhiza Bunge (Tanshen)	DIMS	7T FT-ICR-MS (ESI source; SORI-CID)	(Li et al., 2008)

Schisandra chinensis	DIMS	7T FT-ICR-MS (ESI source; CID)	(Huang et al., 2007)
	DIMS	7T FT-ICR-MS (ESI source; CID)	(Huang et al., 2008)
Schisandra sphenanthera (Fruits)	DIMS	7T FT-ICR-MS (ESI source; CID)	(Huang et al., 2008)
Solanum lycopersicum cultivars (Tomato)	HPLC	LTQ-FT-ICR-MS (ESI source; CID)	(Iijima et al., 2013)
Sorghum bicolor and *Neptunia lutea*	DIMS	15 T FT-ICR-MS (ESI source); 15 T FT-ICR-MS (MALDI source)	(Reeves et al., 2020)
Stemona tuberosa		7T FT-ICR-MS	(Khamko et al., 2013)
Vaccinium myrtillus (Bilberries)	DIMS	7T FT-ICR-MS (ESI source; CID)	(Xiao et al., 2017)
Vaccinium oxycoccos (Cranberries)	DIMS	7T FT-ICR-MS (ESI source; CID)	(Xiao et al., 2017)
Vaccinium uliginosum (Blueberries)	DIMS	7T FT-ICR-MS (ESI source; CID)	(Xiao et al., 2017)

The significance of plants, in particular medicinal plants, in human health cannot be overlooked. Plants have been used since ancient times as resources of molecules with medicinal properties, due to the presence of naturally occurring compounds, and today many of the modern pharmaceuticals are still produced indirectly from plant extracts or from specific plant compounds. Hence, there is an urge to further investigate the "black box" of plant metabolites with medicinal potential to uncover which compounds possess the desired properties and biological activities for human body.

The FT-ICR-MS was first used to specifically characterize plant compounds with health beneficial properties by Warburton and Bristow (Warburton and Bristow, 2006). Six kavalactones present in kava (*Piper methysticum*) roots were investigated by FT-ICR-MS (Warburton and Bristow, 2006). This plant is known for its relaxing and calming properties and its extracts have been used in herbal medicine over the last 2000 years, with preparations of kava being commercialized as capsules and fluid extracts. However, some reports of liver toxicity have questioned the safety of kava-containing products and extracts. The utilization of FT-ICR-MS in kava root extracts allowed the determination of their elemental formula and structural confirmation, leading to the identification of kavalactones with high certainty.

Further studies with FT-ICR-MS have followed with the aim of, not only characterizing plant bioactive compounds, but also to improve the detection methods of these compounds (**Table 1.2**). Xin Huang and co-workers developed a method for *Schisandra chinensis*, whose ripe fruits are a famous tonic in traditional Chinese medicine, to detect and

analyze its lignan constituents, the major bioactive compounds present in this plant with anti-hepatotoxic, anti-asthmatic and central nervous system protecting properties (Huang et al., 2008, 2007). Some plant compounds with decreased incidence or treatment of some diseases have also been investigated by FT-ICR-MS. *Acanthopanax senticosus* leaves were screened to identify α-glucosidase inhibitors which have potential anti-diabetic applications (Zhou et al., 2012), and *Fallopia convolvulus* was analyzed to identify compounds responsible for estrogenic activity (Brennan et al., 2013). Two compounds, emodin and rhodoeosein, were identified as being responsible for estrogenic activity (Brennan et al., 2013).

More recently, Vidal-Gutiérrez and co-workers identified and quantified by FT-ICR-MS cucurbitacins, the main group of compounds found in *Ibervillea sonorae*, which have demonstrated apoptotic and anti-tumoral activities in cervical cancer cells. One new cucurbitacin was also identified in this work (Vidal-Gutiérrez et al., 2021).

Other similar studies applied FT-ICR-MS for the detection of phenolic compounds, oligosaccharides, anthocyanidins and others (Huong et al., 2012; Iijima et al., 2013; Khamko et al., 2013; Kuhnert, 2010; Li et al., 2008; Y. J. Park et al., 2017; Pollier et al., 2011; Reeves et al., 2020; Sakaguchi et al., 2008; Xiao et al., 2017; Yang et al., 2019; Zhang et al., 2010), (**Table 1.2**).

Besides therapeutically active substances, plants also play a great role in supplying food for personal care of mankind. Hence, a detailed knowledge of their metabolites is crucial to understanding the relation between food composition and health properties to attract more customers which will increase plants market value. Also, marketable plants are subject to phytosanitary treatments, thus the study of the presence of these compounds in plants ready to consume is a must for food safety controls. Several studies focused on the evaluation of plants and crops for human consumption to enhance their value and/or attract more consumers (Kuhnert, 2010; Y. J. Park et al., 2017; Pollier et al., 2011; Reeves et al., 2020; Sakaguchi et al., 2008; Xiao et al., 2017). As an example, Ting Xiao and co-workers evaluated the polyphenolic profiles of different berries (blueberry, bilberry, mulberry and cranberry) by FT-ICR-MS (Xiao et al., 2017). The study revealed thirty-nine polyphenols including: 26 anthocyanins, 9 flavonoids and 4 phenolic acids were identified accurately. Their results provided not only a basis for further research on berries but also for the selection of certain berries as potential sources of anthocyanins.

1.6 DISCOVERING VALUE-ADDED PLANT PRODUCTS THROUGH FT-ICR-MS

Plants produce a diverse repertoire of complex small-molecule compounds which can be used in pharmaceutical and industrial products (Fischer et al., 2015). But to move from proof-of-concept experiments to commercial production, it is important to shift the focus from the untargeted and target identification of molecules, and start building-up reliable plant products reference databases, useful to guarantee food authenticity and freshness, and to support consumers, further nutraceutical evaluations and industries. This will ensure quality, purity and yield aspects that determine commercial feasibility. Some plant products with important industrial value are, for example, wood and cork, fibers, fatty oils, vegetable fats and essential oils, sugars and starches, papers, resins, among others.

Recently, interesting studies have been published in the metabolic profiling of plant products using FT-ICR-MS (**Table 1.3**).

Table 1.3 - FT-ICR-MS plant products metabolomics studies (alphabetical order by plant species name). Tesla (T); Direct-infusion mass spectrometry (DIMS); Electrospray ionization (ESI); Atmospheric pressure chemical ionization (APCI); Linear Trap Quadrupole (LTQ); Collision-induced dissociation (CID).

Plant (species)	Product	Experimental conditions		Reference
Acer (Maple) and *Quercus alba* (White oak)	Veneers	DIMS	12 T FT-ICR-MS (ESI source)	(He et al., 2019)
Coffea arabica (Arabica) and *Coffea canephora* var. *robusta* (Robusta)	Coffee	DIMS	LTQ-(7.2 T)FT-ICR-MS (ESI source)	(Garrett et al., 2012)
Cocos nucifera (Coconut)	Water	DIMS	9.4 T FT-ICR-MS (ESI source)	(Costa et al., 2015)
Medicago sativa (Alfalfa), *Phaseolus vulgaris* (Bean), *Hordeum vulgare* (Barley), *Zea mays* (Maize), *Triticum aestivum* (Wheat), *Lolium perenne* (Ryegrass) and *Cucurbita maxima* (Pumpkin)	Root exudates	DIMS	15 T FT-ICR-MS (ESI source)	(Miao et al., 2020)
Quercus (Oak barrel), grain varieties and *Saccharum officinarum* (Sugarcane)	Whisky, Rum and wood barrel samples	DIMS	12 T FT-ICR-MS (ESI source)	(Roullier-Gall et al., 2018)

			4.7 T FT-ICR-MS (ESI	
Satureja montana	Essential oil	DIMS	and APCI sources;	(Vitanza et al., 2019)
			CID)	
Triticum aestivum (Hard white wheat)	Bran samples	DIMS	FT-ICR-MS (ESI and APCI sources)	(Matus-Cádiz et al., 2008)
Vitis species	Red and white wines	DIMS	12 T FT-ICR-MS (ESI source)	(Gougeon et al., 2009)
	Red and white wines	DIMS	12 T FT-ICR-MS (ESI source)	(Roullier-Gall et al., 2014)
	White wines	DIMS	FT-ICR-MS	(Romanet et al., 2021a)

From the different studies published, it can be highlighted the utilization of FT-ICR-MS, to detect and quantify Arabica *(Coffea arabica)* coffee adulterations by Robusta *(Coffea canephora* var. *robusta)* coffee (Garrett et al., 2012). The admixture of Robusta coffee is illegal into high-quality Arabica coffee; thus, it is crucial for the coffee industry to investigate the coffee's quality in a fast and precise manner. Rafael Garrett and co-workers developed a method to quantify blends of Robusta and Arabica coffee as well as to investigate the identity of the major compounds responsible for the distinction between the coffee varieties using FT-ICR-MS together with other mass spectrometry techniques (Garrett et al., 2012).

As already mentioned, FT-ICR-MS was also used to characterize the metabolome of *V. vinifera* cv. Pinot noir's leaves to assess their potential as a source of bioactive nutraceutical compounds (Marisa Maia et al., 2019a).

The chemical composition of wine has mostly been studied using targeted analyses of selected metabolites (Bi et al., 2018; Flamini and De Rosso, 2006; Pinu, 2018). However, the chemical diversity of wine composition can be unraveled through an untargeted approach if using an ultra-high-resolution mass spectrometry, like FT-ICR-MS, providing an instantaneous image of complex interacting processes. The analysis of barrel-aged wines by an untargeted metabolomics approach by FT-ICR-MS, revealed that 10-year-old wines still show a geographic metabolic signature of the forest location where oaks of the barrel in which they were aged have grew (Gougeon et al., 2009). Most recently, Romanet and co-workers applied FT-ICR-MS to explore the chemical diversity associated with the antioxidant capacity of white wines (Romanet et al., 2021). More than 350 molecular markers were found to be correlated with wines with higher antioxidant capacity (Romanet et al., 2021). Bottled white and red wines from different appellations in Burgundy were also analyzed by FT-ICR-MS to characterize wine complexity and identify markers that can separate wines (Roullier-Gall et al., 2014). Roullier-Gall and co-workers also analyzed 150 whisky samples from 49 different distilleries in 7 countries, ranging from 1-day new made spirit to 43 years of maturation with different types of barrel (Roullier-Gall et al., 2018). FT-ICR-MS analysis revealed some

interesting results: the impact of the wood history on the distillate's composition during barrel aging. Whiskies could be differentiated according to the history of the barrel used for the maturation, regardless of the cereal source. Also, the comparison of barrel aged rums and whiskies revealed specific metabolic signatures (Roullier-Gall et al., 2018).

Coconut water was also analyzed by FT-ICR-MS to verify its quality after storage and characterize the chemical compounds produced during natural ageing (Costa et al., 2015).

The study of anti-microbial activities of marketable products are also extremely important for food security. Vitanza and co-workers characterized the metabolite profile of commercial essential oil of *Satureja montana* to evaluate its antimicrobial properties, both alone and combined with gentamicin towards gram-negative and gram-positive bacterial strains, through the combination of FT-ICR-MS and antibacterial activity experiments (Vitanza et al., 2019).

1.7 A DEEPER ANALYSIS OF PLANT CELLS AND CELL COMPARTMENTS' METABOLITES BY FT-ICR-MS

Plants sense all the external stresses present in the environment, get stimulated and then generate appropriate cellular responses. The stimuli received from the sensors located on the cell surface or cytoplasm are transferred to the transcriptional machinery situated in the nucleus, with the help of various signal transduction pathways (Gull et al., 2019). This leads to major differential metabolic changes making the plant tolerant/prepared against the stress. Hence, studying plant cells and different cellular compartments allows a broader understanding of cell dynamics (**Table 1.4**).

Table 1.4 - FT-ICR-MS plant cells and cell compartments metabolomics studies. Tesla (T); Direct-infusion mass spectrometry (DIMS); Electrospray ionization (ESI); Sustained off-resonance irradiation (SORI); Collision-induced dissociation (CID).

Plant (species)	Cell / Cell compartment	Experimental conditions		Reference
Arabidopsis thaliana	Cells	DIMS	7T FT-ICR-MS (ESI source)	(Kai et al., 2009)
	Cells	DIMS	7T FT-ICR-MS (ESI source; SORI-CID)	(Nakamura et al., 2007)
	Intact vacuoles	DIMS	12 T FT-ICR-MS (ESI source)	(Ohnishi et al., 2018)
Vitis vinifera (Grapevine)	Apoplast	DIMS	7 T FT-ICR-MS (ESI source)	(Figueiredo et al., 2021)

FT-ICR-MS was applied to profile the metabolome of *A. thaliana* cell cultures, overexpressing P450-genes to identify and characterize its pathway (Kai et al., 2009). Cytochromes P450 of higher plants play crucial roles in both primary and secondary metabolism processes, such as catalysis and synthesis of structurally diverse specialized metabolites important in essential ecological roles and constitute a valuable resource for the development of new drugs (Shang and Huang, 2019). An FT-ICR-MS based metabolomics scheme was successfully implemented to clarify the P450 functions and fatty acid hydroxylation activity of *A. thaliana CYP78A7* gene was reported (Kai et al., 2009). Also in *A. thaliana* cell cultures, metabolites behind light/dark regulation were investigated, leading to the identification of 40 and 8 ions, respectively in negative and positive ionization modes, to growth conditions (Nakamura et al., 2007). Moreover, it was suggested that accumulations of several phenylpropanoids, a disaccharide and a trisaccharide were prominent in the light condition (Nakamura et al., 2007).

Both these studies opened new insights, not only for the use of plant cell cultures to similar studies, but also to explore their compartments.

This approach was also applied to plant compartments such as the vacuoles and the extracellular space (i.e., apoplast). Non-target analysis with FT-ICR-MS of *A. thaliana* culture-suspension cells identified 1106 *m/z* signals only present in vacuoles (Ohnishi et al., 2018). The apoplastic fluid of grapevine leaves was also evaluated by FT-ICR-MS. A total of 1100 and 1657 putative metabolites were annotated for *V. vinifera* cv. Trincadeira and *V. vinifera* cv. Regent, being 514 common to both grapevine genotypes (Figueiredo et al., 2021).

Although there is still much to be discovered about metabolic functions and pathways in cells and cell compartments, these studies demonstrate the advantage of using an ultra-high-resolution and mass accuracy technique. The exact identification of metabolites and its correlation is a step forward in the comprehension of cellular mechanisms.

1.8 MALDI-FT-ICR-MS: SPATIAL DISTRIBUTION OF PLANT METABOLITES

Besides the identification of metabolites in the overall system or in specific plant compartments, it is also important to understand the spatial distribution of metabolites and their respective accumulation pattern. Mass spectrometry imaging (MSI) has proven to be a very powerful tool, with several advantages, being the most important the ability to simultaneously determine the exact location and distribution of specific or multiple metabolites in a single experiment in a complex biological material, typically plant tissue sections (Bjarnholt et al., 2014; Boughton et al., 2016).

There are several Laser Desorption Ionization (LDI) techniques available nowadays (Boughton et al., 2016), being the Matrix Assisted Laser Desorption Ionization (MALDI) mass spectrometry, by far the most commonly used form of LDI. In MALDI the analyte/tissue is co-crystallized with a chemical matrix, which absorbs the laser energy and releases the analytes into the gas-phase in a process leading to ionization (Bjarnholt et al., 2014; Boughton et al., 2016). The addition of the matrix has several advantages. Not only does it allow to specify the type of compounds to analyze but also, since the energy of the laser light is absorbed by the matrix and not directly by the analytes, MALDI is considered a soft ionization as well as ESI, enabling researchers to detect very small levels of detectable biological analytes, making it an excellent technique for metabolomics studies.

In a MSI experiment, pixels are established by virtually defining an array of discrete spots over the sample area. The laser is fired several times in each pixel before moving to the next spot. For each coordinate individual mass spectra are collected representing all the ionizable molecules on that spot. The combination of all spectra allows the reconstruction of an image with the intensity values of the ionized molecules, representing the spatial distribution of all molecules along the sample, which can be compared with an optical image of the sample (Barkauskas et al., 2009; Boughton et al., 2016). MALDI-MSI has been adopted for the direct visualization of plant tissues and the investigation of plant biology as well. The studies range from studying the mechanisms of plant responses to both abiotic and biotic stresses and symbiotic relationships, to fundamental ecophysiological important processes (reviewed by Qin et al., 2018). An important point to have in consideration when performing plant tissues analysis is sample preparation, which continues to be the major bottleneck of this technique. All the major concerns when performing MSI in plants have been reviewed in Bjarnholt et al., 2014; Bodzon-Kulakowska & Suder, 2016; Boughton et al., 2016; Grassl et al., 2011. A detailed characterization of complex plant tissues by MALDI-MSI requires an instrument that is capable of high mass resolving power, mass accuracy and dynamic range. FT-ICR-MS is the technique for such analysis as it offers the highest mass spectral performance for MALDI-MSI experiments (Bowman et al., 2020). Coupling of MALDI to FT-ICR for MSI analysis, has several limitations. Mass spectrometry imaging experiments of large samples, at very high spatial resolutions, need higher measurement times, which are limited by the length of FT-ICR acquisition times (Buck et al., 2016). As it was previously mentioned, this subject can be addressed by increasing the magnetic field strength. Also, the complexity of the biological sample, due to a vast array of concentrations from different biomolecules with different chemistries and molecular sizes present, may generate an ion suppression effect, making the MSI analysis less sensitive (Boughton et al., 2016). The addition of matrix to a sample generates high-abundance low-weight ion species which leads to significant interfering signals, being also a limitation. Therefore, upon MSI experiments with high-performance analyzers, such as FT-ICR, there is a significant balance between acquisition

speed, spatial resolution and sensitivity (Boughton et al., 2016; Buck et al., 2016). Although several plant metabolic studies appeared using MALDI-MSI (reviewed in Qin et al., 2018), few MSI studies combined MALDI and FT-ICR-MS (Alcantara et al., 2020; Gorzolka et al., 2014; Sarabia et al., 2018; Takahashi et al., 2015), (**Table 1.5**).

Table 1.5 - MALDI-FT-ICR-MS plant metabolomics studies (alphabetical order by plant species name). Tesla (T); matrix-assisted laser desorption/ionization (MALDI); laser desorption/ionization (LDI).

Plant (species)	Experimental conditions	Reference
Arabidopsis thaliana tissues (seedlings and roots)	9.4 T FT-ICR-MS (MALDI and LDI sources)	(Takahashi et al., 2015)
Cannabis leaves and *Jatropha curca*	9.4 T FT-ICR-MS (MALDI and LDI sources)	(dos Santos et al., 2019)
Erythroxylum coca leaves	FT-ICR-MS (MALDI source)	(Dos Santos et al., 2021)
Hordeum vulgare cv. *Optic* (Barley) seeds	FT-ICR-MS (MALDI source)	(Gorzolka et al., 2014)
Hordeum vulgare cv. Hindmarsh (Uniform barley)	7 T XR-FT-ICR-MS (MALDI source)	(Sarabia et al., 2018)
Manihot esculenta Crantz. (Cassava)	7 T FT-ICR-MS (MALDI source)	(Alcantara et al., 2020)

MALDI-FT-ICR-MSI was applied to barley seeds and roots to study the spatial distribution and profiles of metabolites, their characterization and quantify their change (Gorzolka et al., 2014). Barley is one of the model organisms to investigate the cereal germination process that involves complex interactions between different organs that lead to the growth of the plant.

MALDI-FT-ICR-MSI was applied to germinated barley seeds for the detailed localization of metabolites in longitudinal and transversal seed sections (Gorzolka et al., 2014). Several compounds responsible for the prevention of pathogen infestation in seeds, as well as distinct localization patterns within seed organs were identified (Gorzolka et al., 2014). Also, the high-mass resolution of MALDI-FT-ICR-MSI was also used in barley roots to reveal the detailed spatial distribution of metabolites, such as lipids, in response to an abiotic stress, salinity stress (Sarabia et al., 2018).

In another study, an improved method of MALDI-FT-ICR-MSI was developed to achieve a higher-resolution and higher mass accuracy and applied to analyze the distribution of small metabolites in *A. thaliana* roots (Takahashi et al., 2015). Most recently, Dos Santos and co-workers optimized and studied the spatial distribution of alkaloids in *Erythroxylum coca* leaves (Dos Santos et al., 2021). Three matrices were tested and 2,5-dihydroxybenzoic acid

(DHB) was selected as the best matrix. Different tissue thicknesses were also evaluated, to study the inner part of the leaf tissue, and alkaloids and flavonoid molecules were detected.

MALDI-FT-ICR-MSI can also be used for industrial purposes. Heavy metal soil contaminations are very problematic and cause severe negative impacts on human health. Development of cost-effective methods of heavy metals extraction, such as Hg and Au, may offer significant benefits through remediation of contaminated land and extraction of valuable resources. In a recent study, Hg and Au localization in cassava roots were explored for these heavy metals phytoextraction. The results of Alcantara and co-workers using MALDI-FT-ICR-MSI indicated that exposure to Hg and Au did not disturb the plant tissues, being the plants healthy and alive at the time of harvest (Alcantara et al., 2020).

All these studies open new insights for plant metabolomics studies. Also, it is anticipated that MALDI-FT-ICR-MSI approaches will bring a new level of understanding to metabolomics as scientists will be encouraged to consider spatial heterogeneity of metabolites in descriptions of metabolic pathway regulation.

1.9   TANDEM MS AND *IN SILICO* PREDICTION TOOLS IN PLANT METABOLOMICS

In mass spectrometry experiments, the selection and isolation of specific ion species from the mixture and their fragmentation or ion–molecule reactions, allows their thorough characterization. This approach is denominated tandem mass spectrometry or MS/MS (Gross, 2017). The output of MS/MS is a mass spectrum of all the fragments generated by the isolated and fragmented analyte. This approach, by the isolation of a single analyte precursor to obtain a mass spectrum containing only its fragments, provides MS metabolomics studies with structural information of the molecules under analysis, allowing an unequivocal identification of the compounds.

Another important point to have in consideration in MS/MS, are the currently available chemical spectral libraries of raw and validated identified compounds in public databases (Tada et al., 2019). These platforms are essential to identify which metabolites are present in a sample. The fragmentation pattern of the unknown analytes present in the sample can be matched with tandem MS spectra of reference standards and other already identified compounds, allowing an accurate and unambiguous metabolite identification, which still remains the major bottleneck in metabolomics data interpretation (Ara et al., 2021; Cao et al., 2021; Chaleckis et al., 2019; Guijas et al., 2018; Horai et al., 2010; Scheubert et al., 2017; Wang et al., 2016; Wohlgemuth et al., 2016).

One of the alternative approaches used to annotate an unknown fragmentation mass spectrum is using *in silico* predictions, one of the key focuses in computational mass spectrometry research (Agahi et al., 2020; Djoumbou-Feunang et al., 2019; Krettler and Thallinger, 2021; Ruttkies et al., 2016).

Different studies have been published presenting new methods that facilitate the identification of small molecules from tandem MS experiments, even without spectral reference data or a large set of fragmentation rules (Dührkop et al., 2015; Hufsky et al., 2014; Krettler and Thallinger, 2021; Rogers et al., 2009; Ruttkies et al., 2016; Wolf et al., 2010). Also, web-based facilities have been created to help the analysis of raw or processed metabolomics mass spectrometric data, displaying the metabolites identified, changes in their experimental abundance and the metabolic pathways in which they occur (Leader et al., 2011).

One of the challenges of *in silico* annotation remains the multiple candidate structures predicted for each fragmentation spectrum meaning that the user still must visually inspect the predictions from a candidate list. Thus, defining new algorithms with improved quality and annotation rates is crucial (Böcker, 2017; Li et al., 2013; Silva et al., 2018).

Albeit recent technological equipment improvements, the complexity and diversity of plants surpasses these advances. The complete understanding of intricate metabolic pathways, step by step, is mainly incomplete to this diversity of specialized metabolites. To tackle this challenge, different approaches have been used through the years to study metabolites in plants, such as the identification of genes related to metabolites production and functions, utilization of protein sequences to predict enzymatic functions on specific points at the metabolic pathway and gene co-expression networks (Adio et al., 2011, 2011; Chae et al., 2014; Karp et al., 2011; Menikarachchi et al., 2013; Moore et al., 2020; Saito et al., 2008; Schläpfer et al., 2017; Tohge et al., 2005; Wisecaver et al., 2017). Despite innovative experimental approaches, all the metabolites detected need to be identified. Thus, high precision mass spectrometry data needs to be annotated so that the results can be displayed in specific databases. These databases contain linked information of genomes, biological pathways, diseases, drugs and chemical substances, allowing the depth comprehension of the compounds analyzed (Booth et al., 2013; Misra, 2021).

However, there is still a wide gap between the known and unknown as all these experimental approaches have high error rates and depend on the plant material and type of analysis. Thus, multiple network analysis tools have been developed to deal with these flaws and *in silico* metabolomics studies is appearing as an alternative approach (Desmet et al., 2021). In the last few years, computational advances, and the availability of libraries with fragmentation patterns information, made it possible to perform classification and predict plant chemical structures based on computational methods (Cao et al., 2021; Moore et al.,

2020; Peters et al., 2021; Ruttkies et al., 2016; Scheubert et al., 2017; Toubiana et al., 2019). As a result, several databases and tools have been established (Cottret et al., 2010; de Groot et al., 2009; Ellis et al., 2008; Li et al., 2013; Wicker et al., 2016; Yousofshahi et al., 2015). These platforms allow the prediction of the metabolism and creation of networks by computationally generating the enzymatic products of a particular compound (Desmet et al., 2021). *In silico* algorithms also allow the creation of predicted compound databases, helping and guiding laboratory experiments (Zhu et al., 2016).

A recent study by Toubiana and co-workers combined network analysis and machine learning, to predict metabolic pathways from tomato metabolomics data (Toubiana et al., 2019). Also, with bryophytes, Peters and co-workers presented an automated *in silico* compound classification framework to annotate metabolites using an untargeted data from mass spectrometry experiments (Peters et al., 2021).

Albeit these approaches seem to bring a new perspective for plant metabolomics studies, there are still some limitations. The majority of these *in silico* approaches were designed to perform analysis in model plants, e.g., *A. thaliana*, being unclear how these methods work in other species and, therefore, even though similarity-based approaches may be used to surpass the first problem, it is challenging to transfer annotation information across species without having high error rates (Moore et al., 2020; Yu et al., 2004). Nevertheless, a recent study employed machine learning strategies, where knowledge from *A. thaliana* was transferred to predict specialized metabolism genes functions of cultivated tomatoes (Moore et al., 2020).

1.10 THE GRAPEVINE METABOLOME AS A CASE STUDY

Grapevine (*Vitis vinifera* L.) accompanied the development of human culture and its history. Based on both archaeological and historical studies, it is clear that the cultivation and domestication of grapevines, the production of wine and commercialization of grapevine products has always been an important part of the human culture (Terral et al., 2010). Both wine and table grape made this crop global importance to increase and nowadays it is among the most important and cultivated fruit crops in the world.

The *Vitaceae* family comprises the *Vitis* genus, with about 80 species (Organisation of Vine and Wine, 2019). The genus *Vitis* comprises two sub-genera: *Muscadinia* and *EuVitis* differing in morphological, anatomical and cytological characters. The *Muscadinia* sub-genera comprise three species, *V. rontundifolia, V. rotundifoliavar. munsoniana* and *V. popenoii*, while the *EuVitis* includes *Vitis vinifera*, with the subspecies *V. vinifera* ssp. *sylvestris* (wild vines) and

Vitis vinifera ssp. v*inifera* (or sativa), the domesticated one (**Figure 1.3**), (This et al., 2006; Wan et al., 2013).
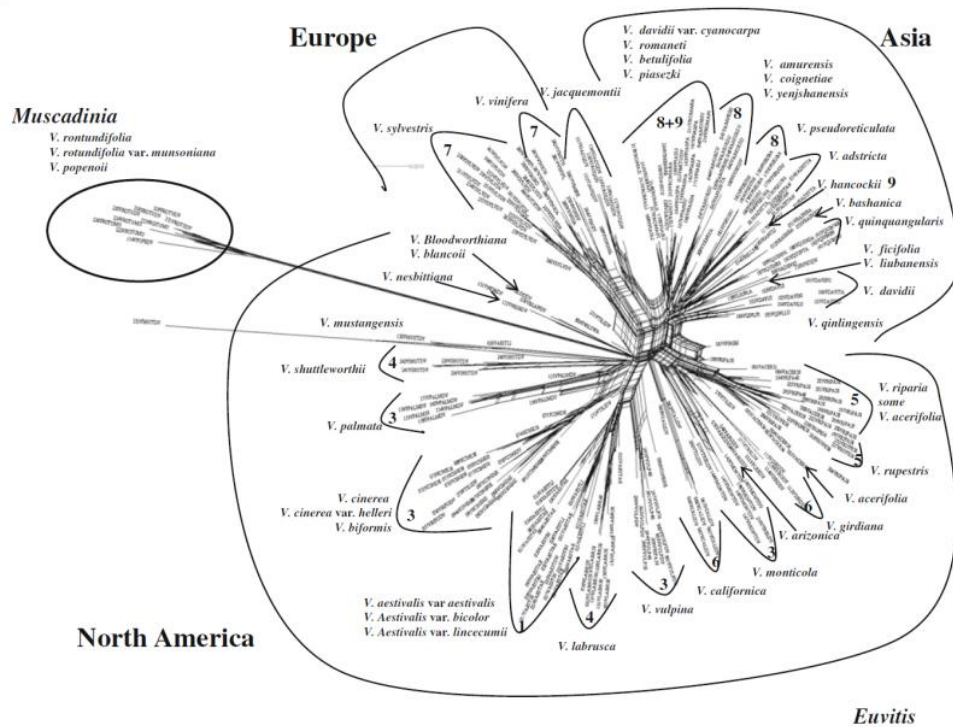
Figure 1.3 - Phylogenetic analysis of North American, Asian and European *Vitis* species (image from Wan et al., 2013).

Within their native habitat in the temperate regions of the world, there are about 28 wild *Vitis* species indigenous to North America and about 30 wild *Vitis* species indigenous to East Asia (Liang et al., 2019). *Vitis vinifera* ssp. *sylvestris* is the only wild *Vitis* native to Europe and Near East, and it is believed to be the wild progenitor for almost 10000 domesticated grapevine cultivars known today (Liang et al., 2019). Although there are over 80 *Vitis* species globally distributed (Organisation of Vine and Wine, 2019), the most cultivated is the *Vitis vinifera* ssp. v*inifera*. The cultivated *Vitis vinifera* comprises up to 5000 cultivars used for wine production and grapes' commercialization (Liang et al., 2019).

Grapevine plays a key role in many countries' economy, with a global market size of 30 billion euros (Organisation of Vine and Wine, 2020). As a result of its easy cultivation and numerous applications, in 2020, the current global vine area for fresh and dried table grapes, wine grapes and intermediate products was 7.3 mha (Organisation of Vine and Wine, 2020). In Portugal, 194 kha surface area is under vines, distributed into 14 main regions, for wine production: *Península de Setúbal*, *Lisboa*, *Tejo*, *Bairrada*, *Vinho Verde*, *Dão*, *Távora-Varosa*, *Porto-Douro*, *Trás-os-Montes*, *Beira interior*, *Alentejo*, *Algarve*, *Açores* and *Madeira* (**Figure 1.4**)

(http://www.winesofportugal.info/). In 2020, Portugal produced 6.4 million hectolitres of wine, of which 3.1 were exported, making the country the 11th world wine producer and the 5th in Europe. The total revenue of this industry was 846 million euros (International Organisation of Vine and Wine, 2020). Portugal has nearly 250 autochthonous grapevine varieties, unique in the world, which enables the country to make unique wines with distinctive flavours (http://www.winesofportugal.info/).
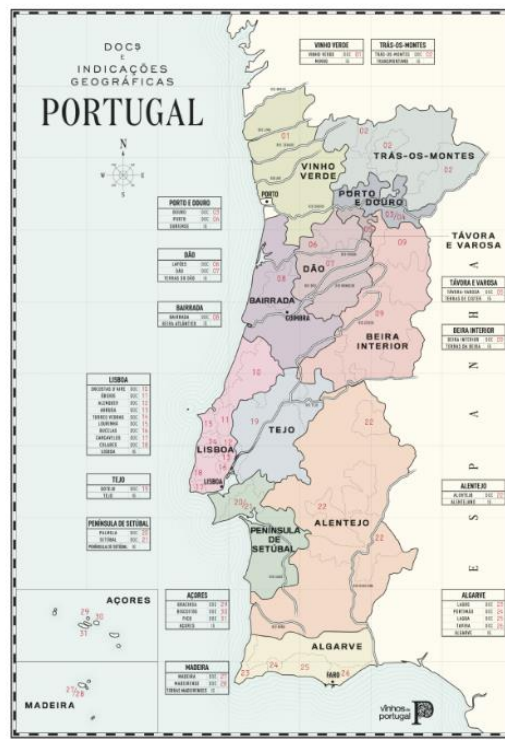
Figure 1.4 - Representation of the Portuguese wine producing regions (image from http://www.winesofportugal.info/).

Although wine and grapes are the major commercialized grapevine products, in some countries such as Turkey, Saudi Arabia, Greece, Bulgaria, Romania and Vietnam, some grapevine varieties are especially grown for fresh and brined leaves consumption (Koşar et al., 2007; Rizzuti et al., 2013; Sat et al., 2002). Some health benefits of grapevine leaves have been demonstrated in inflammatory disorders, pain, bleeding and high blood pressure treatments. Their anti-oxidant and regenerative properties have been described to protect and retard oxidative processes (Ali et al., 2010; Dani et al., 2010; Ledesma-Escobar and Luque de Castro, 2015; Orhan et al., 2007; Pari and Suresh, 2008; Fleming, 2000) and some dermo-cosmetic industries are using grapevine leaves compounds in their dermo-cosmetic products (e.g., Caudalie). These properties, nutritional value, taste and quality are due to a diversity of secondary bioactive metabolites like phenolic compounds, organic acids, lipids and

carbohydrates and therefore, grapevine leaves are considered a healthy food (Lima et al., 2016). However, the majority of these studies are focused in already known health related compounds.

Another important topic to discuss is *Vitis vinifera* susceptibility towards pathogens. *Vitis* exhibit difference resistance and susceptibility degrees towards pathogens. Both American and Asian *Vitis* species possess high tolerance to pathogens while *Vitis vinifera* exhibits different levels of disease susceptibility and tolerance. The wild grapevines (ssp. *sylvestris*) exhibit tolerant traits with different levels of tolerance to pathogens and the cultivated grapevines (ssp. *vinifera*), although susceptible possess different degrees of susceptibility ranging from highly susceptible to less susceptible (http://www.vivc.de/).

Among the most economically important grapevine diseases are downy mildew [caused by the oomycete *Plasmopara viticola* (Berk. & Curt.) Berl. & de Toni) Beri, et de Toni], powdery mildew [(caused by the fungus *Erysiphe necator* (Schweinf.) Burrill) and gray mold (caused by the fungus *Botrytis cinerea* Pers.), (**Figure 1.5**).

Both *P. viticola* and *E. necator* are obligatory biotroph pathogens, as they retrieve nutrients from living tissues and develop structures to invade the cell and to obtain metabolism products, without killing the plant. This lifecycle contrasts with that of necrotrophic pathogens, *B. cinerea*, which actively kill the host tissues as it colonizes and thrive on the contents of dead or dying cells (Laluk and Mengiste, 2010). The mode of infection of these pathogens also differs. *P. viticola* invades the plant through the stomatal cavity on the abaxial side of the leaves (Gessler et al., 2011) and *E. necator* promote wounds in the tissue, by the secretion of lytic enzymes, from which it will enter the plant (Gadoury et al., 2012). *B. cinerea* enters the host through an infection at wound site (**Figure 1.5**), (Prins et al., 2000).

A	**B**	**C**
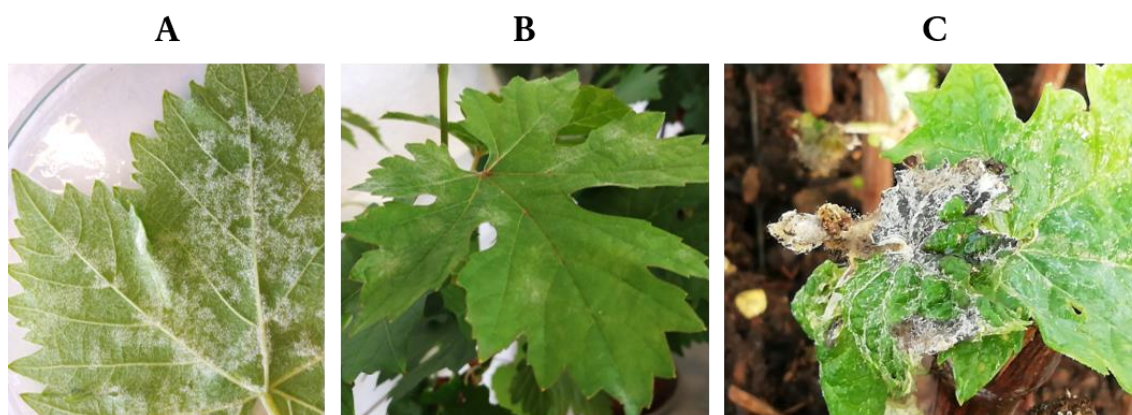
Figure 1.5 – Disease-associated symptoms of (**A**) *Plasmopara viticola*, (**B**) *Erysiphe necator* and (**C**) *Botrytis cinerea* in grapevine.

With adequate climate conditions, these pathogens affect all the green parts of the plant, reducing berry quality and yield, with significant production losses, reaching up to 75% of an entire crop. The preventive application of chemical products is winegrowers' most used approach to control these pathogens (**Figure 1.6**).

Figure 1.6 - Portuguese Bayer – Crop Science recommended treatments through grapevine season (image from https://cropscience.bayer.pt/).

However, chemical products are not entirely efficient and in a climate change scenario, several pathogen outbreaks are being reported (Casagrande et al., 2011; Delmotte et al., 2014; Peressotti et al., 2010). In the last decade, there was an increasing demand for more sustainable agricultural practices. Guidelines from the European Union demand a reduction and sustainable use of pesticides (Directive 2009/128/EC and Goals of the 2030 Agenda for Sustainable Development). Hence winegrowers are forced to reduce the use of pesticides, becoming of higher importance the development of alternative strategies. Having this in mind, producers reinforce the need to create new varieties through breeding programs, that combine the effective and durable tolerances to these pathogens with good berry quality and preserve their unique properties for wine production (Gómez-Zeledón et al., 2013; Merdinoglu et al., 2010; Toffolatti et al., 2012). Tolerance to pathogens in hybrid plants is achieved by crossing suitable parent lines or cultivars and the subsequent selection in the offspring to identify desired combinations of traits. Since American and Asian *Vitis* species have high tolerance against pathogens, they are being used in cross breeding programs with *V. vinifera* towards the development of new cultivars (Alleweldt and Possingham, 1988; Gómez-Zeledón et al., 2013; Toffolatti et al., 2012). Successful examples of this breeding strategy are the cultivars *V. vinifera* Regent, Solaris and Bianca, which display a broad tolerance to *P. viticola*, *E. necator* and *B. cinerea* and have a good berry quality for wine production (Basler and Pfenninger, 2003; Buonassisi et al., 2017; Eibach and Töpher, 2003;

Ruehl et al., 2015). Resistance breeding requires several years to accomplish and the majority of the resulting hybrids did not succeed in the market since they are unsuitable for the production of high quality wines (Buonassisi et al., 2017; Toffolatti et al., 2012). Second, fungi/oomycetes can overcome grapevine defence mechanisms due to their short generation time, the fact that it is outnumbered compared to the host and, depending on the strain virulence, it can modulate the host defence responses (Casagrande et al., 2011; Peressotti et al., 2010; Toffolatti et al., 2012; Zhan et al., 2002). One example is the tolerant hybrid Bianca that, although exhibits different levels of tolerance to *P. viticola*, when it is in contact with a more virulent strain of *P. viticola*, the pathogen surpasses the hybrid defences and infect the plant (Toffolatti et al., 2012).

In crop breeding programs, marker-assisted selection (MAS) is often employed to accelerate and enhance cultivar development, via selection during the juvenile phase and parental selection prior to crossing. Quantitative trait locus (QTL) mapping is currently the most commonly used approach to dissect the genetic factors underlying complex traits. Any new or advanced resulting selection method on the genomic or phenotypic level can bridge the gap between marker development and MAS implementation.

The metabolomics field have a particularly important contribution in this area. Plant metabolites are the end point of cellular metabolism, generally the first to be affected by changing conditions, and are capable of acting as biomarkers for plant selection (Fiehn, 2002). Hence, the combination of metabolomics with QTLs could reveal genomic regions associated to metabolic variations. In fact, some studies start to appear where metabolic QTLs are used as tools for assisting crops' improvement (Abdelrahman et al., 2018; Carreno-Quintero et al., 2012; Gong et al., 2013; Hill et al., 2015; Khan et al., 2012; Wen et al., 2015).

However, the complexity of grapevine metabolism brings huge challenges to the analytical technologies employed in current metabolomics programs, and powerful analytical tools are required for the separation and characterization of this high compound diversity present in the biological sample.

In grapevine research, several metabolomics studies focused on grape growth, development and ripening mainly due to the interest to understand the physiological and biochemical events that determine grape and wine quality (Cuadros-Inostroza et al., 2016; Smart et al., 2006). Also, the metabolome analysis of grapevine berries of a determined cultivar (Deluc et al., 2007; Fortes et al., 2011; Grimplet et al., 2009; Zamboni et al., 2010) or to a particular kind of stress condition (Ali et al., 2012; Batovska et al., 2009, 2008; Hong et al., 2012) was also investigated. All these were performed using Nuclear magnetic resonance (NMR) spectroscopy and based on the analysis of a single extract from leaves. In this case,

albeit using 1D and 2D NMR techniques, the number of metabolites identified was no more than 30 (Ali et al., 2009). The application of gas chromatography coupled to mass spectrometry (GC-MS) for grapevine leaves analysis allowed the detection of around 100 metabolites (Batovska et al., 2008). When using mass spectrometry coupled to liquid chromatography (LC-MS), although the identification and quantification of grapevine metabolites was possible, there were only identified 135 primary metabolites (sugars, amino acids, organic acids and amines) in a 30-minutes hydrophilic interaction LC run (Gika et al., 2012).

To achieve higher sensitivity and maximum metabolome coverage, Fourier Transform Ion Cyclotron Resonance mass spectrometry (FT-ICR-MS) is a promising analytical technique to tackle such challenge. In fact, several studies have been published using FT-ICR-MS to uncover grapevine metabolism (Adrian et al., 2017; Becker et al., 2013; Maia et al., 2016; Nascimento et al., 2019).

The majority of these works focused on the compatible and incompatible interaction of grapevine with *P. viticola* and the identification of possible resistance/susceptibility associated infection biomarkers. More grapevine studies, with and without pathogen infection, with FT-ICR-MS can shed light on the global changes occurring in grapevine metabolism which is fundamental to enhance plant fitness, increase stress tolerance, discover new natural pharmaceutical compounds applications and increase plant market value.

The main goals of this PhD dissertation were:

- Unravel through an untargeted metabolomics approach by FT-ICR-MS the metabolic composition of grapevine leaves;
- Understand the constitutive associated metabolic traits that differentiate tolerant and susceptible grapevine genotypes;
- Uncover grapevine main metabolic alterations after *P. viticola* inoculation through untargeted FT-ICR-MS analysis and MALDI-FT-ICR-MS imaging.

1.11 REFERENCES

Abdelrahman, M., Burritt, D.J., Tran, L.-S.P., 2018. The use of metabolomic quantitative trait locus mapping and osmotic adjustment traits for the improvement of crop yields under environmental stresses. Seminars in Cell & Developmental Biology 83, 86–94. https://doi.org/10.1016/j.semcdb.2017.06.020

Adio, A.M., Casteel, C.L., De Vos, M., Kim, J.H., Joshi, V., Li, B., Juéry, C., Daron, J., Kliebenstein, D.J., Jander, G., 2011. Biosynthesis and Defensive Function of N Δ-Acetylornithine, a Jasmonate-Induced Arabidopsis Metabolite. The Plant Cell 23, 3303–3318. https://doi.org/10.1105/tpc.111.088989

Adrian, M., Lucio, M., Roullier-Gall, C., Héloir, M.-C., Trouvelot, S., Daire, X., Kanawati, B., Lemaître-Guillier, C., Poinssot, B., Gougeon, R., Schmitt-Kopplin, P., 2017. Metabolic Fingerprint of PS3-Induced Resistance of Grapevine Leaves against Plasmopara viticola Revealed Differences in Elicitor-Triggered Defenses. Front Plant Sci 8, 101. https://doi.org/10.3389/fpls.2017.00101

Agahi, F., Juan, C., Font, G., Juan-García, A., 2020. In silico methods for metabolomic and toxicity prediction of zearalenone, α-zearalenone and β-zearalenone. Food and Chemical Toxicology 146, 111818. https://doi.org/10.1016/j.fct.2020.111818

Aharoni, A., Ric de Vos, C.H., Verhoeven, H.A., Maliepaard, C.A., Kruppa, G., Bino, R., Goodenowe, D.B., 2002a. Nontargeted metabolome analysis by use of Fourier transform ion cyclotron mass spectrometry. OMICS 6, 217–234. https://doi.org/doi:10.1089/15362310260256882

Aharoni, A., Ric de Vos, C.H., Verhoeven, H.A., Maliepaard, C.A., Kruppa, G., Bino, R., Goodenowe, D.B., 2002b. Nontargeted Metabolome Analysis by Use of Fourier Transform Ion Cyclotron Mass Spectrometry. OMICS: A Journal of Integrative Biology 6, 217–234. https://doi.org/10.1089/15362310260256882

Alcantara, H.J.P., Jativa, F., Doronila, A.I., Anderson, C.W.N., Siegele, R., Spassov, T.G., Sanchez-Palacios, J.T., Boughton, B.A., Kolev, S.D., 2020. Localization of mercury and gold in cassava (Manihot esculenta Crantz). Environ Sci Pollut Res Int 27, 18498–18509. https://doi.org/10.1007/s11356-020-08285-3

Ali, K., Maltese, F., Choi, Y.H., Verpoorte, R., 2010. Metabolic constituents of grapevine and grape-derived products. Phytochemistry Reviews 9, 357–378. https://doi.org/10.1007/s11101-009-9158-0

Ali, K., Maltese, F., Figueiredo, A., Rex, M., Fortes, A.M., Zyprian, E., Pais, M.S., Verpoorte, R., Choi, Y.H., 2012. Alterations in grapevine leaf metabolism upon inoculation with Plasmopara viticola in different time-points. Plant science 191, 100–107.

Ali, K., Maltese, F., Zyprian, E., Rex, M., Choi, Y.H., Verpoorte, R., 2009. NMR Metabolic Fingerprinting Based Identification of Grapevine Metabolites Associated with Downy Mildew Resistance. Journal of Agricultural and Food Chemistry 57, 9599–9606. https://doi.org/10.1021/jf902069f

Aliferis, K.A., Jabaji, S., 2012. FT-ICR/MS and GC-EI/MS Metabolomics Networking Unravels Global Potato Sprout's Responses to Rhizoctonia solani Infection. PLoS ONE 7, e42576. https://doi.org/10.1371/journal.pone.0042576

Alleweldt, G., Possingham, J.V., 1988. Progress in grapevine breeding. Theoret. Appl. Genetics 75, 669–673. https://doi.org/10.1007/BF00265585

Allwood, J.W., Parker, D., Beckmann, M., Draper, J., Goodacre, R., 2011. Fourier Transform Ion Cyclotron Resonance Mass Spectrometry for Plant Metabolite Profiling and Metabolite Identification, in: Hardy, N.W., Hall, R.D. (Eds.), Plant Metabolomics, Methods in Molecular Biology. Humana Press, Totowa, NJ, pp. 157–176. https://doi.org/10.1007/978-1-61779-594-7_11

Andrews, G.L., Simons, B.L., Young, J.B., Hawkridge, A.M., Muddiman, D.C., 2011. Performance Characteristics of a New Hybrid Quadrupole Time-of-Flight Tandem Mass Spectrometer (TripleTOF 5600). Anal. Chem. 83, 5442–5446. https://doi.org/10.1021/ac200812d

Ara, T., Sakurai, N., Takahashi, S., Waki, N., Suganuma, H., Aizawa, K., Matsumura, Y., Kawada, T., Shibata, D., 2021. TOMATOMET: A metabolome database consists of 7118 accurate mass values detected in mature fruits of 25 tomato cultivars. Plant Direct 5, e00318. https://doi.org/10.1002/pld3.318

Aranìbar, N., Singh, B.K., Stockton, G.W., Ott, K.H., 2001. Automated mode-of-action detection by metabolic profiling. Biochem Biophys Res Commun 286, 150–155. https://doi.org/10.1006/bbrc.2001.5350

Arbona, V., Gómez-Cadenas, A., 2016. Metabolomics of Disease Resistance in Crops. Curr Issues Mol Biol 19, 13–30. https://doi.org/10.21775/9781910190357.04

Aston, F.W., 1920a. Isotopes and Atomic Weights. Nature 105, 617–619. https://doi.org/10.1038/105617a0

Aston, F.W., 1920b. LIX. The mass-spectra of chemical elements. The London, Edinburgh, and Dublin Philosophical Magazine and Journal of Science 39, 611–625. https://doi.org/10.1080/14786440508636074

Aston, F.W., 1919. LXXIV. A positive ray spectrograph. The London, Edinburgh, and Dublin Philosophical Magazine and Journal of Science 38, 707–714. https://doi.org/10.1080/14786441208636004

Barkauskas, D.A., Kronewitter, S.R., Lebrilla, C.B., Rocke, D.M., 2009. Analysis of MALDI FT-ICR mass spectrometry data: a time series approach. Anal Chim Acta 648, 207–214. https://doi.org/10.1016/j.aca.2009.06.064

Barrow, M.P., Burkitt, W.I., Derrick, P.J., 2005. Principles of Fourier transform ion cyclotron resonance mass spectrometry and its application in structural biology. Analyst 130, 18. https://doi.org/10.1039/b403880k

Basler, P., Pfenninger, H., 2003. DISEASE-RESISTANT CULTIVARS AS A SOLUTION FOR ORGANIC VITICULTURE. Acta Horticulturae 681–685. https://doi.org/10.17660/ActaHortic.2003.603.94

Batovska, D.I., Todorova, I.T., Nedelcheva, D.V., Parushev, S.P., Atanassov, A.I., Hvarleva, T.D., Djakova, G.J., Bankova, V.S., Popov, S.S., 2008. Preliminary study on biomarkers for the fungal resistance in Vitis vinifera leaves. Journal of Plant Physiology 165, 791–795. https://doi.org/10.1016/j.jplph.2007.09.005

Batovska, D.I., Todorova, I.T., Parushev, S.P., Nedelcheva, D.V., Bankova, V.S., Popov, S.S., Ivanova, I.I., Batovski, S.A., 2009. Biomarkers for the prediction of the resistance and susceptibility of grapevine leaves to downy mildew. Journal of Plant Physiology 166, 781–785. https://doi.org/10.1016/j.jplph.2008.08.008

Beck, S., Stengel, J., 2016. Mass spectrometric imaging of flavonoid glycosides and biflavonoids in Ginkgo biloba L. Phytochemistry 130, 201–206. https://doi.org/10.1016/j.phytochem.2016.05.005

Becker, L., Poutaraud, A., Hamm, G., Muller, J.-F., Merdinoglu, D., Carré, V., Chaimbault, P., 2013. Metabolic study of grapevine leaves infected by downy mildew using negative ion electrospray – Fourier transform ion cyclotron resonance mass spectrometry. Analytica Chimica Acta 795, 44–51. https://doi.org/10.1016/j.aca.2013.07.068

Beckmann, M., Parker, D., Enot, D.P., Duval, E., Draper, J., 2008. High-throughput, nontargeted metabolite fingerprinting using nominal mass flow injection electrospray mass spectrometry. Nat Protoc 3, 486–504. https://doi.org/10.1038/nprot.2007.500

Behnke, K., Kaiser, A., Zimmer, I., Brüggemann, N., Janz, D., Polle, A., Hampp, R., Hänsch, R., Popko, J., Schmitt-Kopplin, P., Ehlting, B., Rennenberg, H., Barta, C., Loreto, F., Schnitzler, J.-P., 2010. RNAi-mediated suppression of isoprene emission in poplar transiently impacts phenolic metabolism under high temperature and high light intensities: a transcriptomic and metabolomic analysis. Plant Mol Biol 74, 61–75. https://doi.org/10.1007/s11103-010-9654-z

Beynon, J.H., 1956. The use of the mass spectrometer for the identification of organic compounds. Mikrochim Acta 44, 437–453. https://doi.org/10.1007/BF01216629

Bi, H., Xi, M., Zhang, R., Wang, C., Qiao, L., Xie, J., 2018. Electrostatic Spray Ionization-Mass Spectrometry for Direct and Fast Wine Characterization. ACS Omega 3, 17881–17887. https://doi.org/10.1021/acsomega.8b02259

Bino, R.J., Hall, R.D., Fiehn, O., Kopka, J., Saito, K., Draper, J., Nikolau, B.J., Mendes, P., Roessner-Tunali, U., Beale, M.H., Trethewey, R.N., Lange, B.M., Wurtele, E.S., Sumner, L.W., 2004. Potential of metabolomics as a functional genomics tool. Trends Plant Sci 9, 418–425. https://doi.org/10.1016/j.tplants.2004.07.004

Bjarnholt, N., Li, B., D'Alvise, J., Janfelt, C., 2014. Mass spectrometry imaging of plant metabolites--principles and possibilities. Nat Prod Rep 31, 818–837. https://doi.org/10.1039/c3np70100j

Blair, S.L., MacMillan, A.C., Drozd, G.T., Goldstein, A.H., Chu, R.K., Paša-Tolić, L., Shaw, J.B., Tolić, N., Lin, P., Laskin, J., Laskin, A., Nizkorodov, S.A., 2017. Molecular Characterization of Organosulfur Compounds in Biodiesel and Diesel Fuel Secondary Organic Aerosol. Environ. Sci. Technol. 51, 119–127. https://doi.org/10.1021/acs.est.6b03304

Böcker, S., 2017. Searching molecular structure databases using tandem MS data: are we there yet? Current Opinion in Chemical Biology, Omics 36, 1–6. https://doi.org/10.1016/j.cbpa.2016.12.010

Bodzon-Kulakowska, A., Suder, P., 2016. Imaging mass spectrometry: Instrumentation, applications, and combination with other visualization techniques. Mass Spectrom Rev 35, 147–169. https://doi.org/10.1002/mas.21468

Booth, S.C., Weljie, A.M., Turner, R.J., 2013. COMPUTATIONAL TOOLS FOR THE SECONDARY ANALYSIS OF METABOLOMICS EXPERIMENTS. Computational and Structural Biotechnology Journal 4, e201301003. https://doi.org/10.5936/csbj.201301003

Boughton, B.A., Thinagaran, D., Sarabia, D., Bacic, A., Roessner, U., 2016. Mass spectrometry imaging for plant biology: a review. Phytochem Rev 15, 445–488. https://doi.org/10.1007/s11101-015-9440-2

Bowman, A.P., Blakney, G.T., Hendrickson, C.L., Ellis, S.R., Heeren, R.M.A., Smith, D.F., 2020. Ultra-High Mass Resolving Power, Mass Accuracy, and Dynamic Range MALDI Mass Spectrometry Imaging by 21-T FT-ICR MS. Anal. Chem. 92, 3133–3142. https://doi.org/10.1021/acs.analchem.9b04768

Brennan, J.C., Denison, M.S., Holstege, D.M., Magiatis, P., Dallas, J.L., Gutierrez, E.G., Soshilov, A.A., Millam, J.R., 2013. 2,3-cis-2R,3R-(−)-epiafzelechin-3-O-p-coumarate, a novel flavan-3-ol isolated from Fallopia convolvulus seed, is an estrogen receptor agonist in human cell lines. BMC Complement Altern Med 13, 133. https://doi.org/10.1186/1472-6882-13-133

Buck, A., Balluff, B., Voss, A., Langer, R., Zitzelsberger, H., Aichler, M., Walch, A., 2016. How Suitable is Matrix-Assisted Laser Desorption/Ionization-Time-of-Flight for Metabolite Imaging from Clinical Formalin-Fixed and Paraffin-Embedded Tissue Samples in Comparison to Matrix-Assisted Laser Desorption/Ionization-Fourier Transform Ion Cyclotron Resonance Mass Spectrometry? Anal. Chem. 88, 5281–5289. https://doi.org/10.1021/acs.analchem.6b00460

Buonassisi, D., Colombo, M., Migliaro, D., Dolzani, C., Peressotti, E., Mizzotti, C., Velasco, R., Masiero, S., Perazzolli, M., Vezzulli, S., 2017. Breeding for grapevine downy mildew resistance: a review of "omics" approaches. Euphytica 213. https://doi.org/10.1007/s10681-017-1882-8

Cao, L., Guler, M., Tagirdzhanov, A., Lee, Y.-Y., Gurevich, A., Mohimani, H., 2021. MolDiscovery: learning mass spectrometry fragmentation of small molecules. Nat Commun 12, 3718. https://doi.org/10.1038/s41467-021-23986-0

Cao-Ngoc, P., Leclercq, L., Rossi, J.-C., Hertzog, J., Tixier, A.-S., Chemat, F., Nasreddine, R., Al Hamoui Dit Banni, G., Nehmé, R., Schmitt-Kopplin, P., Cottet, H., 2020. Water-Based Extraction of Bioactive Principles from Blackcurrant Leaves and Chrysanthellum americanum: A Comparative Study. Foods 9, 1478. https://doi.org/10.3390/foods9101478

Carreno-Quintero, N., Acharjee, A., Maliepaard, C., Bachem, C.W.B., Mumm, R., Bouwmeester, H., Visser, R.G.F., Keurentjes, J.J.B., 2012. Untargeted Metabolic Quantitative Trait Loci Analyses Reveal a Relationship between Primary Metabolism and Potato Tuber Quality1[W][OA]. Plant Physiol 158, 1306–1318. https://doi.org/10.1104/pp.111.188441

Casagrande, K., Falginella, L., Castellarin, S.D., Testolin, R., Di Gaspero, G., 2011. Defence responses in Rpv3-dependent resistance to grapevine downy mildew. Planta 234, 1097–1109. https://doi.org/10.1007/s00425-011-1461-5

Castro-Moretti, F.R., Gentzel, I.N., Mackey, D., Alonso, A.P., 2020. Metabolomics as an Emerging Tool for the Study of Plant-Pathogen Interactions. Metabolites 10. https://doi.org/10.3390/metabo10020052

Chae, L., Kim, T., Nilo-Poyanco, R., Rhee, S.Y., 2014. Genomic Signatures of Specialized Metabolism in Plants. Science 344, 510–513. https://doi.org/10.1126/science.1252076

Chaleckis, R., Meister, I., Zhang, P., Wheelock, C.E., 2019. Challenges, progress and promises of metabolite annotation for LC-MS-based metabolomics. Curr Opin Biotechnol 55, 44–50. https://doi.org/10.1016/j.copbio.2018.07.010

Chen, F., Ma, R., Chen, X.-L., 2019. Advances of Metabolomics in Fungal Pathogen-Plant Interactions. Metabolites 9. https://doi.org/10.3390/metabo9080169

Chen, J., Ge, Z., Zhu, W., Xu, Z., Li, C., 2014. Screening of Key Antioxidant Compounds of Longan (*Dimocarpus longan* Lour.) Seed Extract by Combining Online Fishing/Knockout, Activity Evaluation, Fourier Transform Ion Cyclotron Resonance Mass Spectrometry, and High-Performance Liquid Chromatography Electrospray Ionization Mass Spectrometry Methods. J. Agric. Food Chem. 62, 9744–9750. https://doi.org/10.1021/jf502995z

Cho, E., Witt, M., Hur, M., Jung, M.-J., Kim, S., 2017. Application of FT-ICR MS Equipped with Quadrupole Detection for Analysis of Crude Oil. Anal. Chem. 89, 12101–12107. https://doi.org/10.1021/acs.analchem.7b02644

Choi, Y.H., Tapias, E.C., Kim, H.K., Lefeber, A.W.M., Erkelens, C., Verhoeven, J.T.J., Brzin, J., Zel, J., Verpoorte, R., 2004. Metabolic Discrimination of Catharanthus roseus

Leaves Infected by Phytoplasma Using 1H-NMR Spectroscopy and Multivariate Data Analysis. Plant Physiology 135, 2398–2410. https://doi.org/10.1104/pp.104.041012

Comisarow, M.B., Marshall, A.G., 1996. The Early Development of Fourier Transform Ion Cyclotron Resonance (FT-ICR) Spectroscopy. Journal of Mass Spectrometry 31, 581–585. https://doi.org/10.1002/(SICI)1096-9888(199606)31:6<581::AID-JMS369>3.0.CO;2-1

Comisarow, M.B., Marshall, A.G., 1974a. Fourier transform ion cyclotron resonance spectroscopy. Chemical Physics Letters 25, 282–283. https://doi.org/10.1016/0009-2614(74)89137-2

Comisarow, M.B., Marshall, A.G., 1974b. Fourier transform ion cyclotron resonance spectroscopy. Chemical Physics Letters 25, 282–283. https://doi.org/10.1016/0009-2614(74)89137-2

Comisarow, M.B., Marshall, A.G., 1974c. Frequency-sweep fourier transform ion cyclotron resonance spectroscopy. Chemical Physics Letters 26, 489–490. https://doi.org/10.1016/0009-2614(74)80397-0

Costa, H.B., Souza, L.M., Soprani, L.C., Oliveira, B.G., Ogawa, E.M., Korres, A.M.N., Ventura, J.A., Romão, W., 2015. Monitoring the physicochemical degradation of coconut water using ESI-FT-ICR MS. Food Chemistry 174, 139–146. https://doi.org/10.1016/j.foodchem.2014.10.154

Cottret, L., Wildridge, D., Vinson, F., Barrett, M.P., Charles, H., Sagot, M.-F., Jourdan, F., 2010. MetExplore: a web server to link metabolomic experiments and genome-scale metabolic networks. Nucleic Acids Research 38, W132–W137. https://doi.org/10.1093/nar/gkq312

Crockford, D.J., Holmes, E., Lindon, J.C., Plumb, R.S., Zirah, S., Bruce, S.J., Rainville, P., Stumpf, C.L., Nicholson, J.K., 2006. Statistical heterospectroscopy, an approach to the integrated analysis of NMR and UPLC-MS data sets: application in metabonomic toxicology studies. Anal Chem 78, 363–371. https://doi.org/10.1021/ac051444m

Cuadros-Inostroza, A., Ruíz-Lara, S., González, E., Eckardt, A., Willmitzer, L., Peña-Cortés, H., 2016. GC–MS metabolic profiling of Cabernet Sauvignon and Merlot cultivars during grapevine berry development and network analysis reveals a stage- and cultivar-dependent connectivity of primary metabolites. Metabolomics 12. https://doi.org/10.1007/s11306-015-0927-z

Dani, C., Oliboni, L.S., Agostini, F., Funchal, C., Serafini, L., Henriques, J.A., Salvador, M., 2010. Phenolic content of grapevine leaves (Vitis labrusca var. Bordo) and its neuroprotective effect against peroxide damage. Toxicology in Vitro 24, 148–153. https://doi.org/10.1016/j.tiv.2009.08.006

de Groot, M.J.L., van Berlo, R.J.P., van Winden, W.A., Verheijen, P.J.T., Reinders, M.J.T., de Ridder, D., 2009. Metabolite and reaction inference based on enzyme specificities. Bioinformatics 25, 2975–2982. https://doi.org/10.1093/bioinformatics/btp507

Dehmelt, H.G., 1952. Kernquadrupolspektren in zwei Bortrialkylen. Z. Physik 133, 528–531. https://doi.org/10.1007/BF01336865

Dehmelt, H.G., 1951a. Quadrupolresonanzfrequenzen des kristallinen Broms. Z. Physik 130, 480–482. https://doi.org/10.1007/BF01328439

Dehmelt, H.G., 1951b. Quadrupol-Resonanzfrequenzen von J127-Kernen in kristallinen kovalenten Jodverbindungen. Z. Physik 130, 356–370. https://doi.org/10.1007/BF01340172

Dehmelt, H.-G., 1950. Kernquadrupolfrequenzen in kristallinen Jodverbindungen. Naturwissenschaften 37, 398–398. https://doi.org/10.1007/BF00738365

Dehmelt, H.G., Krüger, H., 1951a. über das Quadrupolresonanzspektrum in kristallinem Antimontrichlorid und das Verhältnis der Antimonkernquadrupolmomente. Z. Physik 130, 385–391. https://doi.org/10.1007/BF01340174

Dehmelt, H.G., Krüger, H., 1951b. Quadrupol-Resonanzfrequenzen von Cl- und Br-Kernen in kristallinem Dichloräthylen und Methylbromid. Z. Physik 129, 401–415. https://doi.org/10.1007/BF01379591

Dehmelt, H.-G., Krüger, H., 1950. Kernquadrupolfrequenzen in festem Dichloräthylen. Naturwissenschaften 37, 111–112. https://doi.org/10.1007/BF00623717

Delmotte, F., Mestre, P., Schneider, C., Kassemeyer, H.-H., Kozma, P., Richart-Cervera, S., Rouxel, M., Delière, L., 2014. Rapid and multiregional adaptation to host partial resistance in a plant pathogenic oomycete: evidence from European populations of Plasmopara viticola, the causal agent of grapevine downy mildew. Infect. Genet. Evol. 27, 500–508. https://doi.org/10.1016/j.meegid.2013.10.017

Deluc, L.G., Grimplet, J., Wheatley, M.D., Tillett, R.L., Quilici, D.R., Osborne, C., Schooley, D.A., Schlauch, K.A., Cushman, J.C., Cramer, G.R., 2007. Transcriptomic and metabolite analyses of Cabernet Sauvignon grape berry development. BMC Genomics 8, 429. https://doi.org/10.1186/1471-2164-8-429

Desmet, S., Brouckaert, M., Boerjan, W., Morreel, K., 2021. Seeing the forest for the trees: Retrieving plant secondary biochemical pathways from metabolome networks. Computational and Structural Biotechnology Journal 19, 72–85. https://doi.org/10.1016/j.csbj.2020.11.050

Devaux, P.G., Horning, M.G., Horning, E.C., 1971. Benzyloxime Derivatives of Steroids. A New Metabolic Profile Procedure for Human Urinary Steroids Human Urinary Steroids. Analytical Letters 4, 151–160. https://doi.org/10.1080/00032717108059686

Djoumbou-Feunang, Y., Fiamoncini, J., Gil-de-la-Fuente, A., Greiner, R., Manach, C., Wishart, D.S., 2019. BioTransformer: a comprehensive computational tool for small

molecule metabolism prediction and metabolite identification. Journal of Cheminformatics 11, 2. https://doi.org/10.1186/s13321-018-0324-5

Dole, M., Mack, L.L., Hines, R.L., Mobley, R.C., Ferguson, L.D., Alice, M.B., 1968. Molecular Beams of Macroions. J. Chem. Phys. 49, 2240–2249. https://doi.org/10.1063/1.1670391

Dos Santos, N.A., de Almeida, C.M., Gonçalves, F.F., Ortiz, R.S., Kuster, R.M., Saquetto, D., Romão, W., 2021. Analysis of Erythroxylum coca Leaves by Imaging Mass Spectrometry (MALDI-FT-ICR IMS). J Am Soc Mass Spectrom 32, 946–955. https://doi.org/10.1021/jasms.0c00449

dos Santos, N.A., de Souza, L.M., Pinto, F.E., de J. Macrino, C., de Almeida, C.M., Merlo, B.B., Filgueiras, P.R., Ortiz, R.S., Mohana-Borges, R., Romão, W., 2019. LDI and MALDI-FT-ICR imaging MS in *Cannabis* leaves: optimization and study of spatial distribution of cannabinoids. Anal. Methods 11, 1757–1764. https://doi.org/10.1039/C9AY00226J

Du, Q.-Q., Liu, S.-Y., Xu, R.-F., Li, M., Song, F.-R., Liu, Z.-Q., 2012. Studies on structures and activities of initial Maillard reaction products by electrospray ionisation mass spectrometry combined with liquid chromatography in processing of red ginseng. Food Chemistry 135, 832–838. https://doi.org/10.1016/j.foodchem.2012.04.126

Dührkop, K., Shen, H., Meusel, M., Rousu, J., Böcker, S., 2015. Searching molecular structure databases with tandem mass spectra using CSI:FingerID. PNAS 112, 12580–12585. https://doi.org/10.1073/pnas.1509788112

Eibach, R., Töpher, R., 2003. Success in resistance breeding: "Regent" and its steps into the market. Acta Horticulturae 687–691. https://doi.org/10.17660/ActaHortic.2003.603.95

Ellis, L.B.M., Gao, J., Fenner, K., Wackett, L.P., 2008. The University of Minnesota pathway prediction system: predicting metabolic logic. Nucleic Acids Research 36, W427–W432. https://doi.org/10.1093/nar/gkn315

Fenn, J.B., Mann, M., Meng, C.K., Wong, S.F., Whitehouse, C.M., 1989. Electrospray ionization for mass spectrometry of large biomolecules. Science 246, 64–71. https://doi.org/10.1126/science.2675315

Ferreira, F.P.S., Morais, S.R., Bara, M.T.F., Conceição, E.C., Paula, J.R., Carvalho, T.C., Vaz, B.G., Costa, H.B., Romão, W., Rezende, M.H., 2014. Eugenia calycina Cambess extracts and their fractions: Their antimicrobial activity and the identification of major polar compounds using electrospray ionization FT-ICR mass spectrometry. Journal of Pharmaceutical and Biomedical Analysis 99, 89–96. https://doi.org/10.1016/j.jpba.2014.07.003

Fiehn, O., 2002. Metabolomics – the link between genotypes and phenotypes. Plant Mol Biol 48, 155–171. https://doi.org/10.1023/A:1013713905833

Fiehn, O., 2001. Combining Genomics, Metabolome Analysis, and Biochemical Modelling to Understand Metabolic Networks. Comp Funct Genomics 2, 155–168. https://doi.org/10.1002/cfg.82

Figueiredo, J., Cavaco, A.R., Guerra-Guimarães, L., Leclercq, C., Renaut, J., Cunha, J., Eiras-Dias, J., Cordeiro, C., Matos, A.R., Sousa Silva, M., Figueiredo, A., 2021. An apoplastic fluid extraction method for the characterization of grapevine leaves proteome and metabolome from a single sample. Physiol Plantarum 171, 343–357. https://doi.org/10.1111/ppl.13198

Fischer, R., Vasilev, N., Twyman, R.M., Schillberg, S., 2015. High-value products from plants: the challenges of process optimization. Current Opinion in Biotechnology 32, 156–162. https://doi.org/10.1016/j.copbio.2014.12.018

Flamini, R., De Rosso, M., 2006. Mass spectrometry in the analysis of grape and wine proteins. Expert Rev Proteomics 3, 321–331. https://doi.org/10.1586/14789450.3.3.321

Fleming, T., 2000. PDR for herbal medicines, 2., rev. ed. ed. Medical Economics Co, Montvale, N.J.

Foito, A., Stewart, D., 2018. Metabolomics: A High-throughput Screen for Biochemical and Bioactivity Diversity in Plants and Crops. Curr Pharm Des 24, 2043–2054. https://doi.org/10.2174/1381612824666180515125926

Folli, G.S., Souza, L.M., Araújo, B.Q., Romão, W., Filgueiras, P.R., 2020. Estimating the intermediate precision in petroleum analysis by (±)electrospray ionization Fourier transform ion cyclotron resonance mass spectrometry. Rapid Communications in Mass Spectrometry 34, e8861. https://doi.org/10.1002/rcm.8861

Fortes, A.M., Agudelo-Romero, P., Silva, M.S., Ali, K., Sousa, L., Maltese, F., Choi, Y.H., Grimplet, J., Martinez- Zapater, J.M., Verpoorte, R., Pais, M.S., 2011. Transcript and metabolite analysis in Trincadeira cultivar reveals novel information regarding the dynamics of grape ripening. BMC Plant Biol 11, 149. https://doi.org/10.1186/1471-2229-11-149

Gadoury, D.M., Cadle-Davidson, L., Wilcox, W.F., Dry, I.B., Seem, R.C., Milgroom, M.G., 2012. Grapevine powdery mildew (Erysiphe necator): a fascinating system for the study of the biology, ecology and epidemiology of an obligate biotroph. Mol Plant Pathol 13, 1–16. https://doi.org/10.1111/j.1364-3703.2011.00728.x

Garrett, R., Vaz, B.G., Hovell, A.M.C., Eberlin, M.N., Rezende, C.M., 2012. Arabica and Robusta Coffees: Identification of Major Polar Compounds and Quantification of Blends by Direct-Infusion Electrospray Ionization–Mass Spectrometry. J. Agric. Food Chem. 60, 4253–4258. https://doi.org/10.1021/jf300388m

Genga, A., Mattana, M., Coraggio, I., Locatelli, F., Piffanelli, P., Consonni, R., 2011. Plant Metabolomics: A Characterisation of Plant Responses to Abiotic Stresses. Abiotic Stress in Plants - Mechanisms and Adaptations. https://doi.org/10.5772/23844

Gessler, C., Pertot, I., Perazzolli, M., 2011. Plasmopara viticola: a review of knowledge on downy mildew of grapevine and effective disease management. Phytopathologia Mediterranea 50, 3–44. https://doi.org/10.14601/Phytopathol_Mediterr-9360

Ghaste, M., Mistrik, R., Shulaev, V., 2016. Applications of Fourier Transform Ion Cyclotron Resonance (FT-ICR) and Orbitrap Based High Resolution Mass Spectrometry in Metabolomics and Lipidomics. Int J Mol Sci 17. https://doi.org/10.3390/ijms17060816

Giavalisco, P., Hummel, J., Lisec, J., Inostroza, A.C., Catchpole, G., Willmitzer, L., 2008. High-Resolution Direct Infusion-Based Mass Spectrometry in Combination with Whole ^{13}C Metabolome Isotope Labeling Allows Unambiguous Assignment of Chemical Sum Formulas. Anal. Chem. 80, 9417–9425. https://doi.org/10.1021/ac8014627

Giavalisco, P., Köhl, K., Hummel, J., Seiwert, B., Willmitzer, L., 2009. 13C Isotope-Labeled Metabolomes Allowing for Improved Compound Annotation and Relative Quantification in Liquid Chromatography-Mass Spectrometry-based Metabolomic Research. Anal. Chem. 81, 6546–6551. https://doi.org/10.1021/ac900979e

Gika, H.G., Theodoridis, G.A., Vrhovsek, U., Mattivi, F., 2012. Quantitative profiling of polar primary metabolites using hydrophilic interaction ultrahigh performance liquid chromatography-tandem mass spectrometry. J Chromatogr A 1259, 121–127. https://doi.org/10.1016/j.chroma.2012.02.010

Glauser, G., Veyrat, N., Rochat, B., Wolfender, J.-L., Turlings, T.C.J., 2013. Ultra-high pressure liquid chromatography–mass spectrometry for plant metabolomics: A systematic comparison of high-resolution quadrupole-time-of-flight and single stage Orbitrap mass spectrometers. Journal of Chromatography A, State-of-the art of (UHP)LC--MS(--MS) techniques and their practical application 1292, 151–159. https://doi.org/10.1016/j.chroma.2012.12.009

Gohlke, R.S., 1959. Time-of-Flight Mass Spectrometry and Gas-Liquid Partition Chromatography. Anal. Chem. 31, 535–541. https://doi.org/10.1021/ac50164a024

Gómez-Zeledón, J., Zipper, R., Spring, O., 2013. Assessment of phenotypic diversity of Plasmopara viticola on Vitis genotypes with different resistance. Crop Protection 54, 221–228. https://doi.org/10.1016/j.cropro.2013.08.015

Gong, L., Chen, W., Gao, Y., Liu, X., Zhang, H., Xu, C., Yu, S., Zhang, Q., Luo, J., 2013. Genetic analysis of the metabolome exemplified using a rice population. Proceedings of the National Academy of Sciences 110, 20320–20325. https://doi.org/10.1073/pnas.1319681110

Gorzolka, K., Bednarz, H., Niehaus, K., 2014. Detection and localization of novel hordatine-like compounds and glycosylated derivates of hordatines by imaging mass

spectrometry of barley seeds. Planta 239, 1321–1335. https://doi.org/10.1007/s00425-014-2061-y

Gougeon, R.D., Lucio, M., Frommberger, M., Peyron, D., Chassagne, D., Alexandre, H., Feuillat, F., Voilley, A., Cayot, P., Gebefugi, I., Hertkorn, N., Schmitt-Kopplin, P., 2009. The chemodiversity of wines can reveal a metabologeography expression of cooperage oak wood. Proceedings of the National Academy of Sciences 106, 9174–9179. https://doi.org/10.1073/pnas.0901100106

Gowda, G.A.N., Djukovic, D., 2014. Overview of Mass Spectrometry-Based Metabolomics: Opportunities and Challenges. Methods Mol Biol 1198, 3–12. https://doi.org/10.1007/978-1-4939-1258-2_1

Grassl, J., Taylor, N.L., Millar, A.H., 2011. Matrix-assisted laser desorption/ionisation mass spectrometry imaging and its development for plant protein imaging. Plant Methods 7, 21. https://doi.org/10.1186/1746-4811-7-21

Grimplet, J., Cramer, G.R., Dickerson, J.A., Mathiason, K., Van Hemert, J., Fennell, A.Y., 2009. VitisNet: "Omics" integration through grapevine molecular networks. PLoS ONE 4, e8365. https://doi.org/10.1371/journal.pone.0008365

Gross, J.H., 2017. Mass Spectrometry: A Textbook, 3rd ed. Springer International Publishing. https://doi.org/10.1007/978-3-319-54398-7

Guijas, C., Montenegro-Burke, J.R., Domingo-Almenara, X., Palermo, A., Warth, B., Hermann, G., Koellensperger, G., Huan, T., Uritboonthai, W., Aisporna, A.E., Wolan, D.W., Spilker, M.E., Benton, H.P., Siuzdak, G., 2018. METLIN: A Technology Platform for Identifying Knowns and Unknowns. Anal. Chem. 90, 3156–3164. https://doi.org/10.1021/acs.analchem.7b04424

Gull, A., Lone, A.A., Wani, N.U.I., 2019. Biotic and Abiotic Stresses in Plants. Abiotic and Biotic Stress in Plants. https://doi.org/10.5772/intechopen.85832

Haijes, H.A., Willemsen, M., Van der Ham, M., Gerrits, J., Pras-Raves, M.L., Prinsen, H.C.M.T., Van Hasselt, P.M., De Sain-van der Velden, M.G.M., Verhoeven-Duif, N.M., Jans, J.J.M., 2019. Direct Infusion Based Metabolomics Identifies Metabolic Disease in Patients' Dried Blood Spots and Plasma. Metabolites 9, 12. https://doi.org/10.3390/metabo9010012

Hansen, R.L., Guo, H., Yin, Y., Lee, Y.J., 2019. FERONIA mutation induces high levels of chloroplast-localized Arabidopsides which are involved in root growth. Plant J 97, 341–351. https://doi.org/10.1111/tpj.14123

He, L., Rockwood, A.L., Agarwal, A.M., Anderson, L.C., Weisbrod, C.R., Hendrickson, C.L., Marshall, A.G., 2019. Diagnosis of Hemoglobinopathy and β-Thalassemia by 21 Tesla Fourier Transform Ion Cyclotron Resonance Mass Spectrometry and Tandem Mass Spectrometry of Hemoglobin from Blood. Clinical Chemistry 65, 986–994. https://doi.org/10.1373/clinchem.2018.295766

He, Z., Sleighter, R.L., Hatcher, P.G., Liu, S., Wu, F., Zou, H., Olanya, O.M., 2019. Molecular level comparison of water extractives of maple and oak with negative and positive ion ESI FT-ICR mass spectrometry. J Mass Spectrom 54, 655–666. https://doi.org/10.1002/jms.4379

Hendrickson, C.L., Quinn, J.P., Kaiser, N.K., Smith, D.F., Blakney, G.T., Chen, T., Marshall, A.G., Weisbrod, C.R., Beu, S.C., 2015. 21 Tesla Fourier Transform Ion Cyclotron Resonance Mass Spectrometer: A National Resource for Ultrahigh Resolution Mass Analysis. J. Am. Soc. Mass Spectrom. 26, 1626–1632. https://doi.org/10.1007/s13361-015-1182-2

Herzog, R., Schwudke, D., Schuhmann, K., Sampaio, J.L., Bornstein, S.R., Schroeder, M., Shevchenko, A., 2011. A novel informatics concept for high-throughput shotgun lipidomics based on the molecular fragmentation query language. Genome Biol 12, R8. https://doi.org/10.1186/gb-2011-12-1-r8

Hill, C.B., Taylor, J.D., Edwards, J., Mather, D., Langridge, P., Bacic, A., Roessner, U., 2015. Detection of QTL for metabolic and agronomic traits in wheat with adjustments for variation at genetic loci that affect plant phenology. Plant Science 233, 143–154. https://doi.org/10.1016/j.plantsci.2015.01.008

Hipple, J.A., Sommer, H., Thomas, H.A., 1949. A Precise Method of Determining the Faraday by Magnetic Resonance. Phys. Rev. 76, 1877–1878. https://doi.org/10.1103/PhysRev.76.1877.2

Hirai, M.Y., Yano, M., Goodenowe, D.B., Kanaya, S., Kimura, T., Awazuhara, M., Arita, M., Fujiwara, T., Saito, K., 2004. Integration of transcriptomics and metabolomics for understanding of global responses to nutritional stresses in Arabidopsis thaliana. Proc Natl Acad Sci U S A 101, 10205–10210. https://doi.org/10.1073/pnas.0403218101

Hiraoka, K., 2013. Fundamentals of Mass Spectrometry. Springer Science & Business Media.

Hong, Y.-S., Martinez, A., Liger-Belair, G., Jeandet, P., Nuzillard, J.-M., Cilindre, C., 2012. Metabolomics reveals simultaneous influences of plant defence system and fungal growth in Botrytis cinerea-infected Vitis vinifera cv. Chardonnay berries. J. Exp. Bot. 63, 5773–5785. https://doi.org/10.1093/jxb/ers228

Hopfgartner, G., 2011. Can MS fully exploit the benefits of fast chromatography? Bioanalysis 3, 121–123. https://doi.org/10.4155/bio.10.191

Horai, H., Arita, M., Kanaya, S., Nihei, Y., Ikeda, T., Suwa, K., Ojima, Y., Tanaka, Kenichi, Tanaka, S., Aoshima, K., Oda, Y., Kakazu, Y., Kusano, M., Tohge, T., Matsuda, F., Sawada, Y., Hirai, M.Y., Nakanishi, H., Ikeda, K., Akimoto, N., Maoka, T., Takahashi, H., Ara, T., Sakurai, N., Suzuki, H., Shibata, D., Neumann, S., Iida, T., Tanaka, Ken, Funatsu, K., Matsuura, F., Soga, T., Taguchi, R., Saito, K., Nishioka, T., 2010. MassBank: a public repository for sharing mass spectral data for life sciences. J Mass Spectrom 45, 703–714. https://doi.org/10.1002/jms.1777

Horning, E.C., Horning, M.G., 1971. Metabolic Profiles: Gas-Phase Methods for Analysis of Metabolites. Clinical Chemistry 17, 802–809. https://doi.org/10.1093/clinchem/17.8.802

Huang, X., Song, F., Liu, Z., Liu, S., 2008. Structural characterization and identification of dibenzocyclooctadiene lignans in Fructus Schisandrae using electrospray ionization ion trap multiple-stage tandem mass spectrometry and electrospray ionization Fourier transform ion cyclotron resonance multiple-stage tandem mass spectrometry. Analytica Chimica Acta 615, 124–135. https://doi.org/10.1016/j.aca.2008.03.056

Huang, X., Song, F., Liu, Z., Liu, S., 2007. Studies on lignan constituents fromSchisandra chinensis (Turcz.) Baill. fruits using high-performance liquid chromatography/electrospray ionization multiple-stage tandem mass spectrometry. J. Mass Spectrom. 42, 1148–1161. https://doi.org/10.1002/jms.1246

Hufsky, F., Scheubert, K., Böcker, S., 2014. New kids on the block: novel informatics methods for natural product discovery. Nat Prod Rep 31, 807–817. https://doi.org/10.1039/c3np70101h

Hughey, C.A., Rodgers, R.P., Marshall, A.G., 2002. Resolution of 11,000 compositionally distinct components in a single electrospray ionization Fourier transform ion cyclotron resonance mass spectrum of crude oil. Anal Chem 74, 4145–4149. https://doi.org/10.1021/ac020146b

Huong, T.T., Cuong, N.X., Tram, L.H., Quang, T.T., Duong, L.V., Nam, N.H., Dat, N.T., Huong, P.T.T., Diep, C.N., Kiem, P.V., Minh, C.V., 2012. A new prenylated aurone from *Artocarpus altilis*. Journal of Asian Natural Products Research 14, 923–928. https://doi.org/10.1080/10286020.2012.702758

Iijima, Y., Watanabe, B., Sasaki, R., Takenaka, M., Ono, H., Sakurai, N., Umemoto, N., Suzuki, H., Shibata, D., Aoki, K., 2013. Steroidal glycoalkaloid profiling and structures of glycoalkaloids in wild tomato fruit. Phytochemistry 95, 145–157. https://doi.org/10.1016/j.phytochem.2013.07.016

Ingallina, C., Maccelli, A., Spano, M., Di Matteo, G., Di Sotto, A., Giusti, A.M., Vinci, G., Di Giacomo, S., Rapa, M., Ciano, S., Fraschetti, C., Filippi, A., Simonetti, G., Cordeiro, C., Sousa Silva, M., Crestoni, M.E., Sobolev, A.P., Fornarini, S., Mannina, L., 2020. Chemico-Biological Characterization of Torpedino Di Fondi® Tomato Fruits: A Comparison with San Marzano Cultivar at Two Ripeness Stages. Antioxidants 9, 1027. https://doi.org/10.3390/antiox9101027

International Organisation of Vine and Wine, 2020. 2020 Wine Production - OIV First Estimates.

Janz, D., Behnke, K., Schnitzler, J.-P., Kanawati, B., Schmitt-Kopplin, P., Polle, A., 2010. Pathway analysis of the transcriptome and metabolome of salt sensitive and tolerant

poplar species reveals evolutionary adaption of stress tolerance mechanisms. BMC Plant Biol 10, 150. https://doi.org/10.1186/1471-2229-10-150

Jorge, T.F., Rodrigues, J.A., Caldana, C., Schmidt, R., van Dongen, J.T., Thomas-Oates, J., António, C., 2015. Mass spectrometry-based plant metabolomics: Metabolite responses to abiotic stress: MASS SPECTROMETRY-BASED PLANT METABOLOMICS. Mass Spectrometry Reviews n/a-n/a. https://doi.org/10.1002/mas.21449

Junot, C., Fenaille, F., Colsch, B., Bécher, F., 2014. High resolution mass spectrometry based techniques at the crossroads of metabolic pathways: HIGH RESOLUTION MASS SPECTROMETRY FOR METABOLOMICS. Mass Spec Rev 33, 471–500. https://doi.org/10.1002/mas.21401

Junot, C., Madalinski, G., Tabet, J.-C., Ezan, E., 2010. Fourier transform mass spectrometry for metabolome analysis. Analyst 135, 2203. https://doi.org/10.1039/c0an00021c

Kai, K., Hashidzume, H., Yoshimura, K., Suzuki, H., Sakurai, N., Shibata, D., Ohta, D., 2009. Metabolomics for the characterization of cytochromes P450-dependent fatty acid hydroxylation reactions in Arabidopsis. Plant Biotechnology 26, 175–182. https://doi.org/10.5511/plantbiotechnology.26.175

Kaling, M., Kanawati, B., Ghirardo, A., Albert, A., Winkler, J.B., Heller, W., Barta, C., Loreto, F., Schmitt-Kopplin, P., Schnitzler, J.-P., 2015. UV-B mediated metabolic rearrangements in poplar revealed by non-targeted metabolomics: Poplar metabolome under UV stress. Plant Cell Environ 38, 892–904. https://doi.org/10.1111/pce.12348

Kanawati, B., Schmitt-Kopplin, P., 2019. Fundamentals and Applications of Fourier Transform Mass Spectrometry. Elsevier. https://doi.org/10.1016/C2016-0-04234-1

Karas, Michael., Bachmann, Doris., Hillenkamp, Franz., 1985. Influence of the wavelength in high-irradiance ultraviolet laser desorption mass spectrometry of organic molecules. Anal. Chem. 57, 2935–2939. https://doi.org/10.1021/ac00291a042

Karas, Michael., Hillenkamp, Franz., 1988. Laser desorption ionization of proteins with molecular masses exceeding 10,000 daltons. Anal. Chem. 60, 2299–2301. https://doi.org/10.1021/ac00171a028

Karp, P.D., Latendresse, M., Caspi, R., 2011. The Pathway Tools Pathway Prediction Algorithm. Standards in Genomic Sciences 5, 424. https://doi.org/10.4056/sigs.1794338

Khamko, V.A., Quang, D.N., Dien, P.H., 2013. Three new phenanthrenes, a new stilbenoid isolated from the roots of *Stemona tuberosa* Lour. and their cytotoxicity. Natural Product Research 27, 2328–2332. https://doi.org/10.1080/14786419.2013.832677

Khan, S.A., Chibon, P.-Y., de Vos, R.C.H., Schipper, B.A., Walraven, E., Beekwilder, J., van Dijk, T., Finkers, R., Visser, R.G.F., van de Weg, E.W., Bovy, A., Cestaro, A., Velasco,

R., Jacobsen, E., Schouten, H.J., 2012. Genetic analysis of metabolites in apple fruits indicates an mQTL hotspot for phenolic compounds on linkage group 16. Journal of Experimental Botany 63, 2895–2908. https://doi.org/10.1093/jxb/err464

Kopka, J., Fernie, A., Weckwerth, W., Gibon, Y., Stitt, M., 2004. Metabolite profiling in plant biology: Platforms and destinations. Genome biology 5, 109. https://doi.org/10.1186/gb-2004-5-6-109

Koşar, M., Küpeli, E., Malyer, H., Uylaşer, V., Türkben, C., Başer, K.H.C., 2007. Effect of Brining on Biological Activity of Leaves of *Vitis vinifera* L. (Cv. Sultani Çekirdeksiz) from Turkey. Journal of Agricultural and Food Chemistry 55, 4596–4603. https://doi.org/10.1021/jf070130s

Kostyukevich, Y.I., Vladimirov, G.N., Nikolaev, E.N., 2012. Dynamically Harmonized FT-ICR Cell with Specially Shaped Electrodes for Compensation of Inhomogeneity of the Magnetic Field. Computer Simulations of the Electric Field and Ion Motion Dynamics. J. Am. Soc. Mass Spectrom. 23, 2198–2207. https://doi.org/10.1007/s13361-012-0480-1

Krettler, C.A., Thallinger, G.G., 2021. A map of mass spectrometry-based in silico fragmentation prediction and compound identification in metabolomics. Briefings in Bioinformatics. https://doi.org/10.1093/bib/bbab073

Kueger, S., Steinhauser, D., Willmitzer, L., Giavalisco, P., 2012. High-resolution plant metabolomics: from mass spectral features to metabolites and from whole-cell analysis to subcellular metabolite distributions. Plant J 70, 39–50. https://doi.org/10.1111/j.1365-313X.2012.04902.x

Kuhnert, N., 2010. Unraveling the structure of the black tea thearubigins. Archives of Biochemistry and Biophysics 501, 37–51. https://doi.org/10.1016/j.abb.2010.04.013

Kuhnert, N., Drynan, J.W., Obuchowicz, J., Clifford, M.N., Witt, M., 2010. Mass spectrometric characterization of black tea thearubigins leading to an oxidative cascade hypothesis for thearubigin formation. Rapid Communications in Mass Spectrometry 24, 3387–3404. https://doi.org/10.1002/rcm.4778

Laluk, K., Mengiste, T., 2010. Necrotroph attacks on plants: wanton destruction or covert extortion? Arabidopsis Book 8, e0136. https://doi.org/10.1199/tab.0136

Lawrence, E.O., Alvarez, L.W., Brobeck, W.M., Cooksey, D., Corson, D.R., McMillan, E.M., Salisbury, W.W., Thornton, R.L., 1939. Initial Performance of the 60-Inch Cyclotron of the William H. Crocker Radiation Laboratory, University of California. Phys. Rev. 56, 124–124. https://doi.org/10.1103/PhysRev.56.124

Lawrence, E.O., Livingston, M.S., 1932. The Production of High Speed Light Ions Without the Use of High Voltages. Phys. Rev. 40, 19–35. https://doi.org/10.1103/PhysRev.40.19

Leader, D.P., Burgess, K., Creek, D., Barrett, M.P., 2011. Pathos: A web facility that uses metabolic maps to display experimental changes in metabolites identified by mass spectrometry. Rapid Communications in Mass Spectrometry 25, 3422–3426. https://doi.org/10.1002/rcm.5245

Ledesma-Escobar, C.A., Luque de Castro, M.D., 2015. Coverage Exploitation of By-Products from the Agrofood Industry, in: Chemat, F., Strube, J. (Eds.), Green Extraction of Natural Products. Wiley-VCH Verlag GmbH & Co. KGaA, pp. 265–306.

Lee, E.D., Mueck, W., Henion, J.D., Covey, T.R., 1989. Real-time reaction monitoring by continuous-introduction ion-spray tandem mass spectrometry. J. Am. Chem. Soc. 111, 4600–4604. https://doi.org/10.1021/ja00195a012

Leon, C., Rodriguez-Meizoso, I., Lucio, M., Garcia-Cañas, V., Ibañez, E., Schmitt-Kopplin, P., Cifuentes, A., 2009. Metabolomics of transgenic maize combining Fourier transform-ion cyclotron resonance-mass spectrometry, capillary electrophoresis-mass spectrometry and pressurized liquid extraction. Journal of Chromatography A 1216, 7314–7323. https://doi.org/10.1016/j.chroma.2009.04.092

Li, H., Song, F., Zheng, Z., Liu, Z., Liu, S., 2008. Characterization of saccharides and phenolic acids in the Chinese herb Tanshen by ESI-FT-ICR-MS and HPLC. J. Mass Spectrom. 43, 1545–1552. https://doi.org/10.1002/jms.1441

Li, L., Li, R., Zhou, J., Zuniga, A., Stanislaus, A.E., Wu, Y., Huan, T., Zheng, J., Shi, Y., Wishart, D.S., Lin, G., 2013. MyCompoundID: Using an Evidence-Based Metabolome Library for Metabolite Identification. Anal. Chem. 85, 3401–3408. https://doi.org/10.1021/ac400099b

Liang, Z., Duan, S., Sheng, J., Zhu, S., Ni, X., Shao, J., Liu, C., Nick, P., Du, F., Fan, P., Mao, R., Zhu, Yifan, Deng, W., Yang, M., Huang, H., Liu, Y., Ding, Y., Liu, X., Jiang, J., Zhu, Youyong, Li, S., He, X., Chen, W., Dong, Y., 2019. Whole-genome resequencing of 472 Vitis accessions for grapevine diversity and demographic history analyses. Nature Communications 10, 1190. https://doi.org/10.1038/s41467-019-09135-8

Lima, A., Bento, A., Baraldi, I., Malheiro, R., 2016. Selection of grapevine leaf varieties for culinary process based on phytochemical composition and antioxidant properties. Food Chemistry 212, 291–295. https://doi.org/10.1016/j.foodchem.2016.05.177

Maccelli, A., Cesa, S., Cairone, F., Secci, D., Menghini, L., Chiavarino, B., Fornarini, S., Crestoni, M.E., Locatelli, M., 2020a. Metabolic profiling of different wild and cultivated Allium species based on high-resolution mass spectrometry, high-performance liquid chromatography-photodiode array detector, and color analysis. Journal of Mass Spectrometry 55, e4525. https://doi.org/10.1002/jms.4525

Maccelli, A., Cesa, S., Cairone, F., Secci, D., Menghini, L., Chiavarino, B., Fornarini, S., Crestoni, M.E., Locatelli, M., 2020b. Metabolic profiling of different wild and cultivated Allium species based on high-resolution mass spectrometry, high-

performance liquid chromatography-photodiode array detector, and color analysis. Journal of Mass Spectrometry 55, e4525. https://doi.org/10.1002/jms.4525

Maia, M., Ferreira, A.E.N., Cunha, J., Eiras-Dias, J., Cordeiro, C., Figueiredo, A., Sousa Silva, M., 2021a. Comparison of the chemical diversity of Vitis rotundifolia and Vitis vinifera cv. 'Cabernet Sauvignon.' Ciência Téc. Vitiv. 36, 1–8. https://doi.org/10.1051/ctv/20213601001

Maia, M., Ferreira, A.E.N., Cunha, J., Eiras-Dias, J., Cordeiro, C., Figueiredo, A., Sousa Silva, M., 2021b. Comparison of the chemical diversity of Vitis rotundifolia and Vitis vinifera cv. 'Cabernet Sauvignon.' Ciência Téc. Vitiv. 36, 1–8. https://doi.org/10.1051/ctv/20213601001

Maia, Marisa, Ferreira, A.E.N., Laureano, G., Marques, A.P., Torres, V.M., Silva, A.B., Matos, A.R., Cordeiro, C., Figueiredo, A., Sousa Silva, M., 2019a. *Vitis vinifera* 'Pinot noir' leaves as a source of bioactive nutraceutical compounds. Food & Function 10, 3822–3827. https://doi.org/10.1039/C8FO02328J

Maia, M., Ferreira, A.E.N., Marques, A.P., Figueiredo, J., Freire, A.P., Cordeiro, C., Figueiredo, A., Silva, M.S., 2018. Uncovering markers for downy mildew resistance in grapevine through mass spectrometry-based metabolomics. Rev. Ciênc. Agr. 41, 48–53. https://doi.org/10.19084/rca.17066

Maia, M., Ferreira, A.E.N., Marques, A.P., Figueiredo, J., Freire, A.P., Cordeiro, C., Figueiredo, A., Sousa Silva, M.S., 2019. Uncovering markers for downy mildew resistance in grapevine through mass spectrometry-based metabolomics. Rev. Ciênc. Agr. 41, 48–53. https://doi.org/10.19084/RCA.17066

Maia, M., Ferreira, A.E.N., Nascimento, R., Monteiro, F., Traquete, F., Marques, A.P., Cunha, J., Eiras-Dias, J.E., Cordeiro, C., Figueiredo, A., Sousa Silva, M., 2020. Integrating metabolomics and targeted gene expression to uncover potential biomarkers of fungal/oomycetes-associated disease susceptibility in grapevine. Sci. Rep. 10, 15688. https://doi.org/10.1038/s41598-020-72781-2

Maia, Marisa, Maccelli, A., Nascimento, R., Ferreira, A.E.N., Crestoni, M.E., Cordeiro, C., Figueiredo, A., Sousa Silva, M., 2019b. Early detection of Plasmopara viticola-infected leaves through FT-ICR-MS metabolic profiling | International Society for Horticultural Science Acta Horticulturae 1248, 575–580. https://doi.org/10.17660/ActaHortic.2019.1248.77

Maia, M., Monteiro, F., Sebastiana, M., Marques, A.P., Ferreira, A.E.N., Freire, A.P., Cordeiro, C., Figueiredo, A., Sousa Silva, M., 2016. Metabolite extraction for high-throughput FTICR-MS-based metabolomics of grapevine leaves. EuPA Open Proteom 12, 4–9. https://doi.org/10.1016/j.euprot.2016.03.002

Makarov, A., 2000. Electrostatic Axially Harmonic Orbital Trapping: A High-Performance Technique of Mass Analysis. Anal. Chem. 72, 1156–1162. https://doi.org/10.1021/ac991131p

Martins, J.L.R., Rodrigues, O.R.L., da Silva, D.M., Galdino, P.M., de Paula, J.R., Romão, W., da Costa, H.B., Vaz, B.G., Ghedini, P.C., Costa, E.A., 2014. Mechanisms involved in the gastroprotective activity of Celtis iguanaea (Jacq.) Sargent on gastric lesions in mice. Journal of Ethnopharmacology 155, 1616–1624. https://doi.org/10.1016/j.jep.2014.08.006

Matus-Cádiz, M.A., Daskalchuk, T.E., Verma, B., Puttick, D., Chibbar, R.N., Gray, G.R., Perron, C.E., Tyler, R.T., Hucl, P., 2008. Phenolic Compounds Contribute to Dark Bran Pigmentation in Hard White Wheat. J. Agric. Food Chem. 56, 1644–1653. https://doi.org/10.1021/jf072970c

Menikarachchi, L.C., Hill, D.W., Hamdalla, M.A., Mandoiu, I.I., Grant, D.F., 2013. In Silico Enzymatic Synthesis of a 400 000 Compound Biochemical Database for Nontargeted Metabolomics. J. Chem. Inf. Model. 53, 2483–2492. https://doi.org/10.1021/ci400368v

Merdinoglu, D., Blasi, P., Wiedemann-Merdinoglu, S., Mestre, P., Peressotti, E., Poutaraud, A., Prado, E., Schneider, C., 2010. Breeding for durable resistance to downy and powdery mildew in grapevine, in: X International Conference on Grapevine Breeding and Genetics 1046. pp. 65–72.

Miao, Y., Lv, J., Huang, H., Cao, D., Zhang, S., 2020. Molecular characterization of root exudates using Fourier transform ion cyclotron resonance mass spectrometry. Journal of Environmental Sciences 98, 22–30. https://doi.org/10.1016/j.jes.2020.05.011

Misra, B.B., 2021. New software tools, databases, and resources in metabolomics: updates from 2020. Metabolomics 17, 49. https://doi.org/10.1007/s11306-021-01796-1

Moore, B.M., Wang, P., Fan, P., Lee, A., Leong, B., Lou, Y.-R., Schenck, C.A., Sugimoto, K., Last, R., Lehti-Shiu, M.D., Barry, C.S., Shiu, S.-H., 2020. Within- and cross-species predictions of plant specialized metabolism genes using transfer learning. in silico Plants 2. https://doi.org/10.1093/insilicoplants/diaa005

Mungur, R., Glass, A.D.M., Goodenow, D.B., Lightfoot, D.A., 2005. Metabolite Fingerprinting in Transgenic *Nicotiana tabacum* Altered by the *Escherichia coli* Glutamate Dehydrogenase Gene. Journal of Biomedicine and Biotechnology 2005, 198–214. https://doi.org/10.1155/JBB.2005.198

Nagornov, K.O., Gorshkov, M.V., Kozhinov, A.N., Tsybin, Y.O., 2014. High-Resolution Fourier Transform Ion Cyclotron Resonance Mass Spectrometry with Increased Throughput for Biomolecular Analysis. Anal. Chem. 86, 9020–9028. https://doi.org/10.1021/ac501579h

Nakabayashi, R., Sawada, Y., Aoyagi, M., Yamada, Y., Hirai, M.Y., Sakurai, T., Kamoi, T., Rowan, D.D., Saito, K., 2016. Chemical Assignment of Structural Isomers of Sulfur-Containing Metabolites in Garlic by Liquid Chromatography–Fourier Transform Ion Cyclotron Resonance–Mass Spectrometry. The Journal of Nutrition 146, 397S-402S. https://doi.org/10.3945/jn.114.202317

Nakabayashi, R., Sawada, Y., Yamada, Y., Suzuki, M., Hirai, M.Y., Sakurai, T., Saito, K., 2013. Combination of Liquid Chromatography–Fourier Transform Ion Cyclotron Resonance-Mass Spectrometry with ^{13}C-Labeling for Chemical Assignment of Sulfur-Containing Metabolites in Onion Bulbs. Anal. Chem. 85, 1310–1315. https://doi.org/10.1021/ac302733c

Nakamura, Y., Kimura, A., Saga, H., Oikawa, A., Shinbo, Y., Kai, K., Sakurai, N., Suzuki, H., Kitayama, M., Shibata, D., Kanaya, S., Ohta, D., 2007. Differential metabolomics unraveling light/dark regulation of metabolic activities in Arabidopsis cell culture. Planta 227, 57–66. https://doi.org/10.1007/s00425-007-0594-z

Nascimento, R., Maia, M., Ferreira, A.E.N., Silva, A.B., Freire, A.P., Cordeiro, C., Sousa Silva, M., Figueiredo, A., 2019. Early stage metabolic events associated with the establishment of Vitis vinifera – Plasmopara viticola compatible interaction. Plant Physiol Biochem 137, 1–13. https://doi.org/10.1016/j.plaphy.2019.01.026

Nicholson, J.K., Lindon, J.C., Holmes, E., 1999. "Metabonomics": understanding the metabolic responses of living systems to pathophysiological stimuli via multivariate statistical analysis of biological NMR spectroscopic data. Xenobiotica 29, 1181–1189. https://doi.org/10.1080/004982599238047

Nobel Prize, 2002. The Nobel Prize in Chemistry 2002 [WWW Document]. NobelPrize.org. URL https://www.nobelprize.org/prizes/chemistry/2002/fenn/facts/ (accessed 4.8.21).

Nobel Prize, 1989. The Nobel Prize in Physics 1989 [WWW Document]. NobelPrize.org. URL https://www.nobelprize.org/prizes/physics/1989/dehmelt/facts/ (accessed 4.8.21).

Nobel Prize, 1939. The Nobel Prize in Physics 1939 [WWW Document]. NobelPrize.org. URL https://www.nobelprize.org/prizes/physics/1939/lawrence/biographical/ (accessed 4.8.21).

Nobel Prize, 1922. The Nobel Prize in Chemistry 1922 [WWW Document]. NobelPrize.org. URL https://www.nobelprize.org/prizes/chemistry/1922/aston/facts/ (accessed 4.8.21).

Nobel Prize, 1906. The Nobel Prize in Physics 1906 [WWW Document]. NobelPrize.org. URL https://www.nobelprize.org/prizes/physics/1906/thomson/facts/ (accessed 4.8.21).

Ogawa, E.M., Costa, H.B., Ventura, J.A., Caetano, L.C., Pinto, F.E., Oliveira, B.G., Barroso, M.E.S., Scherer, R., Endringer, D.C., Romão, W., 2018. Chemical profile of pineapple

cv. Vitória in different maturation stages using electrospray ionization mass spectrometry: Chemical profile of Vitória pineapple. J. Sci. Food Agric 98, 1105–1116. https://doi.org/10.1002/jsfa.8561

Ohnishi, M., Anegawa, A., Sugiyama, Y., Harada, K., Oikawa, A., Nakayama, Y., Matsuda, F., Nakamura, Y., Sasaki, R., Shichijo, C., Hatcher, P.G., Fukaki, H., Kanaya, S., Aoki, K., Yamazaki, M., Fukusaki, E., Saito, K., Mimura, T., 2018. Molecular components of Arabidopsis intact vacuoles clarified with metabolomic and proteomic analyses. Plant and Cell Physiology. https://doi.org/10.1093/pcp/pcy069

Ohta, D., Shibata, D., Kanaya, S., 2007. Metabolic profiling using Fourier-transform ion-cyclotron-resonance mass spectrometry. Anal Bioanal Chem 389, 1469–1475. https://doi.org/10.1007/s00216-007-1650-z

Oikawa, A., Nakamura, Y., Ogura, T., Kimura, A., Suzuki, H., Sakurai, N., Shinbo, Y., Shibata, D., Kanaya, S., Ohta, D., 2006. Clarification of pathway-specific inhibition by Fourier transform ion cyclotron resonance/mass spectrometry-based metabolic phenotyping studies. Plant Physiol. 142, 398–413. https://doi.org/10.1104/pp.106.080317

Oliveira, B.G., Costa, H.B., Ventura, J.A., Kondratyuk, T.P., Barroso, M.E.S., Correia, R.M., Pimentel, E.F., Pinto, F.E., Endringer, D.C., Romão, W., 2016. Chemical profile of mango (Mangifera indica L.) using electrospray ionisation mass spectrometry (ESI-MS). Food Chemistry 204, 37–45. https://doi.org/10.1016/j.foodchem.2016.02.117

Oliver, S.G., Winson, M.K., Kell, D.B., Baganz, F., 1998. Systematic functional analysis of the yeast genome. Trends Biotechnol 16, 373–378. https://doi.org/10.1016/s0167-7799(98)01214-1

Organisation of Vine and Wine, 2020. 2020 State of the world vitivinicultural sector.

Organisation of Vine and Wine, 2019. The distribution of the world's grapevine varieties.

Orhan, D.D., Orhan, N., Ergun, E., Ergun, F., 2007. Hepatoprotective effect of Vitis vinifera L. leaves on carbon tetrachloride-induced acute liver damage in rats. Journal of Ethnopharmacology 112, 145–151. https://doi.org/10.1016/j.jep.2007.02.013

Pari, L., Suresh, A., 2008. Effect of grape (Vitis vinifera L.) leaf extract on alcohol induced oxidative stress in rats. Food and Chemical Toxicology 46, 1627–1634. https://doi.org/10.1016/j.fct.2008.01.003

Park, K., Kim, M., Baek, S., Bae, I., Seo, S.-W., Kim, J., Shin, Y., Lee, Y.-M., Kim, H., 2013. Simultaneous molecular formula determinations of natural compounds in a plant extract using 15 T Fourier transform ion cyclotron resonance mass spectrometry. Plant Methods 9, 15. https://doi.org/10.1186/1746-4811-9-15

Park, S.-G., Anderson, G.A., Bruce, J.E., 2020. Parallel Detection of Fundamental and Sixth Harmonic Signals Using an ICR Cell with Dipole and Sixth Harmonic Detectors. J. Am. Soc. Mass Spectrom. 31, 719–726. https://doi.org/10.1021/jasms.9b00144

Park, S.-G., Anderson, G.A., Bruce, J.E., 2017. Parallel Spectral Acquisition with Orthogonal ICR Cells. J. Am. Soc. Mass Spectrom. 28, 515–524. https://doi.org/10.1007/s13361-016-1573-z

Park, S.-G., Anderson, G.A., Navare, A.T., Bruce, J.E., 2016. Parallel Spectral Acquisition with an Ion Cyclotron Resonance Cell Array. Anal. Chem. 88, 1162–1168. https://doi.org/10.1021/acs.analchem.5b02987

Park, S.-G., Mohr, J.P., Anderson, G.A., Bruce, J.E., 2021. Application of frequency multiple FT-ICR MS signal acquisition for improved proteome research. International Journal of Mass Spectrometry 465, 116578. https://doi.org/10.1016/j.ijms.2021.116578

Park, Y.J., Seong, S.H., Kim, M.S., Seo, S.W., Kim, M.R., Kim, H.S., 2017. High-throughput detection of antioxidants in mulberry fruit using correlations between high-resolution mass and activity profiles of chromatographic fractions. Plant Methods 13, 108. https://doi.org/10.1186/s13007-017-0258-3

Paul, W., Steinwedel, H., 1953. Notizen: Ein neues Massenspektrometer ohne Magnetfeld. Zeitschrift Naturforschung Teil A 8, 448–450. https://doi.org/10.1515/zna-1953-0710

Pelander, A., Decker, P., Baessmann, C., Ojanperä, I., 2011. Evaluation of a High Resolving Power Time-of-Flight Mass Spectrometer for Drug Analysis in Terms of Resolving Power and Acquisition Rate. J. Am. Soc. Mass Spectrom. 22, 379–385. https://doi.org/10.1007/s13361-010-0046-z

Peressotti, E., Wiedemann-Merdinoglu, S., Delmotte, F., Bellin, D., Di Gaspero, G., Testolin, R., Merdinoglu, D., Mestre, P., 2010. Breakdown of resistance to grapevine downy mildew upon limited deployment of a resistant variety. BMC Plant Biology 10, 147. https://doi.org/10.1186/1471-2229-10-147

Peters, K., Balcke, G., Kleinenkuhnen, N., Treutler, H., Neumann, S., 2021. Untargeted In Silico Compound Classification—A Novel Metabolomics Method to Assess the Chemodiversity in Bryophytes. International Journal of Molecular Sciences 22, 3251. https://doi.org/10.3390/ijms22063251

Piasecka, A., Kachlicki, P., Stobiecki, M., 2019. Analytical Methods for Detection of Plant Metabolomes Changes in Response to Biotic and Abiotic Stresses. IJMS 20, 379. https://doi.org/10.3390/ijms20020379

Pinu, F.R., 2018. Grape and Wine Metabolomics to Develop New Insights Using Untargeted and Targeted Approaches. Fermentation 4, 92. https://doi.org/10.3390/fermentation4040092

Pollier, J., Morreel, K., Geelen, D., Goossens, A., 2011. Metabolite Profiling of Triterpene Saponins in *Medicago truncatula* Hairy Roots by Liquid Chromatography Fourier Transform Ion Cyclotron Resonance Mass Spectrometry. J. Nat. Prod. 74, 1462–1476. https://doi.org/10.1021/np200218r

Pollier, J., Moses, T., González-Guzmán, M., De Geyter, N., Lippens, S., Bossche, R.V., Marhavý, P., Kremer, A., Morreel, K., Guérin, C.J., Tava, A., Oleszek, W., Thevelein, J.M., Campos, N., Goormachtig, S., Goossens, A., 2013. The protein quality control system manages plant defence compound synthesis. Nature 504, 148–152. https://doi.org/10.1038/nature12685

Prins, T.W., Tudzynski, P., von Tiedemann, A., Tudzynski, B., Ten Have, A., Hansen, M.E., Tenberge, K., van Kan, J.A.L., 2000. Infection Strategies of Botrytis cinerea and Related Necrotrophic Pathogens, in: Kronstad, J.W. (Ed.), Fungal Pathology. Springer Netherlands, Dordrecht, pp. 33–64. https://doi.org/10.1007/978-94-015-9546-9_2

Qin, L., Zhang, Y., Liu, Y., He, H., Han, M., Li, Y., Zeng, M., Wang, X., 2018. Recent advances in matrix-assisted laser desorption/ionisation mass spectrometry imaging (MALDI-MSI) for *in situ* analysis of endogenous molecules in plants. Phytochemical Analysis 29, 351–364. https://doi.org/10.1002/pca.2759

Qin, Y., Wysocki, R.J., Somogyi, A., Feinstein, Y., Franco, J.Y., Tsukamoto, T., Dunatunga, D., Levy, C., Smith, S., Simpson, R., Gang, D., Johnson, M.A., Palanivelu, R., 2011. Sulfinylated azadecalins act as functional mimics of a pollen germination stimulant in Arabidopsis pistils: Sulfinylated azadecalins and stimulation of pollen germination. The Plant Journal 68, 800–815. https://doi.org/10.1111/j.1365-313X.2011.04729.x

Razzaq, A., Sadia, B., Raza, A., Khalid Hameed, M., Saleem, F., 2019. Metabolomics: A Way Forward for Crop Improvement. Metabolites 9. https://doi.org/10.3390/metabo9120303

Reeves, S.G., Somogyi, A., Zeller, W.E., Ramelot, T.A., Wrighton, K.C., Hagerman, A.E., 2020. Proanthocyanidin Structural Details Revealed by Ultrahigh Resolution FT-ICR MALDI-Mass Spectrometry, ^{1}H–^{13}C HSQC NMR, and Thiolysis-HPLC–DAD. J. Agric. Food Chem. 68, 14038–14048. https://doi.org/10.1021/acs.jafc.0c04877

Rizzuti, A., Caliandro, R., Gallo, V., Mastrorilli, P., Chita, G., Latronico, M., 2013. A combined approach for characterisation of fresh and brined vine leaves by X-ray powder diffraction, NMR spectroscopy and direct infusion high resolution mass spectrometry. Food Chemistry 141, 1908–1915. https://doi.org/10.1016/j.foodchem.2013.05.044

Roberts, L.D., Souza, A.L., Gerszten, R.E., Clish, C.B., 2012. Targeted Metabolomics. Current Protocols in Molecular Biology 98. https://doi.org/10.1002/0471142727.mb3002s98

Rogers, S., Scheltema, R.A., Girolami, M., Breitling, R., 2009. Probabilistic assignment of formulas to mass peaks in metabolomics experiments. Bioinformatics 25, 512–518. https://doi.org/10.1093/bioinformatics/btn642

Romanet, R., Sarhane, Z., Bahut, F., Uhl, J., Schmitt-Kopplin, P., Nikolantonaki, M., Gougeon, R.D., 2021a. Exploring the chemical space of white wine antioxidant capacity: A combined DPPH, EPR and FT-ICR-MS study. Food Chem 355, 129566. https://doi.org/10.1016/j.foodchem.2021.129566

Romanet, R., Sarhane, Z., Bahut, F., Uhl, J., Schmitt-Kopplin, P., Nikolantonaki, M., Gougeon, R.D., 2021b. Exploring the chemical space of white wine antioxidant capacity: A combined DPPH, EPR and FT-ICR-MS study. Food Chemistry 355, 129566. https://doi.org/10.1016/j.foodchem.2021.129566

Roullier-Gall, C., Signoret, J., Hemmler, D., Witting, M.A., Kanawati, B., Schäfer, B., Gougeon, R.D., Schmitt-Kopplin, P., 2018. Usage of FT-ICR-MS Metabolomics for Characterizing the Chemical Signatures of Barrel-Aged Whisky. Frontiers in Chemistry 6. https://doi.org/10.3389/fchem.2018.00029

Roullier-Gall, C., Witting, M., Gougeon, R.D., Schmitt-Kopplin, P., 2014. High precision mass measurements for wine metabolomics. Front. Chem. 2. https://doi.org/10.3389/fchem.2014.00102

Ruehl, E., Schmid, J., Eibach, R., Töpfer, R., 2015. Grapevine Breeding Programs for the Wine Industry, Andrew Reynolds. ed. Woodhead Publishing.

Ruttkies, C., Schymanski, E.L., Wolf, S., Hollender, J., Neumann, S., 2016. MetFrag relaunched: incorporating strategies beyond in silico fragmentation. Journal of Cheminformatics 8, 3. https://doi.org/10.1186/s13321-016-0115-9

Ryhage, Ragnar., Wikstrom, Sten., Waller, G.R., 1965. Mass Spectrometer Used as Detector and Analyzer for Effluent Emerging from a Capillary Gas Liquid Chromatography Column. Anal. Chem. 37, 435–436. https://doi.org/10.1021/ac60222a045

Saito, K., Hirai, M.Y., Yonekura-Sakakibara, K., 2008. Decoding genes with coexpression networks and metabolomics – 'majority report by precogs.' Trends in Plant Science 13, 36–43. https://doi.org/10.1016/j.tplants.2007.10.006

Sakaguchi, Y., Ozaki, Y., Miyajima, I., Yamaguchi, M., Fukui, Y., Iwasa, K., Motoki, S., Suzuki, T., Okubo, H., 2008. Major anthocyanins from purple asparagus (Asparagus officinalis). Phytochemistry 69, 1763–1766. https://doi.org/10.1016/j.phytochem.2008.02.021

Sarabia, L.D., Boughton, B.A., Rupasinghe, T., van de Meene, A.M.L., Callahan, D.L., Hill, C.B., Roessner, U., 2018. High-mass-resolution MALDI mass spectrometry imaging reveals detailed spatial distribution of metabolites and lipids in roots of barley seedlings in response to salinity stress. Metabolomics 14, 63. https://doi.org/10.1007/s11306-018-1359-3

Sat, I.G., Sengul, M., Keles, F., 2002. Use of grape leaves in canned food. Pak. J. Nutr 1, 257–262.

Satou, M., Enoki, H., Oikawa, A., Ohta, D., Saito, Kazunori, Hachiya, T., Sakakibara, H., Kusano, M., Fukushima, A., Saito, Kazuki, Kobayashi, M., Nagata, N., Myouga, F., Shinozaki, K., Motohashi, R., 2014. Integrated analysis of transcriptome and metabolome of Arabidopsis albino or pale green mutants with disrupted nuclear-encoded chloroplast proteins. Plant Mol Biol 85, 411–428. https://doi.org/10.1007/s11103-014-0194-9

Schauer, N., Fernie, A.R., 2006. Plant metabolomics: towards biological function and mechanism. Trends Plant Sci 11, 508–516. https://doi.org/10.1016/j.tplants.2006.08.007

Scherling, C., Roscher, C., Giavalisco, P., Schulze, E.-D., Weckwerth, W., 2010. Metabolomics Unravel Contrasting Effects of Biodiversity on the Performance of Individual Plant Species. PLoS ONE 5, e12569. https://doi.org/10.1371/journal.pone.0012569

Scheubert, K., Hufsky, F., Petras, D., Wang, M., Nothias, L.-F., Dührkop, K., Bandeira, N., Dorrestein, P.C., Böcker, S., 2017. Significance estimation for large scale metabolomics annotations by spectral matching. Nat Commun 8, 1494. https://doi.org/10.1038/s41467-017-01318-5

Schläpfer, P., Zhang, P., Wang, C., Kim, T., Banf, M., Chae, L., Dreher, K., Chavali, A.K., Nilo-Poyanco, R., Bernard, T., Kahn, D., Rhee, S.Y., 2017. Genome-Wide Prediction of Metabolic Enzymes, Pathways, and Gene Clusters in Plants. Plant Physiology 173, 2041–2059. https://doi.org/10.1104/pp.16.01942

Schrader, W., Klein, H.-W., 2004. Liquid chromatography/Fourier transform ion cyclotron resonance mass spectrometry (LC-FTICR MS): an early overview. Anal Bioanal Chem 379. https://doi.org/10.1007/s00216-004-2675-1

Schuhmann, K., Almeida, R., Baumert, M., Herzog, R., Bornstein, S.R., Shevchenko, A., 2012. Shotgun lipidomics on a LTQ Orbitrap mass spectrometer by successive switching between acquisition polarity modes. J Mass Spectrom 47, 96–104. https://doi.org/10.1002/jms.2031

Schuhmann, K., Herzog, R., Schwudke, D., Metelmann-Strupat, W., Bornstein, S.R., Shevchenko, A., 2011. Bottom-up shotgun lipidomics by higher energy collisional dissociation on LTQ Orbitrap mass spectrometers. Anal Chem 83, 5480–5487. https://doi.org/10.1021/ac102505f

Shahbazy, M., Moradi, P., Ertaylan, G., Zahraei, A., Kompany-Zareh, M., 2020. FTICR mass spectrometry-based multivariate analysis to explore distinctive metabolites and metabolic pathways: A comprehensive bioanalytical strategy toward time-course metabolic profiling of Thymus vulgaris plants responding to drought stress. Plant Science 290, 110257. https://doi.org/10.1016/j.plantsci.2019.110257

Shang, Y., Huang, S., 2019. Engineering Plant Cytochrome P450s for Enhanced Synthesis of Natural Products: Past Achievements and Future Perspectives. Plant Communications 1, 100012. https://doi.org/10.1016/j.xplc.2019.100012

Shaw, J.B., Gorshkov, M.V., Wu, Q., Paša-Tolić, L., 2018. High Speed Intact Protein Characterization Using 4X Frequency Multiplication, Ion Trap Harmonization, and 21 Tesla FTICR-MS. Anal. Chem. 90, 5557–5562. https://doi.org/10.1021/acs.analchem.7b04606

Silva, R.R. da, Wang, M., Nothias, L.-F., Hooft, J.J.J. van der, Caraballo-Rodríguez, A.M., Fox, E., Balunas, M.J., Klassen, J.L., Lopes, N.P., Dorrestein, P.C., 2018. Propagating annotations of molecular networks using in silico fragmentation. PLOS Computational Biology 14, e1006089. https://doi.org/10.1371/journal.pcbi.1006089

Smart, D.R., Schwass, E., Lakso, A., Morano, L., 2006. Grapevine Rooting Patterns: A Comprehensive Analysis and a Review. American Journal of Enology and Viticulture 57, 89–104.

Smith, D.F., Podgorski, D.C., Rodgers, R.P., Blakney, G.T., Hendrickson, C.L., 2018. 21 Tesla FT-ICR Mass Spectrometer for Ultrahigh-Resolution Analysis of Complex Organic Mixtures. Anal Chem 90, 2041–2047. https://doi.org/10.1021/acs.analchem.7b04159

Smith, L.G., 1951. A new magnetic period mass spectrometer. Rev Sci Instrum 22, 115–116. https://doi.org/10.1063/1.1745849

Sommer, H., Thomas, H.A., Hipple, J.A., 1951. The Measurement of $\frac{e}{M}$ by Cyclotron Resonance. Phys. Rev. 82, 697–702. https://doi.org/10.1103/PhysRev.82.697

Stephens, W.E., 1946. Pulsed Mass Spectrometer with Time Dispersion. Bulletin of the American Physical Society 21, 22.

Sumner, L.W., Mendes, P., Dixon, R.A., 2003. Plant metabolomics: large-scale phytochemistry in the functional genomics era. Phytochemistry 62, 817–836. https://doi.org/10.1016/s0031-9422(02)00708-2

Tada, I., Tsugawa, H., Meister, I., Zhang, P., Shu, R., Katsumi, R., Wheelock, C.E., Arita, M., Chaleckis, R., 2019. Creating a Reliable Mass Spectral–Retention Time Library for All Ion Fragmentation-Based Metabolomics. Metabolites 9, 251. https://doi.org/10.3390/metabo9110251

Takahashi, K., Kozuka, T., Anegawa, A., Nagatani, A., Mimura, T., 2015a. Development and Application of a High-Resolution Imaging Mass Spectrometer for the Study of Plant Tissues. Plant Cell Physiol 56, 1329–1338. https://doi.org/10.1093/pcp/pcv083

Takahashi, K., Kozuka, T., Anegawa, A., Nagatani, A., Mimura, T., 2015b. Development and Application of a High-Resolution Imaging Mass Spectrometer for the Study of Plant Tissues. Plant Cell Physiol 56, 1329–1338. https://doi.org/10.1093/pcp/pcv083

Tanaka, K., Waki, H., Ido, Y., Akita, S., Yoshida, Y., Yoshida, T., Matsuo, T., 1988. Protein and polymer analyses up to m/z 100 000 by laser ionization time-of-flight mass spectrometry. Rapid Communications in Mass Spectrometry 2, 151–153. https://doi.org/10.1002/rcm.1290020802

Terral, J.-F., Tabard, E., Bouby, L., Ivorra, S., Pastor, T., Figueiral, I., Picq, S., Chevance, J.-B., Jung, C., Fabre, L., Tardy, C., Compan, M., Bacilieri, R., Lacombe, T., This, P., 2010. Evolution and history of grapevine (Vitis vinifera) under domestication: new morphometric perspectives to understand seed domestication syndrome and reveal origins of ancient European cultivars. Annals of Botany 105, 443–455. https://doi.org/10.1093/aob/mcp298

This, P., Lacombe, T., Thomas, M., 2006. Historical origins and genetic diversity of wine grapes. Trends in Genetics 22, 511–519. https://doi.org/10.1016/j.tig.2006.07.008

Thomson, J.J., 1912. XIX. Further experiments on positive rays. The London, Edinburgh, and Dublin Philosophical Magazine and Journal of Science 24, 209–253. https://doi.org/10.1080/14786440808637325

Thomson, J.J., 1910. LXXXIII. Rays of positive electricity. The London, Edinburgh, and Dublin Philosophical Magazine and Journal of Science 20, 752–767. https://doi.org/10.1080/14786441008636962

Thomson, J.J., 1908. LIV. Positive rays. The London, Edinburgh, and Dublin Philosophical Magazine and Journal of Science 16, 657–691. https://doi.org/10.1080/14786441008636543

Thomson, J.J., 1907. XLVII. On rays of positive electricity. The London, Edinburgh, and Dublin Philosophical Magazine and Journal of Science 13, 561–575. https://doi.org/10.1080/14786440709463633

Thomson, J.J., 1897. XL. *Cathode Rays*. The London, Edinburgh, and Dublin Philosophical Magazine and Journal of Science 44, 293–316. https://doi.org/10.1080/14786449708621070

Toffolatti, S.L., Venturini, G., Maffi, D., Vercesi, A., 2012. Phenotypic and histochemical traits of the interaction between Plasmopara viticola and resistant or susceptible grapevine varieties. BMC plant biology 12, 124.

Tohge, T., Nishiyama, Y., Hirai, M.Y., Yano, M., Nakajima, J., Awazuhara, M., Inoue, E., Takahashi, H., Goodenowe, D.B., Kitayama, M., Noji, M., Yamazaki, M., Saito, K., 2005a. Functional genomics by integrated analysis of metabolome and transcriptome of Arabidopsis plants over-expressing an MYB transcription factor. Plant J. 42, 218–235. https://doi.org/10.1111/j.1365-313X.2005.02371.x

Tohge, T., Nishiyama, Y., Hirai, M.Y., Yano, M., Nakajima, J., Awazuhara, M., Inoue, E., Takahashi, H., Goodenowe, D.B., Kitayama, M., Noji, M., Yamazaki, M., Saito, K., 2005b. Functional genomics by integrated analysis of metabolome and transcriptome

of Arabidopsis plants over-expressing an MYB transcription factor: Metabolomics and transcriptomics. The Plant Journal 42, 218–235. https://doi.org/10.1111/j.1365-313X.2005.02371.x

Tomita, M., Nishioka, T. (Eds.), 2005. Metabolomics: the frontier of systems biology. Springer, Tokyo ; New York.

Toubiana, D., Puzis, R., Wen, L., Sikron, N., Kurmanbayeva, A., Soltabayeva, A., del Mar Rubio Wilhelmi, M., Sade, N., Fait, A., Sagi, M., Blumwald, E., Elovici, Y., 2019. Combined network analysis and machine learning allows the prediction of metabolic pathways from tomato metabolomics data. Commun Biol 2, 1–13. https://doi.org/10.1038/s42003-019-0440-4

van Agthoven, M.A., Delsuc, M.-A., Rolando, C., 2011. Two-dimensional FT-ICR/MS with IRMPD as fragmentation mode. International Journal of Mass Spectrometry, Special Issue: In Honor of Tino Gaumann 306, 196–203. https://doi.org/10.1016/j.ijms.2010.10.034

Vestal, M.L., 2011. The Future of Biological Mass Spectrometry. J. Am. Soc. Mass Spectrom. 22, 953–959. https://doi.org/10.1007/s13361-011-0108-x

Viant, M.R., Rosenblum, E.S., Tieerdema, R.S., 2003. NMR-based metabolomics: a powerful approach for characterizing the effects of environmental stressors on organism health. Environ Sci Technol 37, 4982–4989. https://doi.org/10.1021/es034281x

Vidal-Gutiérrez, M., Torres-Moreno, H., Hernández-Gutiérrez, S., Velazquez, C., Robles-Zepeda, R.E., Vilegas, W., 2021. Antiproliferative activity of standardized phytopreparations from Ibervillea sonorae (S. Watson) Greene. Steroids 169, 108824. https://doi.org/10.1016/j.steroids.2021.108824

Vitanza, L., Maccelli, A., Marazzato, M., Scazzocchio, F., Comanducci, A., Fornarini, S., Crestoni, M.E., Filippi, A., Fraschetti, C., Rinaldi, F., Aleandri, M., Goldoni, P., Conte, M.P., Ammendolia, M.G., Longhi, C., 2019. Satureja montana L. essential oil and its antimicrobial activity alone or in combination with gentamicin. Microbial Pathogenesis 126, 323–331. https://doi.org/10.1016/j.micpath.2018.11.025

Walker, L.R., Tfaily, M.M., Shaw, J.B., Hess, N.J., Paša-Tolić, L., Koppenaal, D.W., 2017. Unambiguous identification and discovery of bacterial siderophores by direct injection 21 Tesla Fourier transform ion cyclotron resonance mass spectrometry. Metallomics 9, 82–92. https://doi.org/10.1039/c6mt00201c

Wan, Y., Schwaninger, H.R., Baldo, A.M., Labate, J.A., Zhong, G.-Y., Simon, C.J., 2013. A phylogenetic analysis of the grape genus (Vitis L.) reveals broad reticulation and concurrent diversification during neogene and quaternary climate change. BMC Evolutionary Biology 13, 141. https://doi.org/10.1186/1471-2148-13-141

Wang, M., Carver, J.J., Phelan, V.V., Sanchez, L.M., Garg, N., Peng, Y., Nguyen, D.D., Watrous, J., Kapono, C.A., Luzzatto-Knaan, T., Porto, C., Bouslimani, A., Melnik,

A.V., Meehan, M.J., Liu, W.-T., Crüsemann, M., Boudreau, P.D., Esquenazi, E., Sandoval-Calderón, M., Kersten, R.D., Pace, L.A., Quinn, R.A., Duncan, K.R., Hsu, C.-C., Floros, D.J., Gavilan, R.G., Kleigrewe, K., Northen, T., Dutton, R.J., Parrot, D., Carlson, E.E., Aigle, B., Michelsen, C.F., Jelsbak, L., Sohlenkamp, C., Pevzner, P., Edlund, A., McLean, J., Piel, J., Murphy, B.T., Gerwick, L., Liaw, C.-C., Yang, Y.-L., Humpf, H.-U., Maansson, M., Keyzers, R.A., Sims, A.C., Johnson, A.R., Sidebottom, A.M., Sedio, B.E., Klitgaard, A., Larson, C.B., P, C.A.B., Torres-Mendoza, D., Gonzalez, D.J., Silva, D.B., Marques, L.M., Demarque, D.P., Pociute, E., O'Neill, E.C., Briand, E., Helfrich, E.J.N., Granatosky, E.A., Glukhov, E., Ryffel, F., Houson, H., Mohimani, H., Kharbush, J.J., Zeng, Y., Vorholt, J.A., Kurita, K.L., Charusanti, P., McPhail, K.L., Nielsen, K.F., Vuong, L., Elfeki, M., Traxler, M.F., Engene, N., Koyama, N., Vining, O.B., Baric, R., Silva, R.R., Mascuch, S.J., Tomasi, S., Jenkins, S., Macherla, V., Hoffman, T., Agarwal, V., Williams, P.G., Dai, J., Neupane, R., Gurr, J., Rodríguez, A.M.C., Lamsa, A., Zhang, C., Dorrestein, K., Duggan, B.M., Almaliti, J., Allard, P.-M., Phapale, P., Nothias, L.-F., Alexandrov, T., Litaudon, M., Wolfender, J.-L., Kyle, J.E., Metz, T.O., Peryea, T., Nguyen, D.-T., VanLeer, D., Shinn, P., Jadhav, A., Müller, R., Waters, K.M., Shi, W., Liu, X., Zhang, L., Knight, R., Jensen, P.R., Palsson, B.O., Pogliano, K., Linington, R.G., Gutiérrez, M., Lopes, N.P., Gerwick, W.H., Moore, B.S., Dorrestein, P.C., Bandeira, N., 2016. Sharing and community curation of mass spectrometry data with Global Natural Products Social Molecular Networking. Nat Biotechnol 34, 828–837. https://doi.org/10.1038/nbt.3597

Wang, S., Alseekh, S., Fernie, A.R., Luo, J., 2019. The Structure and Function of Major Plant Metabolite Modifications. Molecular Plant 12, 899–919. https://doi.org/10.1016/j.molp.2019.06.001

Warburton, E., Bristow, T., 2006. Fourier Transform Ion Cyclotron Resonance Mass Spectrometry for the Characterisation of Kavalactones in the Kava Plant: Elemental Formulae Confirmation by Dual Spray Accurate Mass Measurement and Structural Confirmation by Infrared Multiphoton Dissociation and Sustained Off-Resonance Irradiation Collision Induced Dissociation. Eur J Mass Spectrom (Chichester) 12, 223–233. https://doi.org/10.1255/ejms.808

Way, D.A., Ghirardo, A., Kanawati, B., Esperschütz, J., Monson, R.K., Jackson, R.B., Schmitt-Kopplin, P., Schnitzler, J.-P., 2013. Increasing atmospheric CO_2 reduces metabolic and physiological differences between isoprene- and non-isoprene-emitting poplars. New Phytol 200, 534–546. https://doi.org/10.1111/nph.12391

Wen, W., Li, K., Alseekh, S., Omranian, N., Zhao, L., Zhou, Y., Xiao, Y., Jin, M., Yang, N., Liu, H., Florian, A., Li, W., Pan, Q., Nikoloski, Z., Yan, J., Fernie, A.R., 2015. Genetic Determinants of the Network of Primary Metabolism and Their Relationships to

Plant Performance in a Maize Recombinant Inbred Line Population. Plant Cell 27, 1839–1856. https://doi.org/10.1105/tpc.15.00208

Westinghouse Electric International Company, 1943. The Mass Spectrometer: A new electronic method for fast, accurate gas analysis.

Wicker, J., Lorsbach, T., Gütlein, M., Schmid, E., Latino, D., Kramer, S., Fenner, K., 2016. enviPath – The environmental contaminant biotransformation pathway resource. Nucleic Acids Research 44, D502–D508. https://doi.org/10.1093/nar/gkv1229

Wisecaver, J.H., Borowsky, A.T., Tzin, V., Jander, G., Kliebenstein, D.J., Rokas, A., 2017. A Global Coexpression Network Approach for Connecting Genes to Specialized Metabolic Pathways in Plants. The Plant Cell 29, 944–959. https://doi.org/10.1105/tpc.17.00009

Wohlgemuth, G., Mehta, S.S., Mejia, R.F., Neumann, S., Pedrosa, D., Pluskal, T., Schymanski, E.L., Willighagen, E.L., Wilson, M., Wishart, D.S., Arita, M., Dorrestein, P.C., Bandeira, N., Wang, M., Schulze, T., Salek, R.M., Steinbeck, C., Nainala, V.C., Mistrik, R., Nishioka, T., Fiehn, O., 2016. SPLASH, a hashed identifier for mass spectra. Nat Biotechnol 34, 1099–1101. https://doi.org/10.1038/nbt.3689

Wolf, S., Schmidt, S., Müller-Hannemann, M., Neumann, S., 2010. In silico fragmentation for computer assisted identification of metabolite mass spectra. BMC Bioinformatics 11, 148. https://doi.org/10.1186/1471-2105-11-148

Wolff, M.M., Stephens, W.E., 1953. A Pulsed Mass Spectrometer with Time Dispersion. Review of Scientific Instruments 24, 616–617. https://doi.org/10.1063/1.1770801

Xiao, T., Guo, Z., Sun, B., Zhao, Y., 2017. Identification of Anthocyanins from Four Kinds of Berries and Their Inhibition Activity to α-Glycosidase and Protein Tyrosine Phosphatase 1B by HPLC–FT-ICR MS/MS. J. Agric. Food Chem. 65, 6211–6221. https://doi.org/10.1021/acs.jafc.7b02550

Yamazaki, M., Mochida, K., Asano, T., Nakabayashi, R., Chiba, M., Udomson, N., Yamazaki, Y., Goodenowe, D.B., Sankawa, U., Yoshida, T., Toyoda, A., Totoki, Y., Sakaki, Y., Góngora-Castillo, E., Buell, C.R., Sakurai, T., Saito, K., 2013. Coupling Deep Transcriptome Analysis with Untargeted Metabolic Profiling in Ophiorrhiza pumila to Further the Understanding of the Biosynthesis of the Anti-Cancer Alkaloid Camptothecin and Anthraquinones. Plant and Cell Physiology 54, 686–696. https://doi.org/10.1093/pcp/pct040

Yang, J.-B., Liu, Y., Wang, Q., Ma, S.-C., Wang, A.-G., Cheng, X.-L., Wei, F., 2019. Characterization and identification of the chemical constituents of Polygonum multiflorum Thunb. by high-performance liquid chromatography coupled with ultraviolet detection and linear ion trap FT-ICR hybrid mass spectrometry. Journal of Pharmaceutical and Biomedical Analysis 172, 149–166. https://doi.org/10.1016/j.jpba.2019.03.049

Yoshida, T., Tanaka, K., Ido, Y., Akita, S., Yoshida, Y., 1988. Detection of High Mass Molecular Ions by Laser Desorption Time-of-Flight Mass Spectrometry. Journal of the Mass Spectrometry Society of Japan 36, 59–69. https://doi.org/10.5702/massspec.36.59

Yousofshahi, M., Manteiga, S., Wu, C., Lee, K., Hassoun, S., 2015. PROXIMAL: a method for Prediction of Xenobiotic Metabolism. BMC Systems Biology 9, 94. https://doi.org/10.1186/s12918-015-0241-4

Yu, H., Luscombe, N.M., Lu, H.X., Zhu, X., Xia, Y., Han, J.-D.J., Bertin, N., Chung, S., Vidal, M., Gerstein, M., 2004. Annotation Transfer Between Genomes: Protein–Protein Interologs and Protein–DNA Regulogs. Genome Res. 14, 1107–1118. https://doi.org/10.1101/gr.1774904

Zamboni, A., Carli, M.D., Guzzo, F., Stocchero, M., Zenoni, S., Ferrarini, A., Tononi, P., Toffali, K., Desiderio, A., Lilley, K.S., Pè, M.E., Benvenuto, E., Delledonne, M., Pezzotti, M., 2010. Identification of Putative Stage-Specific Grapevine Berry Biomarkers and Omics Data Integration into Networks. Plant Physiol. 154, 1439–1459. https://doi.org/10.1104/pp.110.160275

Zhan, J., Mundt, C.C., Hoffer, M.E., McDonald, B.A., 2002. Local adaptation and effect of host genotype on the rate of pathogen evolution: an experimental test in a plant pathosystem. Journal of Evolutionary Biology 15, 634–647. https://doi.org/10.1046/j.1420-9101.2002.00428.x

Zhang, X.P., Liu, M.S., Pei, Y.H., Zhang, J.Q., Kang, S.L., 2010. Phenylpropionic acid derivates from the bark of Cerbera manghas. Fitoterapia 81, 852–854. https://doi.org/10.1016/j.fitote.2010.05.010

Zhou, H., Xing, J., Liu, Shu, Song, F., Cai, Z., Pi, Z., Liu, Z., Liu, Shuying, 2012. Screening and Determination for Potential α-Glucosidase Inhibitors from Leaves of Acanthopanax senticosus Harms by Using UF-LC/MS and ESI-MSn: Screening and Determination of α-Glucosidase Inhibitors by MS. Phytochem. Anal. 23, 315–323. https://doi.org/10.1002/pca.1360

Zhu, X.-G., Lynch, J.P., LeBauer, D.S., Millar, A.J., Stitt, M., Long, S.P., 2016. Plants in silico: why, why now and what?—an integrative platform for plant systems biology research. Plant, Cell & Environment 39, 1049–1057. https://doi.org/10.1111/pce.12673

CHAPTER II

Vitis vinifera 'Pinot noir' leaves as a source of bioactive nutraceutical compounds

The sections in this chapter are organized differently from the paper.

2 *Vitis vinifera* 'Pinot noir' leaves as a source of bioactive nutraceutical compounds

2.1 ABSTRACT

Agricultural by-products are often hidden sources of healthy plant ingredients. The investigation of the nutritional values of these by-products is essential towards sustainable agriculture and improved food systems. In the vine industry, grape leaves are a bulky side product which is strategically removed and treated as waste in the process of wine production. In this work we performed an untargeted metabolomic profiling of the methanol extract of the leaves of *Vitis vinifera* cultivar 'Pinot noir', analysed their fatty acid content, and estimated their antioxidative capacity, with the purpose of investigating its nutritional and medicinal value. Fourier transform ion cyclotron resonance mass spectrometry (FT-ICR-MS) analysis identified the presence of numerous compounds which are known to possess diverse nutritional and pharmacological properties, particularly polyphenols and phenolic compounds (e.g. caffeic acid, catechin, kaempferol and quercetin), several phytosterols and fatty acids. Fatty acids were the most represented lipids' secondary class, with the essential alpha-linolenic acid being the most abundant in 'Pinot noir' leaves, with a relative content of 42%. Also, we have found that 'Pinot noir' leaves present a high antioxidant capacity, putting grapevine leaves at the top of the list of foods with the highest antioxidative activity. Our findings scientifically confirmed that 'Pinot noir' leaves have a high content and diversity of biologically active phytochemical compounds which make it of exceptional interest for pharmaceutical and food industries.

2.2 INTRODUCTION

Used since ancient times in traditional medicine, plants are a major source of natural bioactive compounds with a wide range of applications in the pharmaceutical, food and cosmetic industries (Cowan, 1999). However, the use of plants as a source of natural products faces quite a few challenges, mainly the availability of the compounds of interest, which can be very low, and the amount of the starting material, not always adequate for industrial extraction purposes (Atanasov et al., 2015). One strategy to overcome these issues is the selection of abundant plant material with high phytochemical content and nutritional value that is normally seen as agricultural waste and turn it into a valuable resource.

Considering its importance in the wine industry, the grapevine (*Vitis vinifera* L.) is considered one of the most important fruit crops in the world, occupying over 7.5 mha of

global area (FAO and OIV, 2019). Currently, there are about 2000 different cultivars of *V. vinifera* used for grape production and grown all over the world (Lacombe et al., 2011). About 50% of the world's produced grape is destined to wine production, a highly strategic industry for the economy of several countries, with 30% being targeted for the commercialization of fresh grapes and the rest is dried or consumed as grape juice or musts (FAO and OIV, 2019). Grapes contain a great diversity of secondary bioactive metabolites, namely vitamins, anthocyanins, flavonoids, polyphenols and stilbenoids, and are already being used for the development of food supplements (Dávalos et al., 2003; Monagas et al., 2006; Nassiri-Asl and Hosseinzadeh, 2009) and in cosmetics (Barbulova et al., 2015). Grapevine's bioactive compounds have been mostly studied at grape level, whereas the vegetative parts, particularly leaves, are still a disregarded by-product of this industry. Grapevine leaves are a very abundant plant material, contain a wide range of phenolic compounds and antioxidants, being already used in traditional medicine for the treatment of bleeding, inflammation, diarrhoea and diabetes-induced hepatic complications (Lacerda et al., 2016; Nassiri-Asl and Hosseinzadeh, 2009). Additionally, vine leaves have already been included in the human diet in several countries of the Mediterranean Basin, both fresh and brined, and therefore are getting the attention from top European wine producers (Rizzuti et al., 2013).

We performed an untargeted metabolomics approach to unfold the global view of the metabolic composition of leaves from *V. vinifera* 'Pinot noir'. This cultivar is one of the world's most planted grapevines, occupying the 12th position worldwide (the 10th position among the wine making cultivars) and representing around 112 kha of planted area (Organisation of Vine and Wine, 2019). Fourier Transform Ion Cyclotron Resonance mass spectrometry (FT-ICR-MS) was used for metabolite profiling, already successfully used in plant metabolomics due to its ultra-high-resolution and ultra-high-mass accuracy (Adrian et al., 2017; Ghaste et al., 2016; Han et al., 2008; Lei et al., 2011; Maia et al., 2016). These performance characteristics allow the assignment of putative metabolite formulae based solely on accurate mass, by exhaustive search and match with computed masses for given chemical series of compounds, in combination with metabolomic database search by accurate mass (Aharoni et al., 2002; Han et al., 2008). In our analysis, lipids, mostly fatty acids, and phytochemical compounds were the most prevalent metabolites. Hence, fatty acids were subsequently quantified and the antioxidant capacity of 'Pinot noir' leaves was determined to assess their potential as a source of nutra-pharmaceutical compounds.

2.3 MATERIALS AND METHODS

2.3.1 Plant material

V. vinifera 'Pinot noir' leaves were collected at the Portuguese Ampelographic Grapevine Collection (CAN, international code PRT051, established in 1988), at INIAV-Dois Portos, located at Quinta da Almoinha, 60 Km north of Lisbon. This vineyard is trained on a double-cordon system, selecting only four canes in each arm. Plants were grafted on SO4 rootstock (Selection Oppenheim 4), in alluvial soil (pH 8.1 at 0-21 cm deep), in temperate oceanic climate (according to Koppen climate system). Sanitary status is controlled for viral diseases and maintained with preventive phytochemical application every 12 to 15 days in growing season. Since the beginning of the season (March 2015) till sampling time (May 2015), mean temperature was 18 °C (T max: 24 °C; T min: 10 °C) and the precipitation had a mean value of 50 mm (reaching 100 mm in April), (data from the Instituto Português do Mar e da Atmosfera). The third to fifth leaves (from the shoot apex) were collected from 5 fully developed plants and were combined in 1 biological replicate, being collected 3 biological replicates for the analysis. Leaves were immediately frozen in liquid nitrogen and stored at -80 °C until analysis.

2.3.2 Metabolite profile analysis by FT-ICR-MS

Metabolite extraction from *V. vinifera* 'Pinot noir' leaves was performed following a previously developed protocol compatible with direct infusion-FT-ICR-MS (Maia et al., 2016). After extraction, the different obtained fractions (chloroform, water, methanol and acetonitrile) were analysed by direct infusion on a 7T-FT-ICR mass spectrometer (Brüker Daltonics), using positive (ESI$^+$) and negative (ESI$^-$) electrospray ionization modes, as previously reported (Maia et al., 2016). Spectra analysis, compound identification and annotation were also performed as previously described (Maia et al., 2016). Compound formulas, obtained from MassTRIX analysis, were used to plot H/C ratios against O/C ratios in a Van Krevelen diagram and build a frequency histogram of CHO, CHON, CHOS and CHONS elemental compositions.

2.3.3 Fatty acid quantification

Fatty acids' methyl esters (FAME) were prepared by direct trans-methylation of fatty acids using ground leaves with a mixture of methanol:sulfuric acid (97.5:2.5, v/v), with

incubation at 70 °C for 1 h. Methyl esters were recovered in the organic phase after addition of petroleum ether:ultrapure water (3:2, v/v). Quantitative analysis of fatty acids was achieved by gas chromatography (3900 Gas Chromatograph, Varian, Palo Alto, CA, USA) equipped with a flame ionization detector, using a fused silica capillary column (0.25 mm i.d. × 50 m, WCOT Fused Silica, CP-Sil 88 for FAME, Varian) at 210 °C. Heptadecanoic acid (C17:0) was used as internal standard.

2.3.4   Indexes of lipid quality determination

Lipid nutritional quality can be assessed through the determination of the indexes of atherogenicity (IA) and thrombogenicity (IT). IA is defined as the relationship between the sum of the main saturated fatty acids (proatherogenic) and the sum of the main classes of unsaturated fatty acids (antiatherogenic), while IT represents the relationship between C16:0 (hexadecanoic acid) and C18:0 (octadecanoic acid; stearic acid), saturated fatty acids (prothrombogenetic) with monounsaturated fatty acids (MUFAs), polyunsaturated fatty acids -n6 (PUFA-n6) and -n3 (PUFA-n3) (antithrombogenetic) (Garaffo et al., 2011). The following equations (**Equation 2.1** and (**Equation 2.2**) were used for the IA and IT calculation:

(**Equation 2.1**)
$$IA = \frac{(C16:0 + C18:0)}{MUFAs + PUFAs_{n3} + PUFAs_{n6}}$$

(**Equation 2.2**)
$$IT = \frac{(C16:0 + C18:0)}{(0.5 \times MUFAs + 0.5 \times PUFAs_{n6} + 3 \times PUFAs_{n3} + (\frac{PUFAs_{n3}}{PUFAs_{n6}})}$$

2.3.5   Antioxidant assay

Total antioxidant capacity was determined in 'Pinot noir' leaves. Total antioxidant capacity was analysed by measuring the Trolox equivalent antioxidant capacity (TEAC), following the previously described protocol (Figueiredo et al., 2017). Briefly, 100 mg of frozen leaves were homogenized in 3 mL 50 mM potassium phosphate buffer pH 7.2, supplemented with 1% (w/v) of insoluble polyvinylpolypyrrolidone (PVPP 40000), at 4°C. After centrifugation at 16000 g for 1 min, the supernatant was collected and used for the assay. Total antioxidant capacity was determined spectrophotometrically at 405 nm using the antioxidant assay kit and Trolox as standard (Sigma-Aldrich, ref. CS0790). The assay was performed in 3 biological replicates, each analysed twice.

72

2.4 RESULTS AND DISCUSSION

2.4.1 *V. vinifera* 'Pinot noir' metabolic profile

A total of 6348 ions (peaks) were identified in ESI$^+$, while in ESI$^-$ 1105 peaks were detected in the metabolic profile of *V. vinifera* 'Pinot noir' leaves. Through the analysis of the four metabolite fractions, nearly 1000 metabolic entities (unique masses) were identified: 785 in positive ionization mode and 151 in negative ionization mode. To provide insight into metabolite diversity and elemental ratios, metabolite formulas were assigned to the detected masses (combining data from positive and negative ion modes), obtaining a total of 857 different formulas. Compound formulas were used to plot H/C ratios against O/C ratios in a Van Krevelen diagram and build a frequency histogram of CHO, CHON, CHOS and CHONS elemental compositions (**Figure 2.1 – A** and **B**).

The highest density of formulas contains H/C ratios between 1 and 2 and O/C ratios between 0 and 0.5. This area corresponds mainly to lipids. Indeed, compound database match and compound taxonomical annotation revealed that within the major metabolic classes, the lipids' class was the most prevalent, accounting for 67% of the total detected metabolome.

Fatty acids (FAs) were the most represented lipids' secondary class (48% of the total lipids, according to LipidMaps classification), followed by prenol lipids, polyketides and sterols (**Figure 2.2**).
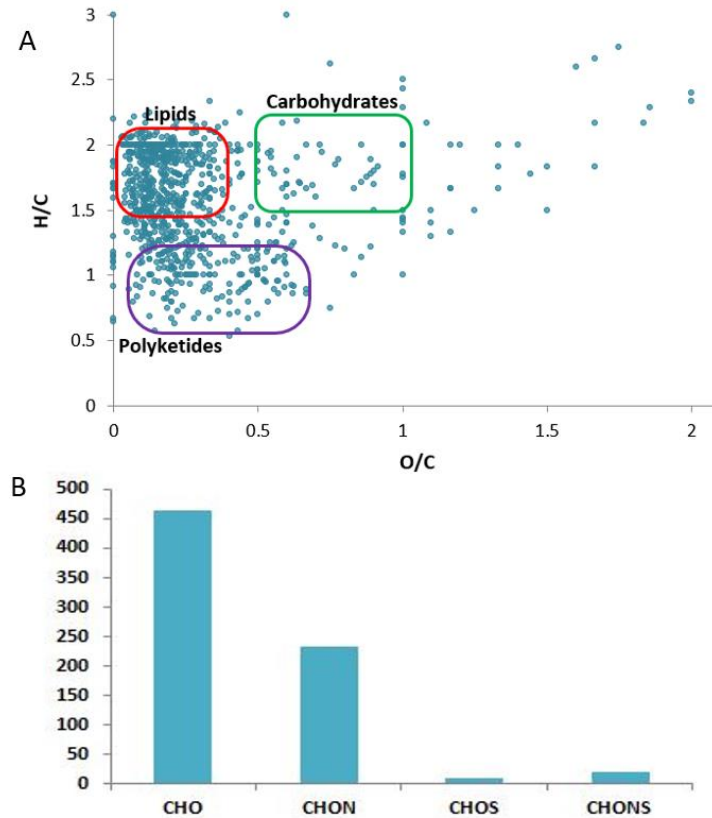
Figure 2.1 - (**A**) Van Krevelen diagram of 'Pinot noir' leaves metabolic composition, built from 857 different formulas. Representative elemental ratio areas for selected groups of compounds are highlighted: lipids in red, carbohydrates in green, and polyketides in purple. (**B**) Frequency histogram of CHO, CHON, CHOS and CHONS elemental compositions in the metabolite formulas displayed in (**A**).
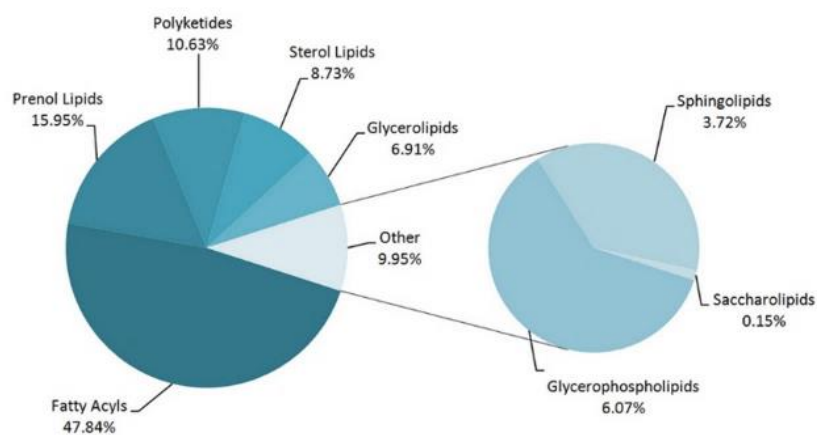
Figure 2.2 - Lipids secondary classes' annotation of grapevine lipids detected by FT-ICR-MS, according to the LipidMaps classification.

2.4.2 Fatty acids

Fatty acid quantification in 'Pinot noir' showed that alpha-linolenic acid (C18:3) was the most abundant FA in leaves (42% of the total quantified FAs). The second most abundant FAs were linoleic acid (C18:2) and palmitic acid (16:0), with 25% and 22% of the total FAs. The essential polyunsaturated fatty acids (PUFAs) C18:2 (omega-6) and C18:3 (omega-3) are not synthesized by human cells (Borsonelo and Galduróz, 2008; Ursin, 2003) but are required to produce long chain PUFAs such as arachidonic and eicosapentaenoic acids, respectively. Therefore, some PUFA have already been included in nutraceutical products (reviewed in Das et al., 2012). These two PUFAs, conserved signalling molecules involved in immune responses (reviewed in Walley et al., 2013), were putatively identified by MS 'Pinot noir' leaves (See **Supplementary Table S2.1** online), most likely from a microbiological source. Less abundant, but also present in significant amounts and also identified by MS, were oleic acid (C18:1), trans-hexadecanoic acid (C16:1t) and stearic acid (C18:0) (See **Supplementary Table S2.1** online). Other FAs identified by MS included docosanedioic acid, dodecanoic acid, eicosanedioic acid and octacosanoic acid (See **Supplementary Table S2.1** online), in agreement with the FA composition recently described for other grapevine cultivars (Laureano et al., 2018).

Grapevine leaves' fatty acids profile was used to assess lipid nutritional quality, through the determination of atherogenicity (IA) and thrombogenicity (IT) health lipid indexes. These indexes are indicators of the effects of fatty acids in human health, mainly their contribution to the prevention of atheroma and thrombus formation. 'Pinot noir' leaves have low IA and IT levels, 0.32 and 0.17 respectively, meaning that they could be part of a healthy diet.

2.4.3 Sterols

Plant sterols (also named phytosterols) are another lipids' secondary class already incorporated in several foods (Korpela et al., 2006) for their ability to interfere with cholesterol absorption. In 'Pinot noir' leaves, we detected several putative sterols, including 22S-hydroxysitosterol, stylisterol B, 16α,17β-Estriol 17-(β-D-glucuronide), 1-hydroxyvitamin D3 3-D-glucopyranoside and several other vitamin D3 derivatives (See **Supplementary Table S2.1** online).

2.4.4 Polyketides

Within the polyketides' subclass, flavonoids and phenolic lipids are the most relevant (reviewed in Brewer, 2011). A highly important antioxidative phenolic acid putatively found in *V. vinifera* 'Pinot noir' was caffeic acid, together with its 3-glucoside and phenethyl ester forms (See **Supplementary Table S2.1** online). Within the phenolic diterpenes, carnosol was putatively identified in 'Pinot noir' leaves (See **Supplementary Table S2.1** online). The extraction of several polyphenols was already optimized from grape seeds to be used in food, cosmetics and pharmaceutical industries (reviewed in Gil-Chávez et al., 2013). Flavonoids were already found in all *V. vinifera* tissues and organs (Ali et al., 2010; Braidot et al., 2008; Hermosín-Gutiérrez et al., 2011; Schoedl et al., 2012). Putatively identified flavonoids in 'Pinot noir' leaves included the most common glycosylated forms and isoforms of kaempferol and quercetin, particularly glucoside, galactoside and glucuronide conjugate forms, rutin, catechin (and/or epicatechin) and gallocatechin (and/or epigallocatechin), (See **Supplementary Table S2.1** online). Plant catechins (flavan-3-ols) are particularly interesting and have been widely used by the pharmaceutical industry as nutraceutical products (Vuong et al., 2010). Together with caffeic acid, catechin and epicatechin were extracted from *Uncaria sinensis* to be used in the treatment of fevers and nervous disorders (reviewed in Gil-Chávez et al., 2013). The dihydroflavonol astilbin, also present in grapes and wine (reviewed in Ali et al., 2010), was detected in 'Pinot noir' leaves. Resveratrol-derived flavonoids were also detected in 'Pinot noir' leaves, namely dihydroresveratrol, 4'-prenyloxyresveratrol and the resveratrol dimer ampelopsin (also named dihydromyrcetin) (See **Supplementary Table S2.1** online). Anthocyanins and anthocyanidins also have antioxidant activity and potential biologically therapeutic effects (reviewed in Brewer, 2011). Glucoside forms of the anthocyanins peonidin and cyanidin, delphinidin 3-O-rutinoside, leucocyanidin and 3-deoxyleucocyanidin were detected in 'Pinot noir' leaves (See **Supplementary Table S2.1** online). An acylated anthocyanin, peonidin 3-(6''-acetylglucoside), was putatively identified for the first time in 'Pinot noir'. These acylated pigments combine their potent antioxidant properties with an increased stability, being therefore more attractive for use as supplements in commercial food products (Giusti and Wrolstad, 2003). Other natural antioxidants putatively detected in 'Pinot noir' leaves included ascorbic and dehydroascorbic acid and alpha-tocopherol (See **Supplementary Table S2.1** online).

2.4.5 Antioxidant capacity of 'Pinot noir' leaves

The presence of polyphenols and phenolic compounds in grapevine leaves suggests that they can be a potential source of antioxidants (reviewed in Lacerda et al., 2016). Indeed,

the metabolic profile of 'Pinot noir' leaves revealed several antioxidant compounds, hinting for a quite relevant antioxidant capacity. We measured the antioxidant activity in 'Pinot noir' leaves using the TEAC (Trolox Equivalents Antioxidant Capacity) method. 'Pinot noir' leaves have a high antioxidant capacity (2402±198 µmol TE/100 g fresh weight (Fw)), comparable to red cabbage (2591 µmol TE/100 g Fw), and higher than strawberries (1846 µmol TE/100 g Fw) or raspberries (1825 µmol TE/100 g Fw), usually considered at the top of the list of foods with significant highest antioxidant activity (Proteggente et al., 2002). Like grape seeds, skin and pomace, already recognized as a good source of antioxidants (Varzakas et al., 2016) grapevine leaves have thus an enormous potential as a source for the extraction of natural antioxidant compounds.

2.5 CONCLUSIONS

The grapevine associated industry is one of the biggest worldwide. Some premium cultivars as 'Pinot noir' are highly cultivated reaching plantation areas of 112 kha. Within this industry, leaves are strategically removed every season, to improve sunlight penetration, air circulation into the vine and grape quality and are considered a waste product. Here, we have shown that 'Pinot noir' leaves have high nutritional potential for human or animal consumption or to be used as a source of bioactive compounds. Grapevine leaves present a high content in fatty acids, with alpha-linolenic acid at the top of the most abundant FA. 'Pinot noir' leaves also contain several antioxidant compounds, particularly phenolic compounds and polyphenols, like caffeic acid, catechin, kaempferol, quercetin and resveratrol-derived flavonoids, with a very interesting antioxidant activity, among other several metabolites with interesting properties in the context of the human health.

Grapevine leaves' potential as source of nutraceuticals has been overlooked. It is time to exploit this abundant natural product as a source of bioactive compounds.

2.6 SUPPLEMENTARY INFORMATION

Supplementary Table S2.1 is available at DOI: https://doi.org/10.1039/c8fo02328j.

2.7 ACKNOWLEDGEMENTS

2.8   REFERENCES

Adrian, M., Lucio, M., Roullier-Gall, C., Héloir, M.-C., Trouvelot, S., Daire, X., Kanawati, B., Lemaître-Guillier, C., Poinssot, B., Gougeon, R., Schmitt-Kopplin, P., 2017. Metabolic Fingerprint of PS3-Induced Resistance of Grapevine Leaves against *Plasmopara viticola* Revealed Differences in Elicitor-Triggered Defenses. Front. Plant Sci. 8. https://doi.org/10.3389/fpls.2017.00101

Aharoni, A., Ric de Vos, C.H., Verhoeven, H.A., Maliepaard, C.A., Kruppa, G., Bino, R., Goodenowe, D.B., 2002. Nontargeted metabolome analysis by use of Fourier transform ion cyclotron mass spectrometry. Omics: a journal of integrative biology 6, 217–234. https://doi.org/doi:10.1089/15362310260256882

Ali, K., Maltese, F., Choi, Y.H., Verpoorte, R., 2010. Metabolic constituents of grapevine and grape-derived products. Phytochemistry Reviews 9, 357–378. https://doi.org/10.1007/s11101-009-9158-0

Atanasov, A.G., Waltenberger, B., Pferschy-Wenzig, E.-M., Linder, T., Wawrosch, C., Uhrin, P., Temml, V., Wang, L., Schwaiger, S., Heiss, E.H., Rollinger, J.M., Schuster, D., Breuss, J.M., Bochkov, V., Mihovilovic, M.D., Kopp, B., Bauer, R., Dirsch, V.M., Stuppner, H., 2015. Discovery and resupply of pharmacologically active plant-derived natural products: A review. Biotechnology Advances 33, 1582–1614. https://doi.org/10.1016/j.biotechadv.2015.08.001

Barbulova, A., Colucci, G., Apone, F., 2015. New Trends in Cosmetics: By-Products of Plant Origin and Their Potential Use as Cosmetic Active Ingredients. Cosmetics 2, 82–92. https://doi.org/10.3390/cosmetics2020082

Borsonelo, E.C., Galduróz, J.C.F., 2008. The role of polyunsaturated fatty acids (PUFAs) in development, aging and substance abuse disorders: Review and propositions. Prostaglandins, Leukotrienes and Essential Fatty Acids 78, 237–245. https://doi.org/10.1016/j.plefa.2008.03.005

Braidot, E., Zancani, M., Petrussa, E., Peresson, C., Bertolini, A., Patui, S., Macrì, F., Vianello, A., 2008. Transport and accumulation of flavonoids in grapevine (*Vitis vinifera* L.). Plant signaling & behavior 3, 626–632. https://doi.org/10.4161/psb.3.9.6686

Brewer, M.S., 2011. Natural Antioxidants: Sources, Compounds, Mechanisms of Action, and Potential Applications. Comprehensive Reviews in Food Science and Food Safety 10, 221–247. https://doi.org/10.1111/j.1541-4337.2011.00156.x

Cowan, M.M., 1999. Plant Products as Antimicrobial Agents. Clin Microbiol Rev 12, 564–582. https://doi.org/10.1128/CMR.12.4.564

Das, L., Bhaumik, E., Raychaudhuri, U., Chakraborty, R., 2012. Role of nutraceuticals in human health. J Food Sci Technol 49, 173–183. https://doi.org/10.1007/s13197-011-0269-4

Dávalos, A., Gómez-Cordovés, C., Bartolomé, B., 2003. Commercial Dietary Antioxidant Supplements Assayed for Their Antioxidant Activity by Different Methodologies. J. Agric. Food Chem. 51, 2512–2519. https://doi.org/10.1021/jf021030j

FAO, OIV, 2019. Table and Dried Grapes: FAO and OIV FOCUS 2016.

Figueiredo, A., Martins, J., Sebastiana, M., Guerreiro, A., Silva, A., Matos, A.R., Monteiro, F., Pais, M.S., Roepstorff, P., Coelho, A.V., 2017. Specific adjustments in grapevine leaf proteome discriminating resistant and susceptible grapevine genotypes to *Plasmopara viticola*. Journal of Proteomics 152, 48–57. https://doi.org/10.1016/j.jprot.2016.10.012

Garaffo, M.A., Vassallo-Agius, R., Nengas, Y., Lembo, E., Rando, R., Maisano, R., Dugo, G., Giuffrida, D., 2011. Fatty Acids Profile, Atherogenic (IA) and Thrombogenic (IT) Health Lipid Indices, of Raw Roe of Blue Fin Tuna (Thunnus thynnus L.) and Their Salted Product "Bottarga." Food and Nutrition Sciences 02, 736. https://doi.org/10.4236/fns.2011.27101

Ghaste, M., Mistrik, R., Shulaev, V., 2016. Applications of Fourier Transform Ion Cyclotron Resonance (FT-ICR) and Orbitrap Based High Resolution Mass Spectrometry in Metabolomics and Lipidomics. International Journal of Molecular Sciences 17, 816. https://doi.org/10.3390/ijms17060816

Gil-Chávez, G.J., Villa, J.A., Ayala-Zavala, J.F., Heredia, J.B., Sepulveda, D., Yahia, E.M., González-Aguilar, G.A., 2013. Technologies for Extraction and Production of Bioactive Compounds to be Used as Nutraceuticals and Food Ingredients: An Overview. Comprehensive Reviews in Food Science and Food Safety 12, 5–23. https://doi.org/10.1111/1541-4337.12005

Giusti, M.M., Wrolstad, R.E., 2003. Acylated anthocyanins from edible sources and their applications in food systems. Biochemical Engineering Journal 14, 217–225. https://doi.org/10.1016/S1369-703X(02)00221-8

Han, J., Danell, R.M., Patel, J.R., Gumerov, D.R., Scarlett, C.O., Speir, J.P., Parker, C.E., Rusyn, I., Zeisel, S., Borchers, C.H., 2008. Towards high-throughput metabolomics using ultrahigh-field Fourier transform ion cyclotron resonance mass spectrometry. Metabolomics 4, 128–140. https://doi.org/10.1007/s11306-008-0104-8

Hermosín-Gutiérrez, I., Castillo-Muñoz, N., Gómez-Alonso, S., García-Romero, E., 2011. Flavonol Profiles for Grape and Wine Authentication, in: Progress in Authentication of Food and Wine, ACS Symposium Series. American Chemical Society, pp. 113–129. https://doi.org/10.1021/bk-2011-1081.ch008

Korpela, R., Tuomilehto, J., Högström, P., Seppo, L., Piironen, V., Salo-Väänänen, P., Toivo, J., Lamberg-Allardt, C., Kärkkäinen, M., Outila, T., Sundvall, J., Vilkkilä, S., Tikkanen, M.J., 2006. Safety aspects and cholesterol-lowering efficacy of low fat dairy products containing plant sterols. Eur J Clin Nutr 60, 633–642. https://doi.org/10.1038/sj.ejcn.1602362

Lacerda, D.S., Costa, P.C., Funchal, C., Gomez, C.D. and R., 2016. Benefits of Vine Leaf on Different Biological Systems. Grape and Wine Biotechnology. https://doi.org/10.5772/64930

Lacombe, T., Martínez Rodríguez, M. del C., This, P., 2011. Grapevine European catalogue: towards a comprehensive list. https://doi.org/10.5073/*Vitis*.2011.50.65-68

Laureano, G., Figueiredo, J., Cavaco, A.R., Duarte, B., Caçador, I., Malhó, R., Sousa Silva, M., Matos, A.R., Figueiredo, A., 2018. The interplay between membrane lipids and phospholipase A family members in grapevine resistance against *Plasmopara viticola*. Sci Rep 8, 14538. https://doi.org/10.1038/s41598-018-32559-z

Lei, Z., Huhman, D.V., Sumner, L.W., 2011. Mass Spectrometry Strategies in Metabolomics. J. Biol. Chem. 286, 25435–25442. https://doi.org/10.1074/jbc.R111.238691

Maia, M., Monteiro, F., Sebastiana, M., Marques, A.P., Ferreira, A.E.N., Freire, A.P., Cordeiro, C., Figueiredo, A., Sousa Silva, M., 2016. Metabolite extraction for high-throughput FTICR-MS-based metabolomics of grapevine leaves. EuPA Open Proteomics 12, 4–9. https://doi.org/10.1016/j.euprot.2016.03.002

Monagas, M., Hernández-Ledesma, B., Gómez-Cordovés, C., Bartolomé, B., 2006. Commercial Dietary Ingredients from *Vitis vinifera* L. Leaves and Grape Skins: Antioxidant and Chemical Characterization. Journal of Agricultural and Food Chemistry 54, 319–327. https://doi.org/10.1021/jf051807j

Nassiri-Asl, M., Hosseinzadeh, H., 2009. Review of the pharmacological effects of *Vitis vinifera* (Grape) and its bioactive compounds. Phytother Res 23, 1197–1204. https://doi.org/10.1002/ptr.2761

Organisation of Vine and Wine, 2019. The distribution of the world's grapevine varieties.

Proteggente, A.R., Pannala, A.S., Paganga, G., Van Buren, L., Wagner, E., Wiseman, S., Van De Put, F., Dacombe, C., Rice-Evans, C.A., 2002. The antioxidant activity of regularly consumed fruit and vegetables reflects their phenolic and vitamin C composition. Free Radic. Res. 36, 217–233. https://doi.org/10.1080/10715760290006484

Rizzuti, A., Caliandro, R., Gallo, V., Mastrorilli, P., Chita, G., Latronico, M., 2013. A combined approach for characterisation of fresh and brined vine leaves by X-ray

powder diffraction, NMR spectroscopy and direct infusion high resolution mass spectrometry. Food Chemistry 141, 1908–1915. https://doi.org/10.1016/j.foodchem.2013.05.044

Schoedl, K., Schuhmacher, R., Forneck, A., 2012. Studying the polyphenols of grapevine leaves according to age and insertion level under controlled conditions. Scientia Horticulturae 141, 37–41. https://doi.org/10.1016/j.scienta.2012.04.014

Ursin, V.M., 2003. Modification of plant lipids for human health: development of functional land-based omega-3 fatty acids. The Journal of nutrition 133, 4271–4274. https://doi.org/10.1093/jn/133.12.4271

Varzakas, T., Zakynthinos, G., Verpoort, F., 2016. Plant Food Residues as a Source of Nutraceuticals and Functional Foods. Foods 5. https://doi.org/10.3390/foods5040088

Vuong, Q.V., Golding, J.B., Nguyen, M., Roach, P.D., 2010. Extraction and isolation of catechins from tea. J Sep Sci 33, 3415–3428. https://doi.org/10.1002/jssc.201000438

Walley, J.W., Kliebenstein, D.J., Bostock, R.M., Dehesh, K., 2013. Fatty acids and early detection of pathogens. Current Opinion in Plant Biology 16, 520–526. https://doi.org/10.1016/j.pbi.2013.06.011

CHAPTER III

Uncovering markers for downy mildew resistance in grapevine through mass spectrometry-based metabolomics

3 Uncovering markers for downy mildew resistance in grapevine through mass spectrometry-based metabolomics

3.1 ABSTRACT

Downy mildew is a major threat to the wine industry and the development of hybrids between *Vitis vinifera* and wild resistant *Vitis* species is a promising strategy to cope with this disease. The discovery of metabolic markers associated with grapevine resistance is paramount. In this work we aim at speeding up the assignment of innate resistance to downy mildew in grapevine cultivars by applying high-resolution mass-spectrometry-based untargeted metabolomics as a profiling and resistance marker discovery method. We compared the susceptible cultivar 'Trincadeira' with the more resistant one 'Regent'. Both cultivars could be easily discriminated based on their metabolic profile and we found several peak features exclusive of each variety.

3.2 INTRODUCTION

Vitis vinifera is one of the most important and cultivated fruit plants in the world, occupying a global area of 7.5 mha and with a global grape production of 7.8 mt in 2016 (Organisation of Vine and Wine, 2017). Most of the produced grape is targeted for wine production, a highly strategic industry for the economy of several countries, Portugal included. With 14 wine producing regions and 190 kha of vineyards, Portugal is the eleventh world wine producer and the fifth in Europe, accounting for ~700 million euros per year of exports (Organisation of Vine and Wine, 2017).

One major threat to the wine industry is downy mildew, caused by the biotrophic oomycete *Plasmopara viticola* (Berk. et Curt.) Berl. et de Toni, infecting all domesticated *V. vinifera* cultivars frequently used for wine production. This pathogen affects leaves, shoots, bunches and fruits, causing quality and yield reduction with significant production and financial losses (Gessler et al., 2011).

Currently used strategies to cope with downy mildew include the intensive use of fungicides, applied soon after the first leaves appear. However, the general recommendations of the European agricultural policy encourage the reduction of pesticides towards environmental sustainability and consumer health. A promising approach is the creation of new cultivars through breeding programs, combining the high degree of resistance against

downy mildew from the wild *Vitis* spp., with the good berry quality of *V. vinifera*. One successful example already used in wine production is the interspecific hybrid 'Regent', developed from *V. vinifera* 'Diana' (Silvaner x Müller-Thurgau cross) and from the interspecific hybrid 'Chambourcin', possessing a higher resistance to downy mildew and other relevant fungal diseases (Gessler et al., 2011).

The complete process of a new cultivar's breeding, from plant crossing to market release, can take about 25 to 30 years. Since grapevine is a perennial crop, the selection process concerning pathogen resistance is only possible 2 to 3 years after plant crossing, after which the more resistant seedlings are kept (Eibach and Töpfer, 2015). Considering the high number of newly developed seedlings, shortening this time would represent a considerable financial benefit to the producers. Hence, any new or advanced selection methods of these new cultivars can lead to a more efficient breeding process.

The discovery of mildew resistance-associated biomarkers in grapevine will allow a quick and accurate identification of the seedlings that inherited the resistant trait soon after germination. Disease-resistance genetic markers have been searched for the past 14 years and quantitative trait loci (QTLs) for resistance to downy mildew were identified (Gessler et al., 2011). Among these, the Resistance to *Plasmopara viticola* (RPV) loci were identified in several *Vitis* species. These loci can be passed into the offspring in cross-breeding programs between *V. vinifera* and other *Vitis* species, but their presence in the cross-bred cultivars does not guarantee resistance to downy mildew (Peressotti et al., 2010). Hence, the resistance of the wild *Vitis* species to *P. viticola* most probably goes beyond the presence of these DNA markers in their genome. Metabolic biomarkers have proven their value to predict phenotypical traits before they are observed (Wolfender et al., 2013). In this area, metabolomics is a powerful tool, for its ability to simultaneously characterize and quantify multiple metabolites (Shepherd et al., 2011). Recently, biomarkers associated with the defence response to downy mildew were identified in a resistant cultivar after leaf inoculation with *P. viticola* (Chitarrini et al., 2017). While most of these studies in grapevine are focused in the metabolic profile of host-pathogen interactions, little is known about the constitutive differences of resistant and susceptible cultivars that could undoubtedly discriminate both groups.

One of the first studies on the discrimination of downy mildew resistant and susceptible grapevine varieties followed a metabolic profiling approach using nuclear magnetic resonance (NMR) (Figueiredo et al., 2008). About 13 metabolites were identified and 7 were differentially accumulated in 'Regent' (more resistant to mildew) and 'Trincadeira' (susceptible). To substantially increase metabolome coverage, in the present work we analysed the same cultivars by Fourier Transform Ion Cyclotron Resonance mass spectrometry (FT-ICR-MS). Due to its ultra-high-resolution and ultra-high-mass accuracy, this

technology is one of the best tools to fingerprint complex samples, allowing very high metabolome coverage (Maia et al., 2016). With this untargeted metabolomics analysis, we increased the number of features detected, significantly increased the ones exclusively present in 'Trincadeira' or 'Regent' and identified several metabolites that discriminate them.

3.3 MATERIALS AND METHODS

3.3.1 Plant material

Vitis vinifera accessions 'Trincadeira' and 'Regent' were collected at the Portuguese Ampelographic Grapevine Collection (CAN, international code PRT051), INIAV-Dois Portos. For each accession, the third to fifth leaves (from the shoot apex) were harvested from 5 fully developed plants and combined in 1 biological replicate, being collected 3 biological replicates for analysis.

3.3.2 Metabolite extraction and FT-ICR-MS analysis

Metabolite extraction was performed as previously reported (Maia, 2016). Only the methanol fraction was analysed by direct infusion on the 7T-FT-ICR mass spectrometer (Brüker Daltonics), in positive electrospray ionization (ESI$^+$) mode. The internal standard leucine enkephalin (YGGFL, Sigma Aldrich Portugal) was added to all samples at a final concentration of 0.5 µg/mL, being considered a mass of $[M+H]^+ = 556.276575$ Da for analysis by ESI$^+$. Spectra were recorded between 100 and 1000 m/z. Spectra analysis and alignment were performed as previously reported (Maia et al., 2016).

3.3.3 Multivariate analysis

Multivariate analysis considering peak intensities (Principal Component Analysis (PCA) and Partial Least Squares - Discriminant Analysis (PLS-DA)) was performed using the program MetaboAnalyst (http://www.metaboanalyst.ca/, (Xia et al., 2015). Missing value imputation was done by substitution by half of the minimum positive value found within the data. Intensity data were normalized to the internal standard (leucine enkephalin), generalized log transformed, and Pareto scaled prior to multivariate methods.

3.3.4 Metabolite identification

The search for candidate compounds among the peaks that clearly discriminate the 'Trincadeira' and 'Regent' cultivars was performed in the MassTRIX database (http://masstrix3.helmholtz-muenchen.de/, (Suhre and Schmitt-Kopplin, 2008). Mass lists were searched in positive ionization mode, considering the adducts $[M+H]^+$, $[M+K]^+$ and $[M+Na]^+$ and 2 ppm as maximum *m/z* deviation from theoretical mass. *Vitis vinifera* was the selected organism and the search was performed in the combined database of KEGG (Kyoto Encyclopedia of Genes and Genomes) / HMDB (Human Metabolome Data Base) / LIPID MAPS without isotopes.

3.4 RESULTS AND DISCUSSION

Metabolomics has been widely used to discriminate samples based on the natural variance in metabolite content (Becker et al., 2013; Gougeon et al., 2009; Plumb et al., 2006; Rhourrhi-Frih et al., 2012). In this approach, metabolite identification is not a requirement for sample discrimination (Becker et al., 2013; Plumb et al., 2006). We performed an untargeted metabolomics analysis by FT-ICR-MS to compare the metabolome between two *V. vinifera* cultivars presenting different degrees of resistance against downy mildew, 'Trincadeira' and 'Regent'. A total of 1912 peaks were detected in *V. vinifera* 'Regent' and 1615 in 'Trincadeira'. Of these, 665 were exclusive to 'Regent' and 368 to 'Trincadeira'. When compared to NMR analysis of the same cultivars (Figueiredo et al., 2008), the metabolic profiling by FT-ICR-MS significantly increased metabolome coverage and the number of cultivar-specific features observed. PCA showed a clear separation between the two cultivars for the first two components (**Figure 3.1 - A**). This separation was confirmed by sample hierarchical clustering using the Euclidean distance for the most significantly different peaks (**Figure 3.1 - B**). Seeking the features most responsible for these differences, we obtained the top 15 of the most discriminatory peaks of a PLS-DA classification model using Variable Importance in Projection (VIP) scores (**Figure 3.1 - C**). Features with a higher VIP score (normally above 1) are regarded as significant in a given model. The top 15 most discriminatory peaks between 'Regent' and 'Trincadeira' present VIP scores between 2 and 3, being therefore highly important in this model.

The search for candidate compounds among the peaks that clearly discriminate the two cultivars was performed in the MassTRIX database. For *V. vinifera* 'Regent', one of these compounds was identified as caffeic acid 3-glucoside. This result corroborated the previous finding using NMR (Figueiredo et al., 2008), which reported the presence of higher amounts

of caffeic acid in 'Regent' when compared to 'Trincadeira'. Two other discriminatory compounds for 'Regent' were oleic acid (C18:1) and its methyl ester form. In *Arabidopsis thaliana*, oleic acid induces the activation of defence responses mediated by jasmonic acid (JA) and represses the salicylic acid (SA) signalling pathway (reviewed in Lim et al., 2017). Indeed, these signalling pathways are highly relevant for grapevine resistance, with the activation of the JA signalling pathway and the interaction between JA and SA being tailored in the defence response against *P. viticola* (Guerreiro et al., 2016). Another compound only identified in 'Regent', also associated with lipid signalling, was palmitoleic acid (C16:1). This fatty acid also plays a likely role in plant defence against fungal pathogens (reviewed in (Lim et al., 2017).
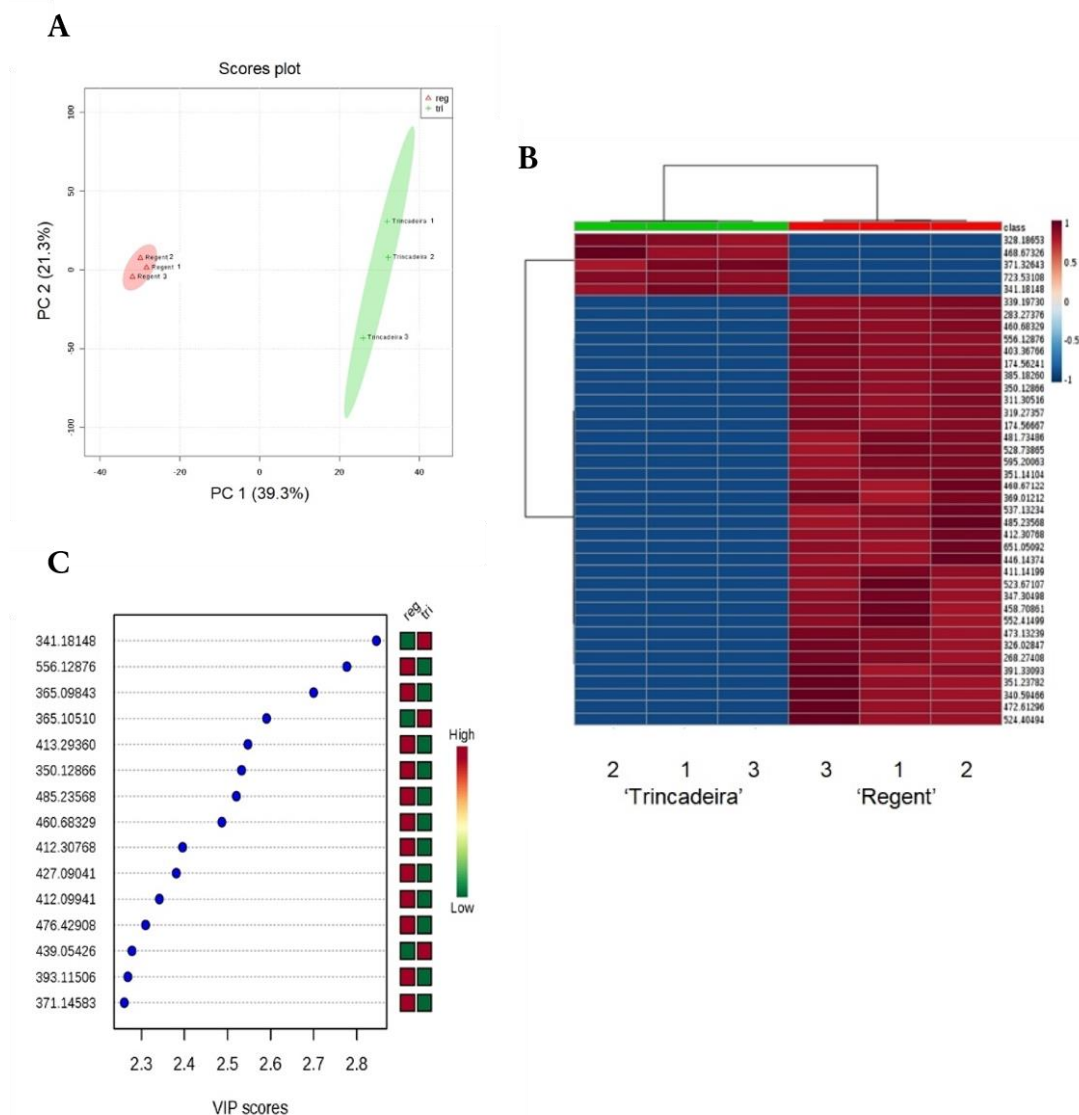
Figure 3.1 - Metabolome difference and discrimination between 'Trincadeira' and 'Regent'. (**A**) PCA scores with sample labels and 95% confidence regions shown. (**B**) Sample hierarchical clustering and heatmap using the top 50 most significant (*t*-test *p*-values) MS peaks. (**C**) Top discriminative peaks in a PLS-DA classification model, shown by decreasing scores of Variable Importance in Projection (VIP) over the first component.

3.5 CONCLUSIONS

Grapevine breeding approaches offer forward-looking perspectives for an environmentally friendly and sustainable viticulture. The discovery of biomarkers will allow a quick and accurate identification of the plantlets that inherited the resistant characteristic soon after germination. Using an untargeted metabolomics approach, based on ultra-high resolution and high-mass accuracy mass spectrometry, we compared two *V. vinifera* cultivars with different degrees of resistance towards the downy mildew. The Portuguese 'Trincadeira' is susceptible to this disease, whereas the interspecific hybrid 'Regent' contains a high degree of resistance. We were able to clearly discriminate both cultivars (without pathogen infection) and identify the most discriminatory compounds. Additionally, we identified features that are exclusive to one or the other cultivar. With the present work, we were able to show the potential of the metabolomics based on ultra-high resolution and ultra-high mass accuracy (FT-ICR-MS). Our work will contribute, not only to grapevine variety discrimination, but also a deeper identification of compounds that participate in the grapevine resistance mechanisms. Moreover, this approach may also contribute for the development of efficient biomarker assays, based on resistance-associated metabolites, to help future breeding programs and introgression line analysis.

3.6 ACKNOWLEDGMENTS

3.7 REFERENCES

Becker, L., Poutaraud, A., Hamm, G., Muller, J.-F., Merdinoglu, D., Carré, V., Chaimbault, P., 2013. Metabolic study of grapevine leaves infected by downy mildew using negative ion electrospray – Fourier transform ion cyclotron resonance mass spectrometry. Analytica Chimica Acta 795, 44–51. https://doi.org/10.1016/j.aca.2013.07.068

Chitarrini, G., Soini, E., Riccadonna, S., Franceschi, P., Zulini, L., Masuero, D., Vecchione, A., Stefanini, M., Di Gaspero, G., Mattivi, F., Vrhovsek, U., 2017. Identification of

Biomarkers for Defense Response to *Plasmopara viticola* in a Resistant Grape Variety. Front. Plant Sci. 8. https://doi.org/10.3389/fpls.2017.01524

Eibach, R., Töpfer, R., 2015. Traditional grapevine breeding techniques, in: Grapevine Breeding Programs for the Wine Industry. Woodhead Publishing, Oxford, pp. 3–22.

Figueiredo, A., Fortes, A.M., Ferreira, S., Sebastiana, M., Choi, Y.H., Sousa, L., Acioli-Santos, B., Pessoa, F., Verpoorte, R., Pais, M.S., 2008. Transcriptional and metabolic profiling of grape (*Vitis vinifera* L.) leaves unravel possible innate resistance against pathogenic fungi. J. Exp. Bot. 59, 3371–3381. https://doi.org/10.1093/jxb/ern187

Gessler, C., Pertot, I., Perazzolli, M., 2011. *Plasmopara viticola*: a review of knowledge on downy mildew of grapevine and effective disease management. Phytopathologia Mediterranea 50, 3–44. https://doi.org/10.14601/Phytopathol_Mediterr-9360

Gougeon, R.D., Lucio, M., De Boel, A., Frommberger, M., Hertkorn, N., Peyron, D., Chassagne, D., Feuillat, F., Cayot, P., Voilley, A., Gebefügi, I., Schmitt-Kopplin, P., 2009. Expressing Forest Origins in the Chemical Composition of Cooperage Oak Woods and Corresponding Wines by Using FTICR-MS. Chem. Eur. J. 15, 600–611. https://doi.org/10.1002/chem.200801181

Guerreiro, A., Figueiredo, J., Sousa Silva, M., Figueiredo, A., 2016. Linking Jasmonic Acid to Grapevine Resistance against the Biotrophic Oomycete *Plasmopara viticola*. Front Plant Sci 7. https://doi.org/10.3389/fpls.2016.00565

Lim, G.-H., Singhal, R., Kachroo, A., Kachroo, P., 2017. Fatty Acid– and Lipid-Mediated Signaling in Plant Defense. Annual Review of Phytopathology 55, 505–536. https://doi.org/10.1146/annurev-phyto-080516-035406

Maia, M., 2016. Metabolic characterization of grapevine leaves: first clues towards biomarkers discovery (Masters' Thesis). Universidade de Lisboa, Portugal.

Maia, M., Monteiro, F., Sebastiana, M., Marques, A.P., Ferreira, A.E.N., Freire, A.P., Cordeiro, C., Figueiredo, A., Sousa Silva, M., 2016. Metabolite extraction for high-throughput FTICR-MS-based metabolomics of grapevine leaves. EuPA Open Proteom 12, 4–9. https://doi.org/10.1016/j.euprot.2016.03.002

Organisation of Vine and Wine, 2017. 2017 OIV Statistical Report on World Vitiviniculture.

Peressotti, E., Wiedemann-Merdinoglu, S., Delmotte, F., Bellin, D., Di Gaspero, G., Testolin, R., Merdinoglu, D., Mestre, P., 2010. Breakdown of resistance to grapevine downy mildew upon limited deployment of a resistant variety. BMC Plant Biology 10, 147. https://doi.org/10.1186/1471-2229-10-147

Plumb, R.S., Johnson, K.A., Rainville, P., Shockcor, J.P., Williams, R., Granger, J.H., Wilson, I.D., 2006. The detection of phenotypic differences in the metabolic plasma profile of three strains of Zucker rats at 20 weeks of age using ultra-performance liquid chromatography/orthogonal acceleration time-of-flight mass spectrometry. Rapid Commun Mass Spectrom 20, 2800–2806. https://doi.org/10.1002/rcm.2655

Rhourrhi-Frih, B., West, C., Pasquier, L., André, P., Chaimbault, P., Lafosse, M., 2012. Classification of natural resins by liquid chromatography-mass spectrometry and gas chromatography-mass spectrometry using chemometric analysis. J Chromatogr A 1256, 177–190. https://doi.org/10.1016/j.chroma.2012.07.050

Shepherd, L.V., Fraser, P., Stewart, D., 2011. Metabolomics: a second-generation platform for crop and food analysis. Bioanalysis 3, 1143–1159. https://doi.org/10.4155/bio.11.61

Suhre, K., Schmitt-Kopplin, P., 2008. MassTRIX: mass translator into pathways. Nucl. Acids Res. 36, W481–W484. https://doi.org/10.1093/nar/gkn194

Wolfender, J.-L., Rudaz, S., Choi, Y.H., Kim, H.K., 2013. Plant metabolomics: from holistic data to relevant biomarkers. Curr. Med. Chem. 20, 1056–1090. https://doi.org/10.2174/0929867311320080009

Xia, J., Sinelnikov, I.V., Han, B., Wishart, D.S., 2015. MetaboAnalyst 3.0—making metabolomics more meaningful. Nucleic Acids Res 43, W251–W257. https://doi.org/10.1093/nar/gkv380

CHAPTER IV

Comparison of the chemical diversity of *Vitis rotundifolia* and *Vitis vinifera* cv. 'Cabernet sauvignon'

4 Comparison of the chemical diversity of *Vitis rotundifolia* and *Vitis vinifera* cv. 'Cabernet sauvignon'

4.1 ABSTRACT

Grapevine is one of the most important fruit plants in the world, mainly due to its grapes and related products, with a highly economic and cultural importance. Every year, vineyards are affected by several pathogen outbreaks and the only way to control them is through preventive applications of agrochemicals every 12 to 15 days. This approach is not sustainable and not always effective. The *Vitis* genus comprise different species that exhibit varying levels of resistance to pathogens, thus the understanding of the innate resistance/susceptibility mechanisms of these different *Vitis* species is crucial to cope with these threats. In this work, an untargeted metabolomics approach was followed, using Fourier transform-ion cyclotron resonance mass spectrometry (FT-ICR-MS), to analyse the metabolic chemical diversity of two *Vitis* species: *Vitis rotundifolia* (resistant to pathogens) and *V. vinifera* cv. 'Cabernet Sauvignon' (susceptible to pathogens). Chemical formulas from both *Vitis* were used to build Van Krevelen diagrams and compositional space plots, which do not require full metabolite identification and provide an easy comparison method. Based only on these visualization tools, it was shown that the *V. rotundifolia* metabolome is more complex than the metabolome of *V. vinifera* cv. 'Cabernet Sauvignon'. Moreover, the regions that present a higher density are associated to lipids, polyketides and carbohydrates. Also, *V. rotundifolia* metabolome presented a higher ratio O/C compounds.

4.2 INTRODUCTION

The history of the grapevine is long and extremely complex with different theories and is present in the human culture since ancient times. Geographical and archaeological studies show that cultivation and domestication of grapevine appear to have occurred between the 7000 and the 4000 BC (García and Revilla, 2013; Fortes and Pais, 2016), with fermentation processes being developed since 6000 BC (Terral et al., 2010). Despite its importance, only one grapevine species was domesticated, while the others remain practically wild.

The genus *Vitis* comprises two sub-genera: *Muscadinia* and *EuVitis* differing in morphological, anatomical and cytological characters. The *Muscadinia* sub-genera comprise three species, while the *EuVitis* includes *Vitis vinifera*, with the subspecies sylvestris (wild vines) and *vinifera* (or sativa), the domesticated one. A great majority of cultivars, now widely

cultivated for fruit, juice and mainly for wine belong to *Vitis vinifera* subsp. *vinifera* (Sefc et al., 2003; This et al., 2006).

Due to its cultural and economic importance, *V. vinifera* is considered one of the most important fruit crops in the world, with a global market size of 31 billion euros (Organisation of Vine and Wine, 2019). However, it is highly susceptible to different pathogens, such as *Plasmopara viticola* (Berk. & Curt.) Berl. & de Toni) Beri, et de Toni, *Erysiphe necator* (Schweinf.) Burrill and *Botrytis cinerea* Pers., the causal agents of downy, powdery mildew and gray mold, respectively, requiring preventive applications of chemical products for disease control. On the other hand, *Muscadinia* species exhibit varying levels of resistance to the pathogens. Understanding the innate molecular basis resistance/susceptibility mechanisms of these different *Vitis* species became crucial for the development of new *V. vinifera* varieties, more resistant to pathogens. Recently, our group showed that the metabolome of *V. vinifera* cultivars is different from other *Vitis* species (Maia et al., 2020a) with different degrees of tolerance/susceptibility to fungal and oomycete related pathogens, highlighting the importance of chemical fingerprinting and its relevance in the identification of resistance/susceptibility-related biomarkers.

The ultra-high-resolution and ultra-high-mass accuracy Fourier Transform Ion Cyclotron Resonance mass spectrometry (FT-ICR-MS) is considered to be superior to any other analytical technique and is one of the best approaches to perform untargeted analysis of complex samples (Kuhnert et al., 2020). Due to its characteristics, it allows the detection of a large number of analytes in a single experiment providing a chemical fingerprint of any given sample and a reliable information on the elemental composition of all analytes detected (Gougeon et al., 2009; Kuhnert et al., 2020; Wu et al., 2004). Such characteristics allow the characterization of different samples, *e.g*: wine (Roullier-Gall et al., 2018, 2017), black tea (Kuhnert et al., 2010), coffee (Jaiswal et al., 2012) and grapevine leaves (Adrian et al., 2017; Becker et al., 2013; Maia et al., 2020a, 2016).

Untargeted analysis of complex samples generates very complex mass spectrum (Gutiérrez Sama et al., 2018), making the analysis challenging due to the difficulty to easily represent and visualize the data. Hence the validation of graphical methods supporting the interpretation and comparison of FT-ICR-MS complex data is very important. Two types of graphical representation were developed, allowing a comprehensive interpretation of complex mass spectrometry data from untargeted metabolomics approaches, both based only on the identified chemical formulas: two-dimensional van Krevelen (VK) diagrams displaying H/C (hydrogen/carbon) versus O/C (oxygen/carbon) ratios (Van Krevelen, 1950) and compositional space plots that use double-bond equivalents (DBE) values (Brockman et al., 2018; Gutiérrez Sama et al., 2018; Kew et al., 2017; Mann et al., 2015; Wu et al., 2004).

Analyzing the elemental composition of the different samples allows the qualitative comparison between series of related samples in terms of their chemical complexity. Van Krevelen diagrams and compositional space plots convey simple, albeit qualitative information on the main molecular classes represented (Adrian et al., 2017; Gutiérrez Sama et al., 2018; Roullier-Gall et al., 2017, 2014; Tziotis et al., 2011). Moreover, in VK diagrams, the H/C ratio is related to the degree of separation, whereas the O/C ratio is related to oxidation (Wu et al., 2004). In plants, the degree of oxidation of certain compounds and their saturation are extremely important as they can be associated to defence responses to biotic and abiotic stresses (Torres et al., 2006). This tool has been mainly used in organic matter samples but due to its easy application to the analysis of complex samples, VK diagrams have recently been used to discriminate samples of biological origin. So far, these plots have been used to study the volatile profile of varietal olive oils from Alentejo region (Martins et al., 2020), satureja essential oils (Maccelli et al., 2020), bottle-aged Chardonnay wines (Roullier-Gall et al., 2017) and for early detection of grapevine leaves' infection (Maia et al., 2019).

The present work aimed to compare the chemical diversity of two *Vitis* species (*Vitis rotundifolia* and *V. vinifera* cv. 'Cabernet Sauvignon'), without any stress, with different resistance levels to pathogens, through an untargeted metabolomics approach. In this study, both van Krevelen (VK) diagrams and compositional space plots were applied to the comparison of *Vitis rotundifolia* and *V. vinifera* cv. 'Cabernet Sauvignon' metabolomes in order to identify visually differences between both metabolomes and associate their resistance/susceptibility to pathogens to these metabolic differences. Grapevine genotypes were selected according to their resistance/susceptibility towards pathogens and importance in the wine industry. *V. rotundifolia*, the best known *Muscadinia* species, originated in the south-eastern United States serves as a rootstock to cope with the high sensitivity of European grapevines to *Phylloxera* disease (Fortes and Pais, 2016). Also, *V. rotundifolia* is highly resistant to the different pathogens (https://www.vivc.de/). *Vitis vinifera* cv. 'Cabernet Sauvignon' is one of the most planted grapevine cultivar in the world, covering an area of 341000 ha, and one of the most widely distributed across the world, mainly grown in China, France, Chile, the United States, Australia, Spain, Argentina, Italy and South Africa (Organisation of Vine and Wine, 2017). This cultivar, widely cultivated worldwide, is highly susceptible to different pathogens.

4.3   MATERIALS AND METHODS

4.3.1   Plant material

Vitis vinifera cv. 'Cabernet Sauvignon' and *Vitis rotundifolia* leaves were collected in the spring (May) from field grown plants belonging to the Portuguese Ampelographic Grapevine Collection (CAN, international code PRT051, established in 1988), at INIAV-Estação Vitivinícola Nacional (Dois Portos). CAN occupy nearly 2 ha of area with homogeneous modern alluvial soils (lowlands) as well as well drained soil. For all accessions in the field, a unique cultivar rootstock was used - Selection Oppenheim 4 (SO4) and each accession come from one unique plant. The climate in this region is temperate with dry and mild summer. The degree of resistance of the genotypes was accessed through bibliographic searches following the classification of International Organisation of Vine and Wine (OIV) (https://www.oiv.int) and *Vitis* International Variety Catalogue (VIVC) (https://www.vivc.de/). For plant material collection, the best possible health status was guaranteed. The third to fifth leaves, from the shoot to apex, were collected from seven fully developed plants and immediately frozen in liquid nitrogen. Leaves were stored at –80 ºC until analysis. Three biological replicates were considered for analysis. Plant material was ground in liquid nitrogen and used for metabolite extraction in the week after material collection.

4.3.2   Metabolite extraction and FT-ICR-MS analysis

Metabolite extraction from *V. vinifera* cv. 'Cabernet Sauvignon' and *V. rotundifolia* leaves was performed following a previously developed protocol (Maia et al., 2016), with minor modifications (Maia et al., 2020a). Briefly, after metabolite extraction with different solvents, the methanol fraction collected was diluted 1000-fold in methanol and analysed by direct infusion on an Apex Qe 7-Tesla Fourier Transform Ion Cyclotron Resonance Mass Spectrometer (7T-FT-ICR-MS, Brüker Daltonics). Leucine enkephalin (YGGFL, Sigma Aldrich) was added to all replicates as internal standard ($[M+H]^+$ = 556.276575 Da or $[M-H]^-$ = 554.262022 Da). For positive ion mode analysis (ESI^+), formic acid (Sigma Aldrich, MS grade) was added to all replicates at a final concentration of 0.1% (v/v). Spectra were acquired at both positive (ESI^+) and negative (ESI^-) electrospray ionization modes and recorded between 100 and 1000 m/z, as previously described (Maia et al., 2020a).

4.3.3   Data processing and chemical formula analysis

For all mass spectra, single point calibration with leucine enkephalin was performed using Data Analysis 5.0 (Brüker Daltonics, Bremen, Germany). Peaks were considered at a minimum signal-to-noise ratio of 4. For each replicate of *V. vinifera* 'Cabernet Sauvignon' and *V. rotundifolia*, mass lists were extracted. The metabolomics data are available in figshare data repository (Maia et al., 2020b). Putative assigned formulas were calculated using Data Analysis 5.0 smart formula tool following the upper formula ($C_{78}H_{126}O_{27}P_9S_{14}N_{20}$) and lower formula ($C_1H_1O_0P_0S_0N_0$). Formulas were exported to build van Krevelen (VK) diagrams, for compositional space analysis and determination of the elemental composition. The H/C ratio versus the O/C ratio for every compound in the sample were calculated and plotted, double bond equivalents (DBE) values were calculated according to (**Equation 4.1**) based on the CcHhOoNnSn molecular formula of each compound and plotted as a function of the number of carbon atoms. For elemental composition analysis, putative assigned formulas from each replicate were firstly combined and formulas presented only in one replicate were excluded. Only formulas presented in 2/3 replicates were considered for the analysis. Chemical formulas detected in each *Vitis* were divided in seven classes (CHO, CHOS, CHON, CHONS, CHOP, CHONP, CHONSP, OTHER) according to the chemical elements present: carbon, hydrogen, oxygen, nitrogen, sulphur, phosphorus and other.

(**Equation 4.1**) $$DBE = C - \frac{H}{2} + \frac{N}{2} + 1$$

4.4   RESULTS AND DISCUSSION

There is an increasing demand for more sustainable agricultural practices. In fact, since 2009, guidelines from the European Union (Directive 2009/128/EC) demand a reduction and sustainable use of pesticides (Scoones, 2016). To cope with these demands, researchers have been trying to uncover the defence /resistance grapevine mechanisms through "omics" studies aiming to help producers and industries for a sustainable viticulture (Buonassisi *et al.*, 2017; Li and Yan, 2020). Hence, the comparison of different *Vitis* genotypes with different resistance/susceptibility levels towards pathogens may allow a better understanding of these mechanisms. Since the metabolome is the first to be affected by changing conditions and provides information of current state of the organism, the study of different grapevine genotypes metabolomes, without stress, may highlight their innate resistance/susceptibility capabilities (Maia et al., 2020a). Having this in mind, the metabolome of two *Vitis* species, with different resistance levels to various pathogens was analysed in order to compare their chemical diversity and possibly relate their resistance or susceptibility to pathogens.

An untargeted metabolomics analysis using FT-ICR-MS was performed and the number of peaks detected in *V. vinifera* cv. 'Cabernet Sauvignon' in positive ionization mode was around 1600 peaks per replicate and in negative mode was around 750 (**Table 4.1**). In *V. rotundifolia* around 1100 peaks were detected in ESI⁺ and around 600 peaks were detected in ESI⁻ (**Table 4.1**). Replicates results demonstrate a high analytical reproducibility of the data obtained, indicating that the analysis of the metabolome profile of each *Vitis* leaves appears to be sufficiently consistent to distinguish these two *Vitis* species with different resistance levels to various pathogens. To provide insight into metabolite diversity, chemical formulas were assigned to the detected masses of each *Vitis*. A total of 385 and 1227 different formulas were detected respectively in *V. vinifera* "Cabernet Sauvignon" and *V. rotundifolia* (**Table 4.2**).

Table 4.1 - Number of peaks detected with ESI⁺ and ESI⁻ in both *Vitis* genotypes

Vitis	Replicates	Number of peaks detected	
		ESI⁺	ESI⁻
V. vinifera 'Cabernet sauvignon'	CS 1	1642	768
	CS 2	1599	838
	CS 3	1631	710
V. rotundifolia	ROT 1	1162	649
	ROT 2	1091	558
	ROT 3	1092	607

Table 4.2 - Number of elemental formulas detected in both *Vitis* according to their elemental composition: CHO, CHOS, CHON, CHONS, CHOP, CHONP, CHONSP and other.

	Vitis	*V. vinifera* 'Cabernet Sauvignon'		*V. 'Rotundifolia'*	
	Ionization mode	ESI⁻	ESI⁺	ESI⁻	ESI⁺
Number of elemental formulas	CHO	8	6	13	20
	CHOS	0	4	0	39
	CHON	9	38	29	121
	CHONS	3	33	2	140
	CHOP	3	14	15	55
	CHONP	23	111	88	232
	CHONSP	1	45	29	174
	Other	12	75	19	251
	Total by Ionization mode	59	326	195	1032
	Total	385		1227	

Compositional space plots and VK diagrams were generated for both genotypes and ionization modes (**Figure 4.1**) highlighting a wide chemical diversity between the two *Vitis* genotypes under analysis.

The positive ionization mode presented a higher number of peaks and consequently a higher number of chemical formulas (**Table 4.1** and **Table 4.2**) in both species analysed. Empirical regions of metabolic classes of the chemical formulas detected were also created in each VK diagram. The regions that present a higher density are associated to lipids, polyketides and carbohydrates. The lipids class is one of the most represented in both *Vitis* genotypes analysed. *V. rotundifolia* presented a higher number of compounds in the carbohydrate and polyketides region (**Figure 4.1**). In fact, polyketides are secondary metabolites involved in plant defence against pathogens. Within polyketides, flavonoids can be highlighted, considered to be one group of aromatic polyketides. In grapevine, flavonoids have already been identified as been associated to grapevine defences against downy mildew (Buonassisi et al., 2017; Chitarrini et al., 2017; Nascimento et al., 2019). Recently, our group also associated these compounds to resistant/tolerant and susceptible cultivars discrimination in no stress conditions (Maia et al., 2020a). Concerning carbohydrates, these metabolites are important signalling molecules involved in biotic and abiotic stresses (Trouvelot et al., 2014). Moreover, by comparing both samples, it is clear that *V. rotundifolia* presents a higher number of compounds with a higher O/C value, suggesting the presence of a higher number of oxidized compounds. Since plants do not possess mobile defence cells, their innate immunity depends on an effective signal transduction between cells to activate defence responses. One of these signals is the production of reactive oxygen species (ROS) (Torres *et al.*, 2006; Frederickson Matika and Loake, 2014; González-Bosch, 2018). The majority of the studies regarding oxygenated species in plants are performed upon plant challenge with a pathogen and not at a constitutive level (Doke et al., 1996; Figueiredo et al., 2017; Nascimento et al., 2019). Hence, the significance of this accumulation of oxidized compounds observed in *V. rotundifolia* must not be discarded and should be investigated in future experiments.

The DBE vs. the number of carbons were plotted for FT-ICR-MS data (**Figure 4.2**). *Vitis rotundifolia*, in both ionization modes, presented a larger number of compounds with a DBE value and with more carbon atoms in their structure. A recent study with *Vitis vinifera* cv. 'Regent' (a tolerant cultivar to pathogens) and *Vitis vinifera* cv. 'Trincadeira' (a susceptible cultivar to pathogens) infected with *Plasmopara viticola*, showed that, after infection the tolerant cultivar presented a higher content of unsaturated fatty acids which leads to a more fluid and permeable membrane and as a consequence to a better defence response to the pathogen (Laureano et al., 2018). The results obtained, although without pathogen challenge, are consistent with that study. To better understand and investigate this phenomenon, future studies should be performed.

Elemental formulas of each compound detected were also investigated for both genotypes (**Figure 4.3**). Significant differences between the two *Vitis* genotypes were observed, being CHON, CHONS, CHOP, CHONP and CHONSP the elemental formulas with the highest differences and more present in *Vitis rotundifolia* (**Figure 4.3**).
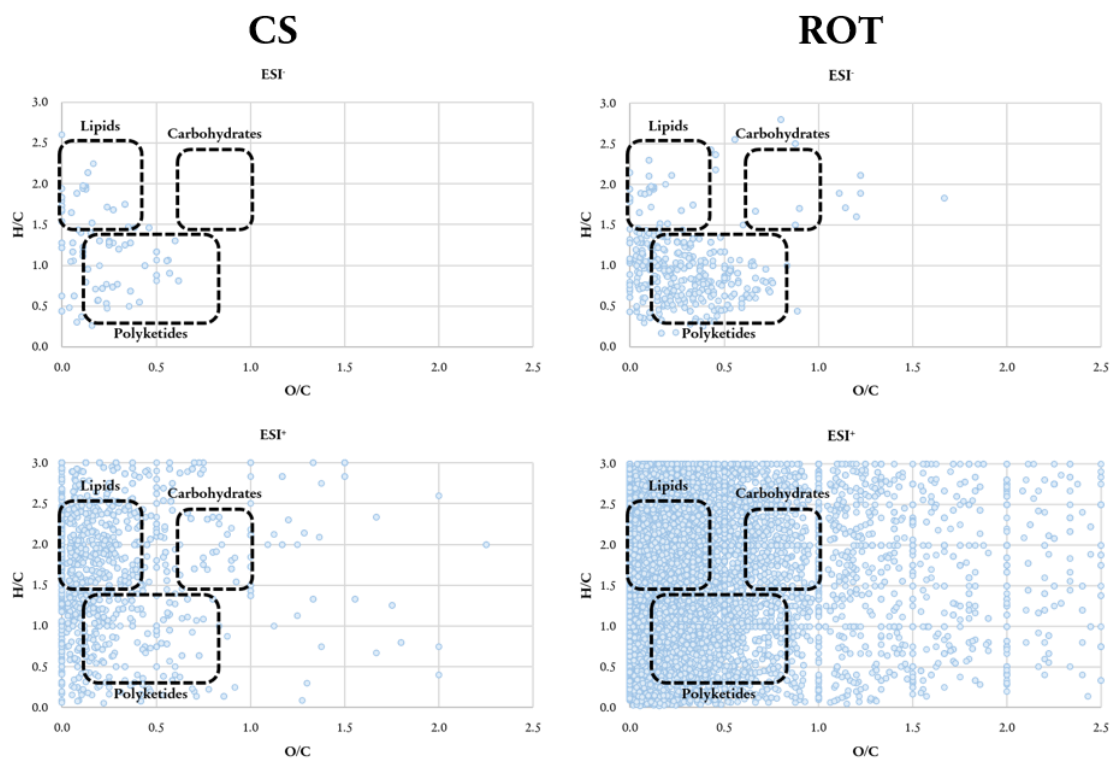
Figure 4.1 - Van Krevelen diagrams of *V. vinifera* cv. 'Cabernet Sauvignon' (CS) and *V. rotundifolia* (ROT) in ESI⁻ and ESI⁺. Areas with the highest point density are highlighted for the three most important major classes of metabolites: lipids, polyketides, carbohydrates.
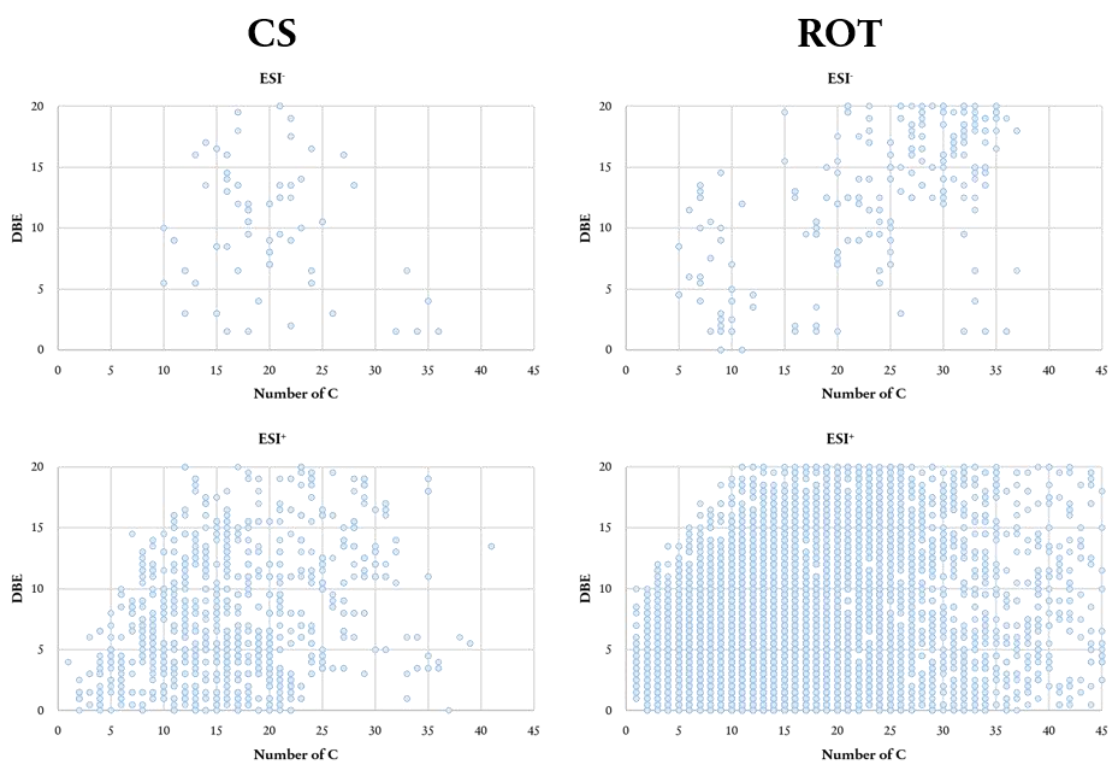
Figure 4.2 - Compositional space plot of *V. vinifera* cv. 'Cabernet Sauvignon' (CS) and *V. rotundifolia* (ROT) in ESI⁻ and ESI⁺.
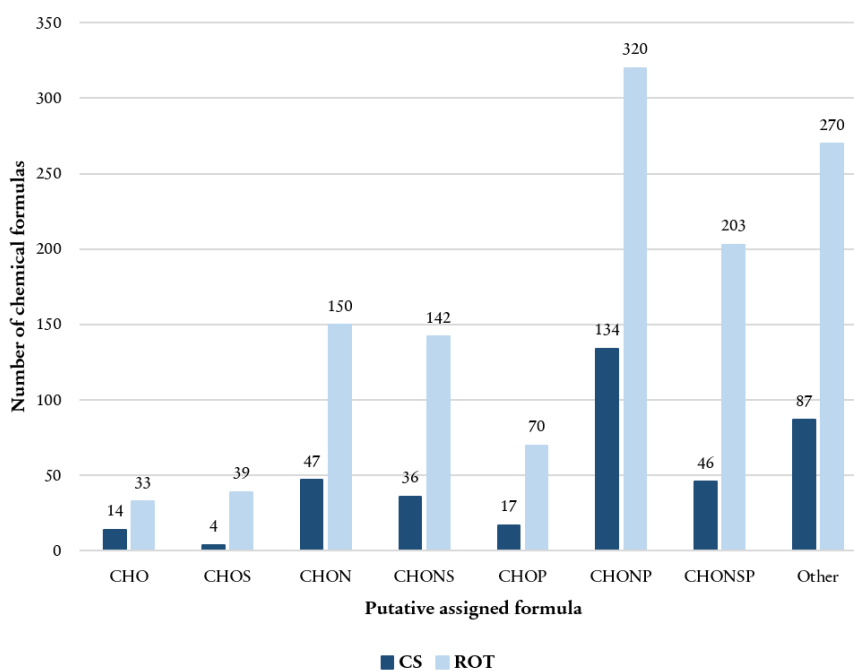
Figure 4.3 - Chemical histogram of *V. vinifera* cv. 'Cabernet Sauvignon' (CS) and *V. rotundifolia* (ROT) according to the elemental formulas detected: CHO, CHOS, CHON, CHONS, CHOP, CHONP, CHONSP and other.

4.5 CONCLUSIONS

In this work, two different *Vitis* genotypes that present different resistance levels towards pathogens were compared at the constitutive metabolic level through different visualization approaches. The results showed that both compositional space plots and VK diagrams allowed a fast comparison of chemical diversity between both metabolomes. Through these visualization techniques, it was shown that *V. rotundifolia* metabolome presented higher complexity than the metabolome from *V. vinifera* 'Cabernet Sauvignon'. Also, higher representation of compounds from the polyketides and carbohydrates groups was found in *V. rotundifolia*, which is in accordance with other studies. The presence of more oxidized compounds in the resistant *Vitis* at the constitutive level was also observed, and further studies should be conducted to better understand if their presence is associated to a higher capability to react upon pathogen challenge. These results open new insights into the study of constitutive compounds in grapevine through the analysis of complex untargeted data through visual tools.

4.6 ACKNOWLEDGEMENTS

4.7 REFERENCES

Adrian, M., Lucio, M., Roullier-Gall, C., Héloir, M.-C., Trouvelot, S., Daire, X., Kanawati, B., Lemaître-Guillier, C., Poinssot, B., Gougeon, R., Schmitt-Kopplin, P., 2017. Metabolic Fingerprint of PS3-Induced Resistance of Grapevine Leaves against *Plasmopara viticola* Revealed Differences in Elicitor-Triggered Defenses. Front Plant Sci 8, 101. https://doi.org/10.3389/fpls.2017.00101

Becker, L., Poutaraud, A., Hamm, G., Muller, J.-F., Merdinoglu, D., Carré, V., Chaimbault, P., 2013. Metabolic study of grapevine leaves infected by downy mildew using negative ion electrospray – Fourier transform ion cyclotron resonance mass

spectrometry. Analytica Chimica Acta 795, 44–51. https://doi.org/10.1016/j.aca.2013.07.068

Brockman, S.A., Roden, E.V., Hegeman, A.D., 2018. Van Krevelen diagram visualization of high resolution-mass spectrometry metabolomics data with OpenVanKrevelen. Metabolomics 14. https://doi.org/10.1007/s11306-018-1343-y

Buonassisi, D., Colombo, M., Migliaro, D., Dolzani, C., Peressotti, E., Mizzotti, C., Velasco, R., Masiero, S., Perazzolli, M., Vezzulli, S., 2017. Breeding for grapevine downy mildew resistance: a review of "omics" approaches. Euphytica 213. https://doi.org/10.1007/s10681-017-1882-8

Chitarrini, G., Soini, E., Riccadonna, S., Franceschi, P., Zulini, L., Masuero, D., Vecchione, A., Stefanini, M., Di Gaspero, G., Mattivi, F., Vrhovsek, U., 2017. Identification of Biomarkers for Defense Response to *Plasmopara viticola* in a Resistant Grape Variety. Front. Plant Sci. 8. https://doi.org/10.3389/fpls.2017.01524

Doke, N., Miura, Y., Sanchez, L.M., Park, H.J., Noritake, T., Yoshioka, H., Kawakita, K., 1996. The oxidative burst protects plants against pathogen attack: Mechanism and role as an emergency signal for plant bio-defence — a review. Gene 179, 45–51. https://doi.org/10.1016/S0378-1119(96)00423-4

Figueiredo, A., Martins, J., Sebastiana, M., Guerreiro, A., Silva, A., Matos, A.R., Monteiro, F., Pais, M.S., Roepstorff, P., Coelho, A.V., 2017. Specific adjustments in grapevine leaf proteome discriminating resistant and susceptible grapevine genotypes to *Plasmopara viticola*. Journal of Proteomics 152, 48–57. https://doi.org/10.1016/j.jprot.2016.10.012

Fortes, A.M., Pais, M.S., 2016. Grape (*Vitis* species), in: Nutritional Composition of Fruit Cultivars. Elsevier, pp. 257–286. https://doi.org/10.1016/B978-0-12-408117-8.00012-X

Frederickson Matika, D.E., Loake, G.J., 2014. Redox Regulation in Plant Immune Function. Antioxid Redox Signal 21, 1373–1388. https://doi.org/10.1089/ars.2013.5679

García, R.A.A., Revilla, E., 2013. The Current Status of Wild Grapevine Populations (*Vitis vinifera* ssp sylvestris) in the Mediterranean Basin. The Mediterranean Genetic Code - Grapevine and Olive. https://doi.org/10.5772/52933

González-Bosch, C., 2018. Priming plant resistance by activation of redox-sensitive genes. Free Radical Biology and Medicine, Redox Signalling in Plants and Implications for Mammalian Physiology 122, 171–180. https://doi.org/10.1016/j.freeradbiomed.2017.12.028

Gougeon, R.D., Lucio, M., De Boel, A., Frommberger, M., Hertkorn, N., Peyron, D., Chassagne, D., Feuillat, F., Cayot, P., Voilley, A., Gebefügi, I., Schmitt-Kopplin, P., 2009. Expressing Forest Origins in the Chemical Composition of Cooperage Oak Woods and Corresponding Wines by Using FTICR-MS. Chem. Eur. J. 15, 600–611. https://doi.org/10.1002/chem.200801181

Gutiérrez Sama, S., Farenc, M., Barrère-Mangote, C., Lobinski, R., Afonso, C., Bouyssière, B., Giusti, P., 2018. Molecular Fingerprints and Speciation of Crude Oils and Heavy Fractions Revealed by Molecular and Elemental Mass Spectrometry: Keystone between Petroleomics, Metallopetroleomics, and Petrointeractomics. Energy & Fuels 32, 4593–4605. https://doi.org/10.1021/acs.energyfuels.7b03218

Jaiswal, R., Matei, M.F., Golon, A., Witt, M., Kuhnert, N., 2012. Understanding the fate of chlorogenic acids in coffee roasting using mass spectrometry based targeted and non-targeted analytical strategies. Food Funct. 3, 976–984. https://doi.org/10.1039/C2FO10260A

Kew, W., Blackburn, J.W.T., Clarke, D.J., Uhrín, D., 2017. Interactive van Krevelen diagrams - Advanced visualisation of mass spectrometry data of complex mixtures: Interactive van Krevelen Diagrams. Rapid Communications in Mass Spectrometry 31, 658–662. https://doi.org/10.1002/rcm.7823

Kuhnert, N., Drynan, J.W., Obuchowicz, J., Clifford, M.N., Witt, M., 2010. Mass spectrometric characterization of black tea thearubigins leading to an oxidative cascade hypothesis for thearubigin formation. Rapid Communications in Mass Spectrometry 24, 3387–3404. https://doi.org/10.1002/rcm.4778

Kuhnert, N., D'souza, R.N., Behrends, B., Ullrich, M.S., Witt, M., 2020. Investigating time dependent cocoa bean fermentation by ESI-FT-ICR mass spectrometry. Food Research International 133, 109209. https://doi.org/10.1016/j.foodres.2020.109209

Laureano, G., Figueiredo, J., Cavaco, A.R., Duarte, B., Caçador, I., Malhó, R., Sousa Silva, M., Matos, A.R., Figueiredo, A., 2018. The interplay between membrane lipids and phospholipase A family members in grapevine resistance against *Plasmopara viticola*. Sci Rep 8, 14538. https://doi.org/10.1038/s41598-018-32559-z

Li, Q., Yan, J., 2020. Sustainable agriculture in the era of omics: knowledge-driven crop breeding. Genome Biology 21, 154. https://doi.org/10.1186/s13059-020-02073-5

Maccelli, A., Cesa, S., Cairone, F., Secci, D., Menghini, L., Chiavarino, B., Fornarini, S., Crestoni, M.E., Locatelli, M., 2020. Metabolic profiling of different wild and cultivated Allium species based on high-resolution mass spectrometry, high-performance liquid chromatography-photodiode array detector, and color analysis. Journal of Mass Spectrometry 55, e4525. https://doi.org/10.1002/jms.4525

Maia, M., Ferreira, A.E.N., Nascimento, R., Monteiro, F., Traquete, F., Marques, A.P., Cunha, J., Eiras-Dias, J.E., Cordeiro, C., Figueiredo, A., Sousa Silva, M., 2020a. Integrating metabolomics and targeted gene expression to uncover potential biomarkers of fungal/oomycetes-associated disease susceptibility in grapevine. Sci. Rep. 10, 15688. https://doi.org/10.1038/s41598-020-72781-2

Maia, M., Figueiredo, A., Sousa Silva, M., Ferreira, A., 2020b. Grapevine untargeted metabolomics to uncover potential biomarkers of fungal/oomycetes-associated diseases. figshare. Dataset. https://doi.org/10.6084/m9.figshare.12357314.v1

Maia, M., Maccelli, A., Nascimento, R., Ferreira, A.E.N., Crestoni, M.E., Cordeiro, C., Figueiredo, A., Sousa Silva, M., 2019. Early detection of *Plasmopara viticola*-infected leaves through FT-ICR-MS metabolic profiling. Acta Hortic. 575–580. https://doi.org/10.17660/ActaHortic.2019.1248.77

Maia, M., Monteiro, F., Sebastiana, M., Marques, A.P., Ferreira, A.E.N., Freire, A.P., Cordeiro, C., Figueiredo, A., Sousa Silva, M., 2016. Metabolite extraction for high-throughput FTICR-MS-based metabolomics of grapevine leaves. EuPA Open Proteom 12, 4–9. https://doi.org/10.1016/j.euprot.2016.03.002

Mann, B.F., Chen, H., Herndon, E.M., Chu, R.K., Tolic, N., Portier, E.F., Roy Chowdhury, T., Robinson, E.W., Callister, S.J., Wullschleger, S.D., Graham, D.E., Liang, L., Gu, B., 2015. Indexing Permafrost Soil Organic Matter Degradation Using High-Resolution Mass Spectrometry. PLoS One 10. https://doi.org/10.1371/journal.pone.0130557

Martins, N., Jiménez-Morillo, N.T., Freitas, F., Garcia, R., Gomes da Silva, M., Cabrita, M.J., 2020. Revisiting 3D van Krevelen diagrams as a tool for the visualization of volatile profile of varietal olive oils from Alentejo region, Portugal. Talanta 207, 120276. https://doi.org/10.1016/j.talanta.2019.120276

Nascimento, R., Maia, M., Ferreira, A.E.N., Silva, A.B., Freire, A.P., Cordeiro, C., Sousa Silva, M., Figueiredo, A., 2019. Early stage metabolic events associated with the establishment of *Vitis vinifera – Plasmopara viticola* compatible interaction. Plant Physiol Biochem 137, 1–13. https://doi.org/10.1016/j.plaphy.2019.01.026

Organisation of Vine and Wine, 2019. OIV Statistical Report on World Vitiviniculture.

Organisation of Vine and Wine, 2017. 2017 OIV Statistical Report on World Vitiviniculture.

Roullier-Gall, C., Hemmler, D., Gonsior, M., Li, Y., Nikolantonaki, M., Aron, A., Coelho, C., Gougeon, R.D., Schmitt-Kopplin, P., 2017. Sulfites and the wine metabolome. Food Chem 237, 106–113. https://doi.org/10.1016/j.foodchem.2017.05.039

Roullier-Gall, C., Signoret, J., Hemmler, D., Witting, M.A., Kanawati, B., Schäfer, B., Gougeon, R.D., Schmitt-Kopplin, P., 2018. Usage of FT-ICR-MS Metabolomics for Characterizing the Chemical Signatures of Barrel-Aged Whisky. Frontiers in Chemistry 6. https://doi.org/10.3389/fchem.2018.00029

Roullier-Gall, C., Witting, M., Gougeon, R.D., Schmitt-Kopplin, P., 2014. High precision mass measurements for wine metabolomics. Front. Chem. 2. https://doi.org/10.3389/fchem.2014.00102

Scoones, I., 2016. The Politics of Sustainability and Development. Annual Review of Environment and Resources 41, 293–319. https://doi.org/10.1146/annurev-environ-110615-090039

Sefc, K.M., Steinkellner, H., Lefort, F., Botta, R., Machado, A. da C., Borrego, J., Maletić, E., Glössl, J., 2003. Evaluation of the Genetic Contribution of Local Wild Vines to European Grapevine Cultivars. Am J Enol Vitic. 54, 15–21.

Terral, J.-F., Tabard, E., Bouby, L., Ivorra, S., Pastor, T., Figueiral, I., Picq, S., Chevance, J.-B., Jung, C., Fabre, L., Tardy, C., Compan, M., Bacilieri, R., Lacombe, T., This, P., 2010. Evolution and history of grapevine (*Vitis vinifera*) under domestication: new morphometric perspectives to understand seed domestication syndrome and reveal origins of ancient European cultivars. Annals of Botany 105, 443–455. https://doi.org/10.1093/aob/mcp298

This, P., Lacombe, T., Thomas, M., 2006. Historical origins and genetic diversity of wine grapes. Trends in Genetics 22, 511–519. https://doi.org/10.1016/j.tig.2006.07.008

Torres, M.A., Jones, J.D.G., Dangl, J.L., 2006. Reactive Oxygen Species Signaling in Response to Pathogens. Plant Physiol 141, 373–378. https://doi.org/10.1104/pp.106.079467

Trouvelot, S., Héloir, M.-C., Poinssot, B., Gauthier, A., Paris, F., Guillier, C., Combier, M., Trdá, L., Daire, X., Adrian, M., 2014. Carbohydrates in plant immunity and plant protection: roles and potential application as foliar sprays. Front. Plant Sci. 5. https://doi.org/10.3389/fpls.2014.00592

Tziotis, D., Hertkorn, N., Schmitt-Kopplin, P., 2011. Kendrick-analogous network visualisation of ion cyclotron resonance Fourier transform mass spectra: improved options for the assignment of elemental compositions and the classification of organic molecular complexity. Eur J Mass Spectrom (Chichester) 17, 415–421. https://doi.org/10.1255/ejms.1135

Van Krevelen, D.W., 1950. Graphical-Statistical Method for the Study of Structure and Reaction Processes of Coal. Fuel 29, 269–228.

Wu, Z., Rodgers, R.P., Marshall, A.G., 2004. Two- and Three-Dimensional van Krevelen Diagrams: A Graphical Analysis Complementary to the Kendrick Mass Plot for Sorting Elemental Compositions of Complex Organic Mixtures Based on Ultrahigh-Resolution Broadband Fourier Transform Ion Cyclotron Resonance Mass Measurements. Analytical Chemistry 76, 2511–2516. https://doi.org/10.1021/ac0355449

CHAPTER V

Integrating metabolomics and targeted gene expression to uncover potential biomarkers of fungal/oomycetes-associated disease susceptibility in grapevine

The sections in this chapter are organized differently from the paper.

5 Integrating metabolomics and targeted gene expression to uncover potential biomarkers of fungal/oomycetes-associated disease susceptibility in grapevine

5.1 ABSTRACT

Vitis vinifera, one of the most cultivated fruit crops, is susceptible to several diseases particularly caused by fungus and oomycete pathogens. In contrast, other *Vitis* species (American, Asian) display different degrees of tolerance/resistance to these pathogens, being widely used in breeding programs to introgress resistance traits in elite *V. vinifera* cultivars. Secondary metabolites are important players in plant defence responses. Therefore, the characterization of the metabolic profiles associated with disease resistance and susceptibility traits in grapevine is a promising approach to identify trait-related biomarkers. In this work, the leaf metabolic composition of eleven *Vitis* genotypes was analysed using an untargeted metabolomics approach. A total of 190 putative metabolites were found to discriminate resistant/tolerant from susceptible genotypes. The biological relevance of discriminative compounds was assessed by pathway analysis. Several compounds were selected as promising biomarkers and the expression of genes coding for enzymes associated with their metabolic pathways was analysed. Reference genes for these grapevine genotypes were established for normalisation of candidate gene expression. The leucoanthocyanidin reductase 2 gene (*LAR2*) presented a significant increase of expression in susceptible genotypes, in accordance with catechin accumulation in this analysis group. Up to our knowledge this is the first time that metabolic constitutive biomarkers are proposed, opening new insights into plant selection on breeding programs.

5.2 INTRODUCTION

Grapevine (*Vitis vinifera* L.) is one of the most cultivated fruit plants in the world, with an important economic impact in wine and table grape industries. Of the 80 known and globally distributed *Vitis* species (Organisation of Vine and Wine, 2019a, 2019b), *Vitis vinifera* L. is the mostly used in viticulture. As a result of its easy cultivation, vineyards longevity and numerous applications, in 2018, the global surface area for grapevine production was 7.4 mha (Organisation of Vine and Wine, 2019b). Grapevine cultivation requires preventive applications of agrochemicals to control several diseases, such as downy mildew [*Plasmopara viticola* (Berk. & Curt.) Berl. & de Toni) Beri, et de Toni], powdery mildew [(*Erysiphe necator* syn. *Uncinula necator* (Schweinf.) Burrill), gray mold (*Botrytis cinerea* Pers.) and black rot

(*Guignardia bidwellii* (Ellis) Viala & Ravaz), that affect all the green parts of the plant and grapes (Micheloni, 2017). However, some chemical products are not entirely efficient, with major pathogen outbreaks being reported (Delmotte et al., 2014; Peressotti et al., 2010). Others are more efficient but have highly economic and environmental costs, besides the detrimental effects to human and animal health (Cabras and Angioni, 2000; Lamichhane et al., 2015). Over the last decade, there has been an increasing demand for environmentally friendly agricultural practices. With the general recommendations of the European agricultural policy encouraging the reduction of pesticides towards environmental sustainability and consumer health improvement, alternatives are needed. One possible approach is the creation of more resistant grapevine varieties through cross-breeding programs between wild *Vitis* sp. (resistant) and *V. vinifera* (susceptible), combining resistant traits with highly desired and unique grape properties. Several crossing lines inbreed with American *Vitis* species are currently commercialized as tolerant varieties to fungal pathogens, e.g. Regent, Calardis Blanc, Solaris (Bove and Rossi, 2020; Zini et al., 2019).

In breeding programs, the selection for pathogen resistance traits is only possible 2 to 3 years after plant crossing, after which the more resistant seedlings are kept (Eibach and Töpfer, 2015; Reynolds, 2015). Considering the high number of newly developed seedlings, the establishment of new and advanced selection methods that can shorten this selection time and lead to a more efficient breeding process is a much-needed requirement. Grapevine genotypes possess distinct degrees of resistance to different fungal pathogens (https://www.vivc.de/). Hence, the study of different grapevine genotypes metabolomes, without stress, will uncover the innate metabolic differences between them. The full comprehension of disease resistance or tolerance mechanisms allied with the discovery of fungal/oomycete pathogen resistance-associated biomarkers in grapevine, may allow a quick and accurate identification of the seedlings that inherited the resistant trait soon after germination.

Secondary metabolites have been proven to play an important role in grapevine defences against pathogens. Several studies have been published in pathogen infection conditions which has allowed the metabolite profiling of some grapevine-pathogen interactions through various analytical instruments. Some of these metabolites have been highlighted as possible biomarkers (Ali et al., 2012; Batovska et al., 2009, 2008; Becker et al., 2013; Chitarrini et al., 2017; Figueiredo et al., 2008; Malacarne et al., 2011; Nascimento et al., 2019).

For instance, the accumulation of inositol and caffeic acid are possibly related to the innate resistance (Ali et al., 2012; Figueiredo et al., 2008) and hexadecanoic and the monohydroxycarboxylic acids were associated to grapevine resistance (Batovska et al., 2009).

Moreover, stilbenoids were already reported as key defence compounds involved in grapevine resistance to *Plasmopara viticola*, *Erysiphe necator* and *Botrytis cinerea* (Malacarne et al., 2011; Viret et al., 2018).

Metabolic biomarkers have proven their value to predict phenotypical traits before they are observed (Wolfender et al., 2013). In this area, metabolomics is a powerful tool due to its ability to simultaneously characterize and quantify multiple metabolites (Bennett and Wallsgrove, 1994; Fiehn, 2002; Shepherd et al., 2011). Due to its extreme resolution and ultra-high mass accuracy, Fourier Transform Ion Cyclotron Resonance mass spectrometry (FT-ICR-MS) is particularly powerful for an untargeted metabolome characterization, being successfully used in the study of grapevine chemical profile (Adrian et al., 2017; Maia et al., 2019, 2016; Nascimento et al., 2019). Additionally, metabolomics can also be used to explore metabolic pathways, uncover key enzymes involved in the biosynthesis/catalysis of metabolites and therefore genes associated with a wide range of responses. Metabolomics together with metabolic quantitative trait loci (mQTL) mapping, are being used as tools for assisting crops' improvement, representing a breakthrough advance for the selection of offsprings with relevant traits and identification of trait-associated metabolic biomarkers (Shepherd et al., 2011). This approach has been applied to potato, rice, maize and tomato (Alseekh et al., 2015; Fang et al., 2019; Gong et al., 2013; Toubiana et al., 2012; Wang et al., 2012).

The present work aimed at identifying susceptibility and resistance/tolerance biomarkers through a combined approach based on untargeted metabolite profiling and targeted gene expression analysis. Eleven field grown *Vitis* genotypes (5 *Vitis* species and 6 *Vitis vinifera*) with different resistance levels to fungal/oomycete pathogens were analysed. After an untargeted metabolomics analysis by FT-ICR-MS, the most relevant metabolites discriminating susceptible and resistant/tolerant genotypes were mapped for pathway analysis, allowing the selection of genes coding for pathway key enzymes. A targeted gene expression analysis was performed, preceded by reference gene establishment for this sample set. One candidate was identified as a possible susceptibility-associated biomarker.

5.3 MATERIALS AND METHODS

5.3.1 Plant material

Five wild *Vitis* species, one *Vitis vinifera* subsp. *sylvestris* (wild plants that grow into Portuguese river basins) and five *Vitis vinifera* cultivars were investigated (**Table 5.1**).

The resistance of *Vitis* genotypes was accessed through bibliographic searches following the classification of Organisation Internationale de la Vigne et du Vin (http://www.oiv.int) and the phenotype behaviour observed in field conditions into the Portuguese Ampelographic *Vitis* Collection (CAN). CAN is property of INIAV- Estação Vitivinícola Nacional (Dois Portos), located at Quinta da Almoinha, 60 km north of Lisbon (9º11'19''W; 39º02'31''N; 75m above sea level). Established since 1988 and replicated to a new place in 2013 and 2014, according to maintenance conditions: established in homogeneous modern alluvial soils (lowlands) as well as well drained soil; rootstock of a unique variety (Selection Oppenheim 4 – SO4) was used for all accessions including other *Vitis* species and other rootstocks represented in the field; each accession comes from one unique plant. CAN occupy nearly 2 ha of area and the climate of this region is temperate with dry and mild summer, in almost all regions of the northern mountain system Montejunto-Estrela and the regions of the west coast of Alentejo and Algarve (Peel et al., 2007).

For plant material collection, the best possible health status was guaranteed for all accessions was confirmed: plants were tested for the principal grapevine fungal/oomycetes diseases as well as grapevine viruses (healthy genotypes and synonym accessions were planted in continuous line for didactic proposes); same trailing system (bilateral cordon, Royat), canopy maintenance and agricultural management.

Three leaves (third to fifth from the shoot to apex) were harvested in each one of 7 plants of accession (biological replicate) and immediately frozen in liquid nitrogen and stored at –80 ºC until analysis. All genotypes' leaves were collected in the same day at the same time. Three biological replicates containing leaves from 2-3 different plants were analysed. In overall, four wild *Vitis* species, one *Vitis vinifera* subsp. sylvestris (wild plants that grow into Portuguese river basins) and five *Vitis vinifera* cultivars were used in this experiment (**Table 5.1**).

Table 5.1 - Wild *Vitis* species, *V. vinifera* subsp. *sylvestris* and grapevine cultivars analysed. Species and cultivar names, type of accession, origin and response to fungi pathogens are indicated (information adapted from Dry et al., 2019 and http://www.vivc.de/). Classification of resistance: 1 - very low; 3 - low, 5 - medium, 7 - high, 9 - very high or total. R – Resistant; T – Tolerant; S – Susceptible.

Vitis Species	Subspecies (subsp.) or Cultivar (cv.)	VIVC variety number	Abbreviation	Type of Accession	Origin	Degree of resistance according to OIV descriptor 452			Overall response to fungi/oomycete pathogens
						Plasmopara viticola	*Erysiphe necator*	*Botrytis cinerea*	
V. labrusca	Isabella	5560	LAB	Wild species	United States of America	7	9	unknown	R/T
V. rotundifolia	Muscadinia Rotundifolia Michaux cv. Rotundifolia	13586	ROT	Wild species	United States of America	9	9	unknown	R/T
V. riparia Michaux	Riparia Gloire de Montpellier	4824	RIP	Wild species	United States of America	9	9	unknown	R/T
V. candicans Engelmann	*Vitis* Candicans Engelmann	13508	CAN	Wild species	United States of America	7	9	unknown	R/T
V. rupestris Scheele	Rupestris du lot	10389	RU	Wild species	United States of America	7	7	9	R/T
V. vinifera	subsp. *sylvestris*		SYL	Wild plant	Portugal	3	3	5	R/T
	subsp. *sativa* cv. Regent	4572	REG	Cultivated hybrid (Crossing *V. vinifera* cv. Diana X cv. Chambourcin)	Germany	7	9		R/T
	subsp. *sativa* cv. Riesling Weiss	10077	RL	Cultivated grapevine	Germany	3	3	1/3	S
	subsp. *sativa* cv. Pinot noir	9279	PN	Cultivated grapevine	France	3	3	1/3	S
	subsp. *sativa* cv. Cabernet Sauvignon	1929	CS	Cultivated grapevine	France	1/3	1/3	5	S
	subsp. *sativa* cv. Trincadeira	15685	TRI	Cultivated grapevine	Portugal	1/3	1/3	1/3	S

5.3.2 Metabolite extraction and FT-ICR-MS analysis

Metabolite extraction was performed as previously described (Maia et al., 2016). Briefly, 0.1 g of plant material was extracted with 1 mL of 40% methanol (LC-MS grade, Merck)/40% chloroform (Sigma Aldrich)/20% water (v/v/v). Samples were vortexed, kept in an orbital shaker at room temperature and centrifuged for phase separation. The aqueous/methanol layer was further processed by solid-phase extraction using Merck LiChrolut RP-18 columns, pre-equilibrated and extracted with methanol. The methanol fraction was evaporated under a nitrogen stream and reconstituted in 1 mL of methanol. For FT-ICR-MS analysis, samples were diluted 1000-fold in methanol and human leucine enkephalin (Sigma Aldrich) was added for internal calibration of each mass spectrum ($[M+H]^+ = 556.276575$ Da or $[M-H]^- = 554.262022$ Da). For positive ionization mode analysis (ESI^+), formic acid (Sigma Aldrich, MS grade) was added to all samples at a final concentration of 0.1% (v/v). Samples were analysed by direct infusion on an Apex Qe 7-Tesla Fourier Transform Ion Cyclotron Resonance Mass Spectrometer (7T-FT-ICR-MS, Brüker Daltonics). Spectra were acquired at both positive (ESI^+) and negative (ESI^-) electrospray ionization modes, in the mass range of 100 to 1000 m/z, with an accumulation of 250 scans for each spectrum.

5.3.3 Data pre-processing and profiling by multivariate statistical analysis

Data Analysis 5.0 (Brüker Daltonics, Bremen, Germany) was used to internally calibrate each mass spectrum using leucine enkephalin for single point calibration. Peaks were considered at a minimum signal-to-noise ratio of 4. The data matrix for statistical analysis was created by peak alignment at 1 ppm difference tolerance. Only peaks occurring in more than two thirds of the replicate samples for each cultivar were selected for further analysis. Missing values were imputed by half of the global minimum value of all spectra. Data was normalized by the signal of the standard leucine enkephalin in each sample, transformed using the generalized log-transformation and Pareto scaled. The transformation with generalized log has been shown to correct for heteroscedasticity and reduce the skewness (van den Berg et al., 2006). Two unsupervised methods were applied to investigate the metabolic profile similarities between *Vitis* samples. Sample Hierarchical Clustering (agglomerative) was performed, for each ionization mode, using Euclidian distance as the metric and Ward as the method for cluster aggregation. Principal Component Analysis (PCA) models for each ionization mode were also built, retaining a minimum number of principal components necessary to explain 95% of variance (12 components for ESI^+ PCA and 15 components for ESI^- PCA).

Classifiers for resistant/tolerant (n = 21) vs susceptible (n = 12) genotypes were obtained by building Orthogonal Partial Least Squares Discriminant Analysis (OPLS-DA) models. Two target groups were defined: a "resistant/tolerant" attributed to all the wild *Vitis* plus the domesticated *V. vinifera* 'Regent', and the "susceptible" group, attributed to all the remaining domesticated *V. vinifera* cultivars, for model training. Group labels were encoded as +1, -1, and the signs of the dependent-variable components of the partial least squares fitted models were used as decision rules for classification. Model accuracy, R^2 and Q^2 metrics were estimated by 7-fold stratified cross-validation. For each model, a permutation test was carried out to assess its significance, by sampling 1000 label permutations. All analysis were carried out using the package *metabolinks* (https://github.com/aeferreira/metabolinks), which uses packages scipy (Virtanen et al., 2020) and scikit-learn (Pedregosa et al., 2011).

5.3.4 Univariate statistical analysis, metabolite annotation and pathway mapping

The significance of variables in data matrices for ESI$^+$ and ESI$^-$ was assessed by performing two-tail *t*-tests to compare variables in "resistant/tolerant" (n = 21) and "susceptible" (n = 12) groups. *p*-values were corrected for multiple testing by the Benjamini–Hochberg procedure. An FDR-corrected *p*-value cut-off of 0.01 was used for further consideration of a variable in the analysis. Variables were then sorted according to the fold-change defined as the ratio of the averages of "resistant/tolerant" / "susceptible". A variation of at least $|log2(FC)| \geq 1$ was required for a variable to be considered discriminatory.

For metabolite annotation, the *m/z* values of discriminatory peaks were submitted to MassTRIX 3 server (Suhre and Schmitt-Kopplin, 2008) (http://masstrix.org, accessed in April 2020), allowing for the presence of adducts [M+H]$^+$, [M+K]$^+$ and [M+Na]$^+$ for positive scan mode and the adducts [M-H]$^+$ and [M+Cl]$^-$ for negative mode. A maximum *m/z* deviation of 2 ppm was accepted; "KEGG (Kyoto Encyclopaedia of Genes and Genomes)/HMDB (Human Metabolome Database)/LipidMaps without isotopes" was selected for database search; *Vitis vinifera* was selected as the organism. For compound taxonomical classification, each KeGG's metabolite identifier obtained from the MassTRIX search was further annotated according to the relevant ontologies of KeGG's BRITE hierarchies (Kanehisa et al., 2019), if any existed for the identifier. For the "lipids" ontology the LipidMaps lipid classification system (Fahy et al., 2009) was used. Discriminatory compounds were mapped into metabolic pathways using Pathview (Luo and Brouwer, 2013) (http://pathview.uncc.edu), selecting the *Vitis vinifera* Flavonoid biosynthesis ("vvi00941") and Flavone and Flavonol Biosynthesis ("vvi00944") pathways. For visualization, log2(FC) values were colour coded within the boundaries of -5

(red, abundant in the "susceptible" group) and 5 (blue, abundant in "resistant/tolerant" group).

5.3.5 Total RNA extraction and cDNA synthesis

Total RNA was extracted from the leaves of the different *Vitis* samples using the Spectrum™ Plant Total RNA Kit (Sigma-Aldrich, USA), according to the manufacturer's instructions. Residual genomic DNA (gDNA) contamination was removed with On-Column DNase Digestion I Set (Sigma-Aldrich, USA), following the manufacturer's instructions. After extraction, all RNA samples were quantified, and the purity determined with the absorbance ratios at 260/280 and 260/230 nm using a NanoDrop-1000 spectrophotometer (Thermo Scientific). RNA integrity was verified by agarose gel electrophoresis. To confirm the absence of contaminating gDNA, a quantitative Real-time polymerase chain reaction (qPCR) analysis of a target on the crude of total RNA (Vandesompele et al., 2002b, 2002a) was performed using *EF1α* as target. Complementary DNA (cDNA) was synthesized from 2.5 µg of total RNA using RevertAid®H Minus Reverse Transcriptase (Fermentas, Ontario, Canada) anchored with Oligo(dT)$_{23}$ primer (Sigma-Aldrich, USA), as previously described (Monteiro et al., 2013a). For gene expression analysis, 'Cabernet sauvignon' was not included in the dataset due to the lack of sufficient plant material from the same collection used for metabolomics studies.

5.3.6 Reference genes selection and expression analysis

Ten candidate genes were selected based on their previous description as good qPCR reference genes for *Arabidopsis thaliana* (Czechowski et al., 2005) and grapevine (Monteiro et al., 2013b; Polesani et al., 2010; Reid et al., 2006) (**Table 5.2**). Nine of the selected genes were previously described as reference genes for grapevine: *60S ribosomal protein L18 (60S), small nuclear ribonucleoprotein SmD3* [currently annotated as *Tetratricopeptide repeat protein 7B (TPR7B), elongation factor 1-alpha (EF1α), ubiquitin-conjugating enzyme (UBQ), SAND family protein (SAND), Actin (ACT), glyceraldehyde-3-phosphate dehydrogenase (GAPDH), alpha-tubulin 3-chain (α-TUB)* and *beta-tubulin 1-chain (β-TUB)* (Figueiredo et al., 2012; Gamm et al., 2011; Reid et al., 2006; Selim et al., 2012; Trouvelot et al., 2008). The other gene was retrieved from NCBI (http://www.ncbi.nlm.nih.gov/) as being homologous to *Arabidopsis adaptor protein-2 MU-adaptin (AP2M)*.

118

qPCR analysis was carried out in a StepOne™ Real-Time PCR system (Applied Biosystems, Sourceforge, USA), using Maxima™ SYBR Green qPCR Master Mix (2×) kit (Fermentas, Ontario, Canada), following supplier's instructions. Thermal cycling analysis of all genes was performed under the following conditions: initial denaturation step at 95 °C for 10 min; followed by 40 cycles of denaturation at 95 °C for 15 s plus annealing for 30 s (annealing temperatures for each primer pair were indicated at **Table 5.2**). Each set of reactions included a negative control without cDNA template. Non-specific PCR products were analysed by melting curves (see **Appendix A - Supplementary Figure F5.1 - [A-J]**). Three biological replicates and two technical replicates were used for each sample. To assess the amplification efficiency of each reference/candidate gene, a pool of all cDNA samples was diluted (1:4) and used to generate a five-point standard curve based on a ten-fold dilution series.

Table 5.2 - Candidate reference genes for qPCR. Genes, gene accession numbers, primer sequences (Fw, forward; Rev, reverse), amplicon length (bp, base pairs) and qPCR annealing (Ta) and melting (Tm) temperatures are indicated. *Alternative splicing variant.

Gene (NCBI Accession Number)	Primer sequence (5'-3')	Amplicon length (bp)	Ta (°C)	Tm (°C)
60S (XM_002270599.3)	Fw: ATCTACCTCAAGCTCCTAGTC Rev: CAATCTTGTCCTCCTTTCCT	165	60	79.6
TTC7B (XM_002283371.4)	Fw: GCTCTGTTGTTGAAGATGGG Rev: GGAAGCAGTTTGTAGCATCAG	156	60	79.9
EF1α (XM_002284888.3)	Fw: GAACTGGGTGCTTGATAGGC Rev: ACCAAAATATCCGGAGTAAAAGA	164	60	79.7
UBQ (XR_002030722.1)	Fw: GCCCTGCACTTACCATCTTTAAG Rev: GAGGGTCGTCAGGATTTGGA	75	60	78.9
SAND (XM_002285134.3)	Fw: CAACATCCTTTACCCATTGACAGA Rev: GCATTTGATCCACTTGCAGATAAG	76	60	79.2
GAPDH (XM_002263109.3)	Fw: TCAAGGTCAAGGACTCTAACACC Rev: CCAACAACGAACATAGGAGCA	226	60	81.3
*ACTIN** (XM_019223591.1)	Fw: ATTCCTCACCATCATCAGCA Rev: GACCCCCTCCTACTAAAACT	89	55	77.5
α-TUB (XM_002285685.4)	Fw: CAGCCAGATCTTCACGAGCTT Rev: GTTCTCGCGCATTGACCATA	119	60	78.8
AP2M (XM_002281261.3)	Fw: CCTCTCTGGAATGCCTGATTT Rev: CTTTAGCAGGACGGGGATTTA	89	55	75.0
β-TUB (XM_002275270.3)	Fw: TGAACCACTTGATCTCTGCGACTA Rev: CAGCTTGCGGAGGTCTGAGT	86	60	82.3

5.3.7 Determination of reference gene stability

To evaluate reference gene stability, all *Vitis* genotypes were analysed together and the three publicly available software tools GeNorm v. 3.5 (Vandesompele et al., 2002b), NormFinder (Andersen et al., 2004) and the BestKeeper tool (Pfaffl et al., 2004) were used.

GeNorm is based on the pairwise variation of a single reference candidate gene relative to all other genes. GeNorm algorithm calculates a gene expression stability measure (M value) for each gene, based on the average pairwise expression ratio between a gene and each of the other genes being compared in the analysis. Accordingly, a gene displaying a low M value presents a low variance in its expression. NormFinder is based on a variance estimation approach, which calculates an expression stability value (SV) for each gene analysed. It enables estimation of the overall variation of the reference genes, considering intra and intergroup variations of the sample set. According to this algorithm, genes with lowest SV will be top ranked (Andersen et al., 2004). The BestKeeper tool calculates standard deviation (SD) based on quantification cycle (Cq) values of all candidate reference genes (Pfaffl et al., 2004). Moreover, BestKeeper compares each reference gene to the BestKeeper Index (BKI) and calculate a Pearson correlation coefficient (r). Higher r values suggest more stable expression. Genes with SD less than 1 and with the highest coefficient of correlation have the highest stability. A comprehensive ranking, was established by RefFinder, a tool that integrates GeNorm, Normfinder, BestKeeper, and the comparative ΔCt method, based on the rankings from each program, allows the assignment of an appropriate weight to an individual gene and calculates the geometric mean of their weights for the overall final ranking.

A comprehensive ranking of the candidate reference genes was established by calculating the arithmetic mean of the ranking in each algorithm used, as reported previously (Wang et al., 2012). Each gene was ranked from 1 (most stable) to 11 (least stable). The definition of the optimal number of genes required for normalization was achieved by GeNorm pairwise variation analysis (Tunbridge et al., 2011). Additionally, RefFinder was used as a verification tool of our results (Xie et al., 2012) (https://www.heartcure.com.au/reffinder/).

5.3.8 Selection and expression analysis of genes of interest

Genes encoding for enzymes involved in biosynthetic or catabolic reactions of the discriminatory metabolites were selected based on the fold-change of discriminatory compounds and pathway mapping.

A total of 7 genes were selected for expression analysis, coding for the following enzymes: caffeic acid O-methyltransferase (*COMT*), leucoanthocyanidin reductase 2 (*LAR2*), anthocyanidin reductase (*ANR*); fatty acyl-ACP thioesterase B (*FatB*), myo-inositol monophosphatase (*IMPL1*), flavonoid 3',5'-hydroxylase (*F3'5'H*), and UDP-glucose:flavonoid 3-O-glucosyltransferase (*UFGT*). The selection of the genes followed the criteria of the genes being functionally described as being involved in the biosynthesis/catalysis of the compounds.

The sequences for the genes coding for the enzymes involved in catechin and epicatechin synthesis used in this study were previously described in *Vitis* (Bogs, 2005; Gagné et al., 2009) . The remaining genes were selected by comparison of *Arabidopsis thaliana* homologue genes in the *Vitis vinifera* genome coding genes using the Basic Local Alignment Search Tool (BLAST, https://blast.ncbi.nlm.nih.gov/Blast.cgi). When gene families existed for the selected genes, the choice of the gene was made based on information on the literature regarding its involvement in plant resistance/defence.

Genes of interest selected for gene expression analysis were presented in **Table 5.3**. Non-specific PCR products were also analysed by melting curves (see **Appendix A - Supplementary Figure F5.1 - [K-Q]**). For each gene, both standard curve efficiency and SD were calculated by the Hellemans et al. equations (Hellemans et al., 2007) (**Table 5.3**).

After qPCR analysis, the quantification cycle (Cq) values of the genes of interest in all *Vitis* samples, were extracted and normalized by the geometric mean of the Cqs of *UBQ*, *SAND* and *EF1α*, described in this work as the most stable genes for sample normalization. The ability for each possible gene to discriminate between resistant/tolerant and susceptible cultivars was assessed by testing the homocedasticity of groups with Bartlett's test and by assessing significance of the differences between groups with a Wilcox-Mann-Whitney's U test. All *p*-values were adjusted for false discovery rate using the Benjamini-Hochberg procedure. Results yielding an adjusted *p*-value ≤ 0.05 were considered statistically significant. Bartlett's and Wilcox-Mann-Withney tests were performed in R (R Core Team, 2019), using the 'bartlett.test', 'wilcox.test' and 'p.adjust' functions, respectively.

Table 5.3 - Genes of interest and their encoding enzymes selected for gene expression analysis. EC numbers, gene accession numbers, primer sequences (Fw, forward; Rev, reverse), amplicon length, qPCR annealing (Ta) and melting (Tm) temperatures and amplification efficiency are indicated. *Alternative splicing variants. †Alternative locus variants.

Metabolites	Enzyme	Abbreviation	EC number	Gene NCBI Accession Number	Primer sequence (5'-3')	Amplicon length (bp)	Ta (°C)	Tm (°C)	Amplification efficiency
Caffeic acid	Caffeic acid 3-O-methyltransferase	*COMT*	EC 2.1.1.68	XM_003634113.2	Fw: GTATGACCCCAACAACTATC Rev: GACCATGGGGAGAACTGA	88	60	78.4	1.88±0.02
Catechin	Leucoanthocyanidin reductase 2	*LAR2*	EC 1.17.1.3	NM_001281160.1	Fw: TGTAACCGTGGAAGAAGATGA Rev: ATGAAGATGTCGTGAGTGAAG	92	60	80.6	1.88±0.02
Epicatechin	Anthocyanidin reductase	*ANR*	EC 1.3.1.77	NM_001280956.1	Fw: ATCAAGCCAGCAATTCAAGGA Rev: CAGCTGCAGAGGATGTCAAA	93	60	76.2	1.88±0.006
Dodecanoic acid / Hexadecanoic acid	Palmitoyl-acyl carrier protein thioesterase B	*FatB*	EC 3.1.2.21 / 3.1.2.14	XM_019223124.1	Fw: TCGCAAACCCTAGAAACCAAT Rev: AATGAGGGAAGGAGGAAAATG	112	60	77.5	1.93±0.05
Myo inositol	Myo-inositol monophosphatase*	*IMPL1*	EC 3.1.3.25	XM_002276661.3	Fw: ATCCCAAACGCTACCCAAAAA Rev: TAACAGCTTCCATCACAACCT	119	60	80.9	1.96±0.02
Quercetin / Dihydroquercetin	Flavonoid 3',5'-hydroxylase†	*F3'5'H*	EC 1.14.14.81	XM_003632164.3	Fw: GTGGTGCCGGAGATGTTA Rev: TGCGATGGACGGAATAAAAT	173	56	80.1	1.83±0.05
Quercetin-3-O-glucoside (Isoquercitrin)	UDP-glucose:flavonoid 3-O-glucosyltransferase	*UFGT*	EC 2.4.1.91	AF000372.1	Fw: AGGGGATGGTAATGGCTGT Rev: ATGGGTGGAGAGTGAGTTAG	151	60	84.7	1.97±0.01

5.4 RESULTS

5.4.1 Metabolic differentiation of susceptible and resistant/tolerant *Vitis*

Eleven *Vitis* genotypes with different tolerance to pathogens were analysed. *Vitis* species *V. labrusca*, *V. rotundifolia*, *V. riparia*, and *V. candicans* present a higher resistance/tolerance to both downy and powdery mildews and gray mold (**Table 5.1**). An untargeted metabolomics analysis using FT-ICR-MS, by direct infusion and using electrospray ionization in positive (ESI$^+$) and negative (ESI$^-$) ionization modes was followed. Two unsupervised approaches, principal component analysis (PCA) and hierarchical clustering, were applied to the untargeted metabolomics data to verify the analytical reproducibility and to infer inter-genotype metabolic profile similarities among the various *Vitis* samples (**Figure 5.1**).

Data reproducibility, as seen from the clustering of replicates together, was very high, an indicating that metabolome profiling of *Vitis* leaves appears to be sufficiently sensitive to distinguish the different species and cultivars. Also, in both ionization modes, a trend of separation between wild *Vitis* and *V. vinifera* cultivars can be observed in the PCA score plots (**Figure 5.1 – A, B**). The dendrograms resulting from hierarchical clustering confirm this trend, since two major clusters were formed with these two sample groups (**Figure 5.1 – C, D**). The only exception to this overall trend is *V. rupestris*. It is also apparent that the metabolome profile variation among *V. vinifera* cultivars seems to be larger than variation among wild species' samples (**Figure 5.1 – A, B**). The general trend of separation suggests that the multivariate metabolic phenotypes might be enough to discriminate and predict resistance or susceptibility characteristics. For that purpose, we used our metabolomics data to build classifiers for predicting the resistance or susceptibility of *Vitis* plants from their leaf metabolic profiles. We fitted Orthogonal Partial Least Squares Discriminant Analysis (OPLS-DA) models on MS intensity data using as target the inclusion on either the resistant/tolerant group, defined by all the wild species and cultivar 'Regent', or the susceptible group, defined by all the remaining *V. vinifera* cultivars. Separation classifiers were built for either ESI$^+$ or ESI$^-$ data. Both classifiers showed very good performance. Score plots indicate that the predictor component was able to discriminate between the two groups (**Figure 5.2 – A, B**) in both classifiers. Estimating model performance with 7-fold stratified cross-validation, the overall accuracy was grater that 0.98 and both R^2_Y and Q^2_Y metrics achieve top values with only a few orthogonal components (see **Appendix B - Supplementary Figure F5. - A, B**). Furthermore, by assessing the significance of the models by permutation tests, the accuracy of permuted target label models, estimated by 7-fold stratified cross-validation has a distribution well below the reference accuracy of the non-permuted models which correspond, in both classifiers, to *p*-values of 0.001 (**Figure 5.2 – C, D**).
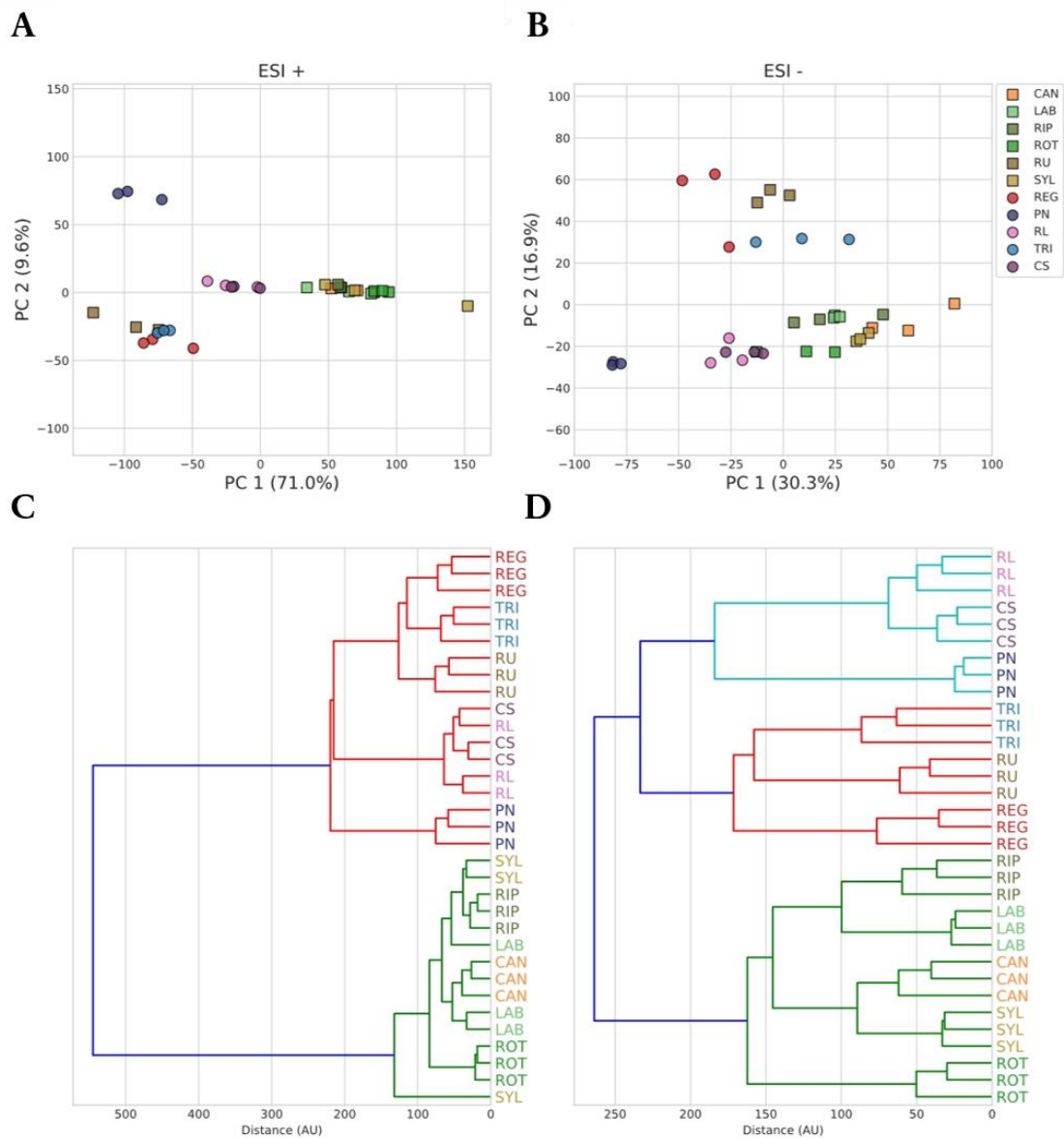
Figure 5.1 - Principal component analysis (PCA) and hierarchical clustering analysis (HCA) of untargeted metabolomics obtained in positive (ESI⁺) and negative (ESI⁻) ionization modes. (**A**, **B**) PCA score plots. Squares represent wild *Vitis*, while circles represent domesticated *V. vinifera*; (**C**, **D**) HCA dendrograms. *Vitis* genotypes abbreviations are indicated in **Table 5.1**. Variance explained by each principal component is indicated in parenthesis.
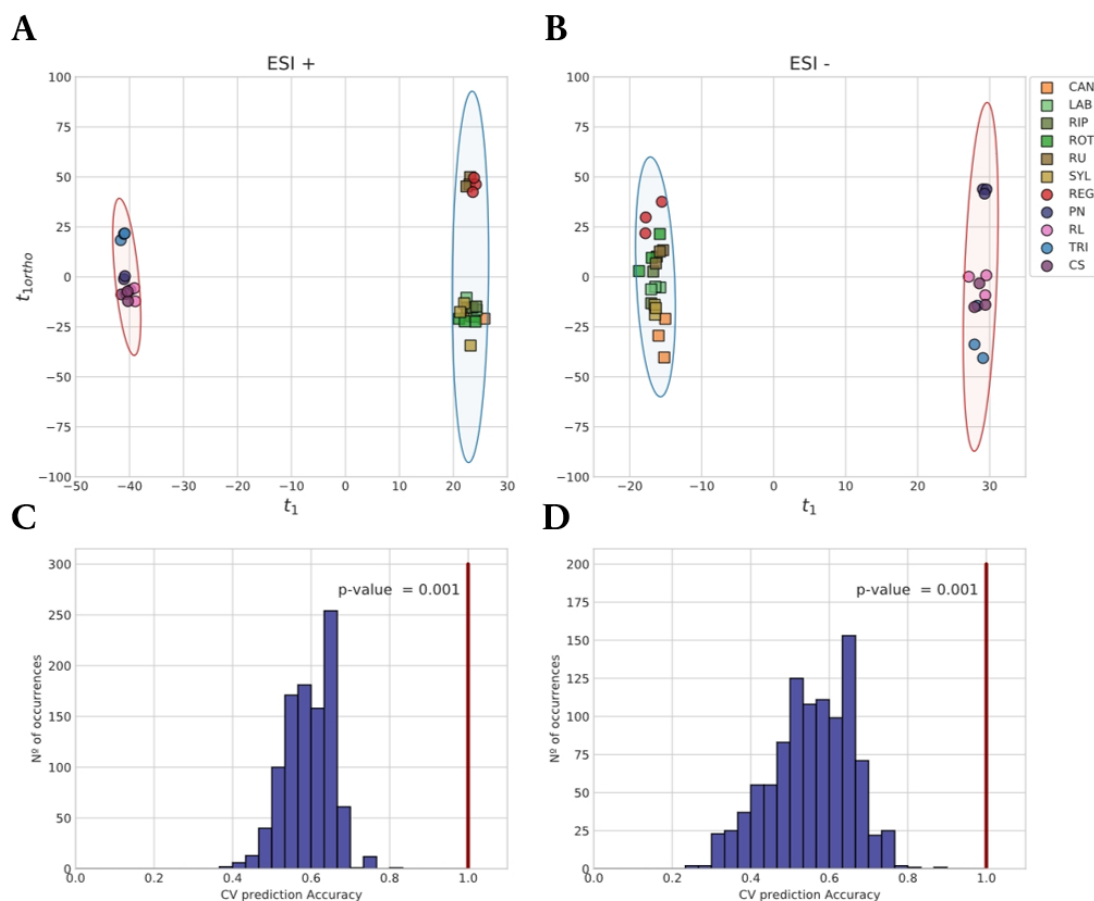
Figure 5.2 - Orthogonal partial least squares discriminant analysis (PLS-DA) models for the classification into resistant/tolerant and susceptible groups using of untargeted metabolomics data obtained in positive (ESI⁺) and negative (ESI⁻) ion modes. (**A**, **B**) Score plots for the predictive and first orthogonal components. Squares represent wild *Vitis*, while circles represent domesticated *V. vinifera*. Confidence ellipses are drawn for the two classification groups: resistant/tolerant (blue) and susceptible (red); (**C**, **D**) Significance diagnostic showing the distribution of predictive accuracy in permutation tests and the *p*-value of the test for accuracy. 1000 permutations were randomly sampled. Vertical lines indicate the accuracy of model with labels non-permuted. Accuracy was estimated by 7-fold stratified cross-validation. *Vitis* genotypes abbreviations are indicated in **Table 5.1**.

Univariate analysis based on the variable intensity changes between resistant/tolerant and susceptible groups allowed the identification of several spectral features with both significant and large variation between the two groups. Even at a significance level of 0.01 for FDR-corrected *p*-values, we found 2535 features with |log2 FC| ≥ 1, 1796 in ESI⁺ and 739 in ESI. A search of these features in MassTRIX (Suhre and Schmitt-Kopplin, 2008) provided a putative identification of some of these peaks. A total of 190 unique masses with significant and large variation between our comparison groups were putatively annotated (see **Supplementary Table S5.1** online).

To understand the biological relevance of these discriminatory compounds in grapevine metabolism, the compounds with KEGG (Kyoto Encyclopaedia of Genes and Genomes) identifiers for database annotation were retrieved and mapped into selected pathogen defence related KEGG pathways using the R package Pathview (**Figure 5.3**). Pathway analysis of flavonoid biosynthesis and flavone and flavonol biosynthesis, mapped 17 and 10 metabolites, respectively (**Figure 5.3**). Among the discriminative putatively identified metabolites, we highlight catechin or epicatechin, leucocyanidin, caffeic acid, hexadecanoid acid derivatives and dodecanoic acid as more abundant in the susceptible *V. vinifera* cultivars. Quercetin 3-O-glucoside (isoquercitrin) and dihydroquercetin, together with several other flavonol 3-O-glucosides, more abundant in the resistant/tolerant plants (see **Supplementary Table S5.1** online).
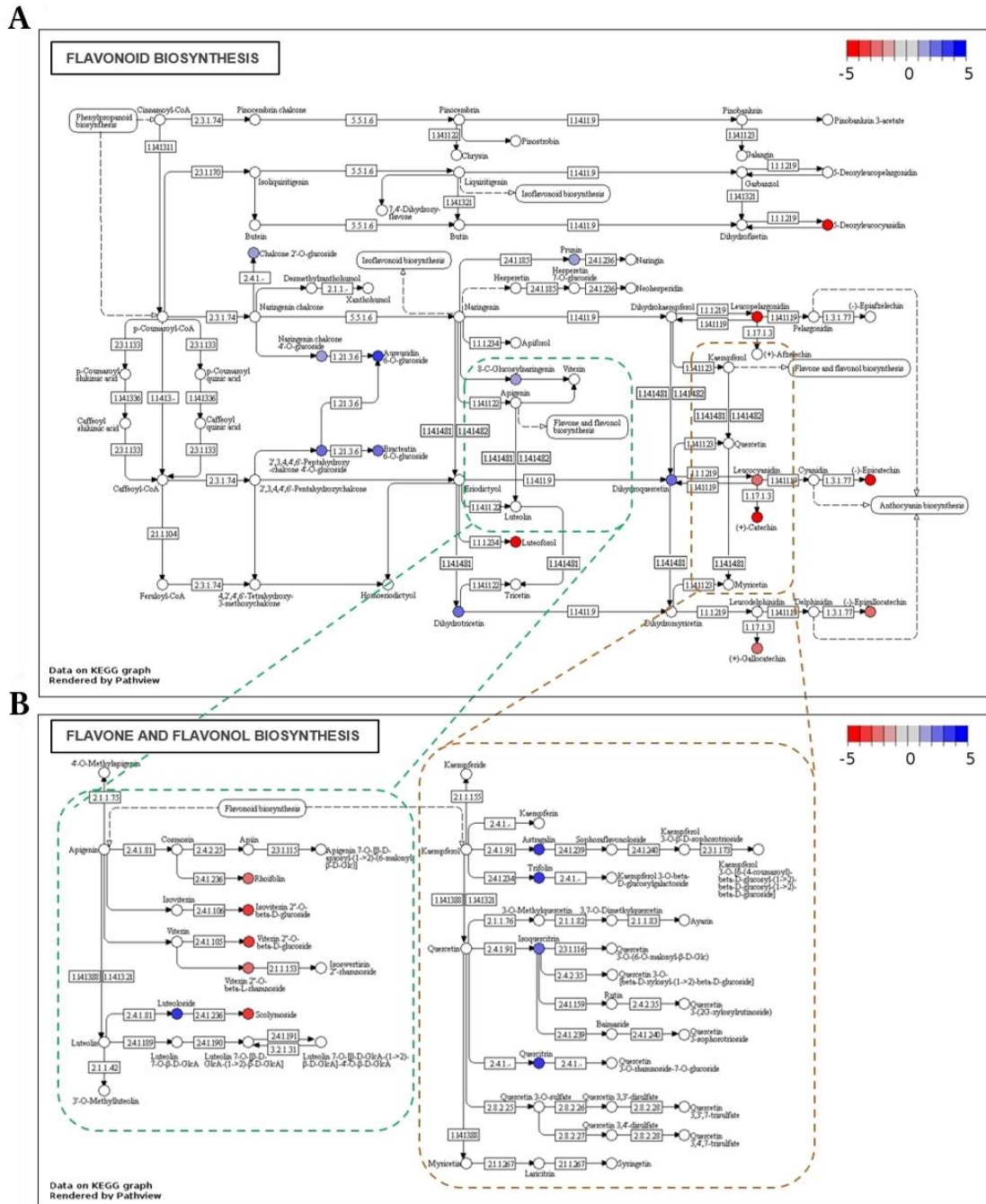
Figure 5.3 - Flavonoid (**A**) and Flavone and flavonol (**B**) biosynthesis pathways from *V. vinifera* showing the discriminatory putative metabolites between resistant/tolerant and susceptible groups (FDR corrected *p*-value < 0.01). Metabolite's KEGG identifiers were used in the R package Pathview, coloured in agreement with their |log2(FC)| values, between resistant/tolerant and susceptible plants: more accumulated in the resistance/tolerance group are blue, more accumulated in the susceptibility group are red and those unchanged are grey, setting the limits between -5 and 5.

5.4.2 Reference gene selection, stability determination and expression analysis

As no reference genes were previously described for non-stressed grapevine genotypes, we selected ten candidate reference genes (RGs) based on their previous description as good qPCR control genes for *Arabidopsis thaliana* (Czechowski et al., 2005) and grapevine (Monteiro et al., 2013a; Polesani et al., 2010; Reid et al., 2006). Nine of the selected genes were formerly described as RGs for grapevine: 60S ribosomal protein L18 (*60S*), tetratricopeptide repeat protein 7B (*TTC7B*)], elongation factor 1-alpha (*EF1α*), ubiquitin-conjugating enzyme (*UBQ*), SAND family protein (*SAND*), glyceraldehyde-3-phosphate dehydrogenase (*GAPDH*), alpha-tubulin 3-chain (*α-TUB*), beta-tubulin 1-chain (*β-TUB*) and actin (*ACT*). Adaptor protein-2 MU-adaptin (*AP2M*) was previously described for *Arabidopsis* (Czechowski et al., 2005) and sequence for its homologue in grapevine was retrieved from NCBI (http://www.ncbi.nlm.nih.gov/) (**Table 5.2**).

Expression stability of the candidate RGs was evaluated by three statistical algorithms, GeNorm, Normfinder and Bestkeeper, and a final rank was established with the RefFinder tool (Castro et al., 2011; Remans et al., 2008). Ranking order of the most stable to the least stable genes is presented **Table 5.4**. In all the *Vitis* species and *V. vinifera* cultivars analysed, genes encoding for UBQ and SAND were ranked as the most stable genes presenting the lowest M value (M = 0.859), followed by *GAPDH* (M = 0.990) and *EF1α* (M = 1.027). For all *Vitis* samples analysed, *UBQ* was considered as the most stable gene with an expression stability value (SV) of 0.552 (**Table 5.4**), followed by *AP2M* (SV = 0.744), *GAPDH* (SV = 0.745) and *β-TUB* (SV = 0.766).

In this study, BestKeeper analysis considered *α-TUB* and *SAND* as the most stable genes for all *Vitis* samples, with standard deviation (SD) values of 0.92 and 1.01, respectively (**Table 5.4**). 60S (SD = 1.07) was the third and *EF1α* (SD = 1.09) was the fourth most stable genes. Considering the 3 algorithms, a final rank was established by RefFinder (Wang et al., 2012). The results revealed that, in grapevine leaves, the four most stable genes for normalization were *UBQ*, *SAND*, *EF1α* and *AP2M* (**Table 5.4**).

Table 5.4 - Candidate reference genes ranking for all *Vitis* samples calculated by GeNorm, NormFinder and BestKeeper. Genes are ordered by the final ranking. SV, Stability value; SD, Standard deviation of Cq value; *r*, Pearson coefficient of correlation; *p*≤0.01. *p*-value associated with the Pearson coefficient of correlation; Ranking order is indicated in parenthesis.

Reference gene	GeNorm	NormFinder	BestKeeper		Ranking mean	Final ranking
	M value	SV	SD	*r*		
UBQ	0.859 (1)	0.552 (1)	1.13 (5)	0.90*	2.33	**1**
SAND	0.859 (1)	0.791 (6)	1.01 (2)	0.81*	3.00	**2**
EF1α	1.027 (3)	0.767 (5)	1.09 (4)	0.85*	4.33	**3**
AP2M	1.105 (4)	0.744 (2)	1.20 (6)	0.86*	4.33	**3**
GADPH	0.990 (2)	0.745 (3)	1.31 (8)	0.90*	4.67	**4**
α-TUB	1.181 (6)	1.122 (7)	0.92 (1)	0.59*	5.00	**5**
β-TUB	1.132 (5)	0.766 (4)	1.21 (7)	0.84*	5.67	**6**
60S	1.245 (7)	1.287 (8)	1.07 (3)	0.63*	6.33	**7**
ACT	1.439 (8)	2.056 (10)	1.63 (9)	0.69*	9.33	**8**
TTC7B	1.602 (9)	1.972 (9)	1.98 (10)	0.78*	10.00	**9**

Based on the putatively identified metabolites, respective metabolic pathways and the existing knowledge regarding markers for pathogen resistance/susceptibility in grapevine, several genes coding for enzymes in the biosynthesis or catabolism of the most discriminating metabolites were selected, namely: quercetin 3-O-glucoside (isoquercitrin), dihydroquercetin, caffeic acid, leucocyanidin, dodecanoic acid, hexadecanoic acid, catechin, epicatechin and myo-inositol. A total of 7 genes were selected for expression analysis, coding for the following enzymes: caffeic acid O-methyltransferase (*COMT*), catalyses the conversion of caffeic acid to ferulic acid; leucoanthocyanidin reductase 2 (*LAR2*), catalyses the synthesis of catechin from leucocyanidin; anthocyanidin reductase (*ANR*), responsible for the synthesis of epicatechin from cyanidin; fatty acyl-ACP thioesterase B (*FatB*), responsible for the synthesis of hexadecanoic acid from hexadecanoyl-ACP and of dodecanoid acid from dodecanoyl-ACP; myo-inositol monophosphatase (*IMPL1*), catalyses the hydrolysis of myo-inositol phosphate into myo-inositol and phosphate; flavonoid 3',5'-hydroxylase (*F3'5'H*), involved in several reactions in the flavonoid biosynthesis pathway; and UDP-glucose:flavonoid 3-O-glucosyltransferase (*UFGT*), catalyses the formation of flavonol 3-O-glucosides, using UDP-glucose as sugar donor (**Table 5.3**). The quantification cycle (Cq) value of the genes of interest in all *Vitis* genotypes were extracted and normalized by the geometric mean of the quantification cycles of *UBQ*, *SAND* and *EF1α*, for data normalization. For each gene, Bartlett's test was used to access homoscedasticity of our samples and the non-parametric Wilcox-Mann-Whitney U test was performed, identifying the discriminating genes between

our comparison groups. Only genes considered statistically significant in both tests (*p*-value < 0.05) were considered to be possible and reliable genetic biomarker (see **Appendix C – Supplementary Table S5.2**). *ANR, UFGT, F3'5'H and FatB* genes were, therefore, excluded (**Figure 5.4**). On the other hand, *COMT, LAR2 and IMPL1* are clearly significantly different between susceptible and resistant/tolerant groups, presenting lower Cq values on the susceptible groups (higher expression) (see **Appendix C – Supplementary Table S5.2**). Among these, the gene with most significance when its level is compared between groups is *LAR2* (**Figure 5.4,** see **Appendix C – Supplementary Table S5.2**), which encodes for the enzyme leucoanthocyanidin reductase 2, responsible for the synthesis of catechin from leucocyanidin and has a higher expression in the group of susceptible plants.
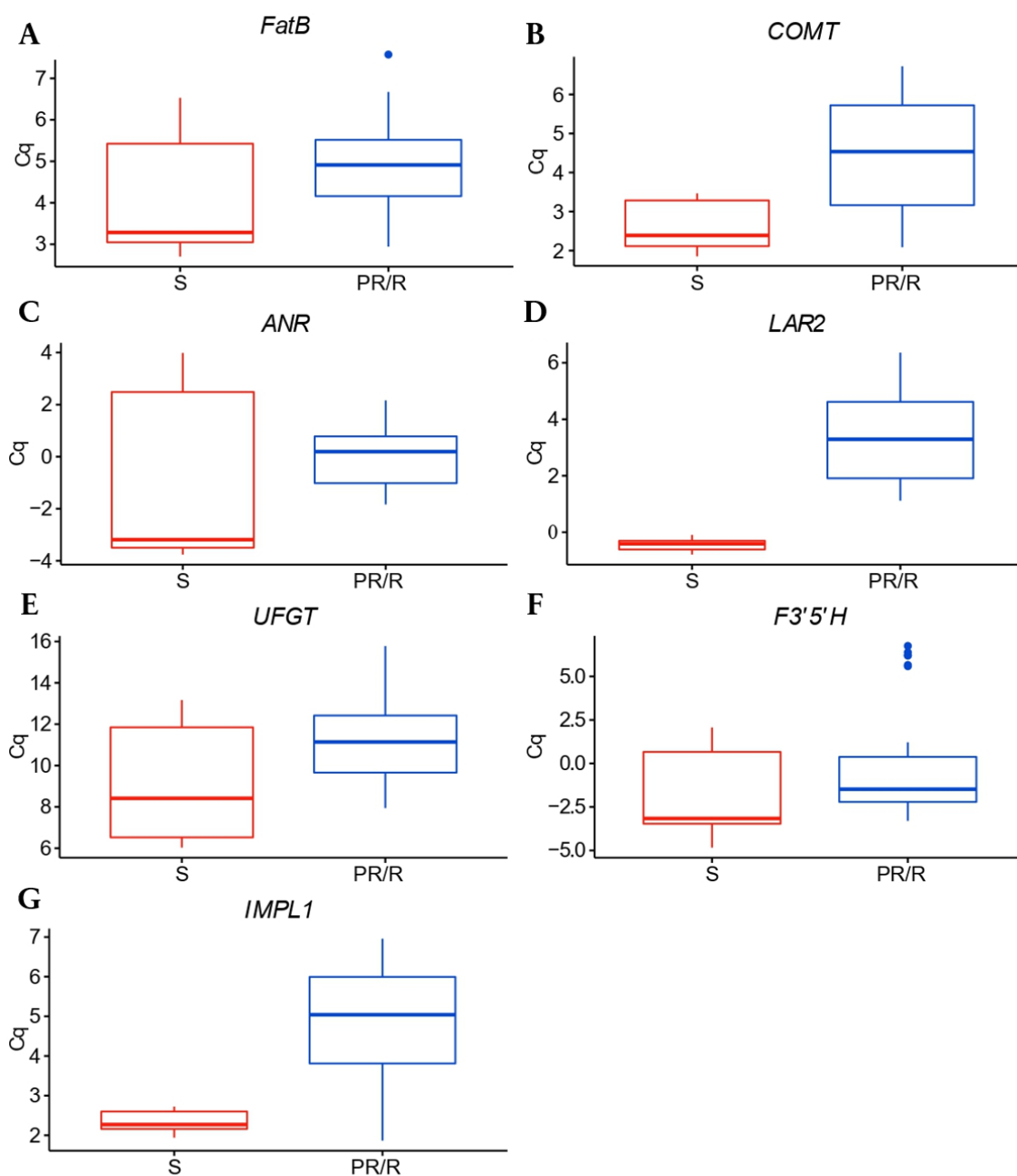
Figure 5.4 - Boxplot of quantification cycles (Cq) values for the different genes of interest in susceptible (S) and tolerant/resistant (PR/R) genotypes. (**A**) *FatB*, (**B**) *COMT*, (**C**) *ANR*, (**D**) *LAR2*, (**E**) *UFGT*, (**F**) *F3'5'H*, (**G**) *IMPL1* (gene names are indicated in **Table 5.3**). Cq values were normalized by the geometric mean of the Cq of *UBQ, SAND* and *EF1α*. Data for susceptible plants are represented in red and data for resistant/tolerant are in blue.

5.5 DISCUSSION

Grapevine is affected by diverse pathogens, particularly fungi and oomycetes, which, if not controlled, can affect the entire vineyard and cause a drastically reduction of the production, berry quality and yield. Downy and powdery mildews, black rot and gray mold gained the European Union's attention and were recently flagged as the grapevine diseases with higher impact in Europe (Micheloni, 2017). European Union is committed to "increase resilience of grape vines to pests and diseases and support the productivity of the sector in sustainable ways", focusing on the breeding of new resistant varieties that maintain the grape qualities for wine production (Micheloni, 2017). Its success depends on the understanding of the innate resistance mechanisms against pathogens and the identification of resistance/susceptibility-related biomarkers towards the development of assays to assist future breeding programs and introgression line analysis. The development of new crossing hybrids by the combination of wild American and Asian *Vitis*, that present innate resistance towards different pathogens (Dry et al., 2019), with *V. vinifera* (susceptible) offer a promising alternative to the use of pesticides and contribute to an environmentally sustainable viticulture. *Vitis riparia* and *V. labrusca*, analysed in our study, exhibit resistant traits to *P. viticola* (Dry et al., 2019) (http://www.vivc.de/) and have been effectively used in for resistance introgression. A successful hybrid example is *V. vinifera* 'Regent', with a broad tolerance to the most significant pathogens (information from http://www.vivc.de/). In breeding programs, the expression of the resistant trait takes too long to be observable in the progeny. The identification of metabolic biomarkers may allow a fast and accurate identification of the seedlings that inherited the resistant traits soon after germination.

The comparison of different *Vitis* metabolomes, without being submitted to any stress, will allow the detection of relevant metabolic variations between grapevine genotypes and uncover potentially innate defence compounds that could be used as biomarkers in breeding-programs.

For that purpose, we have conducted an untargeted metabolome characterization of eleven *Vitis* genotypes presenting different levels of resistance to downy and powdery mildews and black rot. *Vitis vinifera* cultivars Pinot noir, Riesling, Trincadeira and Cabernet sauvignon are susceptible, whereas the inter-specific hybrid *V. vinifera* Regent (that combines both *Vitis vinifera* and American *Vitis* genetic background) and the *V. vinifera* subspecies *sylvestris* present a higher tolerance towards these pathogens, when compared to the other genotypes. From our untargeted metabolomics data, two groups, *V. vinifera* cultivars and wild *Vitis*, were immediately defined and separated based on their metabolic profile. *Vitis rupestris* appears to be an exception to this overall separation trend. However, the metabolic profile of this wild *Vitis* is closer to the interspecific hybrid 'Regent' and cultivar 'Trincadeira'. 'Regent' is

132

considered tolerant to downy and powdery mildews, harbouring one Resistance to *Plasmopara viticola* (RPV) and two Resistance to *Erysiphe necator* (REN) loci (Bove and Rossi, 2020) (http://www.vivc.de/). On 'Regent' pedigree, backcrosses were made with *V. vinifera*, thus, it is expected that its metabolic profile clusters together with *V. vinifera* genotypes. Concerning the metabolome variation, it was observed to be larger in *V. vinifera* cultivars. This difference was somewhat expected, considering that domesticated grapevine cultivars present a genetic background tailored according to breeders most wanted characteristics, as the result of gene transfer during multiple crossings and selection (Bacilieri et al., 2013; Laucou et al., 2011). For the wild species, no agronomic selection events have been pursued and thus they maintain a closer metabolic profile background.

Overall, our data predictor component was capable of discriminate between susceptible and resistant/tolerant grapevine groups. The performance of these predictors is very encouraging in the context of sustainable agricultural practices. The prediction of resistance or susceptibility from plant leaf extracts using extreme-resolution metabolic profiling has the potential to analyse and then select crossed plants in still early development stages of their development, prior to infection, decreasing preventive pesticide use.

For the discriminant analysis, a resistant/tolerant and susceptible group were considered, and 190 metabolites allowed the discrimination between them. Of those, caffeic acid, catechin, epicatechin, leucocyanidin, quercetin-3-O-glucoside and derivatives, and dihydroquercetin, were found to have significant differences between the two groups. Dodecanoic acid and hexadecanoic and myo-inositol derivatives were also found to be discriminative. Some of the identified compounds were already reported as important in grapevine innate resistance (Batovska et al., 2009, 2008; Figueiredo et al., 2008) and others as possible infection-associated resistance/tolerance biomarkers (Chitarrini et al., 2017; Del Río et al., 2004; Kortekamp, 2006; Kortekamp and Zyprian, 2003; Viret et al., 2018). In 2008, Figueiredo and co-workers, compared the metabolic profiles of a tolerant and a susceptible grapevine cultivar (Figueiredo et al., 2008). The accumulation of some metabolites, such as inositol and caffeic acid, was observed and a possible relation to innate resistance towards downy mildew was suggested. Also, the analysis of the leaf surface compounds from different cultivars, displaying different degrees of resistance and susceptibility to *P. viticola*, was reported by Batovska et al. and co-workers (Batovska et al., 2009). In this study, 10 metabolites were highlighted as possible biomarkers for the prediction of downy mildew resistance and susceptibility, in which hexadecanoic acid was related to resistance in grapevine.

Some compounds were also marked as discriminatory between *Vitis* genotypes and linked to higher resistance/susceptibility to pathogens (Becker et al., 2013; Chitarrini et al., 2017; Nascimento et al., 2019). In a time-course infection assay of grapevine leaves with

downy mildew, different metabolites between inoculated and control samples were identified (Chitarrini et al., 2017). Within these metabolites we can highlight quercetin-3-o-glucoside, myo-inositol and hexadecanoic acid, also detected in our study. Moreover, recently, Nascimento and co-workers have identified several metabolic classes, such as flavonoids, associated to grapevine defences against downy mildew (Nascimento et al., 2019). Although stilbenoids are well known plant-derived defence compounds (Malacarne et al., 2011; Viret et al., 2018), no difference in resistant/tolerant and susceptible *Vitis* genotypes was observed at the constitutive level, which is not unexpected as stilbenoids mainly occur as phytoalexins, that are produced dynamically in response to biotic or abiotic stress (Niesen et al., 2013; Teh et al., 2019; Viret et al., 2018).

Discriminative compounds between resistant/tolerant and susceptible *Vitis* genotypes, with KEGG ID were mapped into biochemical pathways, revealing an enrichment in the flavonoid biosynthesis pathway, already described as involved in pathogen response (Mathesius, 2018; Treutter, 2005). These results are in line with previous studies where phenolic compounds were proven to play an important role in biotic and abiotic stress resistance (Braidot et al., 2008; Mattivi et al., 2006; Park and Cha, 2003). Some of these discriminative compounds, that are end products of these pathways, were selected and genes coding for enzymes involved in their metabolic reactions were chosen, particularly from quercetin derivatives, caffeic acid, catechin/epicatechin metabolism, myo-inositol and dodecanoic acid were selected. The expression of these genes was analysed to assess their changes in resistant/tolerant and susceptible plants.

Reference genes for our experimental conditions were defined and candidate gene expression was assessed. Three of the selected genes, *COMT*, *LAR2* and *IMPL1* allowed the discrimination between the susceptible and resistant/tolerant groups. Albeit all these genes showed expression differences between susceptible and resistant/tolerant *Vitis*, *LAR2* (catechin biosynthesis pathway) seems to present a higher discriminative potential. In fact, recent functional genomic studies in grapevine LAR enzymes confirmed that LAR2 is involved in the conversion of leucocyanidin into (+)-catechin and (-)-epicatechin (Yu et al., 2019). Moreover, catechin is a naturally occurring flavonol with high antioxidant properties. It has been previously identified as being involved in grapevine defence mechanisms (Kortekamp, 2006). Also, catechin together with other phenolic compounds, were shown to inhibit the activity of enzymes that are essential for fungal propagation and sporulation of different fungi isolated from Petri-disease-infected grapevines (Del Río et al., 2004). On the other hand, catechin can be degraded by different fungi and used as carbon source for growth (Contreras-Dominguez et al., 2008; Noe et al., 2004; Sambandam and Mahadevan, 1993). Leaves from all susceptible *V. vinifera* cultivars had higher levels of catechin/epicatechin and an over-expression of *LAR2* gene. We hypothesize that, instead of being part of an effective

defence mechanism for the plant, pathogens may be using catechin to develop and establish a successful infection.

5.6 CONCLUSIONS

With this work, we uncovered an important part of the metabolic map of the pathogen-resistance metabolism in grapevine, identifying key metabolic players. By assessing gene expression of key metabolic enzymes, we propose that both catechin/epicatechin and *LAR2* may be putative biomarkers of susceptibility. Despite the fact that further studies have to be conducted with a larger dataset to validate our hypothesis, we consider that our results open new insights towards the development of assays for progeny selection in breeding programs. The study of constitutive expression and accumulation of compounds in grapevine is extremely important as it can uncovered differences associated to resistance/susceptibility to different fungal/oomycete pathogens.

5.7 DATA AVAILABILITY

The metabolomics data that support the findings of this study are available in figshare data repository with the identifier DOI: https://doi.org/10.6084/m9.figshare.12357314 (Maia et al., 2020).

5.8 SUPPLEMENTARY INFORMATION

Supplementary Table S.51 are available at DOI: https://doi.org/10.1038/s41598-020-72781-2. For **Supplementary Figure F5.1**, **Supplementary Figure F5.** and **Supplementary Table S5.2**, consult the Appendices A, B and C, respectively.

5.9 ACKNOWLEDGEMENTS

5.10 REFERENCES

Adrian, M., Lucio, M., Roullier-Gall, C., Héloir, M.-C., Trouvelot, S., Daire, X., Kanawati, B., Lemaître-Guillier, C., Poinssot, B., Gougeon, R., Schmitt-Kopplin, P., 2017. Metabolic Fingerprint of PS3-Induced Resistance of Grapevine Leaves against *Plasmopara viticola* Revealed Differences in Elicitor-Triggered Defenses. Front Plant Sci 8, 101. https://doi.org/10.3389/fpls.2017.00101

Ali, K., Maltese, F., Figueiredo, A., Rex, M., Fortes, A.M., Zyprian, E., Pais, M.S., Verpoorte, R., Choi, Y.H., 2012. Alterations in grapevine leaf metabolism upon inoculation with *Plasmopara viticola* in different time-points. Plant Science 191–192, 100–107. https://doi.org/10.1016/j.plantsci.2012.04.014

Alseekh, S., Tohge, T., Wendenberg, R., Scossa, F., Omranian, N., Li, J., Kleessen, S., Giavalisco, P., Pleban, T., Mueller-Roeber, B., Zamir, D., Nikoloski, Z., Fernie, A.R., 2015. Identification and Mode of Inheritance of Quantitative Trait Loci for Secondary Metabolite Abundance in Tomato. The Plant Cell 27, 485–512. https://doi.org/10.1105/tpc.114.132266

Andersen, C.L., Jensen, J.L., Ørntoft, T.F., 2004. Normalization of real-time quantitative reverse transcription-PCR data: a model-based variance estimation approach to identify genes suited for normalization, applied to bladder and colon cancer data sets. Cancer Res. 64, 5245–5250. https://doi.org/10.1158/0008-5472.CAN-04-0496

Bacilieri, R., Lacombe, T., Le Cunff, L., Di Vecchi-Staraz, M., Laucou, V., Genna, B., Péros, J.-P., This, P., Boursiquot, J.-M., 2013. Genetic structure in cultivated grapevines is linked to geography and human selection. BMC Plant Biology 13, 25. https://doi.org/10.1186/1471-2229-13-25

Batovska, D.I., Todorova, I.T., Nedelcheva, D.V., Parushev, S.P., Atanassov, A.I., Hvarleva, T.D., Djakova, G.J., Bankova, V.S., Popov, S.S., 2008. Preliminary study on biomarkers for the fungal resistance in *Vitis vinifera* leaves. Journal of Plant Physiology 165, 791–795. https://doi.org/10.1016/j.jplph.2007.09.005

Batovska, D.I., Todorova, I.T., Parushev, S.P., Nedelcheva, D.V., Bankova, V.S., Popov, S.S., Ivanova, I.I., Batovski, S.A., 2009. Biomarkers for the prediction of the resistance and susceptibility of grapevine leaves to downy mildew. Journal of Plant Physiology 166, 781–785. https://doi.org/10.1016/j.jplph.2008.08.008

Becker, L., Poutaraud, A., Hamm, G., Muller, J.-F., Merdinoglu, D., Carré, V., Chaimbault, P., 2013. Metabolic study of grapevine leaves infected by downy mildew using negative ion electrospray – Fourier transform ion cyclotron resonance mass spectrometry. Analytica Chimica Acta 795, 44–51. https://doi.org/10.1016/j.aca.2013.07.068

Bennett, R.N., Wallsgrove, R.M., 1994. Secondary metabolites in plant defence mechanisms. New Phytologist 127, 617–633. https://doi.org/10.1111/j.1469-8137.1994.tb02968.x

Bogs, J., 2005. Proanthocyanidin Synthesis and Expression of Genes Encoding Leucoanthocyanidin Reductase and Anthocyanidin Reductase in Developing Grape Berries and Grapevine Leaves. Plant Physiology 139, 652–663. https://doi.org/10.1104/pp.105.064238

Bove, F., Rossi, V., 2020. Components of partial resistance to *Plasmopara viticola* enable complete phenotypic characterization of grapevine varieties. Scientific Reports 10, 1–12. https://doi.org/10.1038/s41598-020-57482-0

Braidot, E., Zancani, M., Petrussa, E., Peresson, C., Bertolini, A., Patui, S., Macrì, F., Vianello, A., 2008. Transport and accumulation of flavonoids in grapevine (*Vitis vinifera* L.). Plant signaling & behavior 3, 626–632. https://doi.org/10.4161/psb.3.9.6686

Cabras, P., Angioni, A., 2000. Pesticide Residues in Grapes, Wine, and Their Processing Products. Journal of Agricultural and Food Chemistry 48, 967–973. https://doi.org/10.1021/jf990727a

Castro, P., Román, B., Rubio, J., Die, J.V., 2011. Selection of reference genes for expression studies in Cicer arietinum L.: analysis of cyp81E3 gene expression against Ascochyta rabiei. Mol Breeding 29, 261–274. https://doi.org/10.1007/s11032-010-9544-8

Chitarrini, G., Soini, E., Riccadonna, S., Franceschi, P., Zulini, L., Masuero, D., Vecchione, A., Stefanini, M., Di Gaspero, G., Mattivi, F., Vrhovsek, U., 2017. Identification of Biomarkers for Defense Response to *Plasmopara viticola* in a Resistant Grape Variety. Front. Plant Sci. 8. https://doi.org/10.3389/fpls.2017.01524

Contreras-Dominguez, M., Roopesh, K., Coronel, A.R., Oduardo, N.G., Guyot, S., Saucedo-Castaneda, G., Perraud, I.G., Roussos, S., Augur, C., 2008. Use of fungal enzymes to study the degradation of specific plant polyphenols 508–518. https://hal.ird.fr/ird-00865346

Czechowski, T., Stitt, M., Altmann, T., Udvardi, M.K., Scheible, W.-R., 2005. Genome-wide identification and testing of superior reference genes for transcript normalization in Arabidopsis. Plant Physiol. 139, 5–17. https://doi.org/10.1104/pp.105.063743

Del Río, J.A., Gómez, P., Báidez, A., Fuster, M.D., Ortuño, A., Frías, V., 2004. Phenolic compounds have a role in the defence mechanism protecting grapevine against the fungi involved in Petri disease. Phytopathologia Mediterranea 43, 87–94. https://doi.org/10.14601/Phytopathol_Mediterr-1736

Delmotte, F., Mestre, P., Schneider, C., Kassemeyer, H.-H., Kozma, P., Richart-Cervera, S., Rouxel, M., Delière, L., 2014. Rapid and multiregional adaptation to host partial resistance in a plant pathogenic oomycete: evidence from European populations of *Plasmopara viticola*, the causal agent of grapevine downy mildew. Infect. Genet. Evol. 27, 500–508. https://doi.org/10.1016/j.meegid.2013.10.017

Dry, I., Riaz, S., Fuchs, M., Sosnowski, M., Thomas, M., 2019. Scion Breeding for Resistance to Biotic Stresses, in: The Grape Genome. Springer, Cham, pp. 319–348.

Eibach, R., Töpfer, R., 2015. Traditional grapevine breeding techniques, in: Grapevine Breeding Programs for the Wine Industry. Woodhead Publishing, Oxford, pp. 3–22.

Fahy, E., Subramaniam, S., Murphy, R.C., Nishijima, M., Raetz, C.R.H., Shimizu, T., Spener, F., van Meer, G., Wakelam, M.J.O., Dennis, E.A., 2009. Update of the LIPID MAPS comprehensive classification system for lipids. J. Lipid Res. 50 Suppl, S9-14. https://doi.org/10.1194/jlr.R800095-JLR200

Fang, C., Fernie, A.R., Luo, J., 2019. Exploring the Diversity of Plant Metabolism. Trends in Plant Science 24, 83–98. https://doi.org/10.1016/j.tplants.2018.09.006

Fiehn, O., 2002. Metabolomics – the link between genotypes and phenotypes. Plant Mol Biol 48, 155–171. https://doi.org/10.1023/A:1013713905833

Figueiredo, A., Fortes, A.M., Ferreira, S., Sebastiana, M., Choi, Y.H., Sousa, L., Acioli-Santos, B., Pessoa, F., Verpoorte, R., Pais, M.S., 2008. Transcriptional and metabolic profiling of grape (*Vitis vinifera* L.) leaves unravel possible innate resistance against pathogenic fungi. J. Exp. Bot. 59, 3371–3381. https://doi.org/10.1093/jxb/ern187

Figueiredo, A., Monteiro, F., Fortes, A.M., Bonow-Rex, M., Zyprian, E., Sousa, L., Pais, M.S., 2012. Cultivar-specific kinetics of gene induction during downy mildew early infection in grapevine. Functional & Integrative Genomics 12, 379–386. https://doi.org/10.1007/s10142-012-0261-8

Gagné, S., Lacampagne, S., Claisse, O., Gény, L., 2009. Leucoanthocyanidin reductase and anthocyanidin reductase gene expression and activity in flowers, young berries and skins of *Vitis vinifera* L. cv. Cabernet-Sauvignon during development. Plant Physiology and Biochemistry 47, 282–290. https://doi.org/10.1016/j.plaphy.2008.12.004

Gamm, M., Héloir, M.-C., Kelloniemi, J., Poinssot, B., Wendehenne, D., Adrian, M., 2011. Identification of reference genes suitable for qRT-PCR in grapevine and application for the study of the expression of genes involved in pterostilbene synthesis. Mol. Genet. Genomics 285, 273–285. https://doi.org/10.1007/s00438-011-0607-2

Gong, L., Chen, W., Gao, Y., Liu, X., Zhang, H., Xu, C., Yu, S., Zhang, Q., Luo, J., 2013. Genetic analysis of the metabolome exemplified using a rice population. PNAS 110, 20320–20325. https://doi.org/10.1073/pnas.1319681110

Hellemans, J., Mortier, G., De Paepe, A., Speleman, F., Vandesompele, J., 2007. qBase relative quantification framework and software for management and automated analysis of real-time quantitative PCR data. Genome Biology 8, R19. https://doi.org/10.1186/gb-2007-8-2-r19

Kanehisa, M., Sato, Y., Furumichi, M., Morishima, K., Tanabe, M., 2019. New approach for understanding genome variations in KEGG. Nucleic Acids Res 47, D590–D595. https://doi.org/10.1093/nar/gky962

Kortekamp, A., 2006. Expression analysis of defence-related genes in grapevine leaves after inoculation with a host and a non-host pathogen. Plant Physiology and Biochemistry 44, 58–67. https://doi.org/10.1016/j.plaphy.2006.01.008

Kortekamp, A., Zyprian, E., 2003. Characterization of Plasmopara-resistance in grapevine using in vitro plants. J. Plant Physiol. 160, 1393–1400. https://doi.org/10.1078/0176-1617-01021

Lamichhane, J.R., Dachbrodt-Saaydeh, S., Kudsk, P., Messéan, A., 2015. Toward a Reduced Reliance on Conventional Pesticides in European Agriculture. Plant Disease 100, 10–24. https://doi.org/10.1094/PDIS-05-15-0574-FE

Laucou, V., Lacombe, T., Dechesne, F., Siret, R., Bruno, J.-P., Dessup, M., Dessup, T., Ortigosa, P., Parra, P., Roux, C., Santoni, S., Varès, D., Péros, J.-P., Boursiquot, J.-M., This, P., 2011. High throughput analysis of grape genetic diversity as a tool for germplasm collection management. Theor Appl Genet 122, 1233–1245. https://doi.org/10.1007/s00122-010-1527-y

Luo, W., Brouwer, C., 2013. Pathview: an R/Bioconductor package for pathway-based data integration and visualization. Bioinformatics 29, 1830–1831. https://doi.org/10.1093/bioinformatics/btt285

Maia, M., Ferreira, A.E.N., Laureano, G., Marques, A.P., Torres, V.M., Silva, A.B., Matos, A.R., Cordeiro, C., Figueiredo, A., Sousa Silva, M., 2019. *Vitis vinifera* "Pinot noir" leaves as a source of bioactive nutraceutical compounds. Food Funct 10, 3822–3827. https://doi.org/10.1039/c8fo02328j

Maia, M., Figueiredo, A., Sousa Silva, M., Ferreira, A., 2020. Grapevine untargeted metabolomics to uncover potential biomarkers of fungal/oomycetes-associated diseases. figshare. Dataset. https://doi.org/10.6084/m9.figshare.12357314.v1

Maia, M., Monteiro, F., Sebastiana, M., Marques, A.P., Ferreira, A.E.N., Freire, A.P., Cordeiro, C., Figueiredo, A., Sousa Silva, M., 2016. Metabolite extraction for high-throughput FTICR-MS-based metabolomics of grapevine leaves. EuPA Open Proteom 12, 4–9. https://doi.org/10.1016/j.euprot.2016.03.002

Malacarne, G., Vrhovsek, U., Zulini, L., Cestaro, A., Stefanini, M., Mattivi, F., Delledonne, M., Velasco, R., Moser, C., 2011. Resistance to *Plasmopara viticola* in a grapevine segregating population is associated with stilbenoid accumulation and with specific

host transcriptional responses. BMC Plant Biol. 11, 114. https://doi.org/10.1186/1471-2229-11-114

Mathesius, U., 2018. Flavonoid Functions in Plants and Their Interactions with Other Organisms. Plants (Basel) 7. https://doi.org/10.3390/plants7020030

Mattivi, F., Guzzon, R., Vrhovsek, U., Stefanini, M., Velasco, R., 2006. Metabolite Profiling of Grape: Flavonols and Anthocyanins. Journal of Agricultural and Food Chemistry 54, 7692–7702. https://doi.org/10.1021/jf061538c

Micheloni, C., 2017. EIP-AGRI Focus Group Diseases and pests in viticulture - STARTING PAPER.

Monteiro, F., Sebastiana, M., Pais, M.S., Figueiredo, A., 2013a. Reference Gene Selection and Validation for the Early Responses to Downy Mildew Infection in Susceptible and Resistant *Vitis vinifera* Cultivars. PLoS ONE 8, e72998. https://doi.org/10.1371/journal.pone.0072998

Monteiro, F., Sebastiana, M., Pais, M.S., Figueiredo, A., 2013b. Reference Gene Selection and Validation for the Early Responses to Downy Mildew Infection in Susceptible and Resistant *Vitis vinifera* Cultivars. PLoS ONE 8, e72998. https://doi.org/10.1371/journal.pone.0072998

Nascimento, R., Maia, M., Ferreira, A.E.N., Silva, A.B., Freire, A.P., Cordeiro, C., Sousa Silva, M., Figueiredo, A., 2019. Early stage metabolic events associated with the establishment of *Vitis vinifera – Plasmopara viticola* compatible interaction. Plant Physiology and Biochemistry 137, 1–13. https://doi.org/10.1016/j.plaphy.2019.01.026

Niesen, D.B., Hessler, C., Seeram, N.P., 2013. Beyond resveratrol: A review of natural stilbenoids identified from 2009–2013. Journal of Berry Research 3, 181–196. https://doi.org/10.3233/JBR-130062

Noe, A.C., Cruz, M., Rodriguez, R., Gutierrez-Sanchez, G., Ramirez-Coronel, A., Augur, C., 2004. Catechin Degradation by Several Fungal Strains Isolated from Mexican Desert. Journal of Microbiology and Biotechnology 14, 426–429.

Organisation of Vine and Wine, 2019a. The distribution of the world's grapevine varieties.

Organisation of Vine and Wine, 2019b. OIV Statistical Report on World Vitiviniculture.

Organisation of Vine and Wine, 2009. 2nd edition of the OIV Descriptor list for grape varieties and *Vitis* species.

Park, H.-J., Cha, H.-C., 2003. Flavonoids from leaves and exocarps of the grape Kyoho. Korean Journal of Biological Sciences 7, 327–330. https://doi.org/10.1080/12265071.2003.9647723

Pedregosa, F., Varoquaux, G., Gramfort, A., Michel, V., Thirion, B., Grisel, O., Blondel, M., Prettenhofer, P., Weiss, R., Dubourg, V., Vanderplas, J., Passos, A., Cournapeau, D., Brucher, M., Perrot, M., Duchesnay, É., 2011. Scikit-learn: Machine Learning in

Python. Journal of Machine Learning Research 12, 2825–2830. https://doi.org/arXiv:1201.0490

Peel, M.C., Finlayson, B.L., McMahon, T.A., 2007. Updated world map of the Köppen-Geiger climate classification. Hydrology and Earth System Sciences 11, 1633–1644. https://doi.org/10.5194/hess-11-1633-2007

Peressotti, E., Wiedemann-Merdinoglu, S., Delmotte, F., Bellin, D., Di Gaspero, G., Testolin, R., Merdinoglu, D., Mestre, P., 2010. Breakdown of resistance to grapevine downy mildew upon limited deployment of a resistant variety. BMC Plant Biology 10, 147. https://doi.org/10.1186/1471-2229-10-147

Pfaffl, M.W., Tichopad, A., Prgomet, C., Neuvians, T.P., 2004. Determination of stable housekeeping genes, differentially regulated target genes and sample integrity: BestKeeper--Excel-based tool using pair-wise correlations. Biotechnol. Lett. 26, 509–515. https://doi.org/10.1023/b:bile.0000019559.84305.47

Polesani, M., Bortesi, L., Ferrarini, A., Zamboni, A., Fasoli, M., Zadra, C., Lovato, A., Pezzotti, M., Delledonne, M., Polverari, A., 2010. General and species-specific transcriptional responses to downy mildew infection in a susceptible (*Vitis vinifera*) and a resistant (V. riparia) grapevine species. BMC genomics 11, 117. https://doi.org/10.1186/1471-2164-11-117

R Core Team, 2019. R: A Language and Environment for Statistical Computing. R Foundation for Statistical Computing, Vienna, Austria.

Reid, K.E., Olsson, N., Schlosser, J., Peng, F., Lund, S.T., 2006. An optimized grapevine RNA isolation procedure and statistical determination of reference genes for real-time RT-PCR during berry development. BMC Plant Biol 6, 27. https://doi.org/10.1186/1471-2229-6-27

Remans, T., Smeets, K., Opdenakker, K., Mathijsen, D., Vangronsveld, J., Cuypers, A., 2008. Normalisation of real-time RT-PCR gene expression measurements in Arabidopsis thaliana exposed to increased metal concentrations. Planta 227, 1343–1349. https://doi.org/10.1007/s00425-008-0706-4

Reynolds, A.G., 2015., in: Grapevine Breeding Programs for the Wine Industry. Elsevier.

Sambandam, T., Mahadevan, A., 1993. Degradation of catechin and purification and partial characterization of catechin oxygenase fromChaetomium cupreum. World J Microbiol Biotechnol 9, 37–44. https://doi.org/10.1007/BF00656513

Selim, M., Legay, S., Berkelmann-Löhnertz, B., Langen, G., Kogel, K.-H., Evers, D., 2012. Identification of suitable reference genes for real-time RT-PCR normalization in the grapevine-downy mildew pathosystem. Plant Cell Rep. 31, 205–216. https://doi.org/10.1007/s00299-011-1156-1

Shepherd, L.V., Fraser, P., Stewart, D., 2011. Metabolomics: a second-generation platform for crop and food analysis. Bioanalysis 3, 1143–1159. https://doi.org/10.4155/bio.11.61

Suhre, K., Schmitt-Kopplin, P., 2008. MassTRIX: mass translator into pathways. Nucl. Acids Res. 36, W481–W484. https://doi.org/10.1093/nar/gkn194

Teh, S.L., Rostandy, B., Awale, M., Luby, J.J., Fennell, A., Hegeman, A.D., 2019. Genetic analysis of stilbenoid profiles in grapevine stems reveals a major mQTL hotspot on chromosome 18 associated with disease-resistance motifs. Horticulture Research 6, 1–11. https://doi.org/10.1038/s41438-019-0203-x

Toubiana, D., Semel, Y., Tohge, T., Beleggia, R., Cattivelli, L., Rosental, L., Nikoloski, Z., Zamir, D., Fernie, A.R., Fait, A., 2012. Metabolic Profiling of a Mapping Population Exposes New Insights in the Regulation of Seed Metabolism and Seed, Fruit, and Plant Relations. PLOS Genetics 8, e1002612. https://doi.org/10.1371/journal.pgen.1002612

Treutter, D., 2005. Significance of flavonoids in plant resistance and enhancement of their biosynthesis. Plant Biol (Stuttg) 7, 581–591. https://doi.org/10.1055/s-2005-873009

Trouvelot, S., Varnier, A.-L., Allegre, M., Mercier, L., Baillieul, F., Arnould, C., Gianinazzi-Pearson, V., Klarzynski, O., Joubert, J.-M., Pugin, A., others, 2008. A β-1, 3 glucan sulfate induces resistance in grapevine against *Plasmopara viticola* through priming of defense responses, including HR-like cell death. Molecular Plant-Microbe Interactions 21, 232–243. https://doi.org/10.1094/MPMI-21-2-0232

Tunbridge, E.M., Eastwood, S.L., Harrison, P.J., 2011. Changed relative to what? Housekeeping genes and normalization strategies in human brain gene expression studies. Biol. Psychiatry 69, 173–179. https://doi.org/10.1016/j.biopsych.2010.05.023

van den Berg, R.A., Hoefsloot, H.C., Westerhuis, J.A., Smilde, A.K., van der Werf, M.J., 2006. Centering, scaling, and transformations: improving the biological information content of metabolomics data. BMC genomics 7, 142. https://doi.org/10.1186/1471-2164-7-142

Vandesompele, J., De Paepe, A., Speleman, F., 2002a. Elimination of primer-dimer artifacts and genomic coamplification using a two-step SYBR green I real-time RT-PCR. Anal. Biochem. 303, 95–98. https://doi.org/10.1006/abio.2001.5564

Vandesompele, J., De Preter, K., Pattyn, F., Poppe, B., Van Roy, N., De Paepe, A., Speleman, F., 2002b. Accurate normalization of real-time quantitative RT-PCR data by geometric averaging of multiple internal control genes. Genome Biol. 3, RESEARCH0034. https://doi.org/10.1186/gb-2002-3-7-research0034

Viret, O., Spring, J.-L., Gindro, K., 2018. Stilbenes: biomarkers of grapevine resistance to fungal diseases. OENO One 52, 235–241. https://doi.org/10.20870/oeno-one.2018.52.3.2033

Virtanen, P., Gommers, R., Oliphant, T.E., Haberland, M., Reddy, T., Cournapeau, D., Burovski, E., Peterson, P., Weckesser, W., Bright, J., van der Walt, S.J., Brett, M., Wilson, J., Millman, K.J., Mayorov, N., Nelson, A.R.J., Jones, E., Kern, R., Larson, E.,

Carey, C.J., Polat, İ., Feng, Y., Moore, E.W., VanderPlas, J., Laxalde, D., Perktold, J., Cimrman, R., Henriksen, I., Quintero, E.A., Harris, C.R., Archibald, A.M., Ribeiro, A.H., Pedregosa, F., van Mulbregt, P., 2020. SciPy 1.0: fundamental algorithms for scientific computing in Python. Nature Methods 17, 261–272. https://doi.org/10.1038/s41592-019-0686-2

Wang, Q., Ishikawa, T., Michiue, T., Zhu, B.-L., Guan, D.-W., Maeda, H., 2012. Stability of endogenous reference genes in postmortem human brains for normalization of quantitative real-time PCR data: comprehensive evaluation using geNorm, NormFinder, and BestKeeper. International Journal of Legal Medicine 126, 943–952. https://doi.org/10.1007/s00414-012-0774-7

Wolfender, J.-L., Rudaz, S., Choi, Y.H., Kim, H.K., 2013. Plant metabolomics: from holistic data to relevant biomarkers. Curr. Med. Chem. 20, 1056–1090. https://doi.org/10.2174/0929867311320080009

Xie, F., Xiao, P., Chen, D., Xu, L., Zhang, B., 2012. miRDeepFinder: a miRNA analysis tool for deep sequencing of plant small RNAs. Plant Mol. Biol. https://doi.org/10.1007/s11103-012-9885-2

Yu, K., Jun, J.H., Duan, C., Dixon, R.A., 2019. VvLAR1 and VvLAR2 Are Bifunctional Enzymes for Proanthocyanidin Biosynthesis in Grapevine. Plant Physiol 180, 1362–1374. https://doi.org/10.1104/pp.19.00447

Zini, E., Dolzani, C., Stefanini, M., Gratl, V., Bettinelli, P., Nicolini, D., Betta, G., Dorigatti, C., Velasco, R., Letschka, T., Vezzulli, S., 2019. R-Loci Arrangement Versus Downy and Powdery Mildew Resistance Level: A *Vitis* Hybrid Survey. Int J Mol Sci 20. https://doi.org/10.3390/ijms20143526

CHAPTER VI

Early detection of *Plasmopara viticola* infected leaves through FT-ICR-MS metabolic profiling

6 Early detection of *Plasmopara viticola* infected leaves through FT-ICR-MS metabolic profiling

6.1 ABSTRACT

Grapevine (*Vitis* (*V.*) *vinifera* L.) is one of the most important crops in the world. The domesticated *V. vinifera* cultivars frequently used for wine production are highly susceptible to different diseases, including downy mildew, caused by *Plasmopara viticola*, one of the most destructive vineyard diseases. Downy mildew affects all the green parts of the vine, causing yield reduction and significant production losses. To cope with this threat, the application of chemical products is currently the mainly strategy, with severe environmental and economic costs. The development of alternative sustainable disease control strategies is crucial. Early detection of infected plants is not easy, since observable disease symptoms normally appear seven to ten days after pathogen inoculation. Thus, the development of early detection techniques is very important to control downy mildew spread.

In the present work, we followed an untargeted metabolomics approach using Fourier Transform Ion Cyclotron Resonance Mass Spectrometry (FT-ICR-MS) to analyse the chemical profile of infected and non-infected grapevine leaves. Chemical formulas were used to build Van Krevelen diagrams and Compositional Space plots, which do not require full metabolite identification and provide an easy screening method. Based only on the chemical profile and representation plots, we were able to discriminate between infected and non-infected grapevine leaves as soon as 24 hours post-inoculation (hpi). Moreover, our results show that lipids, carbohydrates and polyketides are the most altered metabolite groups in *P. viticola*-infected plants when compared to control samples.

6.2 INTRODUCTION

Nowadays, there is an increasing social and political demand for sustainable productions. In viticulture, winegrowers are forced to reduce the use of pesticides. Thus, it is increasingly important to develop alternative strategies. However, the domesticated grapevine used for wine production, *Vitis* (*V.*) *vinifera* L., is highly susceptible to downy mildew, caused by the biotrophic oomycete *Plasmopara* (*P.*) *viticola* (Berk. et Curt.) Berl.et de Toni, one of the most destructive pathogens (Gessler et al., 2011). It may cause severe yield reduction and thus has serious negative economic impact for winegrowers (Figueiredo et al., 2008; Gessler et al., 2011; Gómez-Zeledón et al., 2013; Toffolatti et al., 2012).

Detection of early infections with *P. viticola* in the vineyards is not easy. Normally, infections with this pathogen are only observable when the infection is already established and, with adequate climate conditions, it quickly spreads and affects not only all the susceptible green parts of the plant (leaves, shoots and bunches) but also propagates to surrounding plants (Buonassisi et al., 2017; Gessler et al., 2011). Hence, the development of new techniques that allow an early detection of this infection is extremely important. Metabolomics is a promising tool for the characterization of plant innate pathogen defence responses through the identification of metabolites produced upon plant infection (Arbona and Gómez-Cadenas, 2016). Mass spectrometry based on Fourier Transform Ion Cyclotron Resonance Mass Spectrometry (FT-ICR-MS) is one of the best strategies to perform high throughput untargeted analysis of complex samples (Lim et al., 2016; Marshall et al., 1998), since it is able to resolve thousands of different elemental compositions in a single complex organic mixture (Wu et al., 2004). Recently, our group has developed an efficient metabolite extraction protocol for grapevine leaves compatible with FT-ICR-MS that allowed the identification of more than 800 metabolites (Maia et al., 2016). The high molecular complexity of metabolomics samples generates a very complex mass spectrum (Gutiérrez Sama et al., 2018). It is often difficult to find effective and easily apprehensible visual formats for the representation of these metabolomics data (Kim et al., 2003). To overcome these problems, there are two types of graphical representation that rely on the identified chemical formulas: (i) Van Krevelen (VK) diagrams by plotting H/C (hydrogen to carbon) and O/C (oxygen to carbon) ratios. This representations provide information on the major metabolic classes present on the analysed samples (Brockman et al., 2018; Kew et al., 2017; Mann et al., 2015; Wu et al., 2004); (ii) compositional space plots that use the Double Bond Equivalents (DBE) values, being a good indicator of the molecular structure (Gutiérrez Sama et al., 2018). In this work, we have used this methodology to analyse the chemical composition of a grapevine cultivar upon infection with *P. viticola* and validate the use of the chemical profile, VK diagrams and DBE plots to quickly access and discriminate between infected and non-infected grapevine leaves as soon as 24 hours post inoculation with the pathogen.

6.3 MATERIALS AND METHODS

6.3.1 *Plasmopara viticola* infection

Sporangia of *P. viticola* were collected from infected leaves harvested at the Portuguese Ampelographic grapevine collection (CAN, international code PRT051), INIAV- Dois Portos. After an overnight incubation in the dark, at room temperature and high relative humidity, spores were collected and frozen at -25 °C until further use. *P. viticola* infections were

performed on greenhouse grown plant of *Vitis vinifera* Trincadeira, a susceptible Portuguese cultivar. The abaxial leaf surface was sprayed with a water suspension containing 10^4 sporangia mL^{-1}, while controls were made by spraying the leaves with distilled sterilized water (mock inoculations). Plants were kept for 8 h in a moist chamber and then under greenhouse conditions until symptoms could be observed. The third to fifth leaves (from the shoot apex) were collected at 24 hours post inoculation (hpi) and at least 3 plants were combined to make 1 biological replicate. Leaves were frozen in liquid nitrogen and stored at - 80 ℃.

6.3.2 Metabolite extraction and FT-ICR-MS analysis

Metabolite extraction was done as previously described in Maia et al., 2016 with minor changes. Leaves were ground in liquid nitrogen and used for metabolite extraction. Each biological sample was extracted in a mixture of water: methanol 1:1 (v/v) to obtain a 1 mg/mL solution. Samples were vortexed for 3 min, centrifuged at 1000 *g* for 5 min and diluted to 1:10000 in methanol. Leucine enkephalin (YGGFL, Sigma Aldrich Portugal) was used as internal standard at a final concentration of 0.5 µg/mL and formic acid (Sigma Aldrich, MS grade) was added at a final concentration 0.1% (v/v). Extracted metabolites were analysed by direct infusion electrospray, in positive mode (ESI$^+$), on an Apex Qe 7-Tesla Fourier Transform Ion Cyclotron Resonance Mass Spectrometer (7T-FT-ICR-MS, Brüker Daltonics). Spectra were recorded between 100 and 1000 *m/z* and 100 scans were acquired.

For all mass spectra, internal calibration with Leucine enkephalin mass ([M+H]$^+$ = 556.27657 Da) was used. Raw data for all samples were collected and analysed with the online software Metlin (https://metlin.scripps.edu, Guijas et al., 2018) for compound identification and formula assignment, considering the adducts H$^+$, Na$^+$ and K$^+$, and a mass deviation below 3 ppm (peptides, drugs and toxicants were removed from search). Data from the 3 replicates were combined. Lists were then exported for van Krevelen (VK) diagram, compositional space analysis and frequency histogram of CHO, CHON, CHOS and CHONS elemental compositions. H/C ratio versus the O/C ratio for every compound in the sample were plotted and DBE values were calculated according to (**Equation 6.1**) based on the CcHhOoNnSn molecular formula of each compound and plotted as a function of the number of carbon atoms.

(**Equation 6.1**) $$DBE = C - \frac{H}{2} + \frac{N}{2} + 1$$

6.4 RESULTS AND DISCUSSION

Plasmopara viticola is a obligate biotrophic oomycete pathogen which causes devastating effects on grapevine plants (Armijo et al., 2016; Buonassisi et al., 2017; Gessler et al., 2011; Kamoun et al., 2015; Madden et al., 2000). Different techniques have been used to detect this threat, including molecular biology (Sanagala et al., 2017) and fluorescence analysis (Latouche et al., 2015). However, the detection of early infection is complicated since visible signs of infection only appear after a few days of inoculation and when detected, *P. viticola* has already propagated to other plants (Buonassisi et al., 2017; Gessler et al., 2011). Early detection of mildew infections would contribute for a rapid treatment of those plants and prevent the rapid spreading to the surrounding vines. We propose the use of an untargeted metabolomics approach for the early identification of infected grapevine plants. In this field of complex sample analysis, there are a number of analytical platforms available that allows a chemical profile analysis of different samples being FT-ICR-MS the best methodology. Moreover, using direct infusion of the sample, chromatographic separations are not necessary, saving time in each analysis and increase the metabolome coverage as a higher number of ionised metabolites can be detected. In this work, we analysed the chemical composition of 'Trincadeira' infected leaves with *P. viticola* at 24 hpi by FT-ICR-MS. We identified more than 3500 peaks in the spectra. FT-ICR-MS spectrum for metabolic samples are very complex and the analytical tools available mainly rely on databases, static online platforms and the combination of different analytical programs, which are time consuming. To provide insight into metabolite diversity and elemental ratios, chemical formulas were assigned to the detected masses, leading to a total of 650 different formulas. Van Krevelen diagrams and compositional space plots (**Figure 6.1**) were generated. **Figure 6.1 - A** shows the VK diagram of the control and inoculated samples after 24 hours post inoculation, in positive ionization mode. This representation allows a qualitative identification of the different chemical classes of the compounds present in the different samples. The O/C ratio separate the compounds according to oxidation whereas the H/C ratio allows the separation according to the degree of saturation (Wu et al., 2004). Moreover, VK diagrams are able to provide information about the different chemical classes of compounds that, according to their biochemical properties, can be associated to a specific region of the diagram (Brockman et al., 2018; Wu et al., 2004). Through the VK diagrams plotted for the FT-ICR-MS data of grapevine leaf discs infected with *P. viticola* (**Figure 6.1 - A**), significant differences between the control and inoculated samples are shown. The empirical map created for the main metabolic classes detected identifies the areas with the highest point density: lipids, polyketides and carbohydrates. Furthermore, it is important to highlight the differences in the side regions (0< H/C <1; 1.5< O/C <2.5). Comparing both samples, the inoculated sample has a decreased number of compounds in the lipid region. This result could be due to lipid

peroxidation that leads to a malonaldehyde (MDA) accumulation in response to this biotic stress. Indeed, our recent studies in 'Trincadeira', showed a significant MDA accumulation at 24 hpi with *P. viticola* (Nascimento et al., submitted). This accumulation indicates a disruption of the cellular membrane causing a loss of cellular integrity leading to further reactive oxygen species (ROS) generation.

Regarding compositional space plots, these can be used as a supplement of VK diagrams since DBE values *vs* the number of carbons for specific classes of compounds is a good indicator of the molecular structure. **Figure 6.1 - B**, shows the Double Bond Equivalents as a function of the number of Carbons, in control and inoculated samples 24 hours post inoculation. After infection, there is a higher amount of compound with superior DBE values and with more carbon atoms in their structure. Infection of grapevine with *P. viticola* results in a decrease in the number of compounds in the CHO series, mainly corresponding to carbohydrates. On the other hand, the diversity in CHON series seems to increase (**Figure 6.2**).
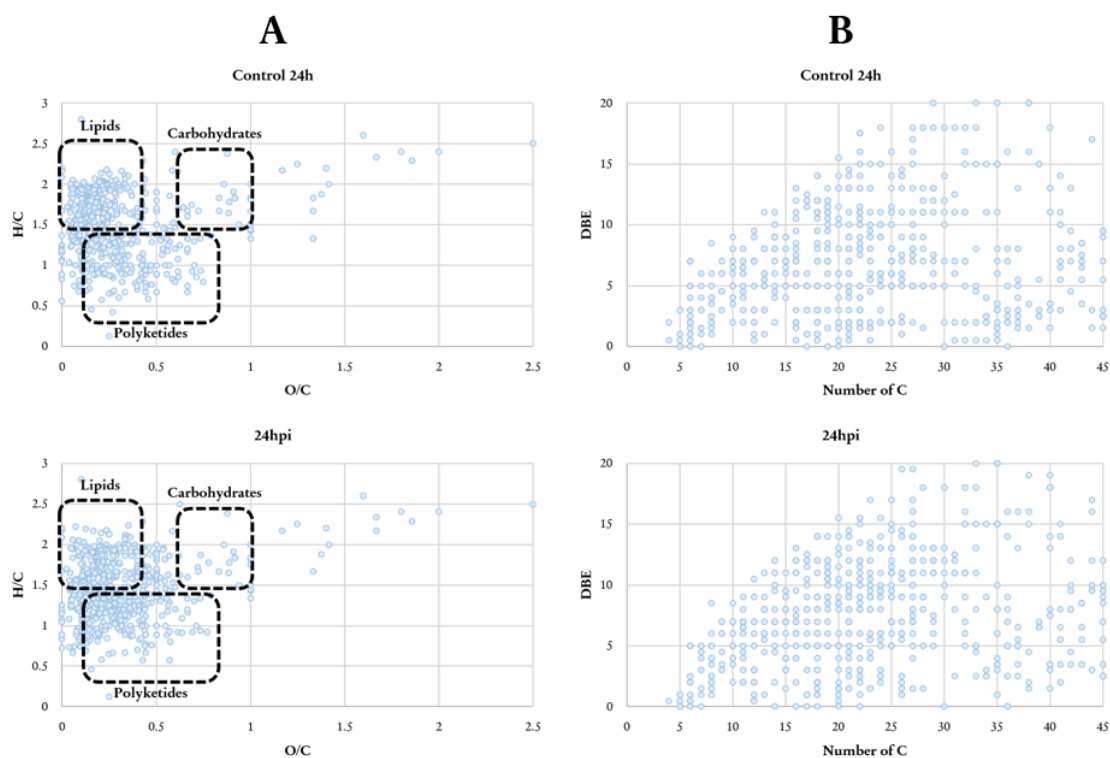

Figure 6.1 – (**A**) Van Krevelen diagram of 'Trincadeira' leaves in control and 24 hpi with *P. viticola*. X-axis represents the O/C ration, and Y-axis the H/C ratio of all the chemical formulas obtained from all spectrum. Plot displays the areas of highest point density for the 3 most important major classes of metabolites: lipids, polyketides, carbohydrates. (**B**) Compositional space plot of 'Trincadeira' leaves in control and 24 hpi with *P. viticola*. X-axis represents the number of carbon atoms and Y-axis the double bond equivalent (DBE) values for the molecules identified.
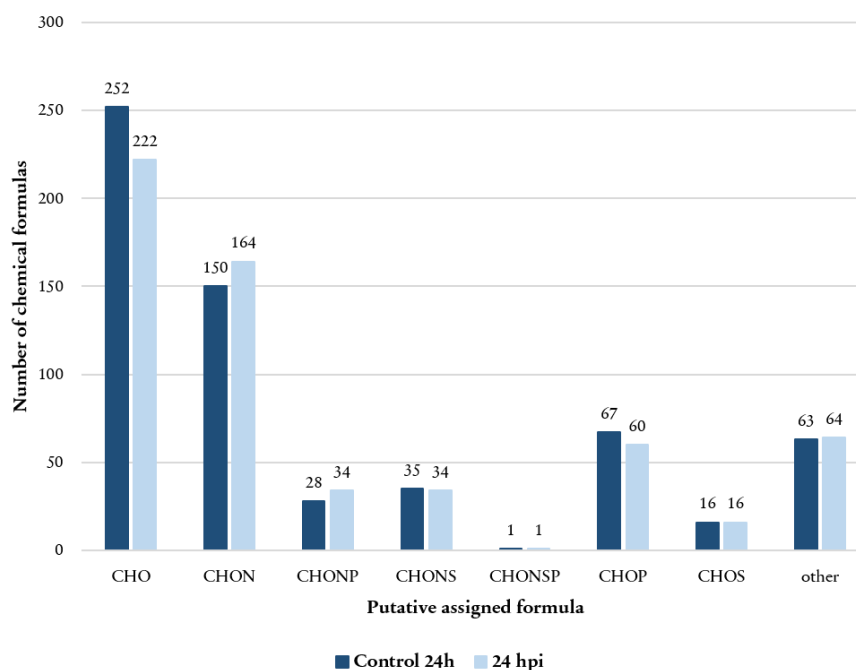
Figure 6.2 - Absolute frequency of compounds in elemental composition series in control and infected 'Trincadeira' grapevine leaves.

6.5   CONCLUSIONS

VK diagrams and compositional space plots are extremely valuable tools to visualize and compare complex data from extreme resolution mass spectrometry analysis, such as those generated by FT-ICR-MS. Also, compounds can be grouped according to their chemical class and specific regions of the VK diagrams can be associated to them. In or work, based on the chemical profile of control and infected samples, we were able to discriminate between infected and non-infected samples, as early as 24 hours after infection.

6.6   ACKNOWLEDGEMENTS

6.7 REFERENCES

Arbona, V., Gómez-Cadenas, A., 2016. Metabolomics of Disease Resistance in Crops. Curr Issues Mol Biol 19, 13–30. https://doi.org/10.21775/9781910190357.04

Armijo, G., Schlechter, R., Agurto, M., Muñoz, D., Nuñez, C., Arce-Johnson, P., 2016. Grapevine Pathogenic Microorganisms: Understanding Infection Strategies and Host Response Scenarios. Frontiers in Plant Science 7. https://doi.org/10.3389/fpls.2016.00382

Brockman, S.A., Roden, E.V., Hegeman, A.D., 2018. Van Krevelen diagram visualization of high resolution-mass spectrometry metabolomics data with OpenVanKrevelen. Metabolomics 14. https://doi.org/10.1007/s11306-018-1343-y

Buonassisi, D., Colombo, M., Migliaro, D., Dolzani, C., Peressotti, E., Mizzotti, C., Velasco, R., Masiero, S., Perazzolli, M., Vezzulli, S., 2017. Breeding for grapevine downy mildew resistance: a review of "omics" approaches. Euphytica 213. https://doi.org/10.1007/s10681-017-1882-8

Figueiredo, A., Fortes, A.M., Ferreira, S., Sebastiana, M., Choi, Y.H., Sousa, L., Acioli-Santos, B., Pessoa, F., Verpoorte, R., Pais, M.S., 2008. Transcriptional and metabolic profiling of grape (*Vitis vinifera* L.) leaves unravel possible innate resistance against pathogenic fungi. Journal of Experimental Botany 59, 3371–3381. https://doi.org/10.1093/jxb/ern187

Gessler, C., Pertot, I., Perazzolli, M., 2011. *Plasmopara viticola*: a review of knowledge on downy mildew of grapevine and effective disease management. Phytopathologia Mediterranea 50, 3–44. https://doi.org/10.14601/Phytopathol_Mediterr-9360

Gómez-Zeledón, J., Zipper, R., Spring, O., 2013. Assessment of phenotypic diversity of *Plasmopara viticola* on *Vitis* genotypes with different resistance. Crop Protection 54, 221–228. https://doi.org/10.1016/j.cropro.2013.08.015

Guijas, C., Montenegro-Burke, J.R., Domingo-Almenara, X., Palermo, A., Warth, B., Hermann, G., Koellensperger, G., Huan, T., Uritboonthai, W., Aisporna, A.E., Wolan, D.W., Spilker, M.E., Benton, H.P., Siuzdak, G., 2018. METLIN: A Technology Platform for Identifying Knowns and Unknowns. Anal. Chem. 90, 3156–3164. https://doi.org/10.1021/acs.analchem.7b04424

Gutiérrez Sama, S., Farenc, M., Barrère-Mangote, C., Lobinski, R., Afonso, C., Bouyssière, B., Giusti, P., 2018. Molecular Fingerprints and Speciation of Crude Oils and Heavy Fractions Revealed by Molecular and Elemental Mass Spectrometry: Keystone

between Petroleomics, Metallopetroleomics, and Petrointeractomics. Energy & Fuels 32, 4593–4605. https://doi.org/10.1021/acs.energyfuels.7b03218

Kamoun, S., Furzer, O., Jones, J.D.G., Judelson, H.S., Ali, G.S., Dalio, R.J.D., Roy, S.G., Schena, L., Zambounis, A., Panabières, F., Cahill, D., Ruocco, M., Figueiredo, A., Chen, X.-R., Hulvey, J., Stam, R., Lamour, K., Gijzen, M., Tyler, B.M., Grünwald, N.J., Mukhtar, M.S., Tomé, D.F.A., Tör, M., Van Den Ackerveken, G., McDowell, J., Daayf, F., Fry, W.E., Lindqvist-Kreuze, H., Meijer, H.J.G., Petre, B., Ristaino, J., Yoshida, K., Birch, P.R.J., Govers, F., 2015. The Top 10 oomycete pathogens in molecular plant pathology. Mol. Plant Pathol. 16, 413–434. https://doi.org/10.1111/mpp.12190

Kew, W., Blackburn, J.W.T., Clarke, D.J., Uhrín, D., 2017. Interactive van Krevelen diagrams - Advanced visualisation of mass spectrometry data of complex mixtures: Interactive van Krevelen Diagrams. Rapid Communications in Mass Spectrometry 31, 658–662. https://doi.org/10.1002/rcm.7823

Latouche, G., Debord, C., Raynal, M., Milhade, C., Cerovic, Z.G., 2015. First detection of the presence of naturally occurring grapevine downy mildew in the field by a fluorescence-based method. Photochem. Photobiol. Sci. 14, 1807–1813. https://doi.org/10.1039/C5PP00121H

Lim, L., Yan, F., Bach, S., Pihakari, K., Klein, D., Lim, L., Yan, F., Bach, S., Pihakari, K., Klein, D., 2016. Fourier Transform Mass Spectrometry: The Transformation of Modern Environmental Analyses. International Journal of Molecular Sciences 17, 104. https://doi.org/10.3390/ijms17010104

Madden, L.V., Ellis, M.A., Lalancette, N., Hughes, G., Wilson, L.L., 2000. Evaluation of a Disease Warning System for Downy Mildew of Grapes. Plant Disease 84, 549–554. https://doi.org/10.1094/PDIS.2000.84.5.549

Maia, M., Monteiro, F., Sebastiana, M., Marques, A.P., Ferreira, A.E.N., Freire, A.P., Cordeiro, C., Figueiredo, A., Sousa Silva, M., 2016. Metabolite extraction for high-throughput FTICR-MS-based metabolomics of grapevine leaves. EuPA Open Proteomics 12, 4–9. https://doi.org/10.1016/j.euprot.2016.03.002

Mann, B.F., Chen, H., Herndon, E.M., Chu, R.K., Tolic, N., Portier, E.F., Roy Chowdhury, T., Robinson, E.W., Callister, S.J., Wullschleger, S.D., Graham, D.E., Liang, L., Gu, B., 2015. Indexing Permafrost Soil Organic Matter Degradation Using High-Resolution Mass Spectrometry. PLoS One 10. https://doi.org/10.1371/journal.pone.0130557

Marshall, A.G., Hendrickson, C.L., Jackson, G.S., 1998. Fourier transform ion cyclotron resonance mass spectrometry: a primer. Mass Spectrom Rev 17, 1–35. https://doi.org/10.1002/(SICI)1098-2787(1998)17:1<1::AID-MAS1>3.0.CO;2-K

Sanagala, R., Moola, A.K., Bollipo Diana, R.K., 2017. A review on advanced methods in plant gene targeting. Journal of Genetic Engineering and Biotechnology 15, 317–321. https://doi.org/10.1016/j.jgeb.2017.07.004

Toffolatti, S.L., Venturini, G., Maffi, D., Vercesi, A., 2012. Phenotypic and histochemical traits of the interaction between *Plasmopara viticola* and resistant or susceptible grapevine varieties. BMC Plant Biol. 12, 124. https://doi.org/10.1186/1471-2229-12-124

Wu, Z., Rodgers, R.P., Marshall, A.G., 2004. Two- and Three-Dimensional van Krevelen Diagrams: A Graphical Analysis Complementary to the Kendrick Mass Plot for Sorting Elemental Compositions of Complex Organic Mixtures Based on Ultrahigh-Resolution Broadband Fourier Transform Ion Cyclotron Resonance Mass Measurements. Analytical Chemistry 76, 2511–2516. https://doi.org/10.1021/ac0355449

CHAPTER VII

MALDI-FT-ICR-MS imaging metabolic snapshot of grapevine-*Plasmopara viticola* interaction

7 Grapevine leaf MALDI-FT-ICR-MS imaging reveals sucrose localisation patterns associated to *P. viticola* development

7.1 ABSTRACT

Grapevine (*Vitis vinifera* L.) is susceptible to the oomycete *Plasmopara viticola*, the causal agent of downy mildew disease. Upon infection, grapevine activates a series of signalling and metabolic pathways, involving secondary metabolites that play a key role in the defence response of the plant. Despite well-established pathways and metabolites involved in this interaction, valuable information on the first recognition-associated molecules on the leaf surface and, particularly, their localisation is still missing. To understand and localise the signalling molecules associated with the susceptibility to this pathogen, we applied Fourier transform-ion cyclotron resonance (FT-ICR) mass spectrometry imaging (MSI) to grapevine leaf discs infected with *P. viticola*. The plant material preparation was optimised, and different matrices and solvents were tested for FT-ICR-MSI analysis. Our data shows that the trichomes present in the abaxial side of the leaf topologically hampers matrix deposition and the ion signal. Preliminary results show that sucrose was more accumulated in leaf discs infected with *P. viticola* in comparison with control leaves. This metabolite presented a non-homogeneous distribution in the leaf disc infected with *P. viticola*. Sucrose was visually more accumulated on the veins of the infected leaves, leading to the hypothesis that sucrose metabolism is being manipulated by the development structures of *P. viticola*. Up to our knowledge this is the first time that sucrose localisation was correlated to *P. viticola* infection sites.

7.2 INTRODUCTION

The development of matrix-assisted laser desorption-ionisation (MALDI) mass spectrometry imaging (MSI) was first reported in 1994 and has been applied to visualise different biomolecules, since 1997 (Caprioli et al., 1997; Spengler et al., 1994). MALDI-MSI has the unique ability to analyse the sample surface directly by combining powerful raster-scan of the sample surface with lasers shots with high mass resolution mass spectrometry (Bjarnholt et al., 2014; Boughton et al., 2016; Grassl et al., 2011). The prime advantage of MALDI-MSI, over other imaging techniques, is not only the ability to identify specific molecules, but also to reveal the distribution of a wide range of biological compounds across the sample section in a label-free and non-targeted mode. Considering that the complexity of biochemical processes occurring in cells, tissues, organs and whole systems is not only

determined by their timing, but also by the localisation of certain molecular events (Kaspar et al., 2011), MALDI-MSI has the advantage to provide high spatial resolution (Bjarnholt et al., 2014; Boughton et al., 2016; Grassl et al., 2011; Kaspar et al., 2011; Schulz et al., 2019). Moreover, MALDI-MSI is a very sensitive technique with the ability to analyse complex samples (Laugesen and Roepstorff, 2003). The analysis of compounds in MALDI-MSI ranges from large biomolecules, such as proteins and peptides, to small molecule compounds such as lipids, sugars, amino acids, phosphorylated compounds and pharmacological and chemical compounds (Alcantara et al., 2020; Carter et al., 2011; Francese et al., 2009; Goodwin et al., 2010; Richard J A Goodwin et al., 2011; Richard J. A. Goodwin et al., 2011; Gorzolka et al., 2014; Grassl et al., 2011; Kaspar et al., 2011; Puolitaival et al., 2008; Sarabia et al., 2018; Solon et al., 2010; Takahashi et al., 2015). MALDI-MSI is also a suitable analytical technique for both polar and nonpolar biomolecules (Rubakhin and Sweedler, 2010a).

To date, the literature of MALDI-MSI in plants is limited when compared to animal studies (Bjarnholt et al., 2014; Boughton et al., 2016). MALDI-MSI has the potential to bring new insights into the molecular analysis of plants by providing high spatial resolution information about metabolic processes and potentially determine changes during plant development or induced by environmental variation. It will provide a means of identifying the localisation of metabolites associated with tissue types, development, disease, genetic variations or following genetic manipulation (Bjarnholt et al., 2014; Boughton et al., 2016). Some reports have used this technique to evaluate the surface distribution of sugars, metabolites and lipids in different plant tissues and organs (Bunch et al., 2004; Burrell et al., 2007; Goto-Inoue et al., 2010; Li et al., 2008; Ng et al., 2007; R. Shroff et al., 2008). For instance, the distribution of epicuticular lipids, waxes and several secondary metabolites, such as flavonoids or alkanes, were measured at the surface of *Arabidopsis thaliana* flowers, leaves and roots (Cha et al., 2009, 2008; Grassl et al., 2011; Jun et al., 2010; Vrkoslav et al., 2010). Moreover, different studies have also used MSI to better understand plant biotic and abiotic stresses (Gorzolka et al., 2014; Hamm et al., 2010; R. Shroff et al., 2008; Shroff et al., 2015; Soares et al., 2015). As an example, this technique has been used to highlight the uneven distribution of specific biological compounds in wheat grains, sampled at various developmental stages and under temperature stress (Takáts et al., 2004). Moreover, it allowed to identify metabolites and other low molecular weight ions in tobacco (*Nicotiana tabacum*) leaves infected with *Phytophtora nicotianae* (Ibáñez et al., 2010). Also, with the increasing demands for a more sustainable agriculture practice, this technique has been used to identify specific agrochemical compounds that are present in the plant or in specific organs of the plant.

In every mass spectrometry imaging-based analysis, the measurement of an analyte intensity is influenced by several factors including analyte extraction efficiency, ionisation

efficiency and consistency of co-crystallisation with the MALDI matrix (Schulz et al., 2019; Schwartz et al., 2003). Sample handling and preparation are crucial to obtain high quality MALDI mass spectra in a reproducible manner (Grassl et al., 2011; Laugesen and Roepstorff, 2003; Schwartz et al., 2003). However, the selection of the MALDI matrix and the optimisation of the preparation protocol are still empirical procedures. The composition of the solvent in which the MALDI matrix is applied on the sample influences the desorption-ionisation of molecules from the tissues. Also, the selection of the optimal matrix, including its crystallisation parameters, for the experiment depends on the type of biological molecules to be analysed. A homogeneous layer of matrix solution, followed by a fast drying of the matrix film should be preferred to avoid the formation of large matrix crystals, that are responsible for critical signal fluctuation in MALDI-MSI profile (known as the matrix effects) (Francese et al., 2009; Grassl et al., 2011; Kaspar et al., 2011; Rubakhin and Sweedler, 2010a). By its ultra-high mass resolving power, Fourier Transform Ion Cyclotron Resonance mass spectrometry (FT-ICR-MS) imaging analysis enables small molecule separation from the complex background of tissue constituents and matrix ions (Bjarnholt et al., 2014; Boughton et al., 2016), which is a very important asset when analysing complex samples such as plant tissues.

Vitis vinifera L. (grapevine) is one of the most important and cultivated fruit plants in the world with a highly economic impact in several countries. Unfortunately, the domesticated *V. vinifera* cultivars frequently used for wine production are highly susceptible to fungal diseases, being the downy mildew, caused by the biotrophic oomycete *Plasmopara viticola* (Berk. et Curt.) Berl.et de Toni, one of the most destructive vineyard diseases. *Plasmopara viticola* is an obligatory biotrophic pathogen. It feeds on the living tissue (grapevine) and develops specific structures to invade the cell and to obtain metabolism products, without killing the plant (Gessler et al., 2011). So far, several potential metabolic biomarkers were identified by comparing the constitutive accumulation of specific metabolites not only in the leaf tissue of different *Vitis* genotypes (Maia et al., 2020), but also in grapevine-pathogen interaction (Adrian et al., 2017; Batovska et al., 2009, 2008; Becker et al., 2013; Nascimento et al., 2019). Their accumulation reflects however the all-leaf tissue metabolome composition/modulation and not the molecules that contribute for the first contact with pathogens at leaf surface. Some studies in grapevine leaves with imaging mass spectrometry are starting to appear to identify the main biological compounds in the leaf surface during the interaction with *Plasmopara viticola* (Becker et al., 2017, 2014; Hamm et al., 2010). However, these studies are only focused on the modulation of specific compounds after pathogen infection, e.g., resveratrol pterostilbene and viniferins.

The present work aimed at analysing *V. vinifera* cv. Trincadeira leaf surface with and without *P. viticola* infection, using MALDI FT-ICR-MS imaging approach. Sample

preparation, including the choice of the MALDI matrix and the matrix deposition solvent, were optimised to uncover the main biological compounds present both constitutively and after pathogen infection.

7.3   MATERIALS AND METHODS

7.3.1   *P. viticola* propagation

Plasmopara viticola spores were collected from infected plants from the vineyard at the Portuguese Ampelographic Grapevine Collection (CAN, international code PRT051, established in 1988) at INIAV-Estação Vitivinícola Nacional (Dois Portos), using a vacuum system and stored at -20 ^{0}C. Inocula was propagated in susceptible *V. vinifera* leaves by spreading a sporangia solution on the abaxial surface of the leaf, with an undefined concentration of *P. viticola* sporangia. After infection, leaves were kept in the dark for the first 8 to 12 hours and then at 25 ^{0}C with natural light conditions, until sporulation appeared in all leaf surface. Spores were collected with a vacuum system and stored at -20 ^{0}C until further use.

7.3.2   Plant material harvesting and *P. viticola* infection assay

The third to fifth fully expanded leaves, from shoot to apex, of *Vitis vinifera* cv. Trincadeira (VIVC variety number: 15685), susceptible to *P. viticola*, were collected at the Portuguese Ampelographic Grapevine Collection. CAN is located at Quinta da Almoinha, 60 km north of Lisbon (9º 11′ 19″ W; 39º 02′ 31″ N; 75 m above sea level). It occupies nearly 2 ha of area with homogeneous modern alluvial soils (lowlands) as well as drained soil. All accessions are grafted on a unique rootstock variety (Selection Oppenheim 4–SO4) and each accession come from one unique plant collected in the field. The climate of this region is temperate with dry and mild summer.

For leaf infections, sporangia viability was confirmed by microscopic observations as described in Kortekamp and co-workers (Kortekamp et al., 2008), prior to inoculation. A suspension containing 50 000 spores/mL was used to infect the abaxial leaf surface. After inoculation, plants were kept for 8 to 12 hours in the dark and kept under natural light conditions at 25 ^{0}C for 96 hours. Leaf discs were then cut and lyophilised at -50 ^{0}C between 2 glass plates, to obtain a planar surface once dried. Mock inoculations were performed by rinsing *Vitis vinifera* cv Trincadeira leaves with water, leaf discs were cut and lyophilised at -

50 ^{0}C. Infection control was accessed 8 days after inoculation with the appearance of typical disease symptoms (see **Appendix D – Supplementary Figure F7.1**).

7.3.3 Matrix coating optimization

MALDI matrices α-cyano-4-hydroxycinnamic acid (HCCA), 2,5-dihydroxybenzoic acid (DHB) and 9-aminoacridine (9-AA) were purchased from Sigma-Aldrich (Overijse, Belgium). Trifluoracetic acid (TFA) was from Sigma-Aldrich, and LC-MS grade acetonitrile (ACN) and methanol (MeOH), were purchase from Biosolve (Valkenswaard, Netherlands). Indium tin oxide (ITO)-coated glass slides were purchased from Bruker Daltonics (Bremen, Germany).

Lyophilised *Vitis vinifera* cv Trincadeira leaf discs were carefully removed from the plates and transferred to the target ITO-glass slide, previously covered with a double-sided adhesive copper tape (StructureProbe INC, West Chester, PA, USA), with the abaxial surface of the leaf facing up. For the analysis of trichome-free leaf discs, after mounting, trichomes were carefully removed using tweezers under a magnifying lens. ITO-glass slides were stored in a vacuum chamber until matrix deposition. Leaf discs were sprayed with the different matrices in different concentrations and solvents (**Table 7.1**). HCCA matrices of 5 mg/mL were prepared using 70:30 (v:v) ACN:H_2O and 70:30 (v:v) MeOH:H_2O with 0.1% (v/v) TFA. In total, 20 layers of this matrix solution were sprayed on the ITO slide using the SunCollect instrument (SunChrom, Friedrichsdorf, Germany). The first layer was sprayed at a flow rate of 10 μL/min. Flow rate was increased by 10 μL/min after each layer until reaching 60 μL/min. DHB matrix was prepared in 50:50 (v:v) ACN:H_2O with 0.1% (v/v) TFA to reach a final concentration of 20 mg/mL according to Seaman and co-workers (Seaman et al., 2014) and fifty matrix layers were sprayed on the ITO slide, as previously described. Solution of 9-AA was prepared at 15 mg/mL in methanol with 0.1% (v/v) TFA according to Rohit Shroff and co-workers (Rohit Shroff et al., 2008). Leaves were spray-coated by using a commercial sprayer. The target plate was kept at around 45 ° angle and the sprayer held at a distance of 20 cm from the plate. This insured that the cone of the spray reaching the target covered the entire leaf. Each spray was followed by 10 seconds of warm air drying. This process was typically carried out 15 times to give maximal signal strength.

Table 7.1 - Different matrices, concentrations and layers used in *Vitis vinifera* cv Trincadeira leaf discs

	Matrix	Concentration	Solvent (% v/v)	Matrix application method	Number of layers
(1)	HCCA	5 mg/mL	70% ACN 30% H_2O 0.1% TFA	SunChrom	20
(2)	HCCA	5 mg/mL	70% MeOH 30% H_2O 0.1% TFA	SunChrom	20
(3)	DHB	20 mg/mL	50% ACN 50% H_2O 0.1% TFA	SunChrom	50
(4)	9-AA	15 mg/mL	100% MeOH 0.1% TFA	Commercial spray	15

7.3.4 MALDI FT-ICR-MS imaging analysis

Microscope images (obtained at the magnification 10 x with an Olympus BX40 microscope) of leaf discs onto ITO-glass slides were acquired to better visualise and select areas of interest in the discs. Also, since the leaf surface is not entirely flat, only the flat areas of the microscopic images were selected for MSI analysis. Two to four small areas of each leaf disc were selected to be analysed (see **Appendix E – Supplementary Figure F7.2**). Analysis was performed using a SolariX XR 9.4T FT-ICR-MS (Bruker Daltonics, Bremen, Germany), fitted with the dual ESI/MALDI ion sources and SmartBeam laser. For each mass spectrum, the following laser parameters were used: 200 laser shots at a repetition rate of 1000 Hz, 60% of power. The raster step size was set at 200 μm. Mass spectrometry images were acquired in positive ionisation mode, in the mass range of 200 to 1000 *m/z*. Red phosphorus solution in pure acetone spotted directly onto the ITO Glass slide was used to calibrate the mass spectrometer before each analysis.

7.3.5 Data analysis

Data were analysed using the imaging mass spectrometry software SCiLS™ Lab 2016b (Bruker Daltonics, Bremen, Germany) for unsupervised spatial identification of discriminative features between control, 96 hpi, and 96 hpi with visible sporulation of *P. viticola* spores. Data were normalised by the total ion count. MALDI FT-ICR-MS chemical images were generated from a colour scale, which represents the normalised intensity of

specific ions. Each pixel of the image is associated with the original mass spectrum that is acquired in a particular position. A spatial localisation of the analytes is provided as a function of the *m/z* values. For metabolite identification, selected *m/z* values were submitted to MassTRIX 3 (Suhre and Schmitt-Kopplin, 2008) server (http://masstrix.org, accessed in April 2021) considering the following parameters: positive scan mode; the adducts [M+H]$^+$, [M+K]$^+$ and [M+Na]$^+$ were considered; a maximum *m/z* deviation of 2 ppm was considered; the organism *Vitis vinifera* was selected; search was performed in the databases "KEGG (Kyoto Encyclopaedia of Genes and Genomes) /HMDB (Human Metabolome DataBase)/LipidMaps without isotopes".

7.4 RESULTS

7.4.1 Preparation of grapevine leaves for analysis: the influence of trichomes

Grapevine leaves have trichomes in the abaxial side (Konlechner and Sauer, 2016), which may hamper the analysis and influence the MSI results (Bjarnholt et al., 2014). Hence, we started by analysing the grapevine leaf discs with and without trichomes to understand if these structures influence the coating of the matrix and to select the leaf discs leading to the best matrix coating. For this analysis, α-cyano-4-hydroxycinnamic acid (HCCA) was the chosen as the matrix as it forms small crystals and hence produces a more homogeneous matrix coating. HCCA was prepared according to (1) in **Table 7.1** (**Materials and Methods section**).

V. vinifera cv. Trincadeira leaf discs' areas analysed with and without trichomes are presented in **Figure 7.1**. In positive-ion mass spectrum, the global intensity of the peaks detected was higher in the leaf disc without trichomes and with a more homogenous intensity detection. These results demonstrate that the matrix was better distributed in the leaf disc without trichomes and consequently a better signal was detected. For further analyses, trichomes were removed from all leaf discs using a tweezer under a magnifying lens. Moreover, to avoid leaf topological interference with the laser, only flat areas of the microscopic images (i.e., corresponding to flat regions on the microscopic image) were selected for MSI analysis.
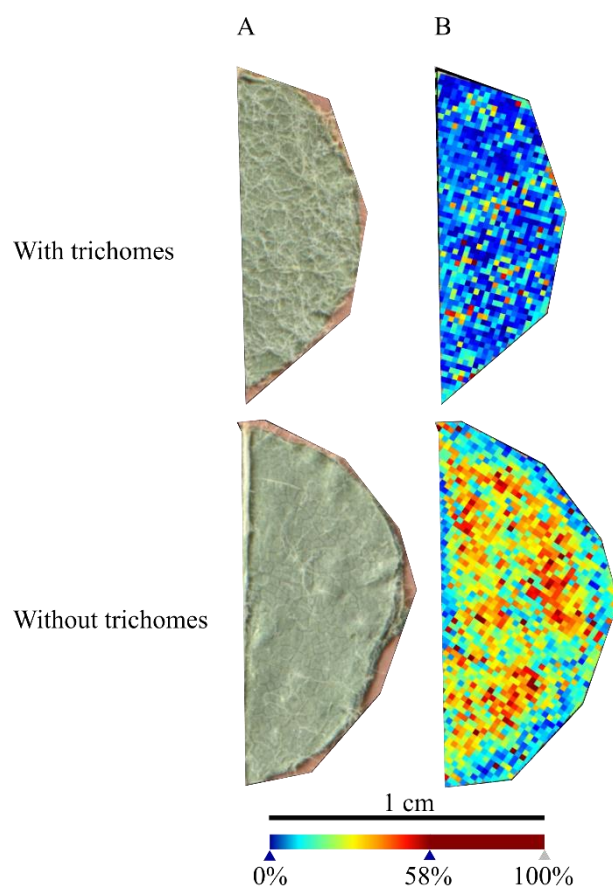
Figure 7.1 – *V. vinifera* cv. Trincadeira leaf discs analysed with and without trichomes; (**A**) Microscopy images of the leaf disc sections analysed; (**B**) MALDI-FT-ICR-MS images reconstructed from all the peaks detected in the leaf discs. Data was normalised by the total ion count.

7.4.2 Different matrix analysis and metabolite detection

After plant material preparation optimisation, and to detect molecules related to the grapevine-*P. viticola* interaction, we tested different matrices already described for MALDI FT-ICR MS imaging analysis of plant tissues (**Table 7.1**).

Matrices α-cyano-4-hydroxycinnamic acid (HCCA), 2,5-dihydroxybenzoic acid (DHB) and 9-aminoacridine (9-AA) were prepared according to **Table 7.1** and applied by spraying on the different *V. vinifera* cv. Trincadeira leaf discs: control (mock inoculated), *96 hpi* (hours post-inoculation) with *P. viticola* without visible sporulation and *96 hpi* with *P. viticola* visible sporulation. HCCA was prepared into two different solvents: MeOH and ACN. HCCA is the most commonly used matrix for small-molecules and different MALDI imaging studies in plant tissues were reported using that matrix in both solvents (Becker et al., 2014; Costa et al., 2013; Seaman et al., 2014; Soares et al., 2015). Microscope images (10x) of leaf discs were taken for a better selection of the leaf discs areas to be analysed (see **Appendix E – Supplementary Figure F7.2**). Selected areas were analysed with an FT-ICR-MS and ion

images were reconstructed from the absolute intensities of the medium mass spectra, showing the exact location of ions on the extension of the leaf area analysed.

The mass spectra of grapevine leaf discs areas obtained from HCCA matrix with MeOH and ACN as solvents were very similar (see **Appendix F – Supplementary Figure F7.3**). These results demonstrate that both solvents can be used for MALDI analysis of grapevine leaf discs. The main differences appeared to be with the matrices DHB and 9-AA. The intensity of the peaks, within the 800 to 900 *m/z* range, was lower (see **Appendix F – Supplementary Figure F7.3**).

These results also demonstrate that removing the physical barrier from the grapevine leaves, trichomes, allows for a better MSI analysis independently of the matrix and solvents used.

Preliminary reconstructed MS images by MS data of all matrices, demonstrated that the ion intensity at *m/z* 365.105 and 381.079 is higher in the leaf discs infected by *P. viticola* than in the control discs (**Figure 7.2**). The highest signals were observed with HCCA in MeOH and, to a lower extent with HCCA in ACN. For DHB and 9-AA, the signal was found much lower and less detectable than with the other matrices.

In a recent study based on the accurate mass measurements by Taylor and co-workers (Taylor et al., 2021), these masses were also detected and correspond to different adducts of disaccharides, the ions at *m/z* 365.105 and 381.079 were putatively identified as the $[M+Na]^+$ and $[M+K]^+$ adducts of sucrose using the MassTRIX database.

In a more detailed analysis, it was visible that the spatial distribution of putatively identified sucrose in the infected grapevine leaf discs is non-homogeneous, as observed in **Figure 7.2**. To evaluate this distribution, the accumulation of these ions was further investigated in the network of small veins and more precisely in the dense parenchyma tissue (**Figure 7.3**). Images of the 96 hpi without visible *P. viticola* sporulation and 96 hpi with visible *P. viticola* sporulation leaf discs were reconstructed from the identified sucrose *m/z* 365.105 ($[M+Na]^+$) as the distribution for *m/z* 381.079 ($[M+K]^+$) was similar but less intense. Our results suggest that sucrose, *m/z* 365.105 ($[M+Na]^+$) and *m/z* 381.079 ($[M+K]^+$), are mainly located around the veins, which is an indicator of the correlation of sucrose at *P. viticola* infection sites (**Figure 7.3**).
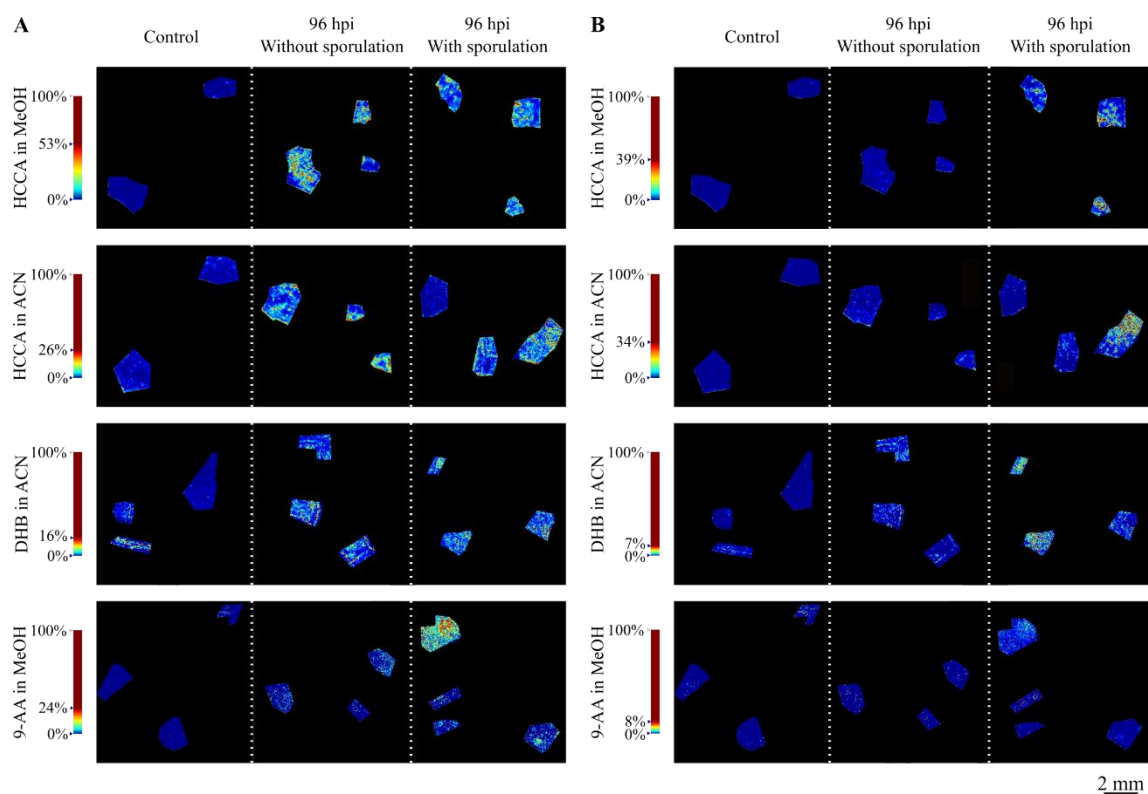
Figure 7.2 – Reconstructed ion images of putatively identified sucrose, (**A**) (*m/z* 365.105, [M+Na]+) and (**B**) (*m/z* 381.079, [M+K]+) adducts, detected with MALDI–FT-ICR-MS imaging using HCCA matrix with MeOH and ACN, DHB matrix and 9-AA matrix. Leaf disc areas analysed from control (mock inoculated), 96 hpi without visible *P. viticola* sporulation and 96 hpi with visible *P. viticola* sporulation are presented. The colour scale of the leaf disc areas indicates the absolute intensity of each pixel (arbitrary units).
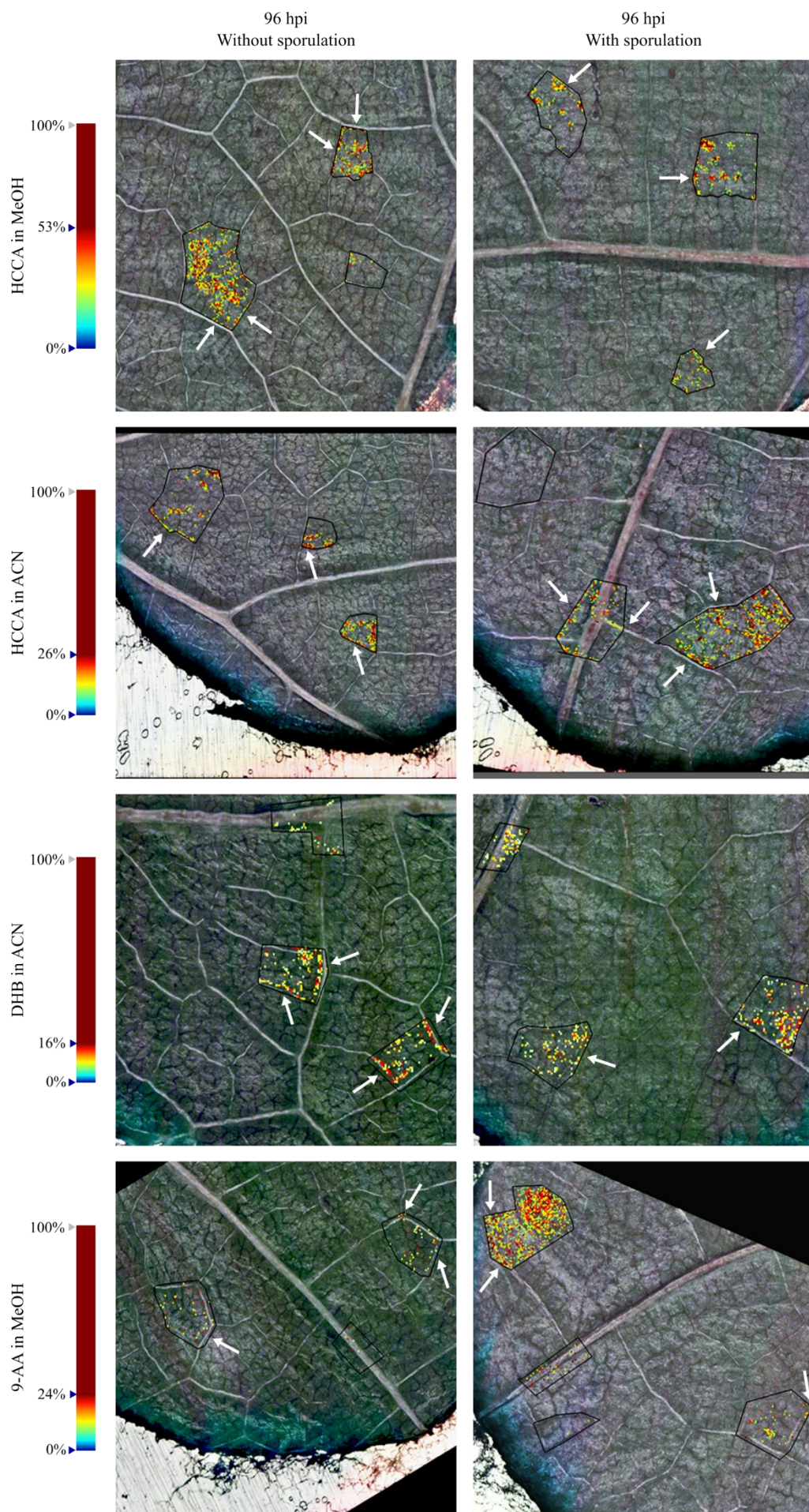
Figure 7.3 - Areas for MALDI-FT-ICR-MS analysis (left) and reconstructed ion images of putatively identified sucrose (*m/z* 365.105, [M+Na]$^+$) (right) in 96 hpi without visible *P. viticola* sporulation and 96 hpi with visible *P. viticola* sporulation. Leaf disc areas detected via MALDI–FT-ICR-MS imaging using HCCA matrix with MeOH and ACN, DHB matrix and 9-AA matrix. The colour scale indicates the absolute intensity of each pixel (arbitrary units). White arrows indicate the visible distribution of putatively identified sucrose along the leaf veins.

7.5   DISCUSSION

Mass spectrometry imaging has been applied to study several plant tissues. However, sample preparation of plant tissues is not easy and continuously seems to be the bottleneck of this technique. This topic has been the major area of interest with the goal to improve sensitivity, specificity and obtain good quality images in a reproducible manner (Schulz et al., 2019).

Sample preparation is a particular challenge, because the visualisation of certain classes of compound relies on specific conditions for optimal ionisation. Careful sample treatment is essential for signal quality and the avoidance of lateral displacement of the analytes (Rubakhin and Sweedler, 2010b). Artefacts can arise at any stage between sample collection and MSI analysis (Rubakhin and Sweedler, 2010b). Although different methodologies have been published through the years to limit these issues, the optimisation of sample preparation is still sample dependent, because of inherent differences in the composition of plant tissues (Grassl et al., 2011; Kaspar et al., 2011).

In plants, trichomes are essential epidermal outgrowths covering most aerial plant tissues and can be found in a very large number of plant species (Huchelmann et al., 2017), including grapevine (Konlechner and Sauer, 2016). Albeit one of the main functions of these structures is to protect the plant from, e.g., herbivorous, insects and fungi, the presence of trichomes in the leaf inhibits the deposition of a homogeneous coating of the matrix. This leads to an inaccurate ionisation of the ions present on the leaf and consequently a misleading detection/identification of the compounds (Bjarnholt et al., 2014). Having this in mind, and since grapevine leaves possess trichomes which could interfere with the analysis, our first approach was to analyse leaf discs with and without trichomes. Our results showed that leaf discs with no trichomes provide a more accurate analysis of the site-specific compounds.

Another important point in sample preparation for MALDI imaging is the matrix. Despite numerous matrices are available to analyse a wide range of biological compounds, it is important to consider the compounds of interest to be analysed in the sample. Selection of

an appropriate matrix is a critical point to obtain a high quality MALDI imaging mass spectrum. For metabolomics analysis, the choice of matrices for metabolite analysis is even more complex, since matrix ions often crowd the low-mass range, limiting confident detection of low-molecular weight analyte ions. For the detection of low-weight molecules, α-cyano-4-hydroxycinnamic acid (HCCA), 2,5-dihydroxybenzoic acid (DHB) and 9-aminoacridine (9-AA) have been found to be the better suited (Calvano et al., 2018; Laugesen and Roepstorff, 2003; Leopold et al., 2018). Besides matrix itself, matrix application, solvent composition (typically methanol or acetonitrile) and mode of application, e.g., sprayer device, movement speed, solvent flow rate, distance between sample and target and/or nozzle temperature, influence the analysis of target molecules from the sample. These parameters are directly related to the size of the matrix crystals formed (Laugesen and Roepstorff, 2003; Leopold et al., 2018; Schulz et al., 2019). The crystallisation between the matrix and the analyte leads to co-crystals which should be as homogeneous as possible, to assure reproducibility and highest sensitivity. Hence, spray is currently the most widespread matrix application technique. Taking this information into account, in this work, HCCA, DHB and 9-AA were tested with MeOH and ACN as solvents using different spraying systems. Our results demonstrate that both solvents can be used for grapevine leaf discs. Also, all matrices appear to be suitable for grapevine leaf disc analysis, within the range of analysis. However, it is important to consider that the intensity of the peaks may be altered according to the matrix used. The *m/z* 365.105 ([M+Na]$^+$) and *m/z* 381.079 ([M+K]$^+$), putatively assigned to sucrose, were commonly identified in all of the matrices and solvents tested presenting high levels of abundance in grapevine leaf discs infected with *P. viticola* when comparing with mock inoculated leaf discs.

Plasmopara viticola infection occurs when the zoospores germinate and penetrate the stomatal cavity on the abaxial side of the leaf, forming a substomatal vesicle. This vesicle gives rise to the primary hyphae and mycelium, which grows through intercellular spaces, enclosed by the veins of the leaf (Fröbel and Zyprian, 2019). The haustorium penetrated the parenchyma cell walls, allowing the contact between the pathogen (*P. viticola*) and the host (grapevine leaves) (Gessler et al., 2011; Yin et al., 2017). Also, this structure may function as a site of molecular exchange of effectors and nutrients between the grapevine and *P. viticola* and block grapevine defence signalling pathways (Yin et al., 2017). In fact, our results demonstrate a correlation of sucrose and the development of *P. viticola* infection structures due to its higher intensity around the veins. There are different hypothesis regarding the roles of sugar transporters in pathogen defence (Bezrutczyk et al., 2018).

Up to our knowledge, our results are the first evidence of sucrose translocation to infection site areas, which lead us to hypothesise that the pathogen, through mycelium development, has gained access to this plant resource, and it is using it to complete its lifecycle

(Aked and Hall, 1993; Bezrutczyk et al., 2018; Gebauer et al., 2017; Sutton et al., 1999). This accumulation is in accordance with our previously results on leaf metabolite profiling by NMR, where we reported higher accumulation of sucrose in *V. vinifera* cv. Trincadeira in the first 48 hours after inoculation with *P. viticola* (Ali et al., 2012). Also, in the all-leaf tissue analysis of *Vitis vinifera* L. 'Marselan', an increase of soluble sugars after 7 dpi (days post-inoculation) was reported (Gamm et al., 2011). The specific location of sucrose needs to be better understood according to the involved biosynthesis pathways and their isomeric composition. Also, sucrose localisation in different *Vitis* genotypes, with different resistance degrees towards pathogens, should be further investigated to understand its role in grapevine defence against pathogens.

The results presented in this article clearly demonstrate the potential of MALDI-FT-ICR-MSI to gain more knowledge on the grapevine-*P. viticola* interaction particularly through the localisation and visual tracking of specific compounds in leaf tissue. Furthermore, our MSI results demonstrate that the analysis methodology works for complex samples, such as grapevine leaves, showing a great potential for application to other plant leaves.

7.6 CONCLUSIONS

Grapevine leaves are quite challenging in obtaining high quality MALDI mass spectra images, as leaves are not entirely flat and possess trichomes, influencing the detection of ions. In this work, we have shown that higher ion signal is achieved in leaf discs without trichomes. Three different matrices were selected (HCCA, DHB and 9-AA), whether dissolved in MeOH or ACN, for leaf discs coating and analysis. HCCA showed the highest signal intensity, independently of the solvent. Reconstructed images by MS allow us to identify sucrose in all the conditions tested. Sucrose ions were more abundant in the infected leaf discs, comparing to control discs. These results are in accordance with previous studies, which describe a variation of accumulation of sucrose in infected *P. viticola* plants. Up to our knowledge, our results are the first visual evidence of the localisation of sucrose translocation in grapevine leaves linked to the development of *P. viticola* infection structures.

7.7 SUPPLEMENTARY INFORMATION

For **Supplementary Figure F7.1**, **Supplementary Figure F7.2** and **Supplementary Figure F7.3**, consult the Appendices D, E and F, respectively.

7.8 ACKNOWLEDGEMENTS

7.9 REFERENCES

Adrian, M., Lucio, M., Roullier-Gall, C., Héloir, M.-C., Trouvelot, S., Daire, X., Kanawati, B., Lemaître-Guillier, C., Poinssot, B., Gougeon, R., Schmitt-Kopplin, P., 2017. Metabolic Fingerprint of PS3-Induced Resistance of Grapevine Leaves against Plasmopara viticola Revealed Differences in Elicitor-Triggered Defenses. Front Plant Sci 8, 101. https://doi.org/10.3389/fpls.2017.00101

Aked, J., Hall, J.L., 1993. The uptake of glucose, fructose and sucrose into the lower epidermis of leaf discs of pea (Pisum sativum L. cv. Argenteum). New Phytologist 123, 271–276. https://doi.org/10.1111/j.1469-8137.1993.tb03735.x

Alcantara, H.J.P., Jativa, F., Doronila, A.I., Anderson, C.W.N., Siegele, R., Spassov, T.G., Sanchez-Palacios, J.T., Boughton, B.A., Kolev, S.D., 2020. Localization of mercury and gold in cassava (Manihot esculenta Crantz). Environ Sci Pollut Res Int 27, 18498–18509. https://doi.org/10.1007/s11356-020-08285-3

Ali, K., Maltese, F., Figueiredo, A., Rex, M., Fortes, A.M., Zyprian, E., Pais, M.S., Verpoorte, R., Choi, Y.H., 2012. Alterations in grapevine leaf metabolism upon inoculation with Plasmopara viticola in different time-points. Plant Science 191–192, 100–107. https://doi.org/10.1016/j.plantsci.2012.04.014

Batovska, D.I., Todorova, I.T., Nedelcheva, D.V., Parushev, S.P., Atanassov, A.I., Hvarleva, T.D., Djakova, G.J., Bankova, V.S., Popov, S.S., 2008. Preliminary study on

biomarkers for the fungal resistance in Vitis vinifera leaves. Journal of Plant Physiology 165, 791–795. https://doi.org/10.1016/j.jplph.2007.09.005

Batovska, D.I., Todorova, I.T., Parushev, S.P., Nedelcheva, D.V., Bankova, V.S., Popov, S.S., Ivanova, I.I., Batovski, S.A., 2009. Biomarkers for the prediction of the resistance and susceptibility of grapevine leaves to downy mildew. Journal of Plant Physiology 166, 781–785. https://doi.org/10.1016/j.jplph.2008.08.008

Becker, L., Bellow, S., Carré, V., Latouche, G., Poutaraud, A., Merdinoglu, D., Brown, S.C., Cerovic, Z.G., Chaimbault, P., 2017. Correlative Analysis of Fluorescent Phytoalexins by Mass Spectrometry Imaging and Fluorescence Microscopy in Grapevine Leaves. Anal Chem 89, 7099–7106. https://doi.org/10.1021/acs.analchem.7b01002

Becker, L., Carré, V., Poutaraud, A., Merdinoglu, D., Chaimbault, P., 2014. MALDI Mass Spectrometry Imaging for the Simultaneous Location of Resveratrol, Pterostilbene and Viniferins on Grapevine Leaves. Molecules 19, 10587–10600. https://doi.org/10.3390/molecules190710587

Becker, L., Poutaraud, A., Hamm, G., Muller, J.-F., Merdinoglu, D., Carré, V., Chaimbault, P., 2013. Metabolic study of grapevine leaves infected by downy mildew using negative ion electrospray – Fourier transform ion cyclotron resonance mass spectrometry. Analytica Chimica Acta 795, 44–51. https://doi.org/10.1016/j.aca.2013.07.068

Bezrutczyk, M., Yang, J., Eom, J.-S., Prior, M., Sosso, D., Hartwig, T., Szurek, B., Oliva, R., Vera-Cruz, C., White, F.F., Yang, B., Frommer, W.B., 2018. Sugar flux and signaling in plant–microbe interactions. The Plant Journal 93, 675–685. https://doi.org/10.1111/tpj.13775

Bjarnholt, N., Li, B., D'Alvise, J., Janfelt, C., 2014. Mass spectrometry imaging of plant metabolites--principles and possibilities. Nat Prod Rep 31, 818–837. https://doi.org/10.1039/c3np70100j

Boughton, B.A., Thinagaran, D., Sarabia, D., Bacic, A., Roessner, U., 2016. Mass spectrometry imaging for plant biology: a review. Phytochem Rev 15, 445–488. https://doi.org/10.1007/s11101-015-9440-2

Bunch, J., Clench, M.R., Richards, D.S., 2004. Determination of pharmaceutical compounds in skin by imaging matrix-assisted laser desorption/ionisation mass spectrometry. Rapid Commun Mass Spectrom 18, 3051–3060. https://doi.org/10.1002/rcm.1725

Burrell, M., Earnshaw, C., Clench, M., 2007. Imaging Matrix Assisted Laser Desorption Ionization Mass Spectrometry: a technique to map plant metabolites within tissues at high spatial resolution. Journal of Experimental Botany 58, 757–763. https://doi.org/10.1093/jxb/erl139

Calvano, C.D., Monopoli, A., Cataldi, T.R.I., Palmisano, F., 2018. MALDI matrices for low molecular weight compounds: an endless story? Anal Bioanal Chem 410, 4015–4038. https://doi.org/10.1007/s00216-018-1014-x

Caprioli, R.M., Farmer, T.B., Gile, J., 1997. Molecular imaging of biological samples: localization of peptides and proteins using MALDI-TOF MS. Anal Chem 69, 4751–4760. https://doi.org/10.1021/ac970888i

Carter, C.L., McLeod, C.W., Bunch, J., 2011. Imaging of phospholipids in formalin fixed rat brain sections by matrix assisted laser desorption/ionization mass spectrometry. J Am Soc Mass Spectrom 22, 1991–1998. https://doi.org/10.1007/s13361-011-0227-4

Cha, S., Song, Z., Nikolau, B.J., Yeung, E.S., 2009. Direct profiling and imaging of epicuticular waxes on Arabidopsis thaliana by laser desorption/ionization mass spectrometry using silver colloid as a matrix. Anal Chem 81, 2991–3000. https://doi.org/10.1021/ac802615r

Cha, S., Zhang, H., Ilarslan, H.I., Wurtele, E.S., Brachova, L., Nikolau, B.J., Yeung, E.S., 2008. Direct profiling and imaging of plant metabolites in intact tissues by using colloidal graphite-assisted laser desorption ionization mass spectrometry. Plant J 55, 348–360. https://doi.org/10.1111/j.1365-313X.2008.03507.x

Costa, M.A., Marques, J.V., Dalisay, D.S., Herman, B., Bedgar, D.L., Davin, L.B., Lewis, N.G., 2013. Transgenic Hybrid Poplar for Sustainable and Scalable Production of the Commodity/Specialty Chemical, 2-Phenylethanol. PLoS ONE 8, e83169. https://doi.org/10.1371/journal.pone.0083169

Francese, S., Dani, F.R., Traldi, P., Mastrobuoni, G., Pieraccini, G., Moneti, G., 2009. MALDI mass spectrometry imaging, from its origins up to today: the state of the art. Comb Chem High Throughput Screen 12, 156–174. https://doi.org/10.2174/138620709787315454

Fröbel, S., Zyprian, E., 2019. Colonization of Different Grapevine Tissues by Plasmopara viticola—A Histological Study. Front. Plant Sci. 10. https://doi.org/10.3389/fpls.2019.00951

Gamm, M., Héloir, M.-C., Bligny, R., Vaillant-Gaveau, N., Trouvelot, S., Alcaraz, G., Frettinger, P., Clément, C., Pugin, A., Wendehenne, D., Adrian, M., 2011. Changes in carbohydrate metabolism in Plasmopara viticola-infected grapevine leaves. Mol Plant Microbe Interact 24, 1061–1073. https://doi.org/10.1094/MPMI-02-11-0040

Gebauer, P., Korn, M., Engelsdorf, T., Sonnewald, U., Koch, C., Voll, L.M., 2017. Sugar Accumulation in Leaves of Arabidopsis sweet11/sweet12 Double Mutants Enhances Priming of the Salicylic Acid-Mediated Defense Response. Front Plant Sci 8. https://doi.org/10.3389/fpls.2017.01378

Gessler, C., Pertot, I., Perazzolli, M., 2011. Plasmopara viticola: a review of knowledge on downy mildew of grapevine and effective disease management. Phytopathologia Mediterranea 50, 3–44. https://doi.org/10.14601/Phytopathol_Mediterr-9360

Goodwin, Richard J. A., Mackay, C.L., Nilsson, A., Harrison, D.J., Farde, L., Andren, P.E., Iverson, S.L., 2011. Qualitative and quantitative MALDI imaging of the positron emission tomography ligands raclopride (a D2 dopamine antagonist) and SCH 23390 (a D1 dopamine antagonist) in rat brain tissue sections using a solvent-free dry matrix application method. Anal Chem 83, 9694–9701. https://doi.org/10.1021/ac202630t

Goodwin, Richard J A, Pitt, A.R., Harrison, D., Weidt, S.K., Langridge-Smith, P.R.R., Barrett, M.P., Logan Mackay, C., 2011. Matrix-free mass spectrometric imaging using laser desorption ionisation Fourier transform ion cyclotron resonance mass spectrometry. Rapid Commun Mass Spectrom 25, 969–972. https://doi.org/10.1002/rcm.4939

Goodwin, R.J.A., Scullion, P., MacIntyre, L., Watson, D.G., Pitt, A.R., 2010. Use of a Solvent-Free Dry Matrix Coating for Quantitative Matrix-Assisted Laser Desorption Ionization Imaging of 4-Bromophenyl-1,4-diazabicyclo(3.2.2)nonane-4-carboxylate in Rat Brain and Quantitative Analysis of the Drug from Laser Microdissected Tissue Regions. Anal. Chem. 82, 3868–3873. https://doi.org/10.1021/ac100398y

Gorzolka, K., Bednarz, H., Niehaus, K., 2014. Detection and localization of novel hordatine-like compounds and glycosylated derivates of hordatines by imaging mass spectrometry of barley seeds. Planta 239, 1321–1335. https://doi.org/10.1007/s00425-014-2061-y

Goto-Inoue, N., Setou, M., Zaima, N., 2010. Visualization of Spatial Distribution of γ-Aminobutyric Acid in Eggplant (Solanum melongena) by Matrix-assisted Laser Desorption/Ionization Imaging Mass Spectrometry. Anal. Sci. 26, 821–825. https://doi.org/10.2116/analsci.26.821

Grassl, J., Taylor, N.L., Millar, A.H., 2011. Matrix-assisted laser desorption/ionisation mass spectrometry imaging and its development for plant protein imaging. Plant Methods 7, 21. https://doi.org/10.1186/1746-4811-7-21

Hamm, G., Carré, V., Poutaraud, A., Maunit, B., Frache, G., Merdinoglu, D., Muller, J.-F., 2010. Determination and imaging of metabolites from *Vitis vinifera* leaves by laser desorption/ionisation time-of-flight mass spectrometry: Imaging of metabolites from *Vitis vinifera* leaves. Rapid Commun. Mass Spectrom. 24, 335–342. https://doi.org/10.1002/rcm.4395

Huchelmann, A., Boutry, M., Hachez, C., 2017. Plant Glandular Trichomes: Natural Cell Factories of High Biotechnological Interest1[OPEN]. Plant Physiol 175, 6–22. https://doi.org/10.1104/pp.17.00727

Ibáñez, A.J., Scharte, J., Bones, P., Pirkl, A., Meldau, S., Baldwin, I.T., Hillenkamp, F., Weis, E., Dreisewerd, K., 2010. Rapid metabolic profiling of Nicotiana tabacum defence

responses against Phytophthora nicotianae using direct infrared laser desorption ionization mass spectrometry and principal component analysis. Plant Methods 6, 14. https://doi.org/10.1186/1746-4811-6-14

Jun, J.H., Song, Z., Liu, Z., Nikolau, B.J., Yeung, E.S., Lee, Y.J., 2010. High-spatial and high-mass resolution imaging of surface metabolites of Arabidopsis thaliana by laser desorption-ionization mass spectrometry using colloidal silver. Anal Chem 82, 3255–3265. https://doi.org/10.1021/ac902990p

Kaspar, S., Peukert, M., Svatos, A., Matros, A., Mock, H.-P., 2011. MALDI-imaging mass spectrometry - An emerging technique in plant biology. Proteomics 11, 1840–1850. https://doi.org/10.1002/pmic.201000756

Konlechner, C., Sauer, U., 2016. Ultrastructural leaf features of grapevine cultivars (Vitis vinifera L. ssp. vinifera). OENO One 50. https://doi.org/10.20870/oeno-one.2016.50.4.51

Laugesen, S., Roepstorff, P., 2003. Combination of two matrices results in improved performance of MALDI MS for peptide mass mapping and protein analysis. J. Am. Soc. Mass Spectrom. 14, 992–1002. https://doi.org/10.1016/S1044-0305(03)00262-9

Leopold, J., Popkova, Y., Engel, K., Schiller, J., 2018. Recent Developments of Useful MALDI Matrices for the Mass Spectrometric Characterization of Lipids. Biomolecules 8, 173. https://doi.org/10.3390/biom8040173

Li, Y., Shrestha, B., Vertes, A., 2008. Atmospheric pressure infrared MALDI imaging mass spectrometry for plant metabolomics. Anal Chem 80, 407–420. https://doi.org/10.1021/ac701703f

Maia, M., Ferreira, A.E.N., Nascimento, R., Monteiro, F., Traquete, F., Marques, A.P., Cunha, J., Eiras-Dias, J.E., Cordeiro, C., Figueiredo, A., Sousa Silva, M., 2020. Integrating metabolomics and targeted gene expression to uncover potential biomarkers of fungal/oomycetes-associated disease susceptibility in grapevine. Sci. Rep. 10, 15688. https://doi.org/10.1038/s41598-020-72781-2

Nascimento, R., Maia, M., Ferreira, A.E.N., Silva, A.B., Freire, A.P., Cordeiro, C., Sousa Silva, M., Figueiredo, A., 2019. Early stage metabolic events associated with the establishment of Vitis vinifera – Plasmopara viticola compatible interaction. Plant Physiol Biochem 137, 1–13. https://doi.org/10.1016/j.plaphy.2019.01.026

Ng, K.-M., Liang, Z., Lu, W., Tang, H.-W., Zhao, Z., Che, C.-M., Cheng, Y.-C., 2007. In Vivo Analysis and Spatial Profiling of Phytochemicals in Herbal Tissue by Matrix-Assisted Laser Desorption/Ionization Mass Spectrometry. Anal. Chem. 79, 2745–2755. https://doi.org/10.1021/ac062129i

Puolitaival, S.M., Burnum, K.E., Cornett, D.S., Caprioli, R.M., 2008. Solvent-Free Matrix Dry-Coating for MALDI Imaging of Phospholipids. J Am Soc Mass Spectrom 19, 882–886. https://doi.org/10.1016/j.jasms.2008.02.013

Rubakhin, S.S., Sweedler, J.V. (Eds.), 2010a. Mass Spectrometry Imaging: Principles and Protocols, Methods in Molecular Biology. Humana Press. https://doi.org/10.1007/978-1-60761-746-4

Rubakhin, S.S., Sweedler, J.V., 2010b. A mass spectrometry primer for mass spectrometry imaging. Mass Spectrometry Imaging: Principles and Protocols 21–49. https://doi.org/10.1007/978-1-60761-746-4_2

Sarabia, L.D., Boughton, B.A., Rupasinghe, T., van de Meene, A.M.L., Callahan, D.L., Hill, C.B., Roessner, U., 2018. High-mass-resolution MALDI mass spectrometry imaging reveals detailed spatial distribution of metabolites and lipids in roots of barley seedlings in response to salinity stress. Metabolomics 14, 63. https://doi.org/10.1007/s11306-018-1359-3

Schulz, S., Becker, M., Groseclose, M.R., Schadt, S., Hopf, C., 2019. Advanced MALDI mass spectrometry imaging in pharmaceutical research and drug development. Current Opinion in Biotechnology 55, 51–59. https://doi.org/10.1016/j.copbio.2018.08.003

Schwartz, S.A., Reyzer, M.L., Caprioli, R.M., 2003. Direct tissue analysis using matrix-assisted laser desorption/ionization mass spectrometry: practical aspects of sample preparation. J Mass Spectrom 38, 699–708. https://doi.org/10.1002/jms.505

Seaman, C., Flinders, B., Eijkel, G., Heeren, R.M.A., Bricklebank, N., Clench, M.R., 2014. "Afterlife Experiment": Use of MALDI-MS and SIMS Imaging for the Study of the Nitrogen Cycle within Plants. Anal. Chem. 86, 10071–10077. https://doi.org/10.1021/ac501191w

Shroff, R., Schramm, K., Jeschke, V., Nemes, P., Vertes, A., Gershenzon, J., Svatoš, A., 2015. Quantification of plant surface metabolites by matrix-assisted laser desorption-ionization mass spectrometry imaging: glucosinolates on *Arabidopsis thaliana* leaves. Plant J 81, 961–972. https://doi.org/10.1111/tpj.12760

Shroff, R., Vergara, F., Muck, A., Svatos, A., Gershenzon, J., 2008. Nonuniform distribution of glucosinolates in Arabidopsis thaliana leaves has important consequences for plant defense. Proceedings of the National Academy of Sciences 105, 6196–6201. https://doi.org/10.1073/pnas.0711730105

Shroff, Rohit, Vergara, F., Muck, A., Svatoš, A., Gershenzon, J., 2008. Nonuniform distribution of glucosinolates in Arabidopsis thaliana leaves has important consequences for plant defense. PNAS 105, 6196–6201. https://doi.org/10.1073/pnas.0711730105

Soares, M.S., da Silva, D.F., Forim, M.R., da Silva, M.F. das G.F., Fernandes, J.B., Vieira, P.C., Silva, D.B., Lopes, N.P., de Carvalho, S.A., de Souza, A.A., Machado, M.A., 2015. Quantification and localization of hesperidin and rutin in Citrus sinensis grafted on C. limonia after Xylella fastidiosa infection by HPLC-UV and MALDI imaging mass

spectrometry. Phytochemistry 115, 161–170. https://doi.org/10.1016/j.phytochem.2015.02.011

Solon, E.G., Schweitzer, A., Stoeckli, M., Prideaux, B., 2010. Autoradiography, MALDI-MS, and SIMS-MS imaging in pharmaceutical discovery and development. AAPS J 12, 11–26. https://doi.org/10.1208/s12248-009-9158-4

Spengler, B., Hubert, M., Kaufmann, R., 1994. MALDI ion imaging and biological ion imaging with a new scanning UV-laser microprobe. Presented at the Proceedings of the 42nd Annual Conference on Mass Spectrometry and Allied Topics, Chicago, p. 1041.

Suhre, K., Schmitt-Kopplin, P., 2008. MassTRIX: mass translator into pathways. Nucl. Acids Res. 36, W481–W484. https://doi.org/10.1093/nar/gkn194

Sutton, P.N., Henry, M.J., Hall, J.L., 1999. Glucose, and not sucrose, is transported from wheat to wheat powdery mildew. Planta 208, 426–430. https://doi.org/10.1007/s004250050578

Takahashi, K., Kozuka, T., Anegawa, A., Nagatani, A., Mimura, T., 2015. Development and Application of a High-Resolution Imaging Mass Spectrometer for the Study of Plant Tissues. Plant Cell Physiol 56, 1329–1338. https://doi.org/10.1093/pcp/pcv083

Takáts, Z., Wiseman, J.M., Gologan, B., Cooks, R.G., 2004. Mass spectrometry sampling under ambient conditions with desorption electrospray ionization. Science 306, 471–473. https://doi.org/10.1126/science.1104404

Taylor, M.J., Mattson, S., Liyu, A., Stopka, S.A., Ibrahim, Y.M., Vertes, A., Anderton, C.R., 2021. Optical Microscopy-Guided Laser Ablation Electrospray Ionization Ion Mobility Mass Spectrometry: Ambient Single Cell Metabolomics with Increased Confidence in Molecular Identification. Metabolites 11. https://doi.org/10.3390/metabo11040200

Vrkoslav, V., Muck, A., Cvačka, J., Svatoš, A., 2010. MALDI imaging of neutral cuticular lipids in insects and plants. J Am Soc Mass Spectrom 21, 220–231. https://doi.org/10.1016/j.jasms.2009.10.003

Yin, X., Liu, R.-Q., Su, H., Su, L., Guo, Y.-R., Wang, Z.-J., Du, W., Li, M.-J., Zhang, X., Wang, Y.-J., Liu, G.-T., Xu, Y., 2017. Pathogen development and host responses to Plasmopara viticola in resistant and susceptible grapevines: an ultrastructural study. Horticulture Research 4, 17033. https://doi.org/10.1038/hortres.2017.33

CONCLUDING REMARKS

In the framework of this PhD dissertation, FT-ICR-MS was used to deepen the knowledge on the metabolome of grapevine, from nutritional value to pathogen resistance. The analysis of *Vitis vinifera* cv. Pinot noir leaves, with the purpose of investigating its nutritional and medicinal value, revealed that grapevine leaves present a high content in fatty acids and contain several antioxidant compounds. Also, 'Pinot noir' leaves presented a high antioxidant capacity, putting grapevine leaves at the top of the list of foods with the highest antioxidative activity.

The metabolic composition of grapevine leaves was unravelled by an untargeted metabolomics approach and the constitutive associated metabolic traits that differentiate tolerant and susceptible grapevine genotypes were elucidated. First, the metabolomes of *Vitis vinifera* cv. Trincadeira (susceptible to pathogens) and *Vitis vinifera* cv. Regent (tolerant to pathogens) were investigated and the obtained results revealed a clear discrimination of both cultivars at the constitutive level. The most discriminatory compounds were identified. Second, through the application of visualization approaches (compositional space plots and van Krevelen diagrams), the metabolome of two different *Vitis* genotypes: *V. rotundifolia* (tolerant to pathogens) and *V. vinifera* 'Cabernet Sauvignon' (susceptible to pathogens); was compared and revealed that *Vitis rotundifolia* metabolome presented higher complexity than the metabolome from *V. vinifera* 'Cabernet Sauvignon'.

Since the analysis of untargeted metabolomic analysis allowed the discrimination of *Vitis* genotypes not only from different species but also from the same *Vitis* species. This approach was used to compare, at the constitutive level, the metabolome of 11 *Vitis* genotypes, with different tolerance degrees to pathogens to uncovered differences associated to resistance/susceptibility to different fungal/oomycete pathogens. Key differentiating metabolic players were identified. Combining a metabolomics approach with gene expression analysis, catechin/epicatechin and *LAR2* were pointed out as putative biomarkers associated to susceptibility towards pathogens.

The main metabolic alterations after *P. viticola* inoculation through untargeted FT-ICR-MS analysis and MALDI-FT-ICR-MS imaging was uncovered. The chemical profile of control and *Vitis vinifera* cv. Trincadeira leaves with *P. viticola* was analysed. Visualization approaches allowed the discrimination of infected and non-infected samples, as early as 24 hours after infection. The analysis of grapevine leaves using untargeted MALDI-FT-ICR-MS imaging revealed that putative sucrose ions were more abundant in the infected leaf discs and visually more abundant in *P. viticola* infection sites.

In sum, the results obtained show that FT-ICR-MS-based metabolomics is essential in grapevine research. This OMICs approach allowed grapevine discrimination and deepened our knowledge on the intricate metabolic networks of grapevine. Several compounds were highlighted as involved in grapevine resistance/susceptibility mechanisms. These results open new insights towards the development of efficient biomarker assays, to help future breeding programs in progeny selection, as well as plant screening on the field.

FUTURE PERSPECTIVES

Grapevine (*Vitis vinifera* L.) has always been an important part of the development of human culture and nowadays is one of the most important cultivated fruit plants in the world, not only due to its food products, but also due to its major economical importance in the wine industry. However, its value goes beyond wine and grapes for consumption, since it contains innumerous secondary metabolites highly important for human health.

The research results obtained during this PhD are transversal to many knowledge areas, from fundamental science to a more applied science and may be used to propose new approaches for a more sustainable viticulture.

Considering a circular economy approach, viticulture is one of the main areas where production waste is undervalued. In Maia et al., (2019), we have underlined the nutritional value of grapevine leaves. Since, some wine producers, are expanding their business to enoturism and opening in the vineyards some specialized restaurants in enogastronomy, the investigation on the nutritional value of grapevine leaves will contribute to increase their use in the Mediterranean diet. Different cultivars should be analysed and compared and carbohydrates, fibres and pigments should be quantified in leaves to improve the knowledge on this by-product. This would trigger the creation of consumable products made with leaves and enhance their market value.

In Maia et al., (2020), we have highlighted a new approach for the identification of constitutive metabolic biomarkers for pathogen tolerance/susceptibility traits. The identification of the accumulation of different compounds, particularly catechin and derivatives, as well as *LAR2* gene expression, in susceptible *Vitis*, opened new doors towards biomarkers discovery. To further continue this study, a higher number of *Vitis* genotypes (>50) should be analysed to validate the identified compounds and the quantification of catechin and other compounds should be performed in all genotypes. In the future it might also be interesting to analyse these compounds in *P. viticola*, *E. necator* and *B. cinerea* infected grapevine leaves, to understand the behaviour of these metabolites upon different pathogen challenges. Each pathogen has a different infection mode and life cycle, hence further metabolomics studies on the interactions of grapevine with pathogens should also be performed to identify disease specific compounds.

Also, in Maia et al., (in preparation), we have highlighted the importance of the visual distribution of putatively identified sucrose in grapevine leaf discs infected with *P. viticola*. Although some studies have reported sucrose accumulation in infected *P. viticola* plants, further studies must be conducted to fully understand the correlation of sucrose and the mode

of propagation of *P. viticola* infection. A time-course analysis should be performed to investigate its accumulation throughout the infection. Also, the tissue localization of more compounds, that are related to *P. viticola* infection, should be investigated.
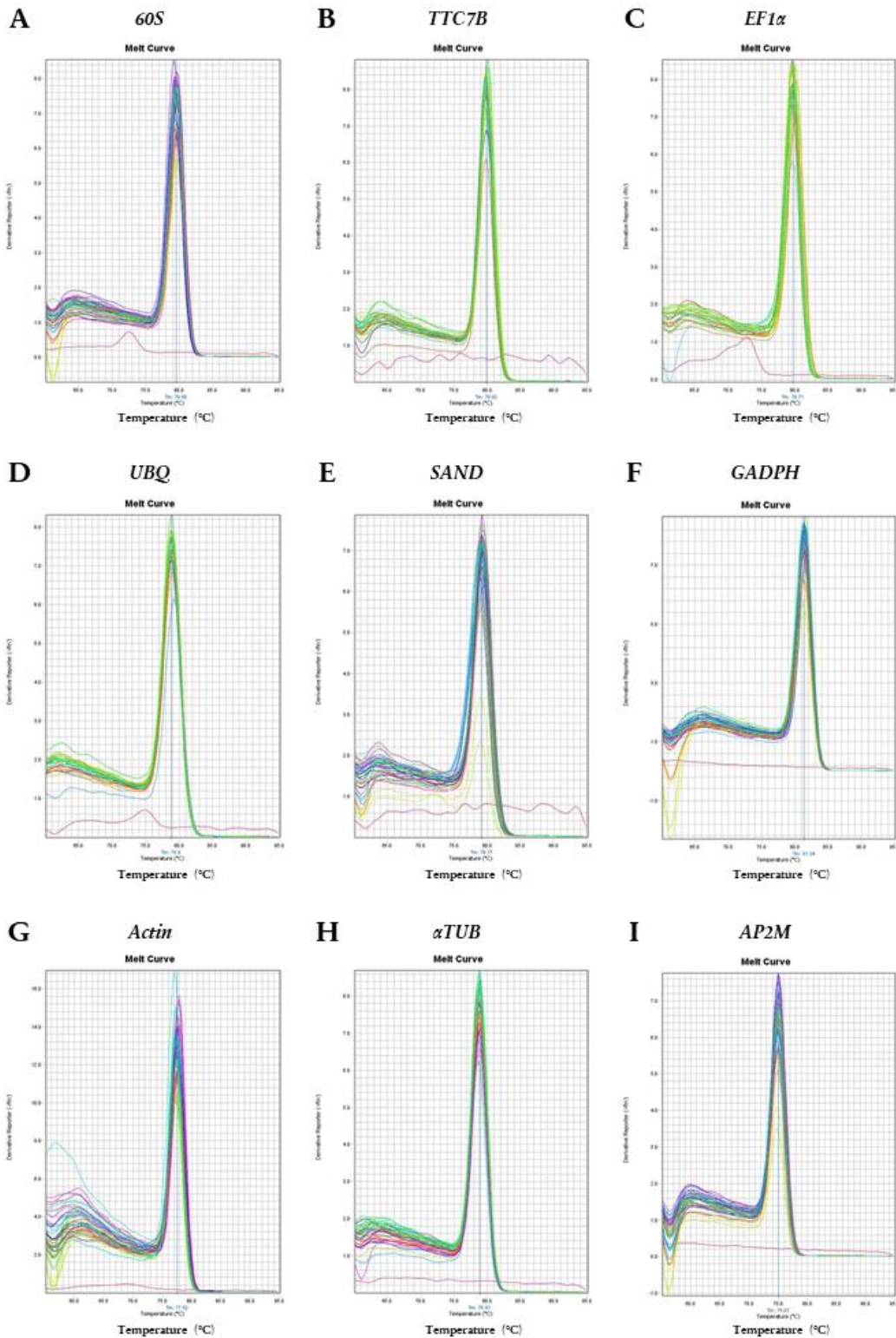
The European Union is committed to "*increase resilience of grape vines to pests and diseases and support the productivity of the sector in sustainable ways*", focusing on the breeding of new resistant varieties that maintain the grape qualities for wine production. Its success depends on the understanding of the innate resistance mechanisms against pathogens and the identification of resistance-related biomarkers towards the development of biomarker assays to assist future breeding programs and introgression line analysis. Future work built upon this thesis may contribute to the development of new selection methods leading to a more efficient breeding process, through early selection of the resistant seedlings, representing a considerable financial benefit to producers.
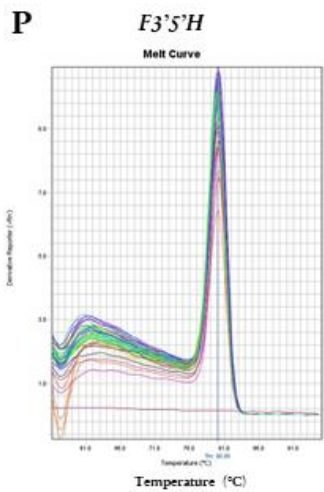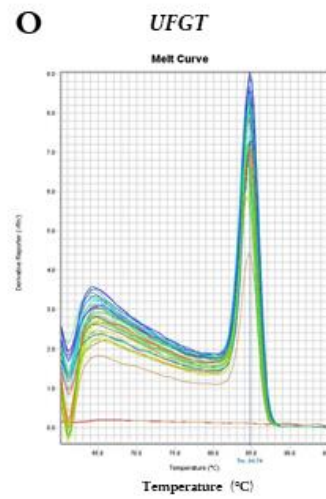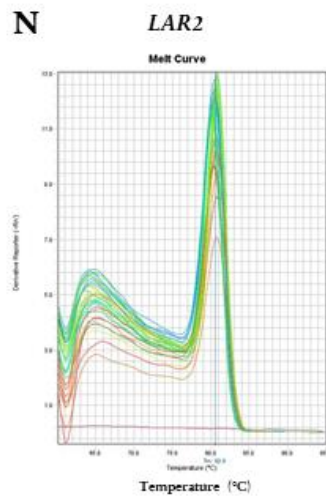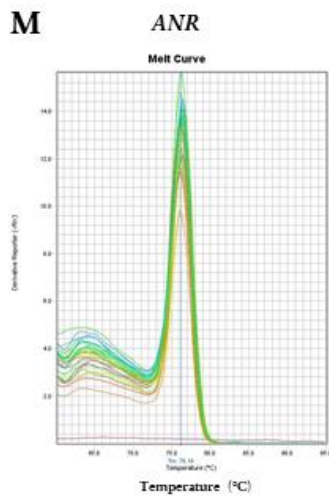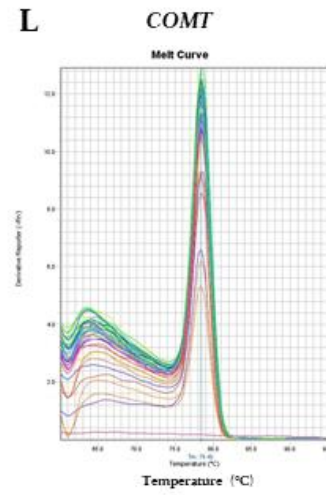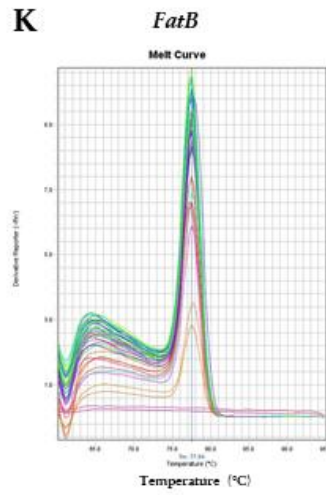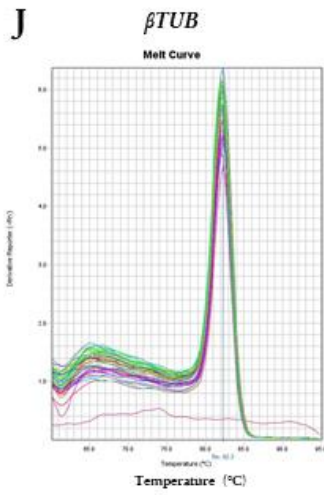
APPENDICES

The appendices presented are from **Chapter V** and **Chapter VII** and were published and submitted, respectively, to Scientific Journals:

1. **Maia, M.**, Ferreira, A.E.N., Nascimento, R., Monteiro, F., Traquete, F., Marques, A.P., Cunha, J., Eiras-Dias, J.E., Cordeiro, C., Figueiredo, A., Sousa Silva, M., 2020. Integrating metabolomics and targeted gene expression to uncover potential biomarkers of fungal/oomycetes-associated disease susceptibility in grapevine. Sci Rep 10, 15688. https://doi.org/10.1038/s41598-020-72781-2

2. **Maia, M.**, McCann, A., Malherbe, C., Far, J., Cunha, J., Eiras-Dias, J., Cordeiro, C., Eppe, G., De Pauw, E., Figueiredo, A., Sousa Silva, M., 2021. Grapevine leaf MALDI-FT-ICR-MS imaging reveals sucrose localisation patterns associated to *P. viticola* development. Metabolites (***Submitted***)
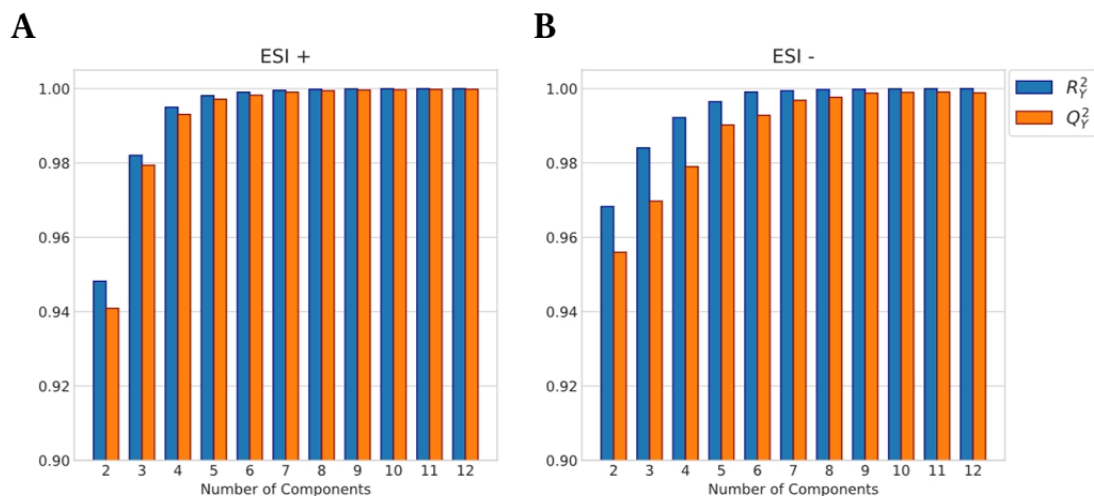
Supplementary Figure F5.1 - Melting curves of reference (**A-J**) and target (**K-Q**) genes. (**A**) 60S; (**B**) TTC7B; (**C**) EF1α; (**D**) UBQ; (**E**) SAND; (**F**) GADPH; (**G**) Actin; (**H**) αTUB; (**I**) AP2M; (**J**) βTUB; (**K**) FatB; (**L**) COMT; (**M**) ANR; (**N**) LAR2; (**O**) UFGT; (**P**) F3'5'H; (**Q**) IMPL1.

J βTUB

Melt Curve

Temperature (°C)

K FatB

Melt Curve

Temperature (°C)

L COMT

Melt Curve

Temperature (°C)

M ANR

Melt Curve

Temperature (°C)

N LAR2

Melt Curve

Temperature (°C)

O UFGT

Melt Curve

Temperature (°C)

P F3'5'H

Melt Curve

Temperature (°C)

Q IMPL1

Melt Curve

Temperature (°C)

188

APPENDIX B

A

B
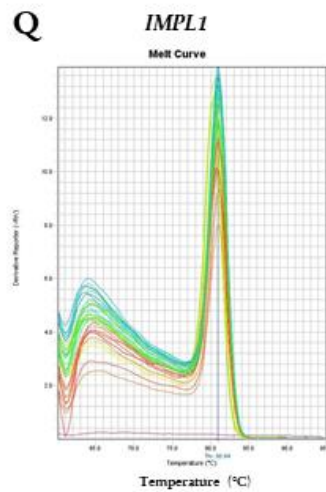
Supplementary Figure F5.2 - Model diagnostics showing fitting (R^2) and prediction ability (Q^2) metrics as a function of the number of components for the orthogonal partial least squares discriminant analysis (OPLS-DA) models for the classification into resistant/partial resistant and susceptible groups using of untargeted metabolomics data obtained in positive (**A**) and negative (**B**) ion modes. Q^2 is calculated from stratified 7-fold cross-validation.

APPENDIX C

Supplementary Table S5.2 - Gene expression analysis in the resistant/partial resistant and susceptible genotypes. Gene names' abbreviations are indicated (full gene names are indicated in **Table 5.3**). Results for Wilcox-Mann-Withney and Bartlett's tests are shown (*p*-value and adjusted *p*-value).

| Gene name abbreviation	Wilcox-Mann-Withney's test		Bartlett's test		*p*-value < 0.05 in both tests
	p-value	Adjusted *p*-value	*p*-value	Adjusted *p*-value	
LAR2	2.50124490706687e-14	2.75136939777356e-13	8.27320583499119e-11	9.1005264184903e-10	*
IMPL1	5.05270155526963e-07	1.38949292769915e-06	3.44493222111252e-09	1.89471272161188e-08	*
COMT	1.52538570732167e-07	5.59308092684614e-07	0.000215009186384817	0.000473020210046597	*
F3'5'H	0.0306640612463527	0.033730467370988	0.284805367322071	0.376956141272915	
FatB	0.0254846858024407	0.0311479493140942	0.120745701618498	0.189743245400497	
UFGT	0.0221037816153451	0.0303926997210995	0.408433132616659	0.408433132616659	
ANR	0.142746053595515	0.142746053595515	6.52974378169775e-08	2.39423938662251e-07	

0h   8dpi
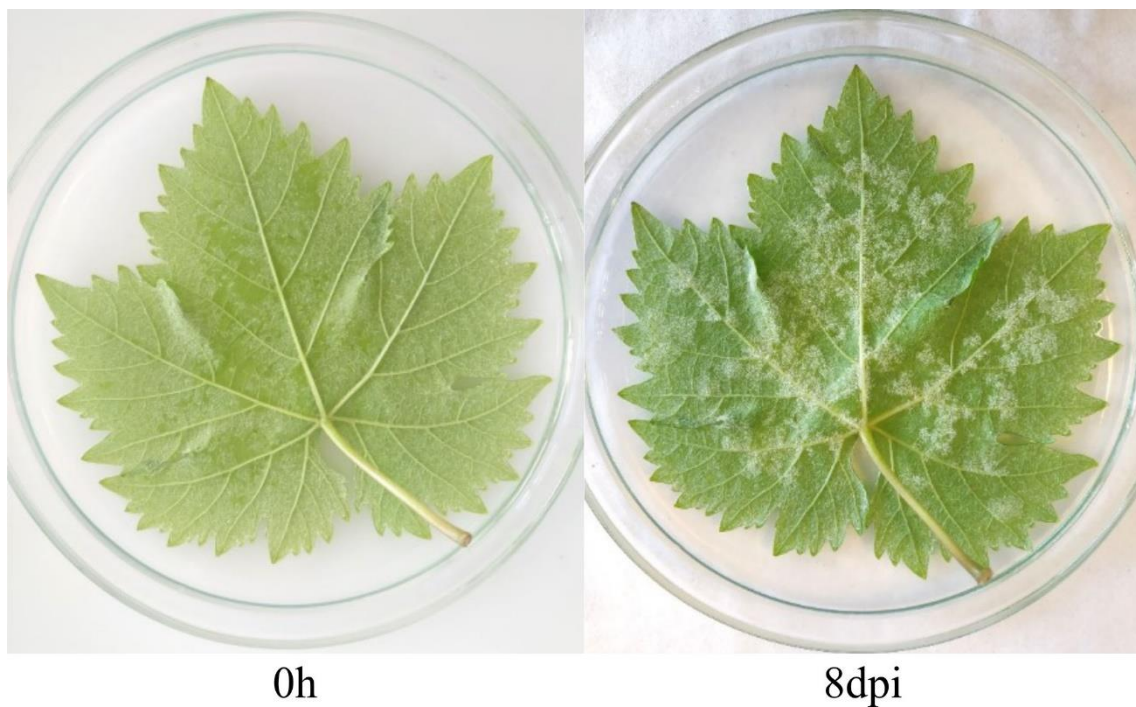
Supplementary Figure F7.2 - *V. vinifera* cv Trincadeira phenotype leaves of non-infected (0 h) and 8 days after inoculation (8 dpi) with *P. viticola*.

APPENDIX E
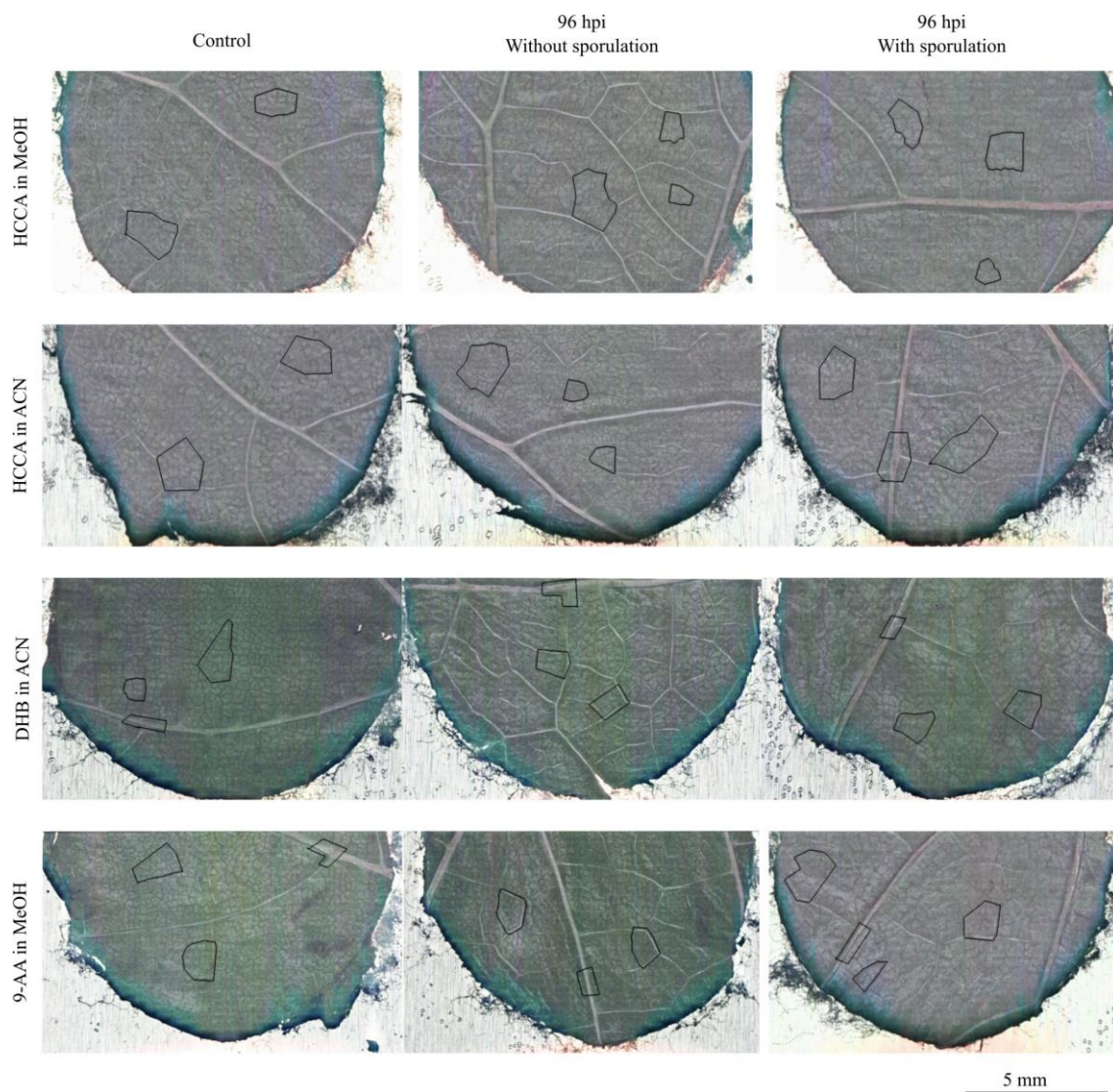
Supplementary Figure F7.2 - Microscope images (10 x) of *Vitis vinifera* cv. Trincadeira. Areas marked with a black line were selected for MALDI-FT-ICR-MS analysis with different matrices and solvents.

APPENDIX F
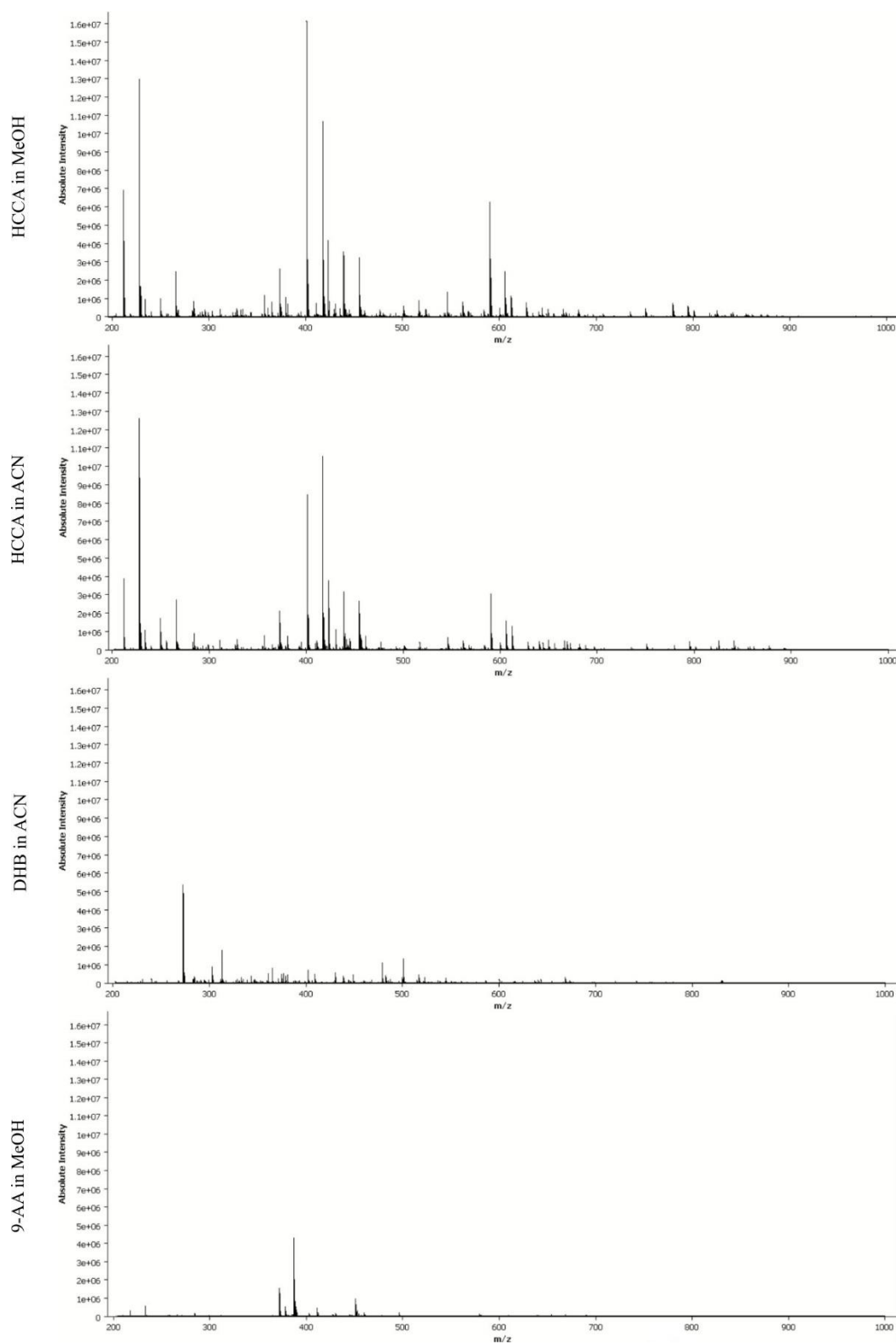
Supplementary Figure F7.3 - MALDI-FT-ICR-MS mean mass spectra of *Vitis vinifera* cv. Trincadeira leaf discs (control, 96 hpi without visible *P. viticola* sporulation and 96 hpi with visible sporulation) in positive ionisation mode. Data was normalised by the total ion count.